

**Pore water biogeochemistry and trace metal dynamics in
deep intertidal flat sediments**

Porenwasser-Biogeochemie und Spurenmetallodynamik in tiefen
intertidalen Wattsedimenten

Dissertation

zur Erlangung des Grades eines Doktors der Naturwissenschaften

– Dr. rer. nat. –

angenommen bei der Fakultät für Mathematik und Naturwissenschaften

der Carl von Ossietzky Universität Oldenburg

von

Melanie Beck

geboren am 12.10.1978 in Wertingen

Erstreferent: Prof. Dr. H.-J. Brumsack

Koreferent: Prof. Dr. J. Rullkötter

Eingereicht am: 26.6.2007

Disputation am: 17.7.2007

Abstract

Intertidal flats are highly dynamic environments, which are subjected to tidal and seasonal variations in light, oxygen supply, organic matter quality and quantity, aggregates, and bottom currents. Sediment geochemistry as well as biogeochemical and hydrological processes in the sediments further vary with depth. The main objective of this thesis was to investigate biogeochemical processes through the analysis of pore waters at different locations in the backbarrier area of Spiekeroog Island and to assess whether seeping pore waters have an impact on the chemistry and the ecosystem of the open water column.

In order to study biogeochemical processes in sediment layers of some metres depth, a multilevel *in situ* pore water sampler was developed, which allows pore water sampling down to 5 m sediment depth. After insertion into the sediment, the sampler stays on site allowing repetitive sampling at identical locations and depth intervals. The new sampler permits the *in situ* extraction of pore water without altering redox-sensitive element concentrations.

Sulphate, dissolved organic carbon, nutrients, and several terminal metabolic products were studied for the identification of organic matter remineralization pathways. Significant correlations between the inorganic products of terminal metabolism (ammonium and phosphate) and sulphate depletion suggest sulphate reduction to be the dominant terminal carbon oxidation pathway. Pore water concentrations of sulphate, ammonium, and phosphate were further used to elucidate the composition of organic matter degraded in the sediment.

Spatial variations of sulphate, dissolved organic carbon, and nutrients reveal that mixed flat sediments, which are richer in clay than sand flat sediments, display a more pronounced depletion of sulphate and a stronger enrichment of metabolic products than sandy sediments. Clay-rich layers are impeding pore water exchange processes resulting

in longer residence times of pore waters and thus enrichments of metabolic products. Differences in sediment structure and hydrological conditions explain spatial variations in pore water depth profiles of margins compared to central parts of tidal flats. Our deep pore water studies further illustrate that seasonal variations of sulphate, dissolved organic matter, and nutrients are not limited to the sediment surface, but are also observed in some metres depths within permeable sandy sediments. When substrate is available, the activity of fermentative microorganisms presumably increase with increasing temperature even in depths of some metres thus stimulating the activity of sulphate reducers by the production of labile organic compounds.

Trace metals (Mn, Fe, Mo, U, Cr, V) show similar general trends with depth close to margins and in central parts of tidal flats. Despite of dynamic biogeochemical, sedimentological, and hydrological conditions prevailing in intertidal flats, the general trends with depth of trace metals are similar to those observed in deep sea environments where constant sedimentation rates dominate. Seasonal sampling revealed that trace metals V and Cr vary seasonally parallel to changes in dissolved organic carbon. Seasonal variations of Mn, Fe, Mo, and U are by contrast limited to the upper decimetres of the sediment depending on factors like organic matter supply, redox stratification, and geochemical composition of the particulate matter deposited on the sediment surface.

Close to the tidal flat margin changes in pore water depth profiles are observed during one tidal cycle which evidence that deep pore water advection affects biogeochemical processes at tidal flat margins. Seasonal variations of sulphate and dissolved organic carbon further support the hypothesis that this zone is affected by deep pore water flow. Therefore, pore waters originating from some metres depth presumably escape at tidal flat margins at low tide. Owing to the enrichment of specific elements in pore water compared to sea water (e.g. nutrients, Mn), seeping pore waters may represent a source for the ecosystem in the open water column.

Kurzfassung

Wattgebiete stellen hoch dynamische Systeme dar. In ihnen ändern sich Licht, Sauerstoffgehalt, Qualität und Quantität des organischen Materials, Aggregate und Strömungsgeschwindigkeiten mit der Tide und den Jahreszeiten. In den Sedimenten variieren des weiteren Lithologie sowie biogeochemische und hydrologische Prozesse mit der Tiefe. Im Mittelpunkt dieser Arbeit stand das Verständnis von biogeochemischen Prozessen, die im Porenwasser des Rückseitenwatts der Insel Spiekeroog ablaufen. Des weiteren sollte der Einfluss von an Platenrändern austretenden Porenwässern auf das Ökosystem in der offenen Wassersäule abgeschätzt werden.

Um biogeochemische Prozesse in mehreren Metern Sedimenttiefe untersuchen zu können, wurde ein Probenahmesystem entwickelt. Dieses ermöglicht die Gewinnung von Porenwasser *in situ* bis in 5 m Tiefe wird. Das Probenahmesystem verbleibt nach dem Einbringen im Sediment. Dadurch wird ermöglicht, dass Proben wiederholt an den gleichen Standorten und in den gleichen Tiefenintervallen gewonnen werden können. Weiterhin ermöglicht die Konstruktion des Probenehmers die Extraktion von Porenwasser, ohne dass Artefakte bei redox-sensitiven Elementen auftreten.

Im Porenwasser wurden Sulfat, gelöster organischer Kohlenstoff, Nährstoffe und mehrere terminale Stoffwechselprodukte bestimmt, um die Abbauege des organischen Materials aufzuklären. Signifikante Korrelationen zwischen den anorganischen Produkten des terminalen Metabolismus (Ammonium und Phosphat) und dem Verbrauch von Sulfat legen nahe, dass Sulfatreduktion den wichtigsten Prozess für die Oxidation von organischem Material darstellt. Die Konzentrationen von Sulfat, Ammonium und Phosphat im Porenwasser wurden auch dafür verwendet, genaueres über die Zusammensetzung des im Sediment abgebauten organischen Materials herauszufinden.

Räumliche Variationen der Konzentrationen an Sulfat, gelöstem organischen Kohlenstoff und Nährstoffen zeigen, dass es in Mischwattsedimenten zu einer stärkeren

Abnahme von Sulfat und einer ausgeprägteren Anreicherung von Stoffwechselprodukten kommt als in Sandwattsedimenten. Tonreiche Lagen erschweren in Mischwattsedimenten Austauschprozesse im Porenwasser, was zu längeren Aufenthaltszeiten und somit stärkeren Anreicherung von Stoffwechselprodukten führt. Räumliche Variationen zeigen sich auch bei einem Vergleich der Tiefenprofile, die in Sedimenten des Platenrandes und der zentralen Gebiete der Plate gewonnen wurden. Diese sind durch Unterschiede in der Sedimentstruktur und den hydrologischen Bedingungen zu erklären. Die über ein Jahr bestimmten Konzentrationen von Sulfat, gelöstem organischen Kohlenstoff und Nährstoffen zeigen, dass saisonale Veränderungen nicht auf die Sedimentoberfläche begrenzt sind, sondern auch in Sedimenttiefen von mehreren Metern zu finden sind. Bei Verfügbarkeit von Substrat scheint die Aktivität von Fermentierern auch in Sedimenttiefen von einigen Metern mit ansteigenden Temperaturen zuzunehmen. Durch das Freisetzen von leicht abbaubaren organischen Verbindungen erhöhen sie somit die Aktivität der Sulfatreduzierer.

Spurenmehalle (Mn, Fe, Mo, U, Cr, V) zeigen in der Nähe des Platenrandes im Allgemeinen ähnliche Trends mit der Tiefe wie in zentralen Bereichen der Plate. Die Tiefenprofile weisen in Wattgebieten trotz der dynamischen biogeochemischen, sedimentologischen und hydrologischen Bedingungen einen ähnlichen Verlauf wie in Kontinentalrandsedimenten auf, in denen zumeist deutlich weniger variable Bedingungen vorherrschen. Monatliche Probenahmen haben gezeigt, dass sich die Konzentrationen der Spurenmehalle V und Cr parallel zu den saisonalen Veränderungen von gelöstem organischen Kohlenstoff entwickeln. Veränderungen der Mn, Fe, Mo und U Konzentrationen über ein Jahr sind vor allem in den obersten Sedimentschichten zu beobachten. Sie sind durch Faktoren wie der Nachlieferung an organischem Material, der Redoxzonierung und der geochemischen Zusammensetzung des auf der Sedimentoberfläche abgelagerten partikulären Materials beeinflusst.

In der Nähe des Platenrandes wurde beobachtet, dass sich der Verlauf der Porenwassertiefenprofile innerhalb eines Tidenzyklus verändert. Dies ist ein deutlicher

Hinweis darauf, dass biogeochemische Prozesse an Platenrändern durch Advektion des Porenwassers in tieferen Sedimentschichten beeinflusst werden. Unterstützt wird die Hypothese, dass dieser Bereich der Plate durch Advektionsprozesse beeinflusst wird, durch die gemessenen saisonalen Konzentrationsveränderungen von Sulfat und gelöstem organischen Kohlenstoff. Es wird daher angenommen, dass Porenwässer aus einigen Metern Sedimenttiefe bei Niedrigwasser an den Platenrändern aus dem Sediment heraussickern. Bezogen auf Komponenten, die im Porenwasser im Vergleich zum Meerwasser angereicht sind (z.B. Nährstoffe, Mn), könnte dieses Porenwasser somit eine Quelle für das Ökosystem in der offenen Wassersäule darstellen.

Table of contents

Abstract	I
Kurzfassung	III
Table of contents	VI
Figure legends	VII
Table legends	XII
1. Introduction	1
1.1. Wadden Sea	1
1.2. Organic matter remineralization in marine sediments	4
1.3. Transport processes in coastal marine sediments	7
1.4. Objectives of the thesis	13
1.5. Outline of the author's contribution	16
2. In situ pore water sampling in deep intertidal flat sediments	19
3. Sulphate, dissolved organic carbon, nutrients and terminal metabolic products in deep pore waters of an intertidal flat	37
4. Spatial, seasonal, and tidal variations of sulphate, dissolved organic carbon, and nutrients in deep pore waters of intertidal flat sediments	63
5. Cycling of trace metals (Mn, Fe, Mo, U, V, Cr) in deep pore waters of intertidal flat sediments	90
6. Non-conservative behaviour of molybdenum in coastal waters: Coupling geochemical, biological, and sedimentological processes	124
7. Conclusions and perspectives	158
8. References	162
Acknowledgements	185
Curriculum vitae	186

Figure legends

(abbreviated)

Fig. 1.1.	Wadden sea area. Picture slightly modified from Marencic et al. (2005).	3
Fig. 1.2.	Conceptual model of organic matter decomposition pathways and the geochemical zonation in marine sediments. Figure reproduced from Jørgensen (2006).	4
Fig. 1.3.	Pressure distribution at a small mound on the sediment surface exposed to unidirectional boundary layer flow. Graph reproduced from Huettel et al. (1998).	8
Fig. 1.4.	Up- and downstream of protruding sediment structures sea water is forced into the sediment leading to high nitrate concentration, while underneath the protrusion anoxic pore water is drawn to the surface reflected in high ammonium concentrations. Graph reproduced from Huettel et al. (1998).	9
Fig. 1.5.	Pore water flow pathways simulated in a tidal flat, which platform is inundated at high tide. Figure modified from Wilson and Gardner (2006).	11
Fig. 1.6.	Surface and deep pore water circulation processes as hypothesized by Billerbeck et al. (2006b). Figure reproduced from Billerbeck et al. (2006b).	12
Fig. 2.1.	<i>In situ</i> pore water sampler	23
Fig. 2.2.	Sampling area located in the tidal backbarrier area of the Island of Spiekeroog, one of the barrier islands of the NW German Wadden Sea. The cross marks the sampling location (Janssand: 53° 44.183' N, 007° 41.904' E).	25
Fig. 2.3.	Comparison of two <i>in situ</i> sampling techniques, our new developed sampler (filled dots) and the AMS TM gas vapour probe kit (open squares).	27

Fig. 2.4.	Pore water depth profiles of Mn, V, Mo, and U. Samples were taken with the <i>in situ</i> sampler in a sandy tidal flat sediment, NW Germany, in April and May 2005.	29
Fig. 2.5.	Pore water depth profiles of SO_4^{2-} , Mn and Mo. Samples taken with the <i>in situ</i> sampler in a sandy tidal flat sediment, NW Germany, on July 19 th 2005.	33
Fig. 2.6.	Seasonal variation of the pore water depth profiles of DOC and SO_4^{2-} .	34
Fig. 3.1.	(A) Study site in an intertidal sand flat (Janssand) in the backbarrier area of Spiekeroog Island, Wadden Sea, Germany. (B) Tidal flat topography.	41
Fig. 3.2.	Depth profiles of parameters characterising the lithology at the sampling site in an intertidal sand flat. The grey bars highlight the clay rich layers of the sediment profile. Depths of about 1.5 to 2.5 m are marked with a hatched area as the sediment is predominantly sandy, with very thin clay layers.	48
Fig. 3.3.	Pore water profiles of Cl^- , pH, NO_3^- , SO_4^{2-} , H_2S , CH_4 , DOC, TA, NH_4^+ , PO_4^{3-} , and H_4SiO_4 , at the sampling site in an intertidal sand flat of the backbarrier area of Spiekeroog Island from April 2006.	50
Fig. 3.4.	Ratios of DOC, TA, NH_4^+ , and PO_4^{3-} concentrations to $(\text{SO}_4^{2-})_{\text{Dep}}$ concentrations. Best-fit linear regressions are calculated for samples from April 2006 separately (A) and for all samples taken from May 2005 till June 2006 (B) at the sampling site described.	53
Fig. 3.5.	Sea water PO_4^{3-} and H_4SiO_4 concentrations determined at a monitoring station in the backbarrier area of Spiekeroog Island in May 2006.	58
Fig. 3.6.	Modelled (continuous line) and measured (points) SO_4^{2-} , NH_4^+ and PO_4^{3-} pore water concentrations.	60
Fig. 4.1.	Sampling locations in two intertidal flats situated in the backbarrier area of Spiekeroog Island, Wadden Sea, Germany. Pore water sampling locations are marked by dots and location numbers increase with increasing distance to the tidal creek.	67

Fig. 4.2.	SiO ₂ , Al ₂ O ₃ , TOC and TS contents of sediment cores taken at locations close to the pore water samplers in the sand flat area (JS1 - JS3) and in the mixed flat area (NN1, NN2) in April 2005.	72
Fig. 4.3.	Chloride, sulphate, DOC, nutrient, total alkalinity, and H ₂ S pore water concentrations determined at three locations in a sand flat area (JS1 - JS3) and at two locations in a mixed flat area (NN1, NN2) in April 2006.	74
Fig. 4.4.	Seasonal variation of sulphate, DOC, total alkalinity, and nutrients at site JS1 close to the tidal creek. Samples were extracted at the same location from May 2005 until June 2006.	76
Fig. 4.5.	Seasonal variation of sulphate, DOC, total alkalinity, and nutrients at site JS2 in the centre of the tidal flat. Samples were extracted at the same location from July 2005 until June 2006.	77
Fig. 4.6.	Minimum and maximum concentrations calculated for specific depths taking all samples into account obtained during 12 sampling campaigns at site JS1 and during 10 campaigns at site JS2.	78
Fig. 4.7.	DOC, NH ₄ ⁺ , TA, and SO ₄ ²⁻ pore water concentrations in samples taken at four different states in a tidal cycle, low tide (LT), rising water level (LT + 4h), high tide (HT), and falling water level (HT + 3h) in June 2006.	80
Fig. 4.8.	Summary of geochemical, biological, and hydrological factors influencing the pore water concentrations in the sand flat Janssand.	88
Fig. 5.1.	(A) Study sites on an intertidal sand flat (JS) in the backbarrier area of Spiekeroog Island, Wadden Sea, Germany. (B) Tidal flat topography.	97
Fig. 5.2.	Trace metal (Fe, Mn, Mo, U, V, Cr) and DOC pore water profiles at site JS1, which is located close to the tidal flat margin of an intertidal sand flat. Samples were taken in April 2006.	102
Fig. 5.3.	Trace metal (Fe, Mn, Mo, U, V, Cr) and DOC pore water profiles at sites JS2 and JS3, located in the central parts of an intertidal sand flat. Samples were taken in April 2006.	106
Fig. 5.4.	Seasonal variation of DOC, V, and Cr at site JS1 close to the tidal creek and at site JS3 in the central parts of the tidal flat.	110

Fig. 5.5.	Seasonal variation of Mn and Fe at sites JS1 and JS2.	112
Fig. 5.6.	Seasonal variation of Mo at sites JS1, JS2, and JS3.	114
Fig. 5.7.	Seasonal variation of U at sites JS1 and JS2.	116
Fig. 5.8.	Mn, Fe, U, Mo, V, and Cr pore water concentrations in samples taken at four different states during a tidal cycle, low tide (LT), rising water level (LT + 4h), high tide (HT), and falling water level (HT + 3h) in June 2006.	119
Fig. 5.9.	Mn, V, and U concentrations in the open water column of the backbarrier area of Spiekeroog Island in August 2002. Samples were obtained close to the tidal inlet of the backbarrier area.	121
Fig. 6.1.	(a) map of the study area showing the sampling sites during several cruises in the Wadden Sea of NW Germany. (b) detailed map of the backbarrier areas of the Islands of Spiekeroog and Langeoog showing the time-series locations in the tidal inlets.	129
Fig. 6.2.	Tidal patterns of suspended particulate matter (SPM) for the Wadden Sea cruises in January and July 2005 (Spiekeroog Island).	136
Fig. 6.3.	Tidal patterns of dissolved Mo and Mo/Al ratios for the Wadden Sea cruises (Spiekeroog Island) from summer 2002 to 2005.	138
Fig. 6.4.	Dissolved Mo of (a) transects from Langeoog Island into the German Bight, and (b) several sampling campaigns at position OB 1 in the tidal inlet of Spiekeroog Island.	140
Fig. 6.5.	Mo/Al and Mn/Al ratios of material (<63 μm) from sediment traps of the backbarrier salt marsh of Langeoog Island from March to November 2005.	141
Fig. 6.6.	Tidal patterns of dissolved Mn and Mn/Al ratios for the Wadden Sea cruises in 2005 (Spiekeroog Island).	143
Fig. 6.7.	Dissolved Mn from several sampling campaigns at position OB 1 in the tidal inlet of Spiekeroog Island during summer and autumn 2005.	144
Fig. 6.8.	Comparison of Mo and Mn pore water profiles between July and November 2005 from two locations at the Janssand tidal flat of the backbarrier area of Spiekeroog Island.	145

- Fig. 6.9.** Correlation diagrams of dissolved Mn and Mo versus aggregate-associated bacteria (normalized to SPM) for surface water samples from the backbarrier area of Spiekeroog Island in July 2005. **151**
- Fig. 6.10.** Illustration of the postulated model for non-conservative behaviour of Mo in coastal waters, which is based on the tight coupling between geochemical, biological, and sedimentological processes. **156**

Table legends

(abbreviated)

Tab. 1.1.	Organic matter remineralization pathways modified from Jørgensen (2006).	5
Tab. 2.1.	Comparison of the <i>in situ</i> AMS sampling technique and the ex situ centrifugation of sediment core slices. The sediment core was not treated under a nitrogen atmosphere.	30
Tab. 3.1.	Stoichiometry of organic matter degradation estimated from slopes of pore water concentrations of total alkalinity TA and sulphate depletion (SO_4^{2-}) _{Dep} against NH_4^+ and PO_4^{3-} concentrations for samples of April 2006 and for all samples taken from May 2005 till June 2006. The ratios of suspended particulate matter and the ratios derived from modelling pore water profiles are displayed.	52
Tab. 5.1.	Replicate analyzes of Cass-4 seawater reference material. Measured and certified values are reported. Accuracy and precision of the measured Cass-4 samples are displayed.	100
Tab. 5.2.	Replicate analyzes of Slew-3 seawater reference material. Measured and certified values are reported. Accuracy and precision of the measured Cass-4 samples are displayed.	100
Tab. 6.1.	Average surface values and ranges of several biological, meteorological, and sedimentological parameters for the Wadden Sea of Spiekeroog Island.	134
Tab. 6.2.	Average surface values and ranges of water temperature, salinity as well as dissolved and particulate geochemical parameters for the Wadden Sea.	137

1. Introduction

Low biogeochemical reaction rates have traditionally been considered to prevail in marine sandy sediments because of their low organic carbon contents. However, it has been demonstrated that sandflats with low organic carbon contents have rates of organic matter remineralization comparable to those of organic-rich mud (D'Andrea et al., 2002; Rusch et al., 2006). The permeability of sand facilitates advective pore water transport through the upper sediment layer supplying oxygen (Ziebis et al., 1996) and dissolved and particulate organic matter (Huettel and Rusch, 2000; Rusch and Huettel, 2000). However, there are few studies, which focused on biogeochemical processes occurring in layers deeper than the sediment surface in permeable sandy sediments. This thesis aims to contribute to the understanding of organic matter and trace metal cycling in permeable sandy sediments with an emphasis on sediment layers of some metres depth. The thesis comprises five studies conducted in the German Wadden Sea. The studies focus on biogeochemical processes and trace metal dynamics in pore waters as well as on the influence of seeping pore waters on the chemistry of the open water column.

1.1. Wadden Sea

The North Sea is a semi-enclosed shelf sea in northern Europe that covers an area of about 575,000 km² at an average water depth of 70 m. It is connected to the Atlantic Ocean in the north and west, whereas the Kattegat represents a connection to the Baltic Sea in the east. At the southern and eastern coast of the North Sea one of the largest tidal flat areas of the world is located, the Wadden Sea, extending for almost 500 km between Den Helder (Netherlands) and Skallingen (Denmark) (Fig. 1.1.). The tidal flat area is located between the coastline and a chain of barrier islands, which are separated by tidal inlets. These inlets connect the tidal flat areas with the open North Sea. The Wadden Sea

covers an area of about 3,300 km², which increases to 5,000 km² including the islands (Flemming and Davis, 1994). Characteristic landscape features of the Wadden Sea are tidal flats, barrier islands, sandbanks, and salt marshes.

Since the end of the last glaciation period about 16,000 years ago sea level has risen by 120 m in the North Sea region (Reise, 2005). The period of rising sea water level was characterized by a fast increase until 7000 BP and by a decelerated rise afterwards. When sea level rise slowed down, barrier spits developed along the southern coastline of the North Sea. These spits supposedly were cut into barrier islands between 7500 and 6000 BP when sea level continued to rise and tidal range increased (Flemming and Davis, 1994; Reise, 2005). Tidal range progressively increased to its present upper mesotidal regime as the water body of the North Sea gradually deepened along with rising sea water level (Chang et al., 2006c). Since about 1000 AD the evolution of the Wadden Sea is influenced by land reclamation and dike construction (Streif, 1990; Flemming and Nyandwi, 1994). Dike building lead to a decrease in deposition of fine particles. Thus, fine to medium sands dominate in the intertidal regions of the German Wadden Sea (Flemming and Nyandwi, 1994; Flemming and Ziegler, 1995)

The tidal flat areas themselves are divided by a system of tidal channels consisting of large main channels and smaller secondary channels. The channel systems of different backbarrier areas are permanently connected to each other, however exchange of huge water masses is limited to high tide periods. The tidal channels further divide the backbarrier area of each island into several tidal flats, which are covered by water at high tide and become exposed to the atmosphere at low tide. Time of exposure varies depending on the geographical situation of the tidal flat because of different tidal ranges in the Wadden Sea area. In the German Bight the tidal range increases from the west (≈ 1.5 m) and the northeast (≈ 1.0 m) to a maximum of about 4 m in the estuary region of Elbe, Weser, and Jade (Flemming and Davis, 1994). Strong hydrodynamic forcing by wind, tides and turbulent water motion make the Wadden Sea a very dynamic ecosystem. It is characterized by high dynamics in salinity, temperature, and oxygen The strong

hydrodynamic regime results in fast transport, dispersion and mixing of dissolved and particulate matter from various sources (Flemming and Ziegler, 1995; Lunau et al., 2006).

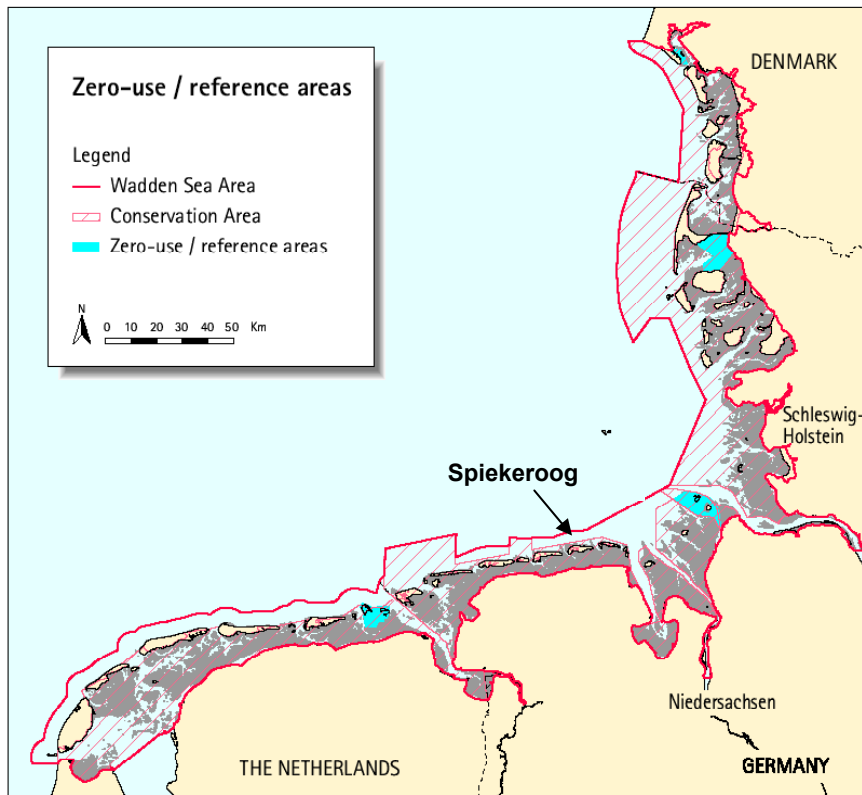


Fig. 1.1.: Wadden sea area. Picture slightly modified from Marencic et al. (2005).

This thesis is embedded in a research project, which focused on the backbarrier area of Spiekeroog Island. Spiekeroog is one of the East-Frisian islands and its backbarrier area is divided into several tidal flats. Two tidal flats with different clay contents were chosen as study area, Janssand and Neuharlingersieler Nacken. Transport of water masses into the backbarrier area occurs over the tidal inlet, the watersheds of neighbouring tidal areas, and a flood gate where fresh water enters the tidal area.

1.2. Organic matter remineralization in marine sediments

Organic matter is either provided to marine sediments by benthic photosynthesis or by dissolved and particulate organic matter synthesised in the open water column and deposited at or infiltrated into sediment surfaces. In marine sediments organic matter constitutes an important food source for benthic fauna and microorganisms. Heterotrophic organisms use organic carbon as an electron donor to obtain energy and as a carbon source to build up biomass. The chemical composition of organic matter can be generalized by $(\text{CH}_2\text{O})_x(\text{NH}_3)_y(\text{H}_3\text{PO}_4)_z$, where the variables x , y , and z depend on the origin and age of the material. Redfield (1958) proposed a stoichiometry of $x = 106$, $y = 16$, and $z = 1$ for fresh marine phytoplankton, however C:N:P ratios of marine organic matter partly differs from this ratio (Atkinson and Smith, 1983).

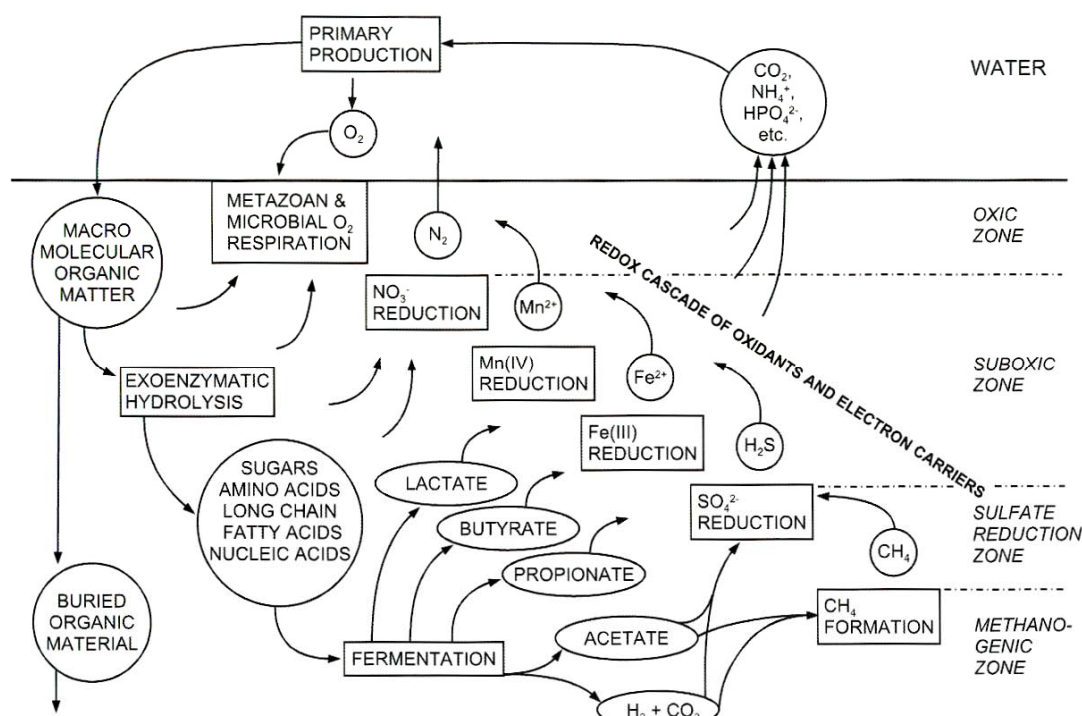


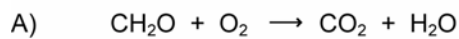
Fig. 1.2.: Conceptual model of organic matter decomposition pathways and the geochemical zonation in marine sediments. Figure reproduced from Jørgensen (2006).

In marine sediments organic matter is mineralized by aerobic and anaerobic processes. In general, aerobic respiration is followed by nitrate reduction, reduction of

Mn(IV) and Fe(III) oxyhydroxides, sulphate reduction and finally methanogenesis (Froelich et al., 1979; Fig 1.2.; Table 1.1.). The succession of the different electron acceptors is based on the energy yield of the reactions. The energy yield of aerobic respiration is highest compared to all other pathways. When a favourable electron acceptor is depleted, the next favourable will be used, with maybe some vertical overlap. The strict vertical zonation of mineralization pathways shown in Figure 1.2. is, however, only valid in diffusion dominated systems. Aerobic and anaerobic remineralization of organic matter leads to incorporation of organic matter into microbial and faunal biomass and to the release of inorganic nutrients and CO₂ (Fig. 1.2.).

Table 1.1.: Organic matter remineralization pathways modified from Jørgensen (2006).

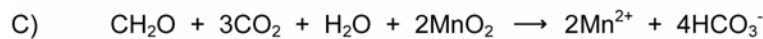
Oxic respiration



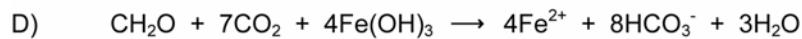
Nitrate reduction



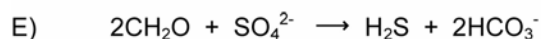
Manganese (IV) reduction



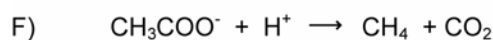
Iron (III) reduction



Sulphate reduction



Methanogenesis



The thermodynamically most efficient process to obtain energy is the oxic respiration of organic material, which takes place in the uppermost centimetres of the sediment where oxygen is present (Table 1.1., reaction A). Oxygen availability in the sediment depends on oxygen penetration depth, which in turn is influenced by the geochemical composition of the sediment and surface topography. Clay-rich sediments have higher porosities than sandy sediments, however their permeability is much lower. The permeability of sand therefore facilitates advective pore water transport and thus oxygen supply in contrast to muddy sediments, where processes are dominated by diffusion

(Ziebis et al., 1996). In general, oxygen penetrates only down to sediment depths of some mm or cm in coastal marine sediments (Brotas et al., 1990; Billerbeck et al., 2006b). Sediment depths where oxygen is present indicate aerobic zones.

In anaerobic zones of the sediment nitrate, Mn and Fe oxyhydroxides, and sulphate are used instead of oxygen as terminal electron acceptors. Based on the high availability of sulphate in marine ecosystems compared to other electron acceptors, sulphate reduction forms the dominant pathway of anaerobic carbon oxidation (Jørgensen, 1982). Several microorganisms that hydrolyse, ferment, and terminally oxidize organic compounds mediate organic matter remineralization in anoxic marine sediments (Alperin et al., 1994; Fig. 1.2.). Hence, the decomposition of organic matter is controlled by several consortia of microorganisms. Often metabolic end products of one step serve as substrate for another. After hydrolysis of complex organic compounds, fermentative organisms are able to degrade mono- and polymers into small organic molecules, which are preferred by terminal oxidizers. Sulphate reducing bacteria prefer short chain carbon molecules, e.g. acetate, lactate or propionate (Finke et al., 2007; Köpke et al., 2005; Sørensen et al., 1981).

The rate of organic matter degradation decreases within the sediment because of less efficient electron acceptors and more refractory organic matter with depth. Refractory organic matter is not a very suitable substrate for bacteria. In marine sediments organic matter was shown to be mainly refractory in greater depth, while easily degradable marine organic matter was only determined in the upper sediment layers (Rusch et al., 1998; Volkman et al., 2000). Bacterial communities thus are affected by the availability and quality of carbon sources (Wilms et al., 2006a). In intertidal flat sediments, sulphate reduction rates were found to be highest in the upper few centimetres of the sediment, but still remained high at 1 m depth and were even detectable in deep layers of some metres (Wilms et al., 2006a).

1.3. Transport processes in coastal marine sediments

Transport processes at the sediment-water interface and in the sediment body are essential for the exchange of solutes and particles and thus for the biogeochemistry in tidal flat sediments. Transport processes include molecular diffusion, where solutes are transported along concentration gradients, and pore water advection, which results in net transport of water. In intertidal sediments permeability, sediment depth, faunal activity, and tidal state determine whether diffusion or advection is the dominant transport process in the sediment.

1.3.1. Surface circulation processes

Fine-grained sediments may accumulate in areas where boundary flows are low. Due to the low hydraulic conductivity, diffusion is the dominant transport process in such beds. In surface sediments where permeability exceeds 10^{-12} m^2 , advective pore water flow dominates the sediment-water exchange, with transport rates that surpass those of molecular diffusion by two orders of magnitude or more (Huettel et al., 2003). During inundation small-scale flow regimes are altered if boundary flows interact with sediment topography (Huettel and Gust, 1992; Ziebis et al., 1996). Pressure gradients are generated by the interaction of bottom currents with sediment topography like ripples leading to advective pore water flow in the upper decimetres of permeable sandy sediments (Huettel et al., 1996; Huettel and Rusch, 2000; Precht and Huettel, 2004). Obstruction of the flow by protruding structures causes local increases of pressure that forces water and suspended particles into sediments, while the acceleration of flow above these protrusions results in a pressure decrease drawing pore water from the sediment (Fig. 1.3.). In coastal environments this transport process is affecting approximately the upper 15 cm of the sedimentary column (Huettel et al., 2003).

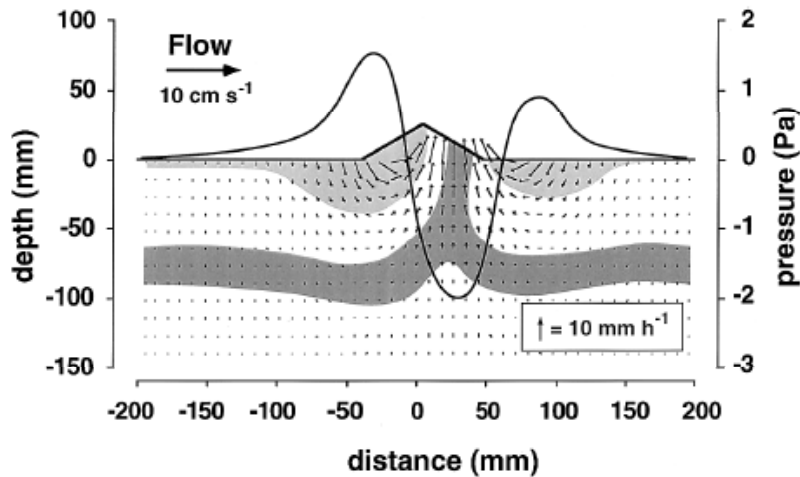


Fig. 1.3.: Pressure distribution at a small mound on the sediment surface exposed to unidirectional boundary layer flow. Areas where sea water is intruding into the sediment are marked in light grey, whereas dark grey indicate areas where pore water is drawn from the sediment. Graph reproduced from Huettel et al. (1998).

Sandy sediments with low organic carbon contents have rates of organic matter remineralization comparable to those of organic-rich muds (Andersen and Helder, 1987; Rusch et al. 2006). Rapid exchange processes at sediment surfaces have been identified as the most important mechanism responsible for enhanced remineralization rates in sandy sediments. The induced pore water flow at the sediment surface is an effective mechanism for rapid exchange of oxygen (Ziebis et al., 1996; Precht et al., 2004; Rusch et al., 2006), dissolved and particulate organic matter (Huettel et al., 1996; Huettel and Rusch, 2000; Rusch and Huettel, 2000), and nutrients (Caetano et al., 1997; Huettel et al., 1998) in permeable sediments. Huettel et al. (1998) showed that oxygenated sea water forced into the sediment when boundary flows are deflected by protruding structures is balanced by pore water ascending from deeper layers creating an anoxic channel where pore water rich in ammonium, Fe^{2+} , and Mn^{2+} can reach the surface (Fig. 1.4.). Through these anoxic channels nutrients, Fe^{2+} , and Mn^{2+} may be supplied to the open water column.

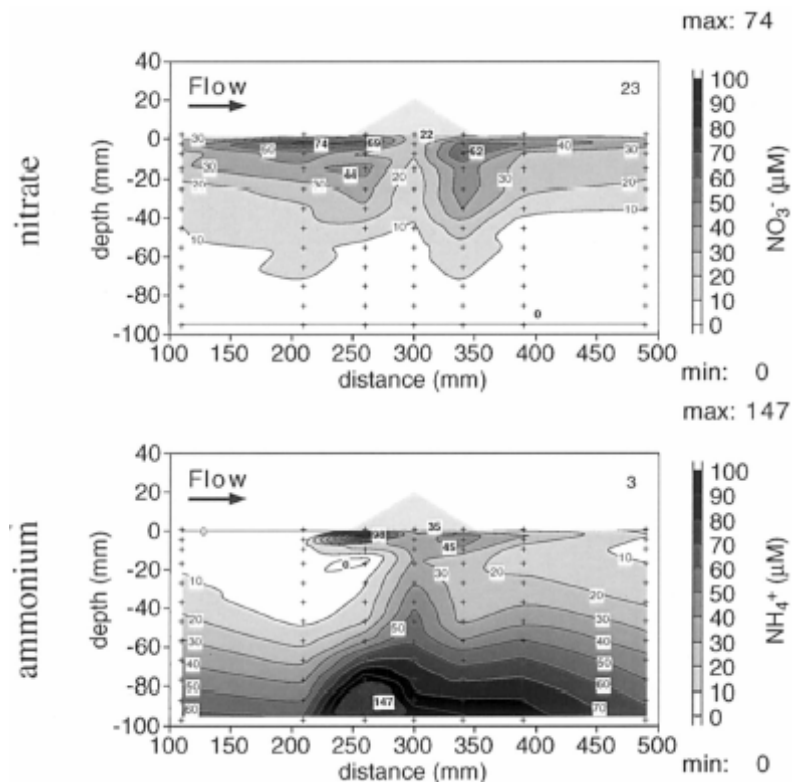


Fig. 1.4.: Up- and downstream of protruding sediment structures sea water is forced into the sediment leading to high nitrate concentration, while underneath the protrusion anoxic pore water is drawn to the surface reflected in high ammonium concentrations. Graph reproduced from Huettel et al. (1998).

Advective pore water exchange at the sediment surface thus leads to the fast recycling of organic matter converting these sediment beds into efficient biocatalytic filters. Therefore, a low content of reactive organic material cannot be interpreted as an indicator for low metabolic activity in these environments, but rather as consequence of rapid turnover and high exchange rates.

1.3.2. Deep circulation processes

Beside advective pore water flow at the sediment surface, intertidal flats are likely influenced by advection in sediment layers of several metres depths (Whiting and Childers, 1989; Howes and Goehring, 1994; Billerbeck et al., 2006b). Especially at tidal flat margins where the surface slopes towards tidal creeks, deep advective pore water

flow seem to be generated driven by the hydraulic gradient between sea water and pore water level at low tide. Wilson and Gardner (2006) constructed numerical models of a generalised tidal creek and marsh to calculate flow pattern and solute exchange between tidal creek and marsh. A scenario where the marsh platform was inundated at high tide showed that water flow occurred primarily in creek banks (Fig. 1.5.). At falling water level and at low tide deep pore water is draining from creek banks, most notably close to the low water line in tidal creeks. At rising water level sea water is intruding into creek banks to a small extent, whereas at high tide when the whole platform is water-saturated pore water flow velocities become negligible.

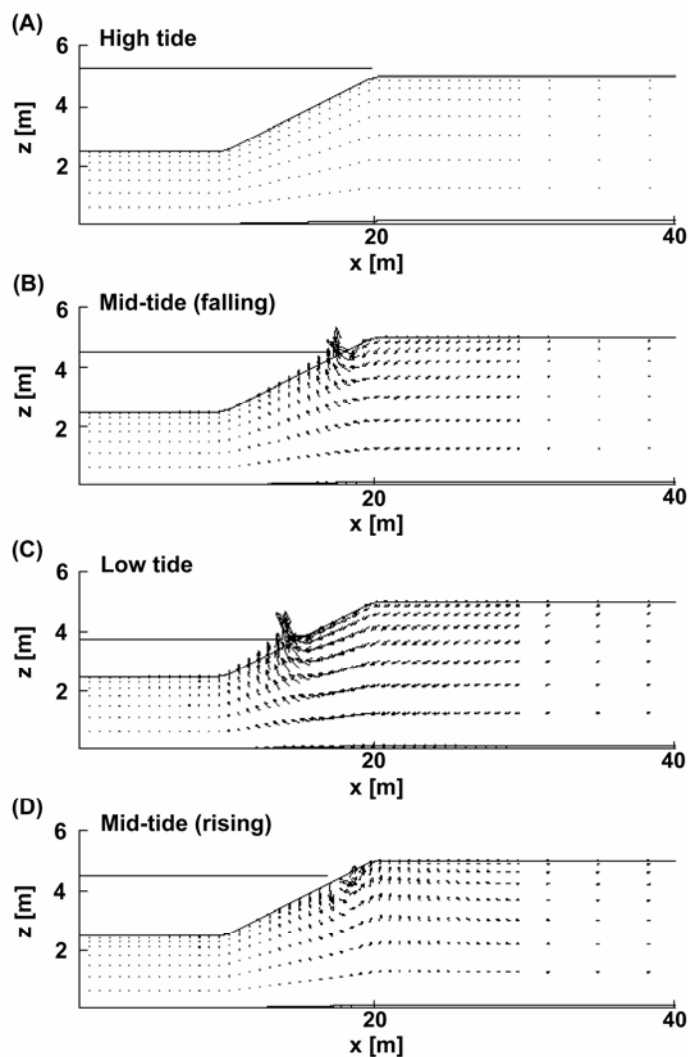


Fig. 1.5.: Pore water flow pathways simulated in a tidal flat, which platform is inundated at high tide.

Figure modified from Wilson and Gardner (2006).

Advective pore water flow generated at tidal flat margins is comparable to processes described as subtidal pumping or submarine groundwater discharge (Riedl et al., 1972; Burnett et al., 2003; Andersen et al., 2005). The coastal aquifer contains the interface where dense sea water with high ionic strength meets lighter fresh water with lower ionic strength. This contrast in physical and chemical properties controls processes at the fresh water/sea water interface beside changes in sea water level and variations in aquifer discharge. Submarine groundwater discharge is thus defined as any water flow on continental margins from the seabed to the coastal ocean (Burnett et al., 2003).

The extent of water exchange in tidally influenced areas depends on sediment permeability and capillarity as well as on tidal range. A larger tidal range should increase exchange by exposing a larger area of the creek bank to drainage (Wilson and Gardner, 2006). In contrast to rapid pore water exchange processes at the sediment surface, fluid flow in deeper parts of the sediment is much slower. For marsh sediments with a hydraulic conductivity of 10^{-4} m s^{-1} , model simulations lasting 60 days showed that groundwater ages are in the order of days close to the creek bank, whereas they increase to 50-60 days with distance to the tidal creek (Wilson and Gardner, 2006). The horizontal flow velocity of pore water in the upper 50 cm of an intertidal flat was determined by following the passage of a fluorescent dye tracer and resulted to vary between 0.3 and 1.0 cm h^{-1} (Billerbeck et al., 2006a). In the studied intertidal flat, flow velocities in sediment layers of some metres depth remain, however, unknown. Billerbeck et al. (2006a) further determined pore water discharge from the sloping margin of this tidal flat by seepage meters. Discharge rates ranged from 2.4 to $4.2 \text{ l m}^{-2} \text{ h}^{-1}$, which is in the same order of magnitude than the rate of $10\text{-}14 \text{ l m}^{-2} \text{ h}^{-1}$ obtained in model results by Wilson and Gardner (2006).

Concerning intertidal flat sediments, Billerbeck et al. (2006b) hypothesized that two circulation processes govern exchange processes (Fig. 1.6.). A rapid 'skin circulation' dominates exchange through the upper centimetres of the sediment. This circulation pattern is characterized by short flow paths, low pore water residence times, and

immediate feedback to the ecosystem. Sediment layers of some metres depth are presumably influenced by a slow 'body circulation' described by long flow paths and pore water residence times. This hypothesis is, however, based on pore water results obtained from the upper decimetres of the sediment and does not include deep pore water analysis.

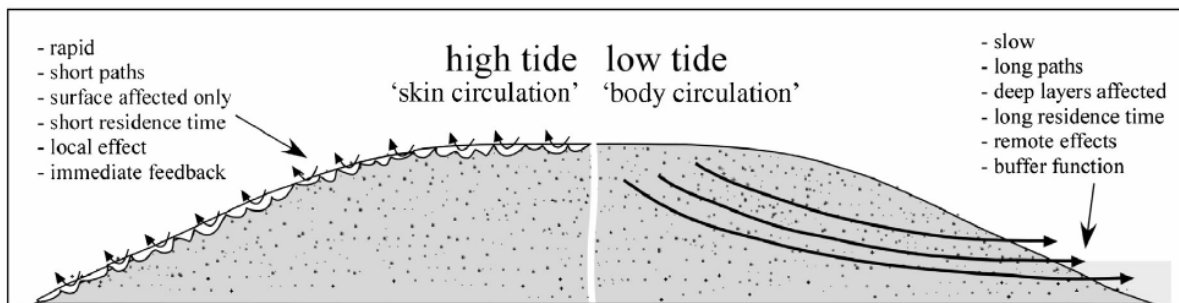


Fig. 1.6.: Surface and deep pore water circulation processes as proposed by Billerbeck et al. (2006b). Figure reproduced from Billerbeck et al. (2006b).

1.4. Objectives of the thesis

The thesis forms part of the Research Group 'BioGeoChemistry of Tidal Flats', which is conducted at the Institute for Chemistry and Biology of the Marine Environment (Oldenburg), University of Oldenburg, Terramare Research Institute (Wilhelmshaven), Senckenberg Institute (Wilhelmshaven), and Max Planck Institute for Marine Microbiology (Bremen). The Research Group aims to better understand biological, chemical, physical, and sedimentological processes in intertidal flat areas. All studies focus on the backbarrier area of Spiekeroog Island. Biogeochemical transformations on particles suspended in the water column, at the sediment water interface and in the sediments are studied. One of the main objectives of the Research Group is the establishment of material budgets based on the knowledge gained about biogeochemical processes and hydrodynamic conditions. The Research Group further tries to develop a comprehensive mathematical model of tidal flat systems which, beyond the initially selected study area, should be applicable to other tidal flat areas and similarly complex systems as well.

The main objective of this thesis was the biogeochemical characterization of pore waters in the backbarrier area of Spiekeroog Island to gain insights into biogeochemical processes in the sediment and to investigate the possible influence of seeping pore waters on the whole ecosystem of the study area. At margins of permeable intertidal flats advective pore water flow does supposedly occur. It was assumed that draining pore waters represent a source to the open water column for those elemental species enriched in pore water compared to sea water. Pore water flow was suggested to occur in some metres depth. Therefore the development of an *in situ* sampling system for the extraction of pore water from layers deeper than 1 m was necessary.

The first study (Chapter 2) describes the development of a new multilevel *in situ* pore water sampler which allows pore water sampling down to 5 m sediment depth. After insertion into the sediment, the sampler stays on site allowing repetitive sampling at identical locations and depth intervals. Depth profiles of redox-sensitive elements are not

affected by oxidation artefacts during extraction, an effect which not always can be eliminated using conventional sampling techniques like centrifugation. The sampler has been successfully used in sediments in the backbarrier tidal flats of Spiekeroog Island.

Chapter 3 presents results of sulphate, dissolved organic carbon, nutrients, and several terminal metabolic products in pore waters down to 5 m sediment depth. This study focuses on one sampling site, which is located at the eastern margin of the Janssand tidal flat close to the main tidal creek. We tried to identify the dominant terminal metabolic pathway. Pore water concentrations of sulphate, ammonium, and phosphate were used to elucidate the composition of organic matter degraded in the sediment. The C:N and C:P ratios estimated for the organic matter were verified by model results.

In Chapter 4 spatial, seasonal, and tidal variations of sulphate, dissolved organic carbon, nutrients and some further metabolic products observed in deep pore waters of intertidal flats are described. Spatial variations of pore water depth profiles were identified in a mixed flat and a sand flat site. Pore waters extracted close to the tidal flat margin were further compared with those of central parts of the same tidal flat. We hypothesized that sediments at the tidal flat margin are influenced by different hydrological and sedimentological processes compared to central parts. The hypothesis could be verified by the identification of seasonal and tidal patterns in pore water composition.

The study presented in Chapter 5 is focused on trace metal dynamics in coastal environments, which undergo seasonal changes in organic carbon supply, redox conditions, and sedimentation of particles. Redox-sensitive trace metals (Mn, Fe, Mo, U, V, Cr) were examined in deep pore waters of an intertidal sand flat. By spatial sampling, the cycling of trace metals in margin areas was compared with central parts of the tidal flat. The general trends with depth observed in intertidal flat sediments were further compared with those determined in deep marine sediments. The influence of seasonal changes in organic matter supply and in particles deposited on the sediment surface was verified by year-round sampling in about monthly intervals.

In Chapter 6 the non-conservative behaviour of molybdenum, which was observed during specific conditions in the open water column of the Wadden Sea, is described. A combined study of geochemical, biological, and sedimentological processes was used to verify mechanisms responsible for the non-conservative behaviour. The main focus of this study was put on molybdenum characteristics in the open water column. However, processes at the sediment surface and in pore water were shown to be essential, too, for a better understanding of the unusual behaviour of molybdenum in the open water column.

Little knowledge about biogeochemical processes in deep pore waters of intertidal flat sediments and about the influence of pore waters on ecosystems in tidal flat areas formed the motivation for the present work. The key questions of the project are summarized as follow:

- Can deep pore waters in tidal flat sediments be extracted without any alteration of redox-sensitive elements and at identical locations over long time periods by our newly developed *in situ* pore water sampler?
- What are the biogeochemical processes that may explain the cycling of sulphate, nutrients, dissolved organic carbon, and trace metals in intertidal flat sediments?
- Does seeping pore water enriched in specific compounds like nutrients or manganese represent a source which may largely account for tidal variations seen in the open water column of the study area?

1.5. Outline of the author's contribution

The thesis comprises five manuscripts, which are presented as chapters. The author's contribution to each of the manuscript is detailed below.

Chapter 2

In situ pore water sampling in deep intertidal flat sediments

A sampling technique was developed for the *in situ* extraction of pore waters down to 5 m depth in intertidal flat sediments. The concept of the sampler was developed by the author, the co-authors, Maik Grunwald, and Helmo Nicolai. The comparison of different sampling techniques in the field was done by the author as was the installation of the newly developed *in situ* pore water sampling technique. All data presented in the manuscript were analyzed by the author herself. The concept of the manuscript and interpretation of the results was developed by the author who also did the writing and editorial handling of the publication, supported by suggestions from Olaf Dellwig, Bernhard Schnetger, and Hans-Jürgen Brumsack. The manuscript was published 2007 in *Limnology and Oceanography: Methods* **5**, 136-144.

Chapter 3

Sulphate, dissolved organic carbon, nutrients and terminal metabolic products in deep pore waters of an intertidal flat

This study addresses biogeochemical processes in deep pore waters of a permeable intertidal sand flat. Results of deep pore water studies are shown and organic matter degradation pathways were identified at one sampling site. The concept of the study was developed by the author who also conducted all sampling campaigns. All samples were analyzed by the author except for nutrient and total alkalinity analyzes as well as sediment analyzes, which were carried out by our lab assistants Carola Lehnert, Eleonore

Gründken, and Martina Wagner. Methane in pore water was analyzed by Maik Grunwald who further provided sea water phosphate and silicate data determined at a monitoring station in the backbarrier area of Spiekeroog Island. Interpretation of the results and writing was done by the author herself, supported by comments from Olaf Dellwig, Bernhard Schnetger, and Hans-Jürgen Brumsack. The modelling part was contributed by Jan Holstein. The manuscript has been submitted to *Biogeochemistry*.

Chapter 4

Spatial, seasonal, and tidal variations of sulphate, dissolved organic carbon, and nutrients in deep pore waters of intertidal flat sediments

This manuscript extends results obtained in sampling campaigns conducted at five different locations in intertidal flats of Spiekeroog Island. In a sand flat area pore water was sampled throughout one year. Close to the tidal flat margin a sampling campaign was further carried out at four different times within one tidal cycle. The sampling strategy of the study was developed by the author who also carried out all sampling campaigns. Carola Lehnert, Eleonore Gründken, and Martina Wagner assisted in analysing nutrients and total alkalinity and performed the sediment analyzes. All data were evaluated and interpreted by the author. Olaf Dellwig, Bernhard Schnetger, and Hans-Jürgen Brumsack supported the author while interpreting the data and writing the publication. The manuscript has been submitted to *Limnology and Oceanography*.

Chapter 5

Cycling of trace metals (Mn, Fe, Mo, U, V, Cr) in deep pore waters of intertidal flat sediments

This study focuses on trace metals cycling in pore waters of an intertidal sand flat. All sampling campaigns, which were carried throughout one year and within one tidal cycle were organized by the author. All trace metal analyzes were further conducted by the author herself. Trace metal data of the open water column of the study area were

provided by Olaf Dellwig. Concept of the publication and discussion of the results was developed by the author, supported by all co-authors. The manuscript has been submitted to *Geochimica et Cosmochimica Acta*.

Chapter 6

Non-conservative behaviour of molybdenum in coastal waters: Coupling geochemical, biological, and sedimentological processes

This study addresses the behaviour of molybdenum in coastal waters of the tidal flat areas in NW Germany and the North Sea. The concept of the study was developed by Olaf Dellwig who also planned all sampling campaigns carried out in the open water column of the backbarrier areas and the North Sea. Pore water data presented in the publication originate from Melanie Beck who also contributed to the interpretation of these data. The manuscript was written by Olaf Dellwig with the help of all co-authors. The manuscript was published 2007 in *Geochimica et Cosmochimica Acta* **71**, 2745-2761.

2. In situ pore water sampling in deep intertidal flat sediments

Melanie Beck, Olaf Dellwig, Kerstin Kolditz, Holger Freund, Gerd Liebezeit, Bernhard Schnetger, Hans-Jürgen Brumsack

This chapter is published in *Limnology and Oceanography: Methods* **5**, 136-144.

Abstract

In this study a multilevel *in situ* pore water sampler is presented which allows pore water sampling down to 5 m sediment depth. The sampler forms a crucial tool to study biogeochemical processes on different time scales in advective pore water systems. After insertion into the sediment, the sampler stays on site allowing repetitive sampling at identical locations and depth intervals. The sampler has been successfully tested for one year in sandy sediments in the backbarrier tidal flats of Spiekeroog Island at the German North Sea coast. Depth profiles of redox sensitive elements show a high depth resolution and are not affected by oxidation artefacts during extraction. Seasonal variations owing to advection and changing microbial activity are apparent for some element species even at sediment depths of 5m.

2.1. Introduction

Pore water studies are essential to understand early diagenetic exchange processes between the sediment and water column in aquatic ecosystems. In permeable systems, like tidal flats or salt-marshes, they are crucial for a better understanding of biogeochemical cycles and fluid flow. Chemical transformations in pore waters, often mediated by microbial activity and redox conditions, regulate exchange processes between the solid and dissolved phase within the sediment. For example, particulate Mn (IV) is transformed into dissolved Mn (II) under anaerobic conditions (e.g. Sundby and Silverberg, 1981; Burdige, 1993; Thamdrup et al., 1994), while dissolved Mo (VI) in sulphide containing solutions is converted to a series of Mo(VI) thioanions ($\text{MoO}_x\text{S}_{4-x}^{2-}$, $x = 0-3$) (Erickson and Helz, 2000; Vorlicek et al., 2004). In solutions containing both sulphide and S(0)-donors (i.e. polysulphides), Mo is transformed into Mo(IV) or Mo(V)₂ polysulphide/sulphide anions, which are easily scavenged by Fe compounds and organic matter (e.g. Helz et al., 1996; Erickson and Helz, 2000; Zheng et al., 2000; Vorlicek et al., 2004).

Numerous techniques have been developed to sample sediment pore water. These can be divided into *ex situ* and *in situ* methods. *Ex situ* methods, which are widely used at present, comprise squeezing or centrifugation of slices of sediment cores. During squeezing, pressure applied to the core forces pore water through a sampling port. In core section squeezers, sediment samples are compressed to retrieve the pore water (Reeburgh, 1967; Sasseville et al., 1974; Robbins et al., 1976). In whole core squeezers, an intact sediment subcore is pressurised and pore water is expelled through a single sampling port at the top or through several sampling ports located at specific depths along the core liner (Bender et al., 1987; Jahnke, 1988). For the extraction of pore water from sediments by centrifugation, special centrifuge tubes are used combining the separation of particles from pore water and the filtration of the resulting fluid (Saager et al., 1990).

A number of artefacts are inherent to *ex situ* methods because the sediment has to be removed from the natural environment for pore water retrieval. Differences in temperature and pressure between the natural environment and the location where the cores are processed potentially affect samples (Bischoff et al., 1970), and oxygen contamination of anaerobic sections can occur even if samples are handled under an inert atmosphere.

In contrast, *in situ* methods like dialysis, rhizon extraction or suction filtration possess less potential for artefacts. In dialysis samplers, a volume of originally deionised water is allowed to equilibrate with sediment pore water (Hesslein, 1976). Dialysis sampling permits a high spatial and temporal resolution. For example, osmosamplers were developed to autonomously collect continuous water samples in remote locations for up to several years (Jannasch et al., 2004). Recently, a rhizon system was developed by Seeberg-Elverfeldt et al. (2005), consisting of a hydrophilic porous polymer tube which is inserted horizontally into the sediment. Pore water flows from the sediment into the space between this porous tube and a central supporting wire, from where it can be sampled via an elastic tube.

Suction filtration forms a third *in situ* method employed for the extraction of pore water. Several apparatus have been developed, with the simplest single level sampler consisting of a modified glass pipette (Makemson, 1972). Howes et al. (1985), Berg and McGlathery (2001), and Nayar et al. (2006) developed modified, more robust versions of single level samplers. Multilevel suction filtration samplers were proposed by Sayles et al. (1973), Montgomery et al. (1981), Watson and Frickers (1990), Hursthouse et al. (1993), and Bertolin et al. (1995). In general, these latter suction samplers consist of a tube equipped with sampling ports at different depths. They are installed in the sediment, mostly by manually driving them into the sediment, and pore water is obtained by the use of suction. For the extraction of pore water, Charette and Allen (2006) presented the application of a suction filtration system which was originally designed for soil gas

sampling by AMS (AMSTM Gas Vapor Probe System, USA). This system can be used to sample multiple depths down to 10 m and is recovered after sampling.

The AMS sampling system represents the only *in situ* method described in the open literature, which allows sampling of pore water in sediment depths exceeding 1 m. Most *in situ* samplers were constructed for the extraction of pore water from the upper decimetres of the sediment at high spatial resolution. Furthermore, most sampling devices were not designed for long term pore water sampling at one location or, in case of osmosamplers, long term sampling would only be possible at a few distinct depth intervals. In order to investigate processes occurring in advective deep pore water systems at depths down to 5 m throughout the year, a new suction sampler was constructed. In this contribution we describe the new *in situ*, multilevel pore water sampler, which is used for sampling pore waters in porous tidal flat sediments at different time scales. The construction of the sampler, its insertion into the sediment as well as the sampling procedure are shown, and examples of pore water profiles obtained are presented.

2.2. Material and Procedures

2.2.1. *In situ* pore water sampler

Sampler construction – A scheme of the new *in situ* pore water sampler designed for retrieval of pore water from depths down to 5 m is shown in Fig. 2.1. Each sampler is composed of a polyethylene (PE) pipe with an outer diameter of 64 mm. Holes were drilled into the sampler walls allowing the insertion of a connector assembly into the pipe which connects the sampling port to teflon tubes with an inner diameter of 4 mm located inside the plastic pipe. The connector is screwed into disc shaped PE plates with an outer diameter of 26 mm which are glued to the outer sampler wall. The sampling ports are covered by two plies of nylon gauze of 100 and 50 μm pore size which serve as pre-filters. The gauzes are attached to the pipe by a second disc shaped PE plate with an outer diameter of 45 mm and a central opening of 9 mm. These plates are fixed to the pipe by

stainless steel screws. These screws are replaced by nylon screws in our latest design. But according to our own experience stainless steel screws had no contamination effect on trace metal analysis. The plates around the sampling ports were installed to prevent vertical flow along the sampler walls while extracting pore water from the sediment. The distribution of the sampling orifices forms a spiral along the pipe to minimize the effect of local sampling on adjacent ports via lateral and vertical flow. The teflon tubes located inside the sampler pipe link the sampling orifice to sampling devices located at the sediment surface. At the top, the sampler is sealed with a removable cap to prevent seawater from entering the teflon tubes.

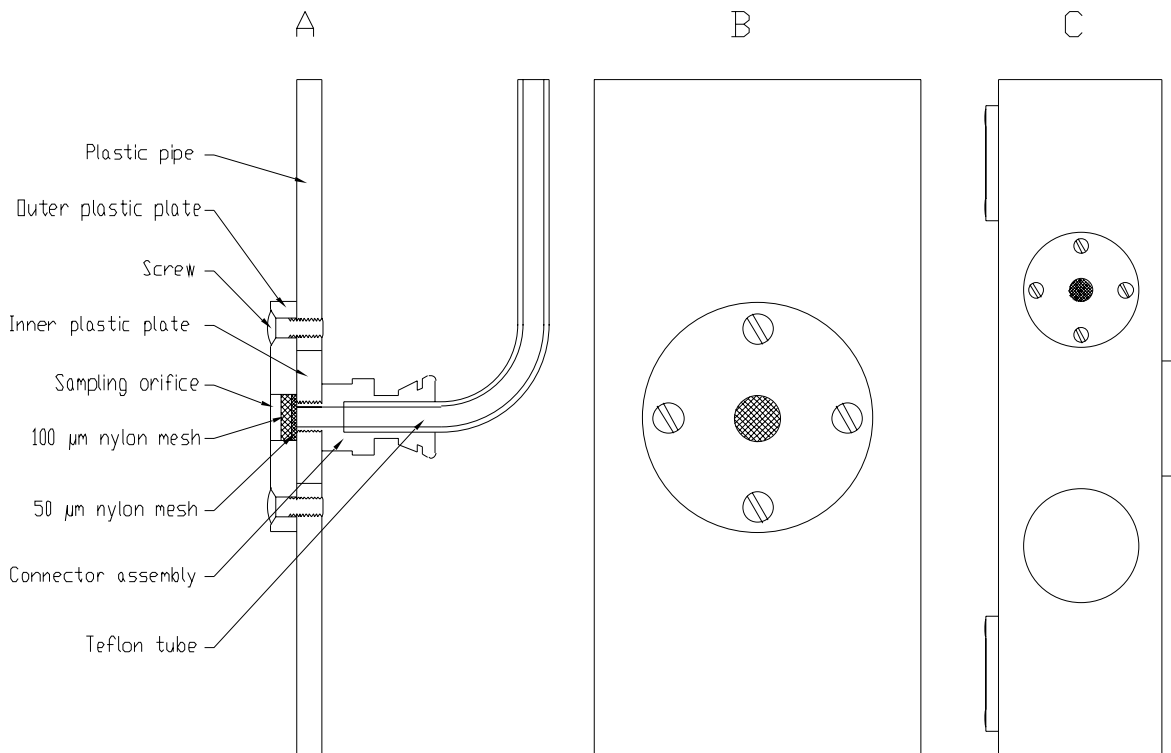


Fig. 2.1.: *In situ* pore water sampler: (A) Vertical cross section of a single sampling port, (B) Close-up of one sampling port from the outside, (C) Part of the sampler showing five sampling ports with a distance of 5 cm between adjacent ports and a rotation angle of 90° around the sampler pipe.

Due to the limited space available within the plastic pipe for teflon tubes, each *in situ* pore water sampling system consists of two samplers. The short sampler (1 m length) has 11 sampling ports at 0.05 m, 0.07 m, 0.10 m, 0.15 m, 0.20 m, 0.25 m, 0.30 m, 0.40 m,

0.50 m, 0.75 m and 1.0 m sediment depth. The long sampler (5 m length) has 10 sampling ports located at 1.0 m, 1.25 m, 1.5 m, 2.0 m, 2.5 m, 3.0 m, 3.5 m, 4.0 m, 4.5 m, and 5.0 m sediment depth.

Insertion of the samplers – For the insertion of the pore water sampler into the sediment, an aluminium tube with an inner diameter of 76 mm was driven into the sediment by a vibro corer to a depth equivalent to the length of the sampler. The sediment inside the aluminium tube was removed by a sediment corer and the pore water sampler was inserted into the empty aluminium tube. Then the aluminium tube was drawn out of the sediment by a tripod while the pore water sampler remained in the sediment. To ensure that the sampler stayed positioned and was not slackened by tidal currents, the inside of the sampler pipe was filled with sand.

Pore water sampling – In sandy water-saturated sediments the pore water sampler enables the extraction of pore fluids via 50 ml PE-syringes. The vacuum generated by a syringe is sufficient to retrieve pore water even from depths of 5 m. However, a transportable vacuum pump (VK2, UMS GmbH, München, Germany) was used where pore water was extracted from sediments with higher contents of clay and silt and from less water-saturated sediments in salt-marshes. The maximum negative pressure applied to the sampling system by the vacuum pump was 700 hPa. Depending on the sampling depth and on the diameter of the teflon tubes used, different volumes of pore water were discarded before taking the sample for analyzes. For depths of up to 1 m, at least 20 ml of pore water were discarded, this volume increased to at least 40 ml for depths of up to 3 m, and to 60 ml for depths exceeding 3 m. The volume necessary to discard resulted from the volume of tubing from the port to the sampling device. The volume of the tubing was 4 ml, 25 ml, and 65 ml for sampling depths of 0.3 m, 2 m and 5 m, respectively. At all sampling ports, pore water samples of 100 ml were extracted for later analysis.

2.2.2. Sampling area

The sampling area is located in the German Wadden Sea, a large tidal flat area located between the Frisian coastline and its barrier islands in Northwest Germany. This study was conducted in the East-Frisian Wadden Sea which is characterized by mesotidal conditions (tidal range 2-4 m). Pore water samples were taken on a sand flat (Janssand) and on a mixed flat (Neuharlingersieler Nacken) of the backbarrier area of the Island of Spiekeroog (Fig. 2.2.).

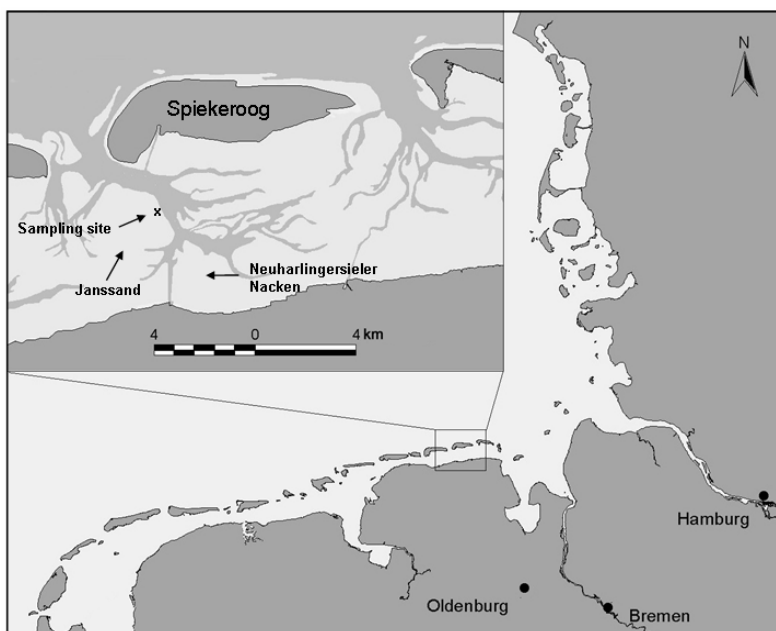


Fig. 2.2.: Sampling area located in the tidal backbarrier area of the Island of Spiekeroog, one of the barrier islands of the NW German Wadden Sea. The cross marks the sampling location (Janssand: 53° 44.183' N, 007° 41.904' E).

The tidal flat is covered by 1 - 2 m of water during high tide, and become exposed for approximately 4 - 6 h during low tide. In the sand flat area sandy sediments predominate, however at depths exceeding 3 m the sands are intermingled with silt-clay layers. The sand flat surface is almost horizontal, except for the margin where the sediment surface slopes towards the main tidal creek. At low tide the distance between the sampling location and the water line is approximately 70 m and the difference in altitude 1.5 m. As

an example, results are presented (see below) from the sampling location on the sand flat which is situated near the main tidal creek (53° 44,183' N; 007° 41,904' E).

2.2.3. Sample analysis

The samples were analyzed for trace elements (Mn, Mo, U, V), SO_4^{2-} , and dissolved organic carbon (DOC). In this study, some results for selected redox sensitive species (SO_4^{2-} , Mn, Mo, U, and V) are presented, and refer to the full set of data which will be published elsewhere.

For the analysis of dissolved metals, the samples were filtered through 0.45 μm SFCA (surfactant-free cellulose acetate) syringe filters. Subboiled HNO_3 was added to obtain a concentration of 1% (v/v) in all samples. Mn, Mo, U and V were analyzed by ICP-MS (Thermo Finnigan MAT Element) in 25-fold dilution. The applied analytical procedure is similar to the method published by Rodushkin and Ruth (1997). Precision and accuracy were checked by the reference seawater standard Cass 4 (Seawater reference material for trace metals, National Research Council, Canada). A solution containing Mn was added to the reference standard to control accuracy and precision of the analyzes as Mn concentrations are much higher in the Wadden Sea pore water than in the original reference material. Precision / accuracy were 4.0% / 2.2% for Mn, 5.8% / 0.8% for Mo, 4.4% / -5.0% for U, and 7.3% / 4.4% for V. Samples for sulphate analysis were filtered through 1.2 μm GF/C filters. Sulphate was analyzed by ion chromatography (Dionex DX 300) in a 250-fold dilution, with standard Atlantic Seawater (Salinity 35.0 (\pm 0.2%); OSIL, UK) used to control the precision (3.0%) and accuracy (-5.3%) of the measurements. Samples for DOC analysis were filtered through 1.2 μm GF/C filters, and 1 ml HCl (6 M) was added to 40 ml sample. DOC was analyzed by high temperature catalytic oxidation using a multi N/C 3000 analyzer (Analytik Jena).

2.3. Assessment

2.3.1. Comparison of sampling techniques

Before our newly developed samplers were installed, the *in situ* AMSTM gas vapour probe kit was used to sample pore water at a nearby location. Due to technical problems, sampling was only possible down to 2 m depth, nevertheless the general trends with depth obtained for SO₄²⁻, Mn, Mo, and U were similar to those using the new *in situ* sampler (Fig. 2.3.). Regarding Mo and U, the decrease in concentration is shifted slightly towards greater depths when the AMS system was used for sampling. This is probably not due to the different sampling techniques, but to the distance between to two sampling locations and the different sampling dates. The results for Mo and U furthermore partly differ in the upper 0.5 m of the sediment as the resolution with depth is better using our sampling technique.

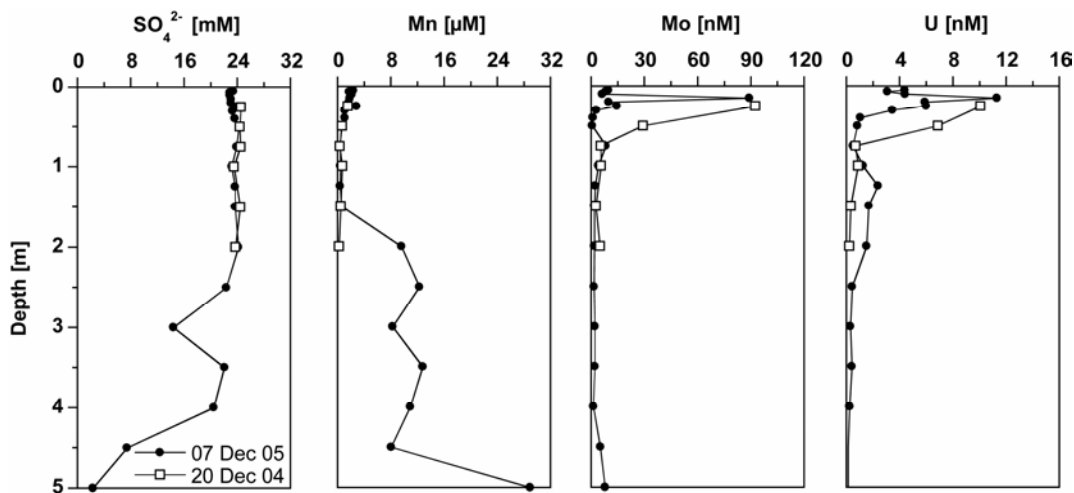


Fig. 2.3.: Comparison of two *in situ* sampling techniques, our new developed sampler (filled dots) and the AMSTM gas vapour probe kit (open squares). Samples taken with the AMS sampler were extracted at a location close to our permanently installed samplers.

Both sampling techniques seem to be suitable to obtain *in situ* pore water samples without altering concentrations of redox sensitive elements by oxidation effects. Preferential flow along the samplers which could falsify the depth profiles would even be

more likely to occur using the AMS system as it has to be redeployed in the sediment for each sampling. However, preferential vertical flow does not seem to occur as it would have an impact on Mo and U concentrations, which decrease from sea water concentrations in the near-surface layers to much lower concentrations at depths where reducing conditions prevail. Compared to the AMS system, the new sampler stays on site after its insertion into the sediment. This offers the possibility of the sediment/pore water system to equilibrate before conducting repetitive samplings at identical locations. We regard this as an important advantage of the new sampling system.

2.3.2. Oxidation effects during sampling

First samples were taken two weeks (April 2005) and seven weeks (May 2005) after the insertion of the samplers into the sediment. At several sampling depths exceeding 0.5 m, Mo and U concentrations were higher in April compared to May (Fig. 2.4.). These changes can be ascribed to oxidation effects still seen in redox sensitive elements like Mo and U even after two weeks of equilibration. The depths profiles obtained from May 2005 onwards remained essentially stable at lower concentration levels in depths exceeding 0.5 m, which supports our hypothesis that oxygen introduced into the sediment during the insertion of the sampler has caused the initially high Mo and U concentrations. We therefore regard both elements as sensitive proxies for oxygen contamination. The oxidation effect seemed less pronounced for Mn and V as the depth profiles of these elements were similar in April and May 2005. V is known to form complexes with DOC (Brumsack and Gieskes, 1983; Wehrli and Stumm, 1989), which are supposed to be less sensitive to oxidation. Regarding Mn, the reaction with O₂ is slow resulting in a half life for Mn(II) disappearance of 340 days at pH ~ 8 in seawater with P_{O₂} ~ 0.21 atm (Morgan, 2005). The results from these first sampling sequences suggest the need of a prolonged equilibration time, which was achieved at least seven weeks after insertion. The accurate equilibration time unfortunately could not be determined as the oxidation artefacts in April

2005 were not evident before a comparison of data was possible with those obtained during later sampling campaigns.

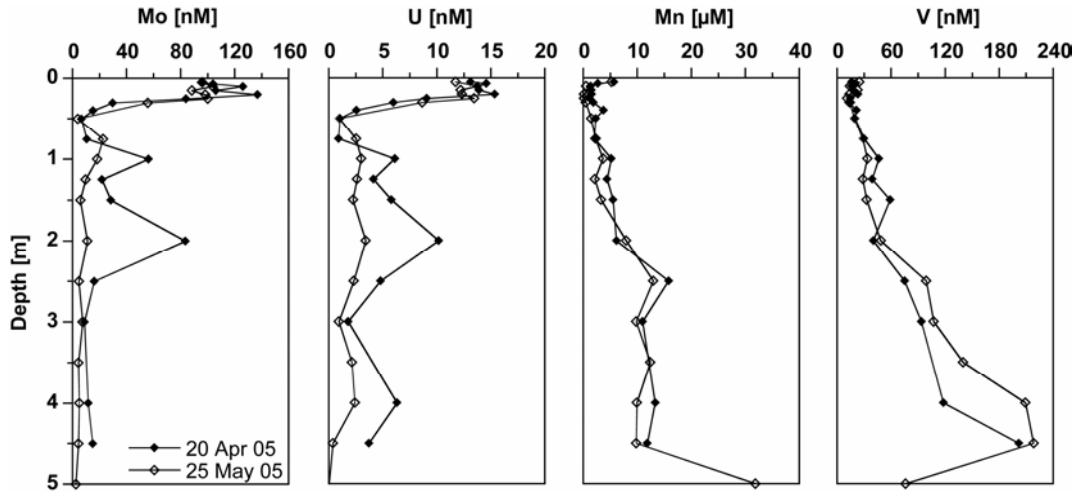


Fig. 2.4.: Pore water depth profiles of Mn, V, Mo, and U. Samples were taken with the *in situ* sampler in a sandy tidal flat sediment, NW Germany, in April and May 2005. The samples in April were extracted after two weeks equilibration time, whereas the samples in May were taken seven weeks after the insertion of the samplers into the sediment.

In November 2004 pore water samples were obtained *in situ* by using the AMSTM gas vapour probe kit and *ex situ* by centrifugation of sediment core material during a sampling carried out on a mixed tidal flat (Neuharlingersieler Nacken). As the sediment core sampling was not performed under N₂ atmosphere, pore water results show the potential oxidation effect on concentrations of redox sensitive elements. Severe artefacts are seen when comparing the results of the two sampling techniques (Tab. 2.1.).

For example, the sample at 1 m sediment depth showed a Mo concentration of 18 nM using the *in situ* AMS technique compared to a concentration of 865 nM in the centrifuged sample. Concentrations of Mo exceeding the sea water level (approximately 105 nM) by more than 8-fold represent oxidation artefacts as the study site is known to be anaerobic below a few centimetres depth. U concentrations in centrifuged pore waters are as well significantly higher than in the *in situ* samples. An opposing effect is seen for Mn as the

oxidation of Mn during the sampling of the core led to lower concentrations in centrifuged pore water samples compared to samples taken *in situ*.

Tab. 2.1.: Comparison of the *in situ* AMS sampling technique and the *ex situ* centrifugation of sediment core slices. The results of the sediment core sampling show the effect of oxygen on concentrations of redox sensitive elements. The sediment core was not treated under a nitrogen atmosphere.

Depth [m]	Mn [μ M]		Mo [nM]		U [nM]	
	<i>in situ</i>	<i>ex situ</i>	<i>in situ</i>	<i>ex situ</i>	<i>in situ</i>	<i>ex situ</i>
0.5	2.2	2.2	19.1	330.8	1.1	16.5
1.0	3.4	1.6	18.0	865.5	3.6	40.3
1.8	8.8	0.1	6.2	528.0	0.3	38.1

2.3.3. Sample volume

The sediment volume from which pore water is extracted by the *in situ* sampler at each sampling port can be calculated via the assumption that this volume is of approximately half-spherical shape around the sampling port. The radius (in cm) of the hemisphere can be described via equation (1)

$$r = \sqrt[3]{\frac{3 \cdot V_{\text{sample}}}{2 \cdot \phi \cdot \pi}} \quad (1)$$

with V_{sample} being the volume of pore water sampled (ml), and ϕ the porosity of the sediment. In this study, about 120 to 160 ml of pore water were extracted at each sampling port depending on the depth of the sampling port and the volume within the tubing necessary to be discarded. The porosity of sandy sediments in the sampling area is approximately 0.45 (B.W. Flemming, pers. comm.). Based on these parameters, a radius of 5.0 cm or 5.5 cm is derived for the resulting hemisphere extracting 120 or 160 ml pore water, respectively. This radius is larger than the smallest distance between the sampling ports in the uppermost part of the sediment. As the rotation angle from one sampling port

to the other is 90° , the distance of adjacent sampling ports is 7.3 cm or 11.5 cm for a difference in depth of 5 m or 10 cm, respectively. Consequently, for a difference in depth of 5 cm the hemispheres of adjacent sampling ports may partly overlap, whereas no overlap of the hemisphere will occur for differences in depth exceeding 10 cm. The sampled hemispheres therefore may have partly interfered for ports located at less than 0.3 m depth. To avoid mixing of pore water in the upper sections of the sediment, smaller volumes of pore water should be sampled at these depths. For a difference in depth of 5 cm between adjacent sampling ports, the maximal pore water volume sampled should be 45 ml. Since the volume of the tubing is less than 10 ml at depths less than 0.3 m, at least 35 ml of sample can be taken for analysis. The volume of pore water, which can be extracted without any overlap of the hemisphere, increases to 180 ml if the difference in distance of adjacent ports is 10 cm. At greater depths, an overlap of the hemispheres around adjacent sampling ports can generally be excluded because the distance between the ports by far exceeds the calculated radius of the hemisphere.

We are assuming that the volume of extracted pore water forms a hemisphere. The extracted volume could also be of ellipsoidal shape, especially at higher flow velocities or during extraction of pore water from sediment layers with changing permeabilities, like alternating sand/mud layers. If the ellipsoid extends perpendicular to the sampler, then the length and width of the ellipsoid would be even smaller than the radius calculated for a hemisphere. In this case the overlap of pore water volumes extracted from adjacent sampling ports would be reduced. Nevertheless, the adaptation of the volume sampled to the distance between the sampling ports remains an important aspect. As the main application of our sampling device is the sampling of pore waters from greater depths, a vertical resolution of less than 5 cm was not considered to be essential. Well adapted sampling devices do exist for high resolution applications in surface sediment. A suitable vertical spacing of the sampling ports of 10 cm is recommended if large pore water volumes of about 100 ml are required. By reducing the extracted pore water volume to 35 ml a vertical spacing of 5 cm is possible. Changing the construction of the sampler by

mounting the sampling ports at an angle of 120° around the sampler tube would allow interference-free sampling of 110 ml at 5 cm depth intervals. Preferential flow along the sampler seem unlikely to occur as the concentrations of several redox-sensitive metal species sharply decrease from sea water-like values in the upper part of the sediment to significantly lower concentrations in deeper layers. For example, Mo concentrations close to the sea water level of 105 nM would have been determined at depths exceeding 0.3 m if sea water percolated along the sampler walls into the sediment.

2.3.4. Pore water profiles

The *in situ* sampler was successfully used to sample pore waters in tidal flat sediments in the coastal area of NW Germany. Examples shown here represent samples from a sandy tidal flat. They highlight both, the importance to obtain *in situ* pore water samples of depths exceeding 1 m as huge changes in element concentrations can be observed below this depth, but also the necessity for a high density of sampling ports in the upper 100 cm of the sediment body, as many processes occur especially in this section (Huettel et al., 1998; Huettel and Rusch, 2000; Rusch and Huettel, 2000).

At the study site, aerobic conditions prevailed only in the upper few cm of the sediment (Billerbeck et al., 2006b). Thus, shortly below the sediment surface, other electron acceptors like SO_4^{2-} are used for microbial organic matter degradation. Consequently, SO_4^{2-} retained sea water concentrations (26 mM at 31 psu) only in the upper 0.5 m of the profile and decreased below this depth (Fig. 2.5.). Due to the reducing conditions in the sediment, high concentrations of dissolved Mn (II) are apparent in the pore waters (Fig. 2.5.). Mo concentrations showed only slight deviations from sea water concentration (110 nM) in the upper part of the sediment (Fig. 2.5.). However, concentrations sharply decreased at depths exceeding 0.3 m, suggesting that soluble MoO_4^{2-} was converted into Mo species which were subsequently scavenged by organic matter or Fe compounds (Helz et al., 1996).

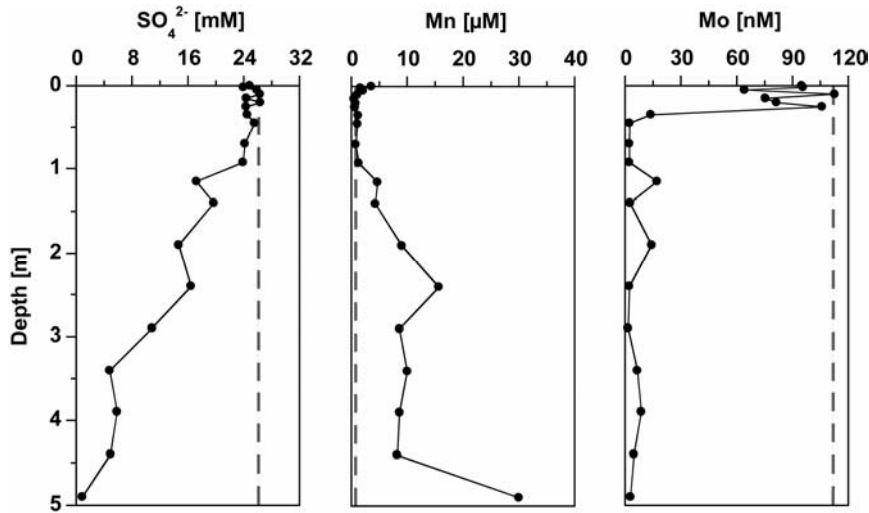


Fig. 2.5.: Pore water depth profiles of SO_4^{2-} , Mn and Mo. Samples taken with the *in situ* sampler in a sandy tidal flat sediment, NW Germany, on July 19th 2005. Dashed lines mark concentrations in the open water column of the tidal flat: SO_4^{2-} calculated for 31 psu, Mn from Dellwig et al. (2007), and Mo from Dellwig, O. (unpublished data).

2.3.5. Seasonal variation

Depth profiles resulting from repetitive sampling at the same location for different seasons are shown for DOC and SO_4^{2-} (Fig. 2.6.). The depth profile for May 2005 represents a characteristic profile for spring and early autumn, whereas the profile for August 2005 is shown as a typical example for the summer months June, July, and August. The depth profile for March 2006 forms a representative profile for samplings from November to April. During the summer months concentrations of SO_4^{2-} decreased more strongly with depth compared to the other seasons, whereas the concentrations of DOC increased in the same time period at depths of about 1 m to 3 m. During autumn and winter the contrary was seen in the deeper part of the sediment, i.e. increased concentrations of SO_4^{2-} and decreased concentrations of DOC. These changes in concentration seem to be caused by advection (Billerbeck et al., 2006a,b; Wilson and Gardener, 2006) and by changing microbial activity due to variations in temperature (Vosjan, 1974).

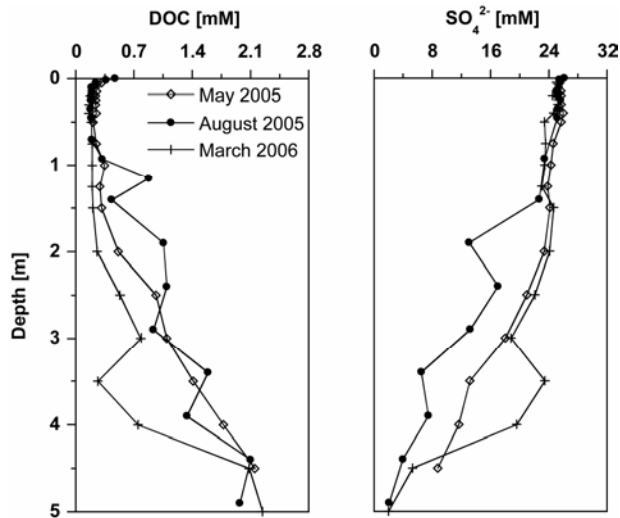


Fig. 2.6.: Seasonal variation of the pore water depth profiles of DOC and SO_4^{2-} . Samples were taken with the *in situ* sampler in a sandy tidal flat sediment, NW Germany.

2.4. Discussion

Bufflap and Allen (1995) discuss possible reasons why pore water sampling methods may alter trace metal concentrations in pore waters. As potential sources of error they list oxidation of anoxic pore waters and sediments, disturbance of sediment cores leading to disruptions of sediment layers, metal contamination and temperature artefacts. In this study, pore water samples were extracted *in situ* and consequently temperature artefacts can be ruled out. With regard to the analysis of trace metals, the sampler was constructed avoiding metal components, and therefore the possibility of metal contamination by components of the sampler is rather unlikely. Oxidation artefacts are the source of error which are most difficult to prevent. However, the installation of the new sampling system definitely prevents any contact of the sample with oxygen.

Another potential source of error is the formation of preferential water paths along the sampler walls, hence smoothing the trends in the depth profiles. The depth profile of Mo with its sharp decrease in concentrations at about 0.3 m depth (Fig. 2.5.), but also strong variations in the concentrations of other elements observed between adjacent sampling ports suggest that this phenomenon can be neglected. If samples are not filtered immediately after extraction, particles present in the pore water can form another source

of error, as trace metals can be adsorbed to or released by such particles. Using the proposed sampler, all samples are pre-filtered during extraction. Furthermore, the samples were filtered immediately after extraction via syringe filters. In principle, it would be possible to use 0.45 µm filters at the sampling ports of the sampler to avoid an additional filtration step. However, this bears the risk of clogging sampling ports by particles.

The *in situ* pore water sampler described in this study offers several new possibilities to gain meaningful insights into the biogeochemical processes occurring in permeable sediments. Compared to *in situ* samplers currently in use, the new sampler allows the extraction of pore waters from several metres depths. For the determination of chemical transformation processes occurring in pore waters of intertidal sediments influenced by advection, sampling of pore waters down to depths of at least several metres is essential. Depth profiles of major and trace elements demonstrate that chemical transformations do not only occur at the sediment-water interface or shortly below the sediment surface, but at greater depth as well.

The new sampler is suitable for studies of seasonal pore water composition as samples can be taken at an identical location for extended periods of time. In permeable sediments influenced by advection the replacement and re-equilibration of pore water is assumed to occur within some hours allowing the determination of pore water compositions within tidal cycles. Furthermore, the permanently installed samplers allow to clearly distinguish between temporal variations and spatial heterogeneity. So far, the new samplers have been used for a period of one year and are still working properly. Even the necessary equilibration time of several weeks is not considered to be disadvantageous in the light of its long lifespan. All these aspects indicate that the new *in situ* sampler is a powerful tool to investigate biogeochemical cycles in tidal flat sediments, salt-marsh soils or in other temporarily inundated environments.

2.5. Comments and recommendations

The sampler proved to be very suitable to sample pore water in permeable water saturated sandy sediments. For the extraction of pore water from muddy sediments (mixed flat Neuharlingersieler Nacken) or partly unsaturated sediments (salt-marsh sediments of Langeoog Island) the sampler is also appropriate, however the sampling is much more time consuming. A further improvement to adapt the sampler to such environments seems possible, e.g. via the enlargement of the sampling port to facilitate the extraction of pore water by extending the area through which suction directly acts on the sediment.

Further fields of application are the analysis of CH₄, N₂O or H₂S contents in the pore water. However, degassing of the sample has to be taken into account once the sample is transferred into sampling containers. In general, pore waters retrieved by this sampler seem to be as suitable for the analysis of dissolved gases as sediment cores where losses of gas are also supposed to occur. For example, a first comparison of CH₄ concentrations determined in samples taken with the *in situ* sampler and in samples from sediment cores showed similar results.

Acknowledgements

The authors would like to thank Helmo Nicolai and his colleagues at TERRAMARE Research Centre for assembling the pore water samplers. His experience and practical suggestions were of great help during the realisation of the project. Furthermore, we wish to thank Malte Groh for his assistance during the sampling campaigns and Alexander Josefowicz, Hans-Harald Berger, and Vebjoern Thingnes for their help during the insertion of the samplers into the sediment. We appreciate the supportive comments made by Jan Axmacher. This study was financially supported by the German Science Foundation (DFG, BR 775/14-4) within the framework of the Research Group 'BioGeoChemistry of Tidal Flats' (FOR 432/2).

3. Sulphate, dissolved organic carbon, nutrients and terminal metabolic products in deep pore waters of an intertidal flat

Melanie Beck, Olaf Dellwig, Jan M. Holstein, Maik Grunwald, Gerd Liebezeit, Bernhard Schnetger, Hans-Jürgen Brumsack

This chapter has been submitted to *Biogeochemistry*.

Abstract

This study addresses deep pore water chemistry in a permeable intertidal sand flat at the NW German coast. Sulphate, dissolved organic carbon (DOC), nutrients, and several terminal metabolic products were studied down to 5 m sediment depth. Significant correlations between the inorganic products of terminal metabolism (NH_4^+ and PO_4^{3-}) and sulphate depletion suggest sulphate reduction to be the dominant terminal carbon oxidation pathway. Pore water concentrations of sulphate, ammonium, and phosphate were used to elucidate the composition of organic matter degraded in the sediment. The thus calculated C:N and C:P ratios were verified by model results. The deep pore water system of permeable intertidal flat margins seems to a large degree be governed by advection, microbiological processes, and lithology, whereas diffusion likely is of minor importance. Water exchange at the sediment surface and in deeper sediment layers converts permeable intertidal sediments into a “bio-reactor” where organic matter is recycled, and nutrients, DOC, and several other terminal metabolic products are released close to the low water line of creek banks. Deep pore waters escaping at tidal flat margins

during low tide presumably form a major source of nutrients and thus may largely account for tidal variations of nutrients in the open water column of the study area.

3.1. Introduction

It has been demonstrated that sandflats with low organic carbon contents have rates of organic matter remineralization comparable to those of organic rich muds (Rusch et al., 2006). The permeability of sand facilitates advective pore water transport through the upper sediment layer in contrast to diffusion-controlled muddy sediments. Rapid exchange between pore water and the overlying water column has been identified as the most important process responsible for enhanced remineralization rates and carbon cycling in sands. During inundation of intertidal sand flats, pressure gradients are generated by the interaction of bottom currents with sediment topography like ripples leading to advective pore water flow in the upper decimetres of permeable sandy sediments (Huettel et al., 1996; Huettel and Rusch, 2000; Precht and Huettel, 2004). The induced pore water flow at the sediment surface is an effective mechanism for rapid exchange of oxygen (Ziebis et al., 1996; Precht et al., 2004; Rusch et al., 2006), dissolved and particulate organic matter (Huettel et al., 1996; Huettel and Rusch, 2000; Rusch and Huettel, 2000), and nutrients (Caetano et al., 1997; Huettel et al., 1998) in permeable sediments. Consequently, advective pore water exchange at the sediment surface leads to fast recycling of organic matter and the removal of metabolic products within a time range of hours and/or days.

Beside advective pore water flow at the sediment surface, intertidal flats are assumed to be influenced by advection in deep sediment layers of several metres depths (Billerbeck et al., 2006b; Wilson and Gardner, 2006). In contrast to rapid pore water exchange processes at the sediment surface, fluid flow in deeper parts of the sediment is presumably much slower. Especially at tidal flat margins where the surface slopes towards tidal creeks, deep advective pore water flow is generated driven by the hydraulic gradient between sea water and pore water level at low tide (Wilson and Gardner, 2006).

This type of advective pore water flow is comparable to processes described as subtidal pumping or submarine groundwater discharge (Riedl et al., 1972; Burnett et al., 2003). Owing to high residence times and long pathways of the pore water, DOC and nutrients are enriched in deep layers compared to the upper section of the sediment.

In tidal flat sediments nutrients and DOC were examined by several authors (Howes and Goehring, 1994; Böttcher et al., 1998; Böttcher et al., 2000; Jahnke et al., 2003; Kuwae et al., 2003; de Beer et al., 2005; Billerbeck et al., 2006b; Magni et al., 2006; Murray et al., 2006; Weston et al., 2006). However, there are few studies which focused on these species in sediment depths exceeding 1 m. Charette and Sholkovitz (2006) determined nutrients and DOC down to about 8 m depth in a subterranean estuary of Waquoit Bay, USA, but focused on trace elements. The understanding of deep pore water processes in tidal flats is, therefore, rather limited.

In this study, sulphate, DOC, nutrients, and several terminal metabolic products were determined in pore waters down to 5 m depth in an intertidal flat from the NW German coast. We will try to decipher biogeochemical and hydrological processes which may govern pore water composition and depth gradients. Pore water analyzes are complemented by a geochemical characterisation of the sedimentary column required to understand pore water concentrations and flow. It has been hypothesized that pore waters from several metres depth are potentially seeping from the tidal flat margin at low tide (Billerbeck et al., 2006b). We intend to provide information on the chemical composition of seeping fluids, which may exert influence on biogeochemical processes in the open water column of the study area. We hypothesize that increases in nutrient concentrations observed in the open water column of the study area (Grunwald et al., 2007) at low tide are mainly due to the release of deep pore water enriched in these species.

3.2. Materials and Methods

3.2.1. Study area

The Wadden Sea, located in the Southern North Sea, forms one of the largest tidal flat areas extending for almost 500 km between Den Helder (Netherlands) and Skallingen (Denmark). In Northwest Germany the tidal flat area is located between the coastline and a chain of barrier islands, which are separated by tidal inlets. These inlets connect the tidal flat areas with the open North Sea. The tidal flat area itself is divided by a tidal channel system consisting of large main channels and smaller secondary channels. Sampling was carried out on the Eastern margin of the intertidal sand flat Janssand, located in the backbarrier area of the Island of Spiekeroog (53° 44,183' N; 007° 41,904' E; Fig. 3.1.).

The study area is characterized by semi-diurnal tides and a tidal range of 2.6 m (Flemming and Davis, 1994). During high tide the Janssand tidal flat is covered by 1 - 2 m of water. It becomes exposed to the air for approximately 6 hours, depending on tidal range and wind direction. During the time of exposure the sediment remains wet. Pore water level was shown to drop gradually to about 10 cm below sediment surface with the lowest point approximately 1.5 h after low tide (Billerbeck et al., 2006a). The Janssand tidal flat surface is almost horizontal, except for the margin where the sediment surface slopes towards the main tidal creek. At low tide the distance between the sampling location and the water line is approximately 70 m and the difference in altitude amounts to about 1.5 m.

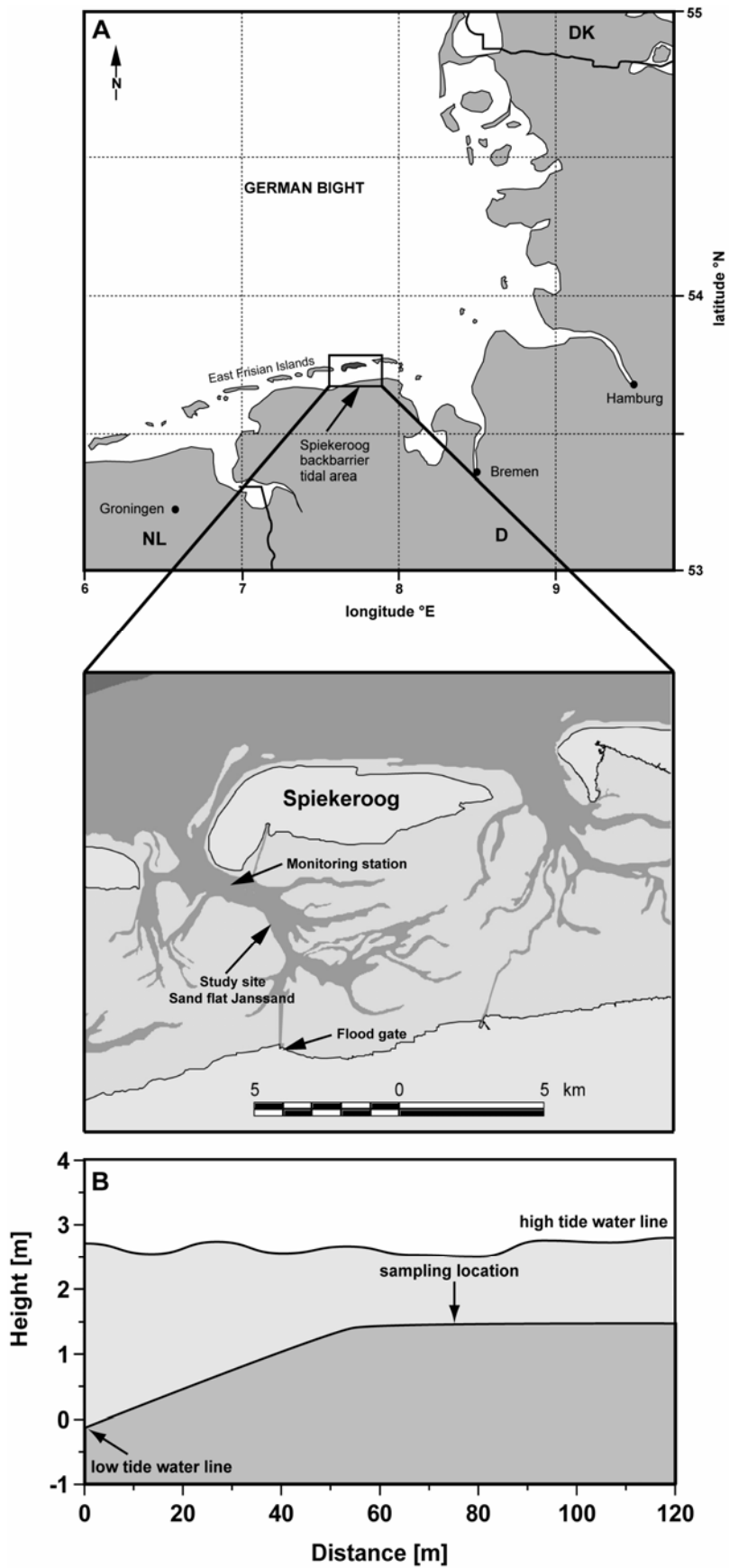


Fig. 3.1.: (A) Study site in an intertidal sand flat (Janssand) in the backbarrier area of Spiekeroog Island, Wadden Sea, Germany. (B) Tidal flat topography.

3.2.2. Sample collection

Pore water – Pore water sampling was carried out using *in situ* samplers described in more detail in Beck et al. (2007). Each sampler is composed of a PE-pipe with sampling ports at 20 depth intervals down to 5 m. Teflon tubings link the sampling orifice to sampling devices located at the sediment surface. Each *in situ* pore water sampling system consists of two samplers. The short sampler (1 m length) has 11 sampling ports at 0.05 m, 0.07 m, 0.10 m, 0.15 m, 0.20 m, 0.25 m, 0.30 m, 0.40 m, 0.50 m, 0.75 m and 1.0 m sediment depth. The long sampler (5 m length) has 10 sampling ports located at 1.0 m, 1.25 m, 1.5 m, 2.0 m, 2.5 m, 3.0 m, 3.5 m, 4.0 m, 4.5 m, and 5.0 m sediment depth. At the top of the sampler PE syringes can be connected to the sampling system to extract pore water from the sediment. Depending on sampling depth and diameter of the teflon tubes, different volumes of pore water were discarded before taking samples for analyzes. All samples were pre-filtered through nylon gauzes of 100 and 50 μm pore size located in front of the sampling orifices and immediately filtered through 1.2 μm GF/C filters after extraction.

Pore water samples described in this paper were taken on April 25th 2006 except for methane samples which were retrieved on March 22nd 2006. For some calculations data obtained in sampling campaigns from May 2005 till June 2006 are used. Samples were analyzed for nutrients (NH_4^+ , PO_4^{3-} , H_4SiO_4 , NO_3^-), sulphate (SO_4^{2-}), sulphide (H_2S), methane (CH_4), dissolved organic carbon (DOC), total alkalinity (TA) and chloride (Cl). Furthermore, the pH value was measured on site using an aliquot of the sample (pH/Cond 340i, WTW, Weilheim, Germany). Samples for the analysis of nutrients, TA, SO_4^{2-} , and Cl were stored in PE vials. Samples for DOC analyzes were acidified by adding 1 ml HCl (6 M) to 40 ml sample and stored in glass bottles. All PE vials were pre-rinsed with ultrapure water prior to use, while all glass bottles were acid washed and rinsed with ultrapure water. All samples were stored at 4-6°C until analysis. The determination of nutrients was conducted the day after sampling.

For the determination of H₂S a certain volume of sample, depending on the expected H₂S concentration, was added to 5 ml of a 10 mM Cd-acetate solution immediately after sampling. A volume of 4 ml sample was used if H₂S concentrations were expected to be lower than 1 mM, whereas 1 ml sample was added for H₂S concentrations exceeding 1 mM. The addition of sample was stopped when yellow fluffs of CdS started to precipitate. Samples for the analysis of CH₄ were filled from the syringe into headspace vials with rubber septa and aluminium crimp seal, and immediately frozen in the field. Degassing of the sample has to be taken into account once the sample is transferred into the bottles, however we tried to minimise this effect.

Sediment core – Within a distance of some metres to the pore water samplers a sediment core was collected in April 2005. An aluminium tube with a diameter of 8 cm was driven into the sediment by a vibration corer to a depth almost equivalent to the length of the sampler. The sediment core was recovered using a lifting block. Sampling of the sediment core was carried out depending on changes in sedimentology.

3.2.3. Pore water analysis

Nutrients – Nutrient concentrations (NH₄⁺, PO₄³⁻, H₄SiO₄, NO₃⁻) were determined photometrically by methods described in Grasshoff et al. (1999) using a spectrophotometer (Spekol 1100, Analytik Jena). Samples containing high concentrations of sulphide were diluted to reduce the effect of sulphide on the formation of coloured complexes, especially for the determination of PO₄³⁻ and H₄SiO₄. Total alkalinity was determined by a spectroscopic method proposed by Sarazin et al. (1999). Solutions containing known concentrations of the analytes were used to check precision and accuracy of the measurements. Precision / accuracy were 5.6% / -2.5% for alkalinity (at 2.5 mM), 5.1% / -3.0% for NH₄⁺ (at 1 mM), 4.8% / 1.2% for PO₄³⁻ (21 µM), and 4.1% / 2.7% for H₄SiO₄ (at 142 µM).

Sulphate – SO_4^{2-} was analyzed by ion chromatography (Dionex DX 300) in a 250-fold dilution, with standard Atlantic Seawater (Salinity 35.0 (\pm 0.2%); OSIL, UK) used to control the precision (3.0%) and accuracy (-5.3%) of the measurements.

Sulphide – For the analysis of H_2S the solution containing the yellow CdS precipitate was filtered through a 0.2 μm syringe filter. The filter was washed with 5 ml 1% (v/v) formic acid and 10 ml ultrapure water to dissolve Cd carbonates also retained on the filter and to remove any excess Cd that did not react with H_2S . The yellow precipitate on the filter was dissolved by adding 10% HCl (v/v), and the filtrate was made up to a constant volume. Cd was analyzed by FAAS (Perkin Elmer AAS 4100) and the H_2S concentration in the samples was calculated based on the Cd concentrations measured as well as CdS stoichiometry.

Dissolved organic carbon – DOC was analyzed by high temperature catalytic oxidation using a multi N/C 3000 analyzer (Analytik Jena, Jena, Germany). Prior to the determination of DOC, the acidified samples were purged by synthetic air to remove any dissolved inorganic carbon. Potassium hydrogen phthalate solutions were used for external calibration and to control precision and accuracy of the measurements. Precision was better than 2.4% and accuracy better than 1.9%.

Chloride – Cl^- was determined by micro titration using a 0.1 mM AgNO_3 solution to titrate a solution composed of 100 μl sample, 5 ml ultrapure water and 100 μl of a K-chromate/-dichromate solution (4.2 g and 0.7 g, respectively, dissolved in 100 ml ultrapure water). Standard seawater of salinity 30.005 (OSIL, UK) was used to control the precision (0.41%) and accuracy (-0.11%) of the measurements.

Methane – For measuring methane concentrations, gas from the headspace of the bottles was injected into a CX-3400 gas chromatograph (Varian, Darmstadt, Germany) equipped with a capillary column (plot-fused silica column no. 7517, 25 m by 0.53 mm, $\text{Al}_2\text{O}_3/\text{KCl}$ coated; Chromopack, Middleburg, The Netherlands) and measured by a flame ionisation detector. Analytical precision was better than 7%.

3.2.4. Sediment analysis

XRF – Sediment samples were freeze dried and homogenised in an agate mill. All samples were analyzed for the major and minor elements Si, Al, Ca, Sr, Ti, and Zr by XRF using a Philips PW 2400 X-ray spectrometer. 600 mg of sample were mixed with 3600 mg of a mixture of dilithiumtetraborate/lithiummetaborate (50% $\text{Li}_2\text{B}_4\text{O}_7$ /50% LiBO_2), preoxidised at 500°C with NH_4NO_3 (p.a.), and fused to glass-beads. Analytical precision and accuracy were better than 5% for all elements.

Bulk parameters – Total carbon (TC) and total sulphur (TS) were determined using an CS 500 IR analyzer (Eltra, Neuss, Germany), while total inorganic carbon (TIC) was analyzed coulometrically by a CM 5012 CO_2 coulometer coupled to a CM 5130 acidification module (UIC, Joliet, USA). Total organic carbon (TOC) was calculated as the difference between TC and TIC. Precision and accuracy of TC, TS, and TIC analyzes were better than at least 3% and 1%, respectively.

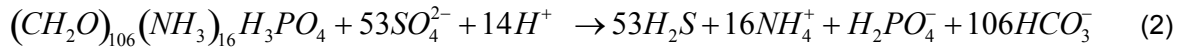
3.2.5. Calculation of sulphate depletion, C:N, and C:P ratios

Sulphate depletion – The pore water depletion in SO_4^{2-} was calculated as proposed by Weston et al. (2006) using the concentrations determined for the specific sediment depths. The depletion in SO_4^{2-} reflects the net amount of SO_4^{2-} consumption, presumably via bacterial SO_4^{2-} reduction, and was calculated according to

$$(\text{SO}_4^{2-})_{\text{Dep}} = \left[(\text{Cl}^-)_{\text{PW}} \cdot (R_{\text{SW}})^{-1} \right] - (\text{SO}_4^{2-})_{\text{PW}} \quad (1)$$

where $(\text{SO}_4^{2-})_{\text{Dep}}$ is the SO_4^{2-} depletion, $(\text{Cl}^-)_{\text{PW}}$ and $(\text{SO}_4^{2-})_{\text{PW}}$ are the pore water concentrations of Cl^- and SO_4^{2-} , and R_{SW} is the molar ratio of Cl^- to SO_4^{2-} in surface sea water ($R_{\text{SW}} = 19.33$). Using Cl^- to compensate for slight changes in salinity due to rain or fresh water input, the hypothetical SO_4^{2-} concentration at a specific depth interval is calculated. The difference between this hypothetical and the actually measured SO_4^{2-} concentration forms an estimate for the metabolic rate of SO_4^{2-} reduction.

Ratios – Carbon to nitrogen (C:N) and carbon to phosphorus (C:P) stoichiometry of the organic matter degraded in the sediment was estimated by a regression analysis of $(SO_4^{2-})_{Dep}$ against NH_4^+ and PO_4^{3-} and multiplying the ratios of $(SO_4^{2-})_{Dep}$ to NH_4^+ and PO_4^{3-} by a factor of 2. This estimation is based on the assumption that the ratio of C to SO_4^{2-} is 2:1 if the oxidation of organic matter is coupled to sulphate reduction according to the equation



where organic matter composition follows the Redfield relationship. Using the Redfield formula represents an approximation as the formula is based on living marine zoo- and phytoplankton and is thus uncertain in buried organic matter (Sholkovitz, 1973). A further approximation is the estimation of the C: SO_4^{2-} ratio in the pore water samples by a regression analysis of $(SO_4^{2-})_{Dep}$ against TA. TA is not totally equivalent to dissolved inorganic carbon (DIC), which should be used for the determination of the C: SO_4^{2-} ratio. The ratios were corrected by the appropriate diffusion coefficients (Weston et al., 2006). Diffusion coefficients described by Boudreau (1997) were used for HCO_3^- , SO_4^{2-} , NH_4^+ and PO_4^{3-} .

3.3. Results

3.3.1. Sediment geochemistry

Depth profiles of parameters characterising the sediment geochemistry at a location close to the pore water samplers are summarized in Figure 3.2. Due to lithological inhomogeneity in the sampling area, the lithology of the sediment core is suggested to differ slightly from the lithology which would be determined at the pore water sampling location. The lithological structure of the sediment core, however, reproduces well the sequence of different sediment layers generally found close to tidal flat margins in the sampling area.

In the study area sandy sediments predominate. However, at depths exceeding 1.8 m the sands are intermingled with silt-clay lenses and layers. Higher amounts of coarse-grained quartz are reflected by enrichments in SiO_2 , whereas higher clay contents are characterized by enrichments in Al_2O_3 . According to Dellwig et al. (2000) the geochemical differentiation between sand, mixed and mud flat based on the SiO_2 content is as follows: sand flat $\text{SiO}_2 > 80\%$, mixed flat SiO_2 65-80%, and mud flat $\text{SiO}_2 < 65\%$. At the sampling site the SiO_2 content of the sediment exceeds 80% down to 1.8 m depth, whereas below this depth SiO_2 contents vary between 60 and 90%. In depths exceeding 1.8 m the Al_2O_3 content ranges from about 3 to 9%. These lithological changes reflect highly variable depositional conditions at the sampling site. The content of total organic carbon (TOC) varies between 0.04 and 2.4% with the highest values found in clay-rich layers. Such TOC contents seem to be typical for sediments in the study area as similar TOC values were determined by Dellwig et al. (2000) for NW German tidal flat sediments. TS contents of the sediment vary between 0.04 and 1%. TOC as well as TS show positive correlations with increasing clay content indicating the importance of organic matter sorption onto clay particles for preservation of both marine and terrestrial organic matter (Baldock et al., 2004).

The highest CaCO_3 contents of up to 12% are determined in clay layers suggesting the incorporation of fine CaCO_3 rich material derived from mussel shells or material already deposited as fine CaCO_3 particles. To differentiate between the sources of the deposited carbonate material, Ca/Sr ratios represent a useful tool as biogenic carbonate and detrital material have different Ca/Sr ratios. As described by Dellwig et al. (1998) biogenic calcite shows Ca/Sr ratios between 210 and 380 (Pingitore and Eastman, 1985), while average shale, which represents the detrital component in sediments has a ratio of about 70 (Wedepohl, 1971). At our sampling site Ca/Sr ratios higher than 210 are determined in the CaCO_3 rich clay layers indicating the presence of biogenic carbonate in these layers. In intervals with high quartz contents Ca/Sr ratios vary between 110 and 160, and the source of the deposited material, therefore, seems to be a mixture of

biogenic carbonate and detrital material, even though feldspars may be of importance as well.

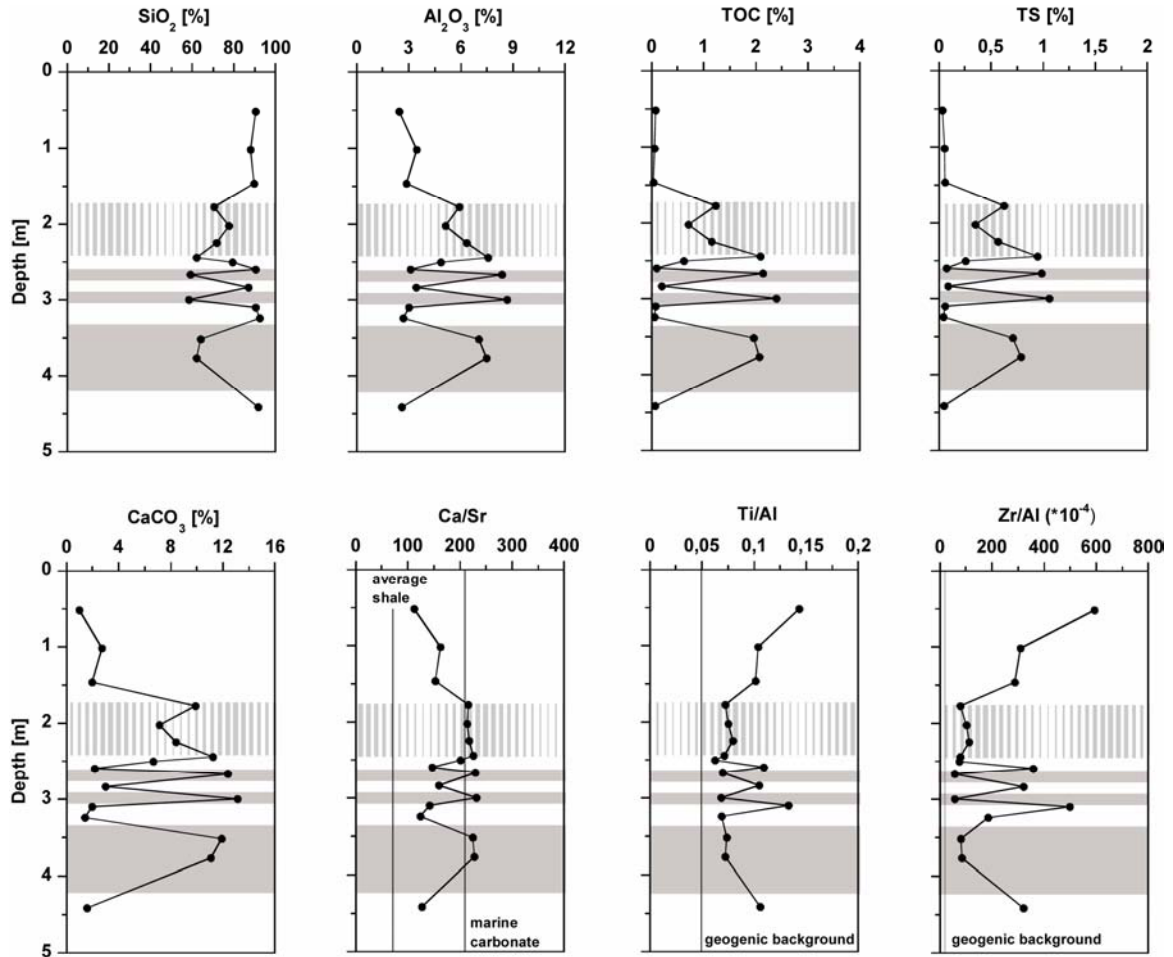


Fig. 3.2.: Depth profiles of parameters characterising the lithology at the sampling site in an intertidal sand flat. The continuous lines indicate the geogenic background in Ti/Al and Zr/Al depth profiles, and the Ca/Sr ratio of average shale and marine carbonate, respectively. The grey bars highlight the clay rich layers of the sediment profile. Depths of about 1.5 to 2.5 m are marked with a hatched area as the sediment is predominantly sandy, with very thin clay layers.

The elements Ti and Zr are indicators of the energetic conditions prevailing during the deposition of the sediment. In Figure 3.2. Ti/Al and Zr/Al ratios are displayed instead of Ti and Zr contents. Aluminium is the element commonly chosen for quantifying the terrigenous-detrital fraction in nearshore sediments (Brumsack, 2006). Any deviation from average shale composition is, therefore, easily recognised in element/Al-ratios. High Ti/Al

and Zr/Al ratios point towards elevated heavy minerals contents (e.g. ilmenite, rutile, zircon), which are found in layers deposited during higher current velocities. Clay minerals in contrast are deposited at low energy conditions. At our sampling site the depth profiles of Ti/Al and Zr/Al show that the depositional conditions changed several times, in accordance with the very dynamic nature of the backbarrier tidal flat area. The time span needed for the sedimentation of such layers may differ significantly, as, for instance, significant sediment redistribution may occur due to wave action during storms (Chang et al., 2006a; Chang et al., 2006b; Christiansen et al., 2006).

3.3.2. DOC, sulphate, and metabolic products in pore water

Depth profiles of sulphate, DOC, nutrients, several metabolic products, chloride, and pH are shown in Figure 3.3. The depth trends shown are typical for the sampling site and were chosen as a representative example for the sampling period from May 2005 to June 2006. Concentrations change within the sampling period of one year, however the trends with depths remain the same. Seasonal variations observed at the sampling site as well as a comparison of depth profiles from different locations in the study area will be presented elsewhere.

The concentrations of Cl^- vary around 500 mM in the entire depth profile with a minimum concentration of 480 mM at 0.75 m depth. Consequently, no subterranean fresh water contribution of the nearby mainland seems to influence the salinity at the sampling location. The pH values vary between 7.8 in the upper part of the sediment and 6.9 at 5 m depth.

Nitrate concentrations in the pore water are below 1 μM except for the upper centimetres where a concentration up to 5.6 μM is determined. In contrast, sea water of the study area shows higher NO_3^- concentrations ranging from about 80 μM at the beginning of April 2006 to about 5 μM in May and June (Grunwald et al., 2007). The slightly elevated NO_3^- pore water concentration at 5 cm depth is either due to seawater introduced by advection at ripples, bioturbation and/or nitrification. The generally low NO_3^-

pore water concentrations imply that seawater NO_3^- introducing into the surface sediment is rapidly denitrified.

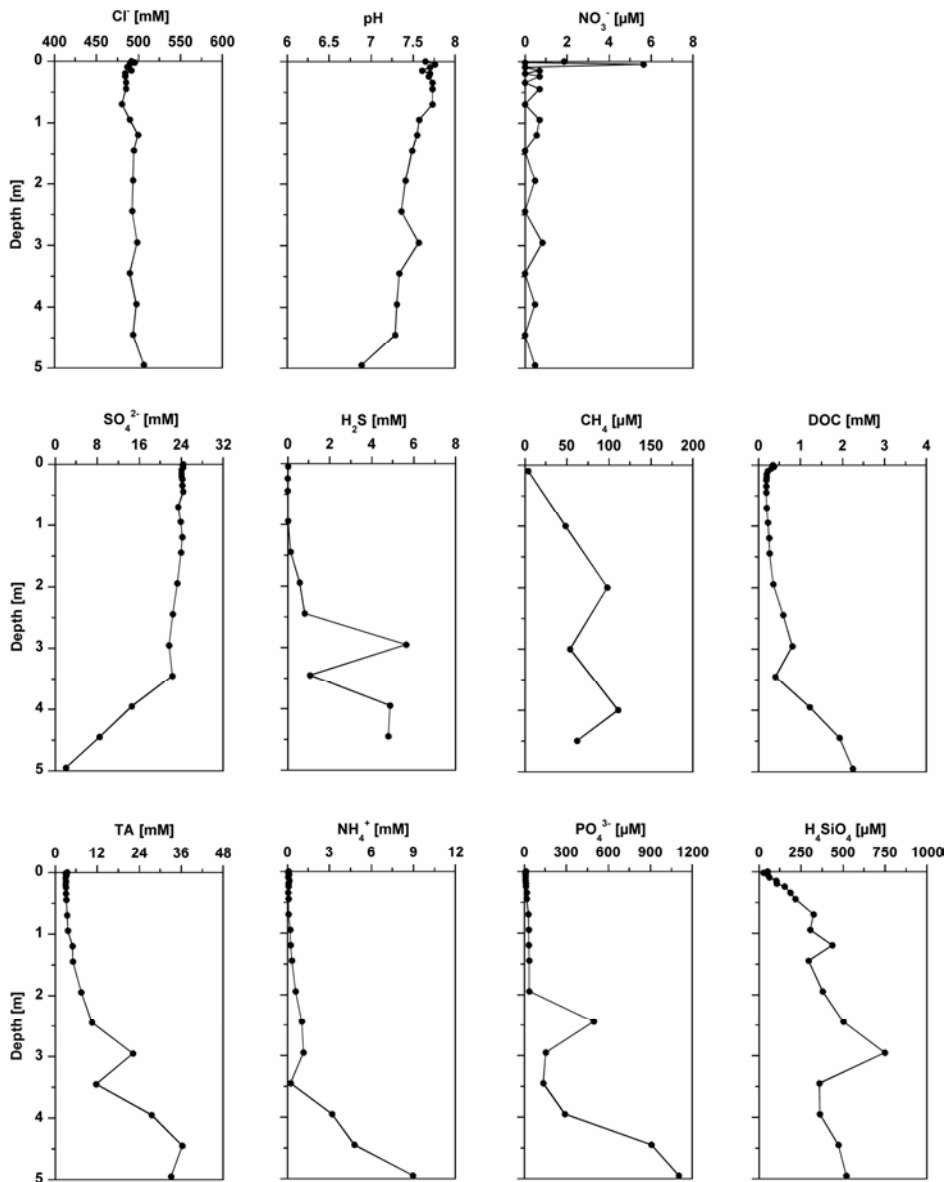


Fig. 3.3.: Pore water profiles of Cl^- , pH, NO_3^- , SO_4^{2-} , H_2S , CH_4 , DOC, TA, NH_4^+ , PO_4^{3-} , and H_4SiO_4 , at the sampling site in an intertidal sand flat of the backbarrier area of Spiekeroog Island from April 2006.

Sulphate is the main electron acceptor used by microorganisms in the sandy sediments of the sampling area. Sulphate reducers were successfully identified in the study area illustrating that high sulphate reduction rates even prevail in deep intertidal

sediments (Wilms et al., 2006a,b; A. Gittel, pers. comm.). Sulphate concentrations close to the sea water value of 26 mM (at salinity 31 in the Wadden Sea) are only determined in the upper part of the sediment, followed by a decrease in SO_4^{2-} concentration caused by the metabolic activity of sulphate reducers. In a sediment depth of 5 m very low concentrations of SO_4^{2-} remain.

Hydrogen sulphide is a terminal metabolic product of SO_4^{2-} reduction. However, H_2S concentrations do not constantly increase with decreasing SO_4^{2-} concentrations at the study site. High H_2S concentrations like e.g. at 3 m depth are assumed to be due to entrapment of H_2S in or below a less permeable clay-rich sediment layer with limited exchange. Furthermore, the concentration of H_2S in the sediment is influenced by the formation of the iron sulphides FeS and FeS_2 (Howarth and Jørgensen, 1984; Moeslund et al., 1994).

Methane shows concentrations of about 5 μM at the sediment surface, and increases to about 100 μM at greater depths. Methane concentrations already start to increase in a sediment depth of about 1 m, where still high concentrations of SO_4^{2-} are found. This possibly illustrates the coexistence of sulphate reducers and methanogens (Wilms et al., 2006b), and/or the upward movement of CH_4 as free gas.

At the sampling site the sandy sediment surface is covered by ripples leading to advective pore water flow at the sediment surface (Huettel et al., 1996; Huettel and Rusch, 2000). Thus, organic material originating from diatoms and dinoflagellates is easily introduced into the upper layers of the sandy sediments and subsequently degraded aerobically and anaerobically. The degradation products are either used by microorganisms for their metabolism, form part of other biogeochemical reactions or become enriched in the sediment pore water, as for example DOC. The concentration of total alkalinity also increases with increasing sediment depth due to decomposition of organic material.

The enrichment of NH_4^+ and PO_4^{3-} with depth reflects the decomposition of organic matter, whereas the increase in H_4SiO_4 concentrations mainly mirrors the dissolution of

biogenic silica. Like the contents of DOC and total alkalinity, the concentrations of NH_4^+ , PO_4^{3-} , and H_4SiO_4 start to increase in sediment depths exceeding some decimetres. At shallower depths these species show concentrations only slightly higher than in seawater of the study area (Schnetger et al., 2000; Dellwig et al., 2007; Grunwald et al., 2007).

3.3.3. Stoichiometry of organic matter degradation

Concentrations of $(\text{SO}_4^{2-})_{\text{Dep}}$ are positively correlated with TA, NH_4^+ , PO_4^{3-} , and DOC. The correlations are displayed for samples taken in April 2006 (Fig. 3.4.A), and for all samples taken from May 2005 until June 2006 (Fig. 3.4.B). The ratio of TA: $(\text{SO}_4^{2-})_{\text{Dep}}$ is 1.7 for the samples from April 2006 and does only slightly change if all samples taken during a one year period are taken into account (Table 3.1.). This ratio is close to the expected ratio of C: $(\text{SO}_4^{2-})_{\text{Dep}}$ of 2, based on Redfield ratios and the assumption that sulphate reduction represents the main metabolic process for organic matter remineralization.

Tab. 3.1.: Stoichiometry of organic matter degradation estimated from slopes of pore water concentrations of total alkalinity TA and sulphate depletion $(\text{SO}_4^{2-})_{\text{Dep}}$ against NH_4^+ and PO_4^{3-} concentrations for samples of April 2006 and for all samples taken from May 2005 till June 2006. The ratios of suspended particulate matter and the ratios derived from modelling pore water profiles are displayed, too.

	C: SO_4^{2-}	C:N	C:P
<i>Suspended particulate matter</i>		7.8*	
<i>Pore water April 2006</i>			
TA	1.7	3.2	77
$(\text{SO}_4^{2-})_{\text{Dep}}$		3.0	75
<i>Pore water model April 2006</i>		3.5 / 4.0 [†]	75
<i>Pore water May 2005 – June 2006</i>			
TA	1.8	2.8	106
$(\text{SO}_4^{2-})_{\text{Dep}}$		2.7	101

* Lunau et al. (2006)

[†] fast degrading organic matter / slowly degrading organic matter

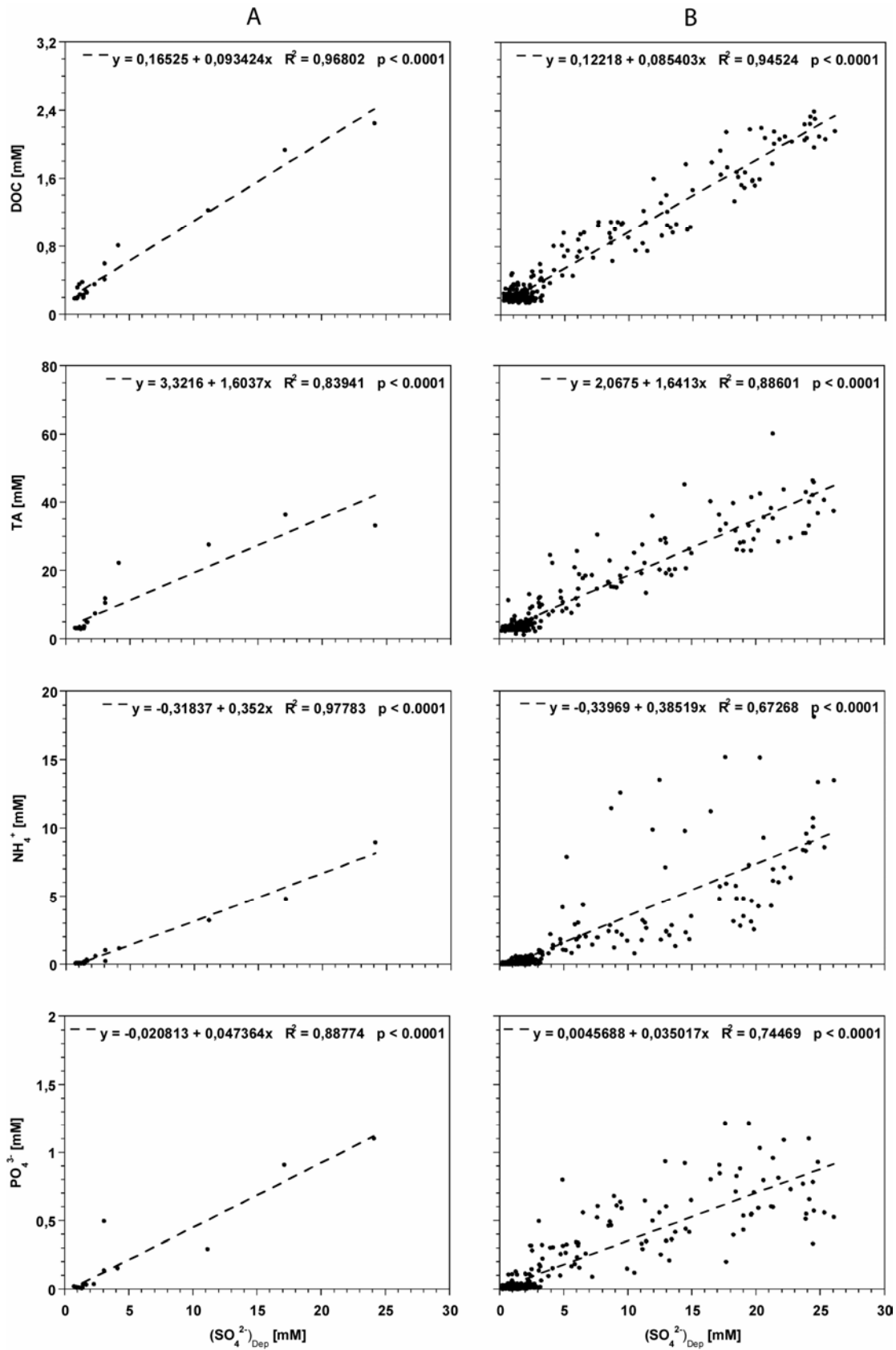


Fig. 3.4.: Ratios of DOC, TA, NH_4^+ , and PO_4^{3-} concentrations to $(\text{SO}_4^{2-})_{\text{Dep}}$ concentrations. Best-fit linear regressions are calculated for samples from April 2006 separately (A) and for all samples taken from May 2005 till June 2006 (B) at the sampling site described.

In fact, methanogenesis is assumed to be responsible for organic matter degradation besides sulphate reduction at the study site. Nevertheless, the approximations used for an estimation of the stoichiometry of organic matter degradation seem to be applicable. Estimates of the C:N ratio of degraded organic matter are 3.1 regarding samples of April 2006 and 2.8 for samples obtained during the whole sampling period of one year (Table 3.1.). The C:P stoichiometry is 76 for samples from April 2006 and 104 for all samples.

3.4. Discussion

3.4.1. Terminal metabolic pathways

In general, the oxidation of organic matter in sediments is coupled to the diminishment of electron acceptors, the use of which depends on their reactivity and availability. Aerobic respiration is followed by nitrate reduction, reduction of Mn^{IV} and Fe^{III} oxides, sulphate reduction and finally methanogenesis (Froelich et al., 1979). In tidal flat sediments, based on the availability of SO_4^{2-} compared to other electron acceptors, sulphate reduction forms the dominant pathway of anaerobic carbon oxidation (Jørgensen, 1982). Due to high lithological variations in tidal flats, different microbial communities are presumably present in sediment layers with different geochemical properties (Wilms et al., 2006c). Therefore, the succession of degradation processes described by Froelich et al. (1979) is often not seen in tidal flat sediments where distinct sediment layers are characterized by different sedimentological, chemical, and biological properties (Wilms et al., 2006a).

In this study, pore water profiles are used to evaluate the pathways of organic matter degradation in an intertidal flat. At the study site the oxygen penetration depth is only a few centimetres (Billerbeck et al., 2006b) and other electron acceptors are thus needed for the degradation of organic matter. Nitrification, denitrification as well as nitrate reduction seem to be closely coupled leading to low NO_3^- concentrations over the entire

depth profile. Methanogenesis occurs in the sediment resulting in CH₄ concentrations up to 100 µM. A conclusion about the depth where methane is actually being produced can however hardly be drawn. Due to concentration gradients and pressure fluctuations induced by tidal cycles, methane will supposedly slowly migrate from its depth of production towards the sediment surface. Thus, upward diffusion may partly explain the existence of elevated methane contents in upper sediment layers. In spite of this, methane can also be produced in the upper sediment layers as methanogenic archaea were detected over the entire depth profile of 5 m in the study area (Wilms et al., 2006b).

In spite of minor methanogenesis occurring in the sediment, sulphate reduction seems to be the dominant pathway of anaerobic organic matter degradation. Sulphate concentrations remain at a high level down to 3.5 m depth and do attain concentrations close to zero only in 5 m depth. Alperin et al. (1994) suggested that sulphate reducing bacteria can no longer metabolize labile DOC when sulphate concentrations drop below ~1 mM. Except in 5 m depth, enough sulphate is thus available as terminal electron acceptor for sulphate reducing bacteria in our study area. The tight coupling of products of organic matter degradation like NH₄⁺, and PO₄³⁻ with (SO₄²⁻)_{Dep} supports this hypothesis (Fig. 3.4.). Advection of pore water within the sediment as well as possible oxidation of H₂S (Fossing and Jørgensen, 1990) could lead to an underestimation of sulphate reduction. However, the general conclusion concerning sulphate reduction as dominant pathway of anaerobic organic matter degradation would remain true. Weston et al. (2006) drew similar conclusions regarding the relevance of organic matter remineralization pathways for intertidal creek-bank sediments in Georgia and South Carolina, USA.

3.4.2. Pore water profiles

Biogeochemical, sedimentological, and hydrological processes may influence the formation of pore water depth profiles. In general, sulphate, DOC, nutrients, total alkalinity, methane, and sulphide show either an increase or decrease with depth depending on whether the species are consumed or produced during organic matter remineralization

(Fig. 3.3.). At the study site concentration gradients do however not always increase or decrease continuously with depth. In depths exceeding 3.5 m sulphate shows a stronger depletion with depth than in the overlying sediment layers, whereas DOC, ammonium and phosphate exhibit a more pronounced enrichment. The depletion in sulphate and enrichment of DOC and nutrients in depths exceeding 3.5 m depth can probably be explained by a displacement of the tidal flat margin. Within 14 years the east tidal flat margin of the Janssand was displaced about 100 m to the east (B.W. Flemming, pers. comm.) suggesting that the sampling location may formerly have been located at the tidal flat margin in contrast to its recent position 75 m away from the low tide water line. In the study area tidal flat margins, especially near the low water line, were shown to be microbially very active (B. Engelen, pers. comm.) resulting in high nutrient concentrations (Billerbeck et al., 2006b). Sediments in depths exceeding 3.5 m which show enrichments in nutrients and DOC thus probably formed part of the former tidal flat margin.

In permeable sediments pore water depth profiles may be further influenced by pore water advection. There are evidences that advection occurs in specific sediment depths at our sampling location close to the tidal flat margin. For example, NH_4^+ shows an unexpected low concentration at 3.5 m depth. The sediment is lithologically composed of layers with different porosities and permeabilities. At 3.5 m depth a sediment layer which is more permeable than the layers above and below seems to promote pore water flow. In the sediment core this permeable layer is geochemically identified as a sandy layer below 3 m depth owing to its high SiO_2 content. The depths of the permeable layer in the sediment core do not exactly match the depth of low NH_4^+ concentrations at the pore water sampling site due to lithological inhomogeneity in the study area. The NH_4^+ depth profile thus implies that NH_4^+ concentrations at 3.5 m depth are influenced by deep pore water advection. The NH_4^+ minimum at 3.5 m depth may be caused via channelled pore water flow from central parts of the sand flat where average NH_4^+ concentrations of about 0.4 mM are determined down to 3.5 m depth. DOC and total alkalinity also show lower concentrations in 3.5 m depth compared to sediment depths above and below. The lower

ammonium, DOC and total alkalinity concentrations in 3.5 m depth may also be due to reduced microbial activity in this depth compared to other sediment layers. Additional data which will be published in a following manuscript, point towards advection as main factor explaining the lower concentrations in 3.5 m (Beck et al., submitted b). Regarding these data, we further suggest that advection also occurs in depths above 3 m, whereas a less permeable layer seems to limit water exchange in 3 m depth.

In several studies advection processes were described in tidal flat sediments (Whiting and Childers, 1989; Howes and Goehring, 1994; Billerbeck et al., 2006a,b; Wilson and Gardner, 2006). All these studies were carried out at locations close to tidal flat margins where a hydraulic gradient is generated between the pore water level in the elevated sand flat and the water level in the tidal creek at low tide. This hydraulic gradient induces pore water flow leading to exchange between the pore water in the sediment and the open water column of the backbarrier area.

Water column PO_4^{3-} and H_4SiO_4 concentrations determined at a monitoring station in the backbarrier area of Spiekeroog Island in May 2006 are shown in Figure 3.5. Concentrations of both species vary depending on the state of the tidal cycle with higher concentrations being determined at low tide. In the study area deep pore water has concentrations 10 to 1000 times higher than sea water (Liebezeit et al., 1996; Schnetger et al., 2000; Grunwald et al., 2007) thus representing a source of nutrients.

Pore water seepage is assumed to explain increases in PO_4^{3-} and H_4SiO_4 concentrations in sea water at low tide. Fresh water, which occasionally flows into the backbarrier area via a flood gate, may additionally represent a nutrient source at low tide. At the flood gate of Neuharlingersiel (Fig. 3.1.) the average PO_4^{3-} and H_4SiO_4 concentrations determined in 2002 and 2003 were 4 μM and 110 μM , respectively (at salinities about 1). As fresh water concentrations are lower than deep pore water concentrations and fresh water does not flow into the backbarrier area at each low tide, pore water seems to represent the main source of nutrients to the open water column and mainly accounts for the tidal variation of certain nutrients in the open water column. This

study on deep pore water in an intertidal flat thus supports hypotheses concerning pore water advection, pore water release at creek banks, and influence of pore water on the open water column composition in the backbarrier area.

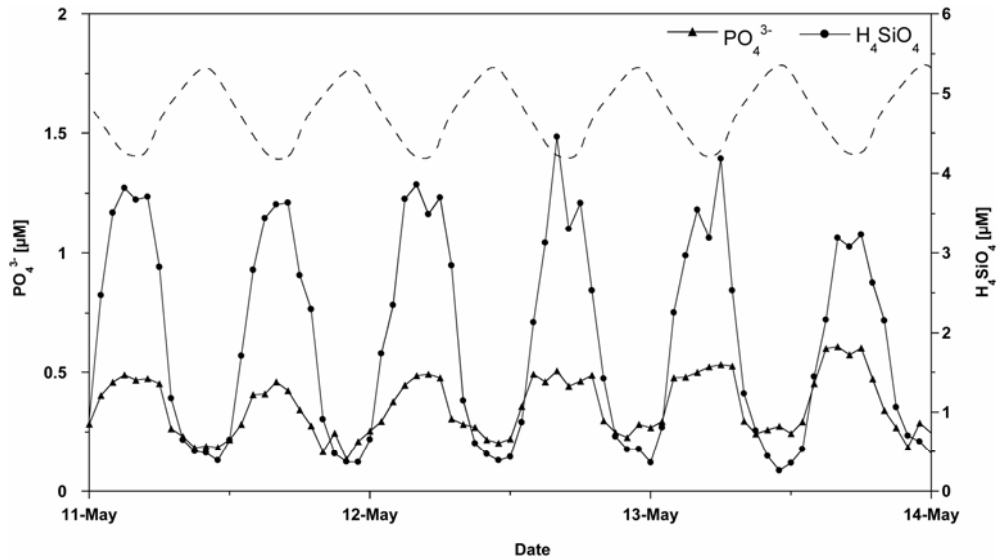


Fig. 3.5.: Sea water PO₄³⁻ and H₄SiO₄ concentrations determined at a monitoring station in the backbarrier area of Spiekeroog Island in May 2006. The dashed line indicates the variations of the water level during tidal cycles.

3.4.3. Organic matter remineralization

DOC concentrations correlate very well with (SO₄²⁻)_{Dep}, with maxima in the zone of maximum sulphate reduction (Fig. 3.4.). However, it is not evident if this correlation is reflecting a single biogeochemical process involving DOC and SO₄²⁻. Hydrolysis and fermenting microorganisms could thus have converted organic matter leading to the production of refractory and labile DOC, whereas the labile part is used by sulphate reducers (Böttcher et al., 1997; Rusch et al., 1998).

The organic matter mineralized at the sampling site seems to be richer in N and P than expected from the Redfield ratio. The C:N and C:P ratios according to Redfield are 6.6 and 106, respectively. According to pore water analyzes, the organic matter at the sampling site has a C:N ratio of about 3 and a C:P ratio of 75-106 (Table 3.1.). The

deviation from the Redfield ratios does not represent a completely unexpected finding as the Redfield ratio is based on average oceanic relationships. Weston et al. (2006) determined C:N ratios between 3.4 and 10 for intertidal creek bank sediments in South Carolina and Georgia, USA, based on the same calculation assumptions made in our study. In our study area suspended particulate matter determined in the open water column has an average C:N ratio of 7.8 (Lunau et al., 2006). Suspended matter is partly incorporated into the sediment where it is in the following degraded by microorganisms (Huettel et al., 1996; Huettel and Rusch, 2000; Rusch and Huettel, 2000). We suggest that the elemental ratios of suspended matter partly explain the elemental composition determined in pore waters. Unfortunately, the C:P ratio of the organic component of the suspended matter was however not determined.

The organic matter composition estimated by regression analyzes was verified by a model approach. For modelling organic matter degradation, sulphate reduction and including subsequent nutrient release to the pore water the generic computer model ISM (Wirtz, 2003) was adopted. It is a partial differential equation solving model describing diffusive transport and biogeochemical processes in aquatic porous media. In the one-dimensional model the sediment column consists of 20 boxes. Using the organic matter decomposition model specified by Boudreau (1992), two particulate organic carbon fractions were specified in the model. The top section of the model (0 - 2.5 m) is free of reactive organic matter, while an average 1% TOC is assumed below this depth. The mid section of the sediment column is separated from the bottom section by a zone at 3.5 m depth in which pore water is continuously replenished with pore water originating from central parts of the tidal flat. This mixing of pore waters from centre and margin of the tidal flat may serve as a surrogate process for advection in a one-dimensional model setup. Due to advection pore water from the centre of the tidal flat is suggested to slowly flow towards the tidal flat margin. As approximation average pore water concentrations determined in 17 different depths down to 3.5 m at a location in the central part of the tidal flat were used (Beck et al., submitted b). This approximation was necessary as the true

pore water flow pathways in the tidal flat are still unknown. The middle and bottom sections are assumed to contain different particulate organic carbon fractions to enable different decay rates and elemental compositions. The organic matter in the mid section is more reactive than in the bottom section and decomposes about twice as fast. During the decomposition of these carbon fractions nutrients are released according to the specific elemental composition of the organic matter. A steady state simulation fitting the observed sulphate and nutrient pore water profiles was obtained by adjusting organic matter decay rates, elemental composition of the organic matter and irrigation rate. Seawater concentrations determined in the study in 1995 and 1996 serve as upper boundary. Lower boundary concentrations are kept constant in order to account for a near linear gradient across the lower boundary.

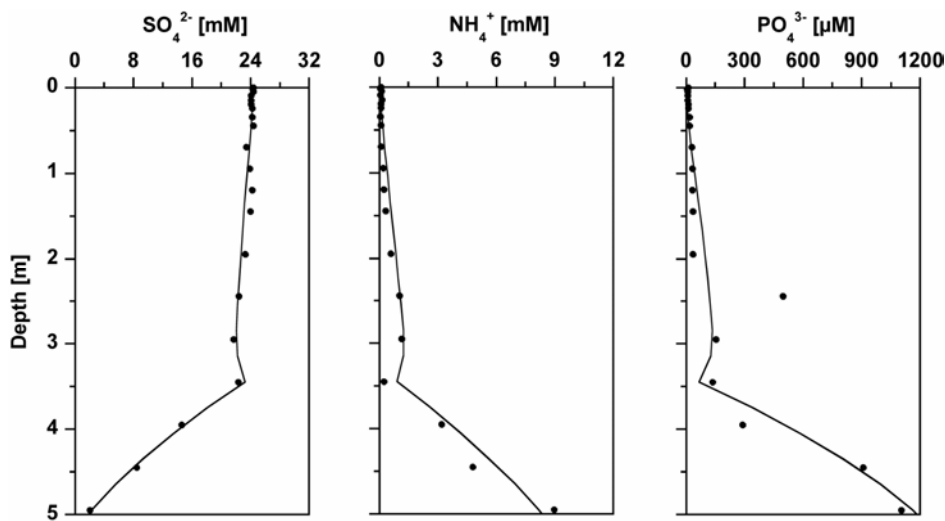


Fig. 3.6.: Modelled (continuous line) and measured (points) SO_4^{2-} , NH_4^+ and PO_4^{3-} pore water concentrations. Same samples as in Figure 3.3. are shown.

Modelling the pore water profiles results in a C:N ratio of 3.5 regarding fast degrading organic matter and 4.0 for slowly degrading organic matter. The modelled C:P ratio is 75 (Fig. 3.6., Table 3.1.). Modelling our pore water profiles thus results in C:N and C:P ratios similar to those calculated by regression analysis (Fig. 3.6.). In the model the unexpectedly high PO_4^{3-} concentration at 2.5 m depth is disregarded. The exclusion of this

PO_4^{3-} concentration in the model setup seems to be of minor importance as a regression analysis of $(\text{SO}_4^{2-})_{\text{Dep}}$ against PO_4^{3-} without the PO_4^{3-} concentration at 2.5 m depth does not result in a significantly different C:P ratio.

Although the study area is affected by advection in specific sediment depths, we assume the calculations concerning C:N and C:P ratios to be applicable as a rough estimation. Regression analyses show good correlations whether only the sampling campaign of April 2006 or all campaigns conducted during one year are regarded (Fig. 3.4.). The estimations of C:N and C:P ratios by regression analysis are further supported by similar results obtained by a model setup (Fig. 3.6.). The model setup uses only diffusional transport except in 3.5 m depth where pore water from central parts of the tidal flat is intruded as simplification of advection processes.

3.5. Conclusions

Biological and chemical processes as well as hydrological and lithological conditions vary with depth leading to changes in pore water concentrations not only in the upper part of the sediment, but down to sediment depths of several metres. In the study area sulphate reduction has been identified as the most important process for organic matter remineralization. Pore water concentrations of sulphate, ammonium, and phosphate have been used to elucidate the composition of organic matter degraded in the sediment. The deep pore water system at tidal flat margins is to a large degree governed by advection and lithology, whereas diffusion seem to be of minor importance. Water exchange at the sediment surface and in deeper sediment layers converts the permeable intertidal sediment into a “bio-reactor”. Pore waters originating from some metres depth are assumed to escape at tidal flat margins at low tide. Deep pore water studies in intertidal flats, which are conducted close to tidal flat margins, thus provide an insight into pore waters supposedly released at creek banks. The release of nutrient-enriched pore waters

presumably accounts for tidal variation of certain nutrients in the water column of the backbarrier area.

Acknowledgements

The authors would like to thank Malte Groh for his valuable assistance during all sampling campaigns and Carola Lehnert and Eleonore Gründken for their assistance during laboratory work. Furthermore, we wish to thank the TERRAMARE Research Centre for providing transportation to the sampling site by boat and especially Helmo Nicolai for his help regarding technical questions. We thank Joris M. Gieskes for his critical reading of a previous version of this manuscript. We gratefully acknowledge the financial support by the German Science Foundation (DFG, BR 775/14-4) within the framework of the Research Group 'BioGeoChemistry of Tidal Flats' (FOR 432/2).

4. Spatial, seasonal, and tidal variations of sulphate, dissolved organic carbon, and nutrients in deep pore waters of intertidal flat sediments

Melanie Beck, Olaf Dellwig, Gerd Liebezeit, Bernhard Schnetger, Hans-Jürgen Brumsack

This chapter has been submitted to *Limnology and Oceanography*.

Abstract

Spatial, seasonal, and tidal variations of sulphate, dissolved organic carbon (DOC), nutrients and associated metabolic products were determined down to 5 m sediment depth in pore waters of intertidal flats located in the German Wadden Sea. Mixed flat sediments which are richer in clay than sand flat sediments are shown to display a more pronounced depletion of sulphate and enrichment of metabolic products. Clay-rich layers hinder pore water exchange processes resulting in longer residence times of pore waters and thus enrichments of metabolic products. Spatial variations of pore water depth profiles have also been determined comparing the tidal flat margin with central parts of a tidal flat. Sediments at the tidal flat margin seem to be influenced by different hydrological and sedimentological processes compared to central parts. Seasonal and tidal variations observed close to the tidal flat margin support the hypothesis that this zone is affected by pore water advection. Our deep pore water studies further illustrate that seasonal variations are not limited to the sediment surface, but can also be observed in sediment depths of some metres. At a location close to the tidal flat margin high temperatures in the summer of 2006 as well as organic matter availability seem to lead to an increase in

microbial activity. This leads to more pronounced sulphate depletion and enrichment in DOC and nutrients in this summer period.

4.1. Introduction

In NW German coastal areas different types of tidal flats can be distinguished depending on sediment composition. In a rough classification tidal flats are divided into sand flats, mixed flats, and mud flats. Sand flats have the highest contents of sand, whereas mud flats show elevated clay contents, and mixed flats represent an intermediate type. In general, clay-rich sediments have higher porosities than sandy sediments. However, smaller pores and the lack of interconnection in clayey sediments may significantly restrict microbial and nutrient mobility compared to sandy sediments (Chapelle and Lovley, 1990). It has been shown that sand flats with low organic carbon contents have rates of organic matter remineralization comparable to those of organic-rich muds (Rusch et al., 2006). The permeability of sand facilitates advective pore water transport in contrast to muddy sediments, where processes are dominated by diffusion.

Rates of organic matter remineralization not only depend on sediment permeability but also on sediment temperature, the availability and quality of the organic matter, and the availability and reactivity of electron acceptors. In general, the oxidation of organic matter in sediments is coupled to the depletion of electron acceptors, the use of which depends on their reactivity and availability. Aerobic respiration is followed by nitrate reduction, reduction of Mn^{IV} and Fe^{III} oxides, sulphate reduction and finally methanogenesis. This succession of degradation processes described by Froelich et al. (1979) is, however, often not seen in tidal flat sediments where distinct sediment layers are characterized by different sedimentological, chemical, and biological properties. In marine sediments, based on the availability of SO_4^{2-} compared to other electron acceptors, sulphate reduction forms the dominant pathway of anaerobic carbon oxidation (Jørgensen, 1982).

In tidal flat sediments which are anoxic beneath a sediment depth of some centimetres, sulphate reduction has been identified as the most important pathway of anaerobic carbon oxidation (Böttcher et al., 2000; Kristensen et al., 2000; Gribsholt and Kristensen, 2003; Weston et al., 2006; Beck et al., submitted a). Rates of sulphate reduction depend on temperature, with increasing rates at higher temperatures (Vosjan, 1974; Kristensen et al., 2000; Koretsky et al., 2003). Furthermore, sulphate reduction rates were shown to be higher in organic-rich muddy sand than in organic-poor coarse sand in intertidal sediments near the Island of Sylt, Germany (Kristensen et al., 2000). Better availability of organic matter thus leads to higher activities of sulphate reducing bacteria. Studies in tidal flats of the backbarrier area of Spiekeroog Island, Germany, support the hypothesis that bacterial communities seem to be affected by the availability and quality of carbon sources (Wilms et al., 2006c). In these intertidal flats, sulphate reduction rates were further found to be highest in the first few centimetres of the sediment, but still remained high at 1 m depth and were even detectable in deep layers of some metres (Wilms et al., 2006a; Köpke et al., in prep.).

Spatial variations in the upper decimetres of tidal flat sediments were studied in several contributions (Kristensen et al., 1997; Gribsholt and Kristensen, 2003; Murray et al., 2006; Sakamaki et al., 2006). Seasonal variations in pore water were determined in the upper decimetres of tidal flat sediments as well (Lerat et al., 1989; Kristensen et al., 1997; Magni and Montani, 2006; Serpa et al., 2007). Variations in temperature, in deposition of organic material, and in macrobenthos activities seem to lead to seasonal variations in nutrient pore water concentrations near the sediment surface (Magni and Montani, 2006). Spatial and seasonal variations in pore waters originating from sediment depths of some metres have, however, remained widely unknown. In tidal flat areas the effects of tidal cycles on the flux of nutrients from the sediment into the open water column were for instance studied by Caetano et al. (1997), Sakamaki et al. (2006), and Yin and Harrison (2000). Rocha (1998) and Kuwae et al. (2003) further determined tidal variations

of pore water depth profiles in the upper 10 cm. Little is known, however, about variations of pore water profiles during one tidal cycle in sediment depths of several metres.

In the present study pore water sampling was carried out at different locations in sand and mixed flats. The pore water composition of a sand flat was compared with that of a mixed flat to evaluate whether pore waters differ due to distinct lithologies and /or biogeochemical processes. Furthermore, the comparison of pore waters originating from different locations within a tidal flat should shed light on the variation of biogeochemical processes and hydrological conditions within a tidal flat. We hypothesize that pore waters extracted close to a tidal flat margin differ from those in the centre of a tidal flat as pore water flow is suggested to be more pronounced at tidal flat margins (Howes and Goehringer, 1994; Billerbeck et al., 2006b; Wilson and Gardner, 2006). A sampling campaign was conducted during one entire tidal cycle aimed to identify changes in pore water depth profiles at a time scale of hours. The knowledge about seasonal pore water variation gained for upper sediment layers (Kristensen et al., 1997; Magni and Montani, 2006) was further extended to sediment depths of 5 m. At three locations in a tidal sand flat pore water was studied at monthly intervals throughout one year.

4.2. Materials and Methods

4.2.1. Study area

The Wadden Sea, located in the Southern North Sea, forms one of the largest tidal flat areas, extending for almost 500 km between Den Helder (Netherlands) and Skallingen (Denmark). The boundary between the North Sea and the Wadden Sea is formed by a chain of barrier islands separated by tidal inlets. In the backbarrier area of these islands, tidal flat areas extend between the coastline and the islands. The backbarrier area of each island is further characterized by a tidal channel system consisting of large main channels and smaller secondary channels. The study area is characterized by semi-diurnal tides and a tidal range of 2.6 m (Flemming and Davis, 1994).

4. Spatial, seasonal, and tidal variations in tidal flat pore waters

Our study was carried out in the backbarrier area of Spiekeroog Island, which represents one of the East Frisian Islands in NW Germany (Fig. 4.1.). The backbarrier area is composed of several tidal flats divided by tidal channels. The tidal flats differ in their sediment composition and their exposure time at low tide depending on their position within the backbarrier area. Pore water studies were conducted at two intertidal flat locations: Janssand (JS) and Neuharlingersieler Nacken (NN).

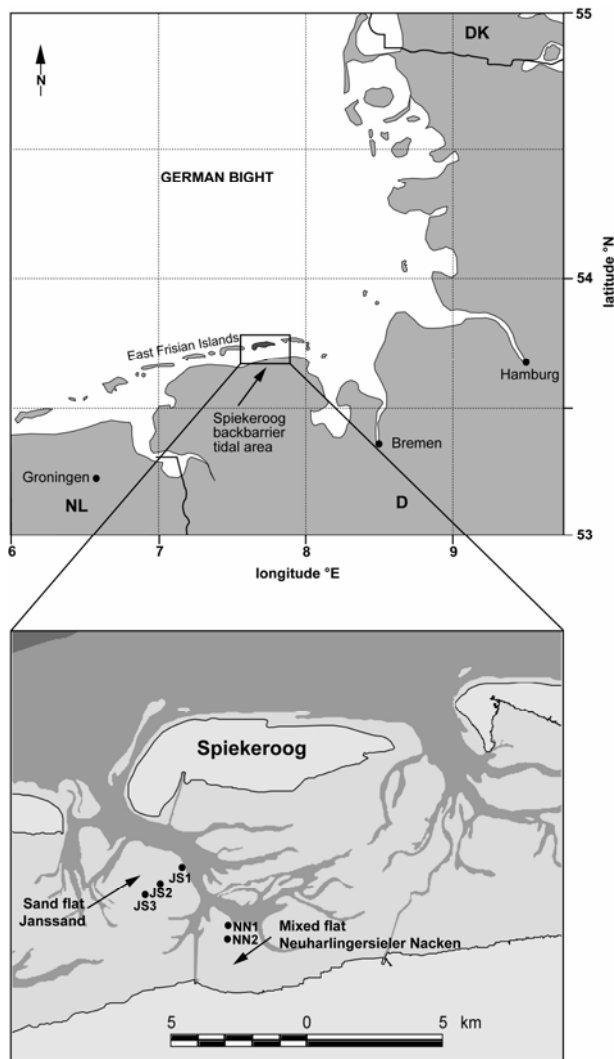


Fig. 4.1.: Sampling locations in two intertidal flats situated in the backbarrier area of Spiekeroog Island, Wadden Sea, Germany. Pore water sampling locations are marked by dots and location numbers increase with increasing distance to the tidal creek.

During high tide the JS tidal flat is covered by 1 - 2 m of water. At low tide it becomes exposed to the atmosphere for approximately 6 hours, depending on tidal range and wind direction. Due to the shorter distance to the coastline and the lower altitude of the tidal flat, the NN tidal flat is only exposed for about 4 hours during low tide. Sampling was carried out at three locations on the JS tidal flat (JS1: 53° 44.183' N, 007° 41.904' E; JS2: 53° 43.962' N, 007° 41.283' E; JS3: 53° 43.844' N, 007° 40.873' E), whereas two locations were chosen on the NN tidal flat (NN1: 53° 43.244' N, 007° 43.737' E; NN2: 53° 43.080' N, 007° 43.706' E). The locations are numbered according to their distance from the tidal flat margin, with number 1 being the one situated closest to the tidal creek. The distance between site JS1 and site JS2 amounts to 800 m, while site JS3 is located 500 m southeast of site JS2.

4.2.2. Pore water sampling

Pore water was extracted using *in situ* samplers described in more detail in Beck et al. (2007). The samplers remained permanently installed in the sediment to allow pore water sampling at the same location over time spans of one year or longer. Briefly, the sampler consists of a pipe with holes drilled into the pipe walls serving as sampling orifices. The sampling ports are linked to sampling devices located at the sediment surface by PTFE (Teflon) tubings. At the top of the sampler PE (polyethylene) syringes are connected to the sampling system to extract pore water from the sediment. Pore water sampling is conducted at 20 different depths, with the upper metre sampled in higher resolution (0.05 m, 0.07 m, 0.10 m, 0.15 m, 0.20 m, 0.25 m, 0.30 m, 0.40 m, 0.50 m, 0.75 m) than deeper sediment layers (1.0 m, 1.25 m, 1.5 m, 2.0 m, 2.5 m, 3.0 m, 3.5 m, 4.0 m, 4.5 m, and 5.0 m). Depending on sampling depth and diameter of the PTFE tubes, different volumes of pore water were discarded before taking samples for analyzes.

Pore water sampling was carried out from April 24th until April 26th 2006 on JS and NN tidal flats to compare pore waters of a sand flat with those of a mixed flat. In order to study the seasonal variation in pore waters, samples were taken on the JS tidal flat throughout

one year. The time interval between consecutive samplings ranged from three to nine weeks. On the JS tidal flat 12 samplings campaigns were conducted at location JS1 from May 2005 to June 2006. At site JS1 pore water was always sampled shortly after low tide at falling water level. At locations JS2 and JS3 sampling campaigns started in July 2005, and 10 campaigns were carried out until June 2006. Furthermore, data of a sampling campaign at site JS1 on June 28th 2006 are presented where pore water was extracted four times during one tidal cycle. Sampling started at low tide and lasted until three hours after high tide.

Pore water samples were analyzed for nutrients (NH_4^+ , PO_4^{3-} , H_4SiO_4), sulphate (SO_4^{2-}), sulphide (H_2S), dissolved organic carbon (DOC), total alkalinity (TA) and chloride (Cl^-). Furthermore, pH was measured on site using an aliquot of the sample (pH/Cond 340i, WTW, Weilheim, Germany). All samples were immediately filtered through 1.2 μm GF/C filters which were pre-heated to 400°C prior to use. Samples for the analysis of nutrients, TA, SO_4^{2-} , and Cl^- were stored in PE vials. Samples for DOC analyzes were acidified by adding 1 ml HCl (6 M) to 40 ml sample and stored in glass bottles. All PE vials were pre-rinsed with ultrapure water prior to use, while all glass bottles were acid washed and rinsed with ultrapure water. All samples were stored at 4-6°C until analysis. The determination of nutrients was conducted within one day after sampling. For the determination of H_2S a certain volume of sample, depending on the expected H_2S concentration, was added to 5 ml of a 10 mM Cd-acetate solution immediately after sampling. A volume of 4 ml sample was used if H_2S concentrations were expected to be lower than 1 mM, whereas 1 ml sample was added for H_2S concentrations exceeding 1 mM. The addition of sample was stopped when yellow fluffs of CdS started to precipitate. At site JS1 temperatures were continuously measured in the sediment using a permanently installed system equipped with Pt 100 sensors (Ahlborn, Munich, Germany) at different depths.

4.2.3. Sediment sampling

Adjacent to the pore water samplers, sediment cores were collected in April 2005. An aluminium tube with a diameter of 8 cm was driven into the sediment by a vibro corer to a depth almost equivalent to the length of the sampler. In compacted sandy sediments the aluminium tube could, however, only be driven to sediment depths of 2.5 and 2.0 m at locations JS2 and JS3. The sediment core was recovered using a lifting block. Sampling of the sediment core was carried out depending on visible lithological changes. Additional drillings were conducted in the centre of the tidal flat using a percussion coring tube.

4.2.4. Pore water analysis

Photometric methods were used to determine NH_4^+ , PO_4^{3-} , H_4SiO_4 (Grasshoff et al., 1999) and total alkalinity (Sarazin et al., 1999). SO_4^{2-} was analyzed by ion chromatography (Dionex DX 300) at 250-fold dilution. A multi N/C 3000 analyzer (Analytik Jena) was used for the analysis of DOC by temperature catalytic oxidation. Cl^- was determined by micro titration (100 μl sample, 5 ml ultrapure water and 100 μl of a K-chromate/-dichromate indicator) with a 0.1 mM AgNO_3 solution. For the analysis of H_2S the solution containing the yellow CdS precipitate was filtered through a 0.2 μm filter using a syringe. After rinsing the filter with 5 ml 1% (v/v) formic acid and 10 ml ultrapure water, the yellow precipitate on the filter was dissolved by adding a known volume of 10% HCl (v/v). Cd was analyzed by FAAS (Perkin Elmer AAS 4100), and the H_2S concentration in the samples was calculated based on CdS stoichiometry. Analytical procedures as well as precision and accuracy of the methods are described in more detail in Beck et al. (submitted a).

4.2.5. Sediment analysis

Sediment samples were freeze dried and homogenised in an agate mill. All samples were analyzed for the major elements Si and Al by XRF using a Philips PW 2400 X-ray

spectrometer. 600 mg of sample were mixed with 3600 mg of a mixture of dilithiumtetraborate/lithiummetaborate (50% $\text{Li}_2\text{B}_4\text{O}_7$ /50% LiBO_2), pre-oxidized at 500°C with NH_4NO_3 (p.a.), and fused to glass-beads. Total carbon (TC) and total sulphur (TS) were determined using an CS 500 IR analyzer (Eltra, Neuss, Germany), while total inorganic carbon (TIC) was analyzed coulometrically by a CM 5012 CO_2 coulometer coupled to a CM 5130 acidification module (UIC, Joliet, USA). Total organic carbon (TOC) was calculated as the difference between TC and TIC.

4.3. Results

4.3.1. Sediment geochemistry

In the backbarrier area of Spiekeroog Island mixed flats with higher clay contents are located closer to the mainland coast, whereas sand flats dominate towards the barrier islands (Flemming and Ziegler, 1995). In Figure 4.2. the contents of SiO_2 , Al_2O_3 , TOC, and TS are shown for the five sampling locations on JS and NN. These four parameters were chosen to roughly describe sediment composition as they document relevant sediment characteristics like sand and clay contents. Sediment geochemistry at location JS1 is described in more detail in Beck et al. (submitted a).

Higher amounts of coarse-grained quartz are reflected by enrichments in SiO_2 , whereas higher contents in clay are characterized by enrichments in Al_2O_3 . The SiO_2 content was proposed to differentiate between sand, mixed, and mud flats (Dellwig et al., 2000): sand flat $\text{SiO}_2 > 80\%$, mixed flat $\text{SiO}_2 65-80\%$, and mud flat $\text{SiO}_2 < 65\%$. In the upper metre of the sediment SiO_2 contents are $> 80\%$ at all locations, however, the generally observed decrease with increasing sediment depth varies depending on the location. At locations JS2 and JS3 SiO_2 and Al_2O_3 contents show no change down to 2.5 m depth. Drilling revealed that sandy sediments dominate down to 5 m depth near site JS2, and down to approximately 3 m near site JS3 (data not shown). Due to its position close to the tidal flat margin where more sediment redistribution occurs, sediment

geochemistry at location JS1 differs from that in the centre of the tidal flat. Sandy and clayey layers alternate at depths exceeding 1.5 m.

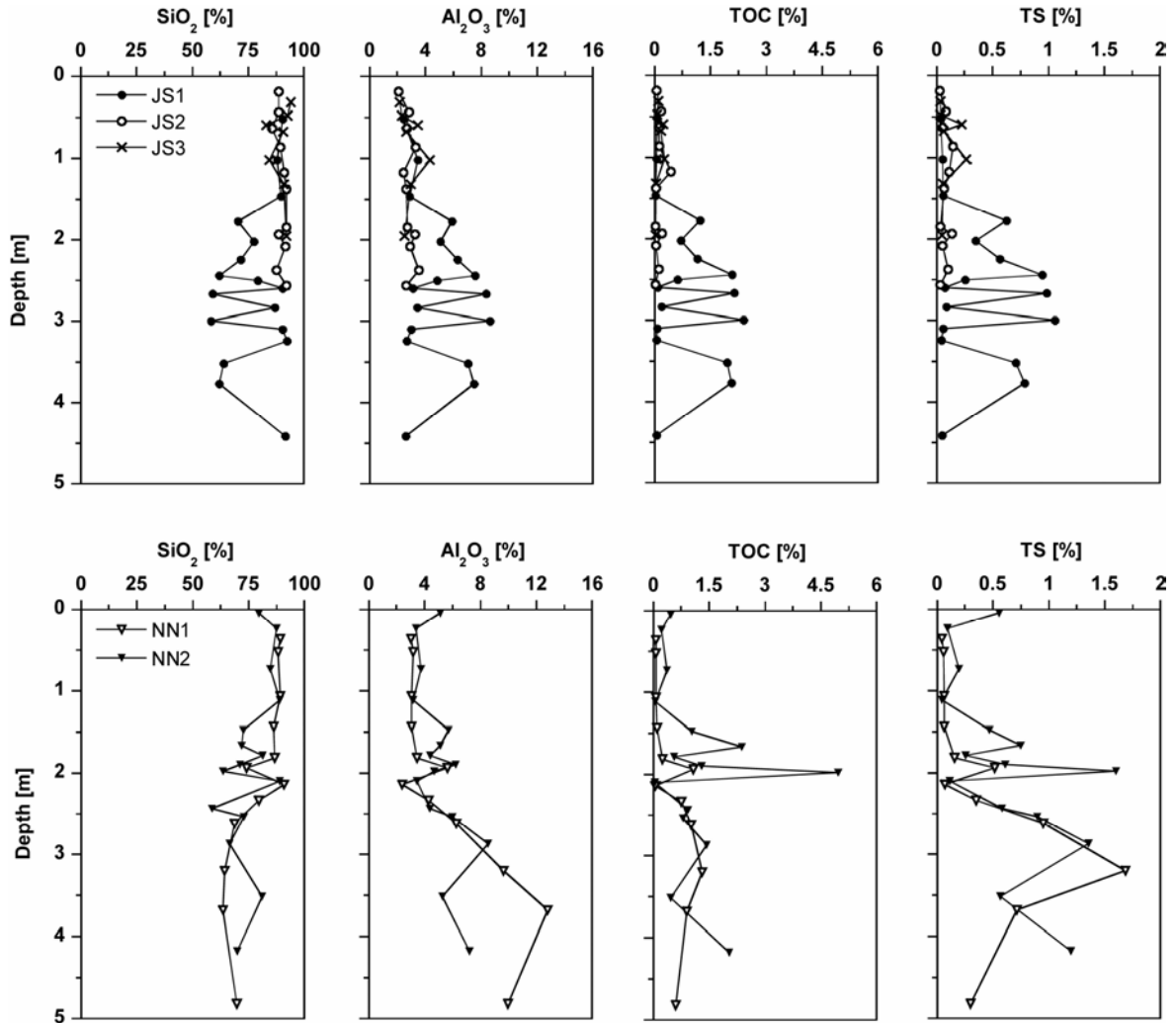


Fig. 4.2.: SiO₂, Al₂O₃, TOC and TS contents of sediment cores taken at locations close to the pore water samplers in the sand flat area (JS1 - JS3) and in the mixed flat area (NN1, NN2) in April 2005.

TOC and TS contents are low in the centre of the tidal flat compared to location JS1 where higher TOC and TS contents are found, especially in clay layers. At greater depths clay contents in the NN tidal flat are comparable to those determined at location JS1. In the NN tidal flat TOC and TS contents are, sometimes, slightly higher than at location JS1. Consequently, sediment geochemistry differs at the three locations on JS tidal flat.

Sediment geochemistry at locations JS1 and NN is rather similar. These locations differ in the number of distinct changes between sandy and clayey layers suggesting that the energetic conditions prevailing during sediment deposition changed more frequently at location JS1. Based on SiO₂ contents (Dellwig et al., 2000), the NN tidal flat is a mixed tidal flat, whereas the JS tidal flat is a sand flat, except for the tidal flat margin, where clay-layers are encountered.

4.3.2. Spatial variations

Pore waters of a sand flat and a mixed flat – In April 2005 pore water sampling was carried out at three locations on JS sand flat and on NN mixed flat to investigate the influence of different lithologies on pore water composition and, therefore, biogeochemical processes. Figure 4.3. shows the depth profiles of chloride, sulphate, DOC, nutrients, TA, and sulphide for three sand flat locations (JS1-JS3) and two mixed flat locations (NN1, NN2). Chloride concentrations remain almost constant at locations JS1 and JS2, whereas at the remaining locations a slight decrease in concentration is observed with depth. The minimum chloride concentrations correspond to a salinity of about 27 ruling out significant fresh water intrusions. However, especially in NN it may well signify the influence of intruding fresher waters from land aquifers. The decrease in sulphate concentrations is more pronounced in the mixed flat than in the sand flat. Especially in the centre of the JS tidal flat, only small sulphate depletions are seen with depth. Products of organic matter mineralization, such as DOC, NH₄⁺, PO₄³⁻, and TA, increase with depth at all sampling locations. However on JS tidal flat these increases are smaller and/or occur at greater sediment depths than on NN tidal flat. For example, DOC concentrations start to increase in the upper decimetres of the sediment at the NN site, whereas they remain almost constant down to some metres depth on JS tidal flat. Regarding H₄SiO₄, the difference between the two tidal flats is less evident, even though the highest concentrations were also determined on NN tidal flat. Sulphide is present in concentrations in the µM range at

locations in the centre of the JS tidal flat. In contrast, sulphide concentrations up to 5.6 mM and 8.2 mM were found at locations JS1 and NN2, respectively.

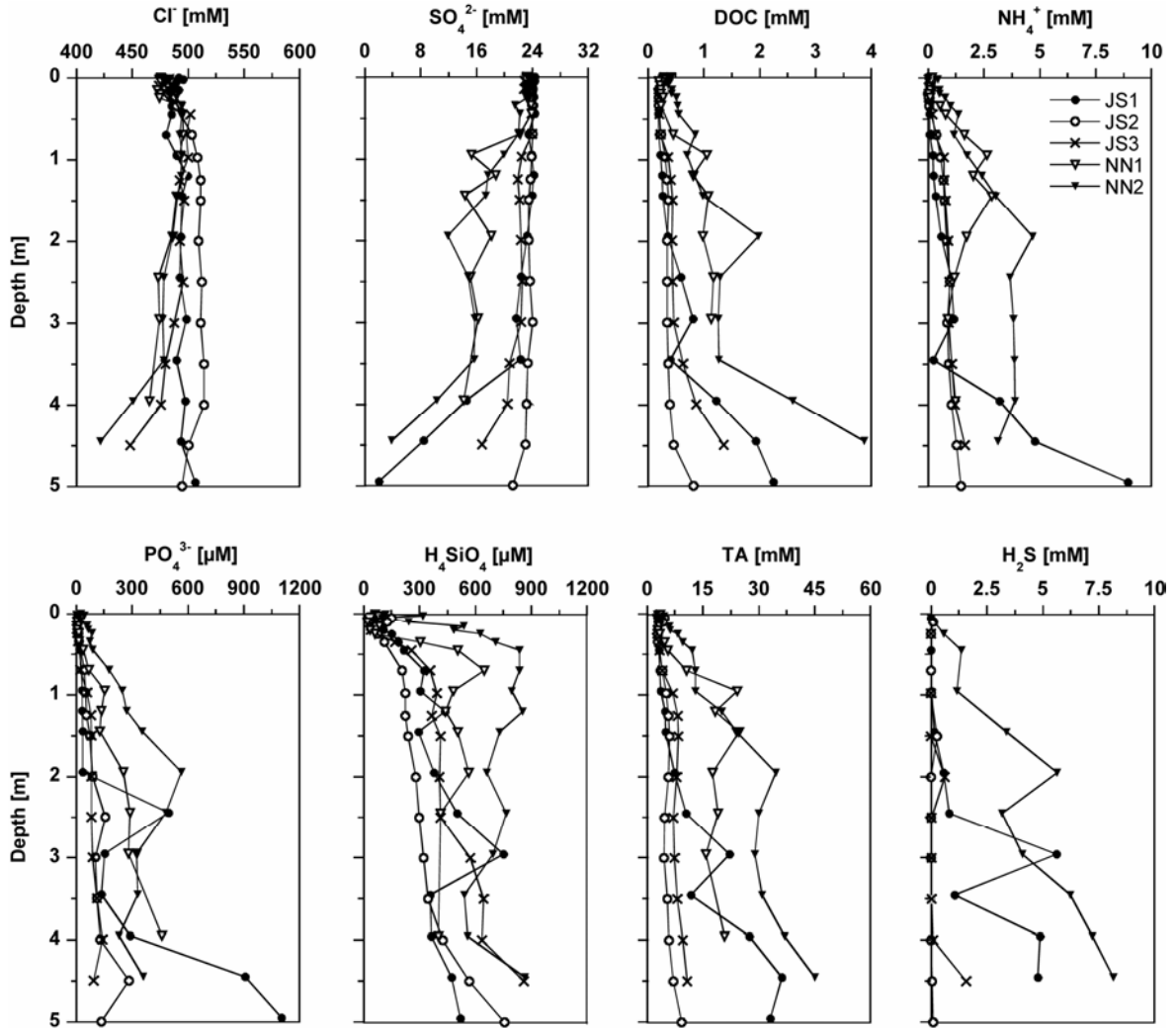


Fig. 4.3.: Chloride, sulphate, DOC, nutrient, total alkalinity, and H₂S pore water concentrations determined at three locations in a sand flat area (JS1 - JS3) and at two locations in a mixed flat area (NN1, NN2) in April 2006.

Pore waters at different locations within a tidal flat – Pore waters at different locations within a tidal flat are utilised to investigate whether biogeochemical processes occurring at locations close to the tidal flat margins differ from those in the centre of the tidal flat. JS sand flat pore waters were sampled at one location close to the tidal flat margin where the sediment slopes towards a tidal creek (JS1), and at two locations positioned in the centre

of the tidal flat (JS2, JS3). At low tide the distance between the sampling location JS1 and the water line is approximately 70 m and the difference in altitude amounts to about 1.5 m.

In Figure 4.3. depth profiles are shown obtained for the three locations in the intertidal sand flat in April 2006. Chloride concentrations are similar, except for the slightly decreasing concentrations to a salinity of about 28 at location JS3. The pH values change slightly between 7.9 and 6.9 with depth (data not shown). In the upper metres of the sediment sulphate is determined at a level almost equivalent to seawater concentrations. Only at greater sediment depths a decrease in sulphate concentration can be observed. Sulphate depletion with depth differs depending on location. At location JS2 no sulphate decrease with depth is seen, whereas a small decrease is observed at location JS3. At location JS1, below 3.5 m, the most intense sulphate depletion occurs. Such location-dependent shapes of depth profiles are also found for DOC, NH_4^+ , PO_4^{3-} , TA, and sulphide. In depths exceeding 3 m the concentrations of these species are higher at location JS1 than at the locations in the centre of the tidal flat.

4.3.3. Seasonal variations

Pore water samples were taken on a monthly basis from May 2005 until June 2006 on the JS intertidal flat. Figure 4.4. shows the seasonal variation of sulphate, DOC, total alkalinity, and nutrient concentrations at site JS1, which is located close to the tidal creek. For sulphate, steep concentration changes are evident in depths exceeding 3 m, whereas in the upper two metres of the sediment essentially seawater concentrations prevail. In the summer months June, July, and August 2005 sulphate concentrations are lower compared to the remaining months, especially at depths between 1 and 4 m. This higher sulphate depletion is only seen in summer 2005 during the sampling period. Temporal patterns of DOC and TA are mirror images to those of sulphate. The nutrients NH_4^+ , and PO_4^{3-} , exhibit higher concentrations during the summer months in 2005 as well. Only small seasonal variations are seen for H_4SiO_4 .

4. Spatial, seasonal, and tidal variations in tidal flat pore waters

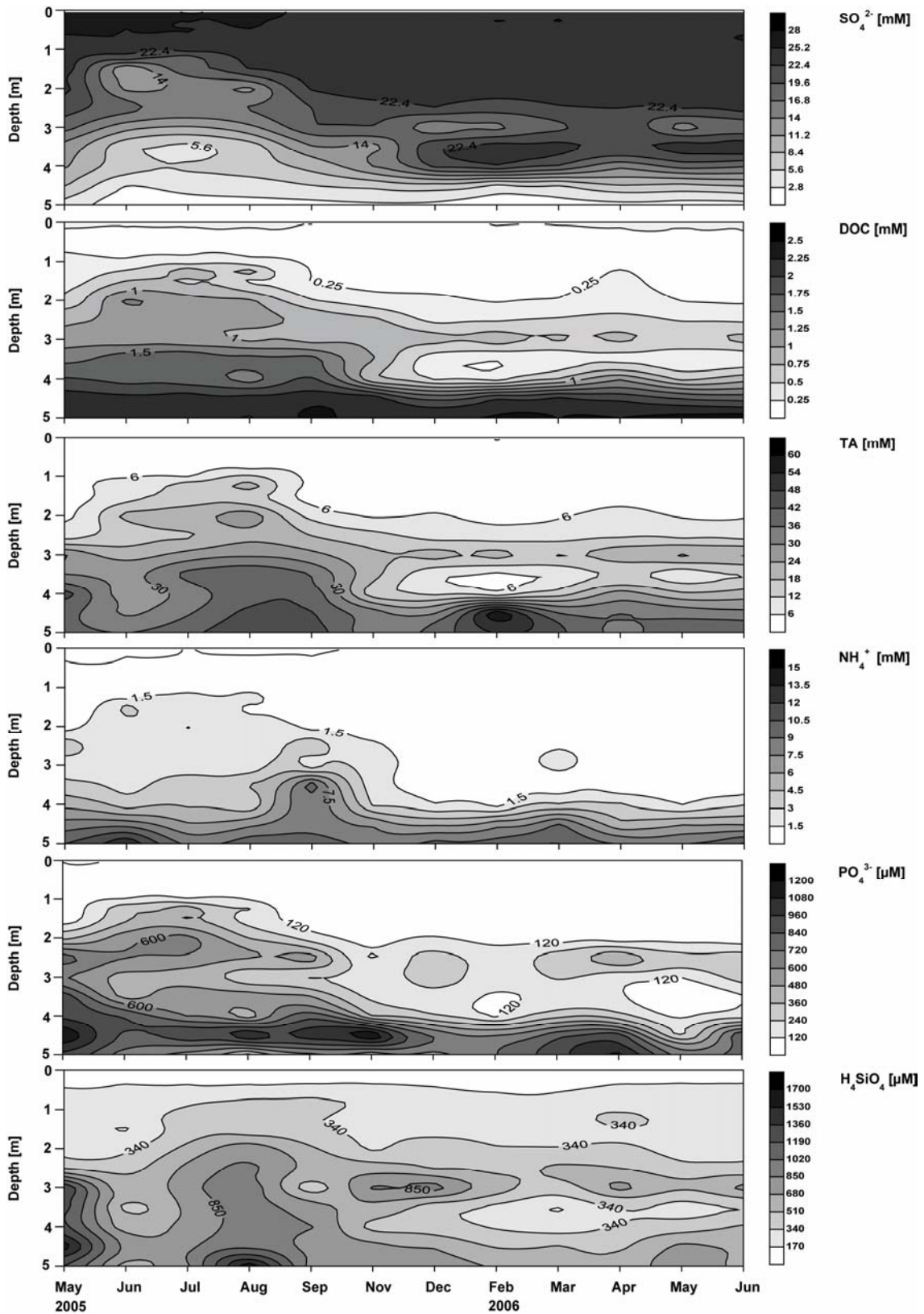


Fig. 4.4.: Seasonal variation of sulphate, DOC, total alkalinity, and nutrients at site JS1 close to the tidal creek. Samples were extracted at the same location from May 2005 until June 2006. Data are interpolated according to Kriging using the program Surfer.

4. Spatial, seasonal, and tidal variations in tidal flat pore waters

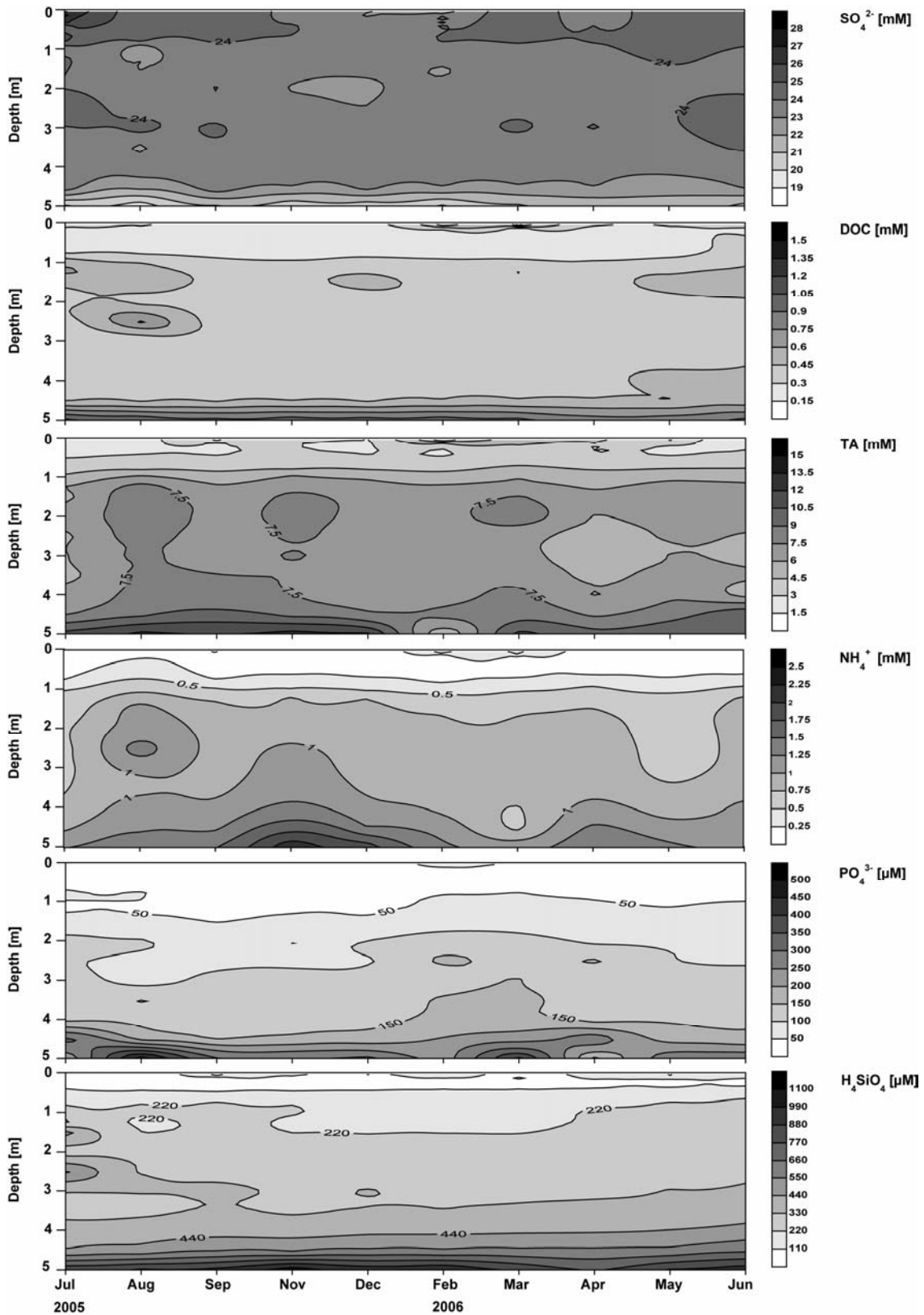


Fig. 4.5.: Seasonal variation of sulphate, DOC, total alkalinity, and nutrients at site JS2 in the centre of the tidal flat. Samples were extracted at the same location from July 2005 until June 2006. Concentration scales are distinct from Figure 4.4. Data are interpolated according to Kriging using the program Surfer.

Figure 4.5. shows seasonal patterns for the same chemical species at site JS2, located in the centre of the intertidal flat (note different concentration scales compared to Fig. 4.5.). In contrast to location JS1, almost no seasonal variations are observed at location JS2. The concentrations of all species remain quite constant within one year, with the steepest concentration gradients always found at the same depth. As in site JS2, little seasonal variations are found at location JS3 (data not shown).

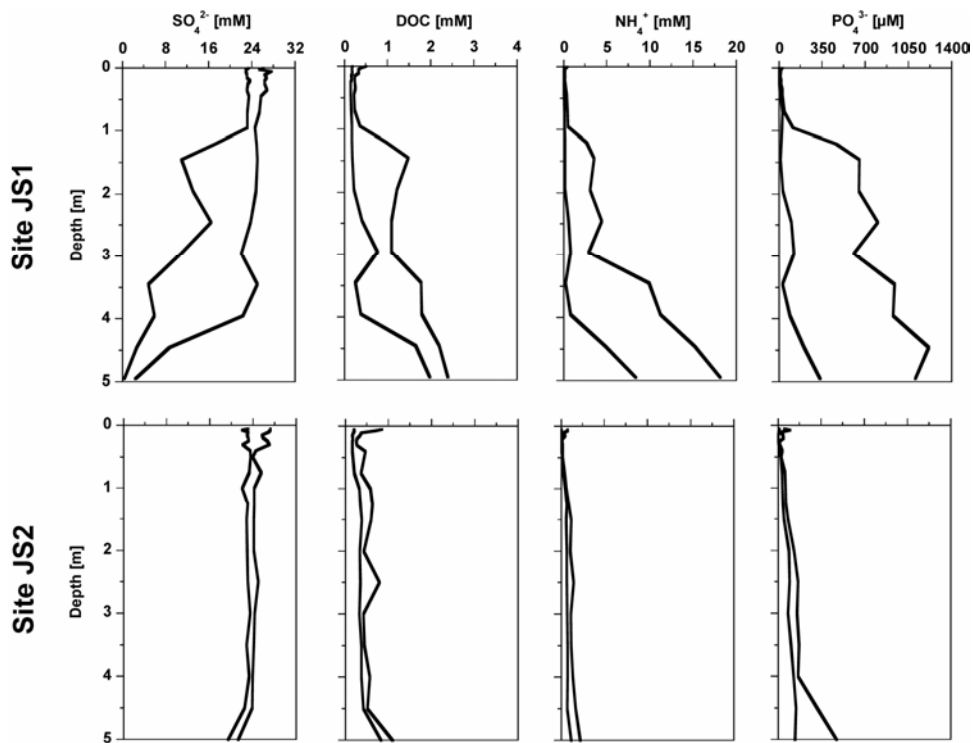


Fig. 4.6.: Minimum and maximum concentrations calculated for specific depths taking all samples into account obtained during 12 sampling campaigns at site JS1 and during 10 campaigns at site JS2. During the sampling period of one year concentrations varied between the minimum and maximum depth profile.

To compare the degree of variations occurring at different sampling locations, minimum and maximum concentrations were calculated for each sediment depth taking all sampling campaigns into account. In Figure 4.6. sulphate, DOC, and nutrient minimum and maximum concentrations are displayed for the locations JS1 and JS2. At site JS3 concentrations vary in a similar range like at site JS2 (data not shown). These minimum

and maximum concentrations illustrate the range of concentrations observed during the sampling period of one year. Concentrations vary most at the location close to the tidal flat margin. Maximum concentrations are up to three times higher than minimum concentrations. In contrast, concentration changes are within a smaller range at locations situated in the centre of the tidal flat. In general, concentrations of all species vary over the entire depth profile leading to distinct minimum and maximum concentrations.

4.3.4. Tidal variations

In June 2006 pore water samples were retrieved at four different time intervals during one tidal cycle at site JS1: at low tide, at mid-tide with rising water level, at high tide, and at mid-tide with falling water level. Depth profiles for DOC, NH_4^+ , TA, and sulphate are shown in Figure 4.7. Tidal concentration changes are seen for DOC, nutrients, and TA with largest variations at 2 to 3 m sediment depth. DOC and NH_4^+ concentrations are increasing two-fold from low to high tide at 2.5 m depth. The concentration variations of sulphate on the other hand are small and within the range of analytical precision.

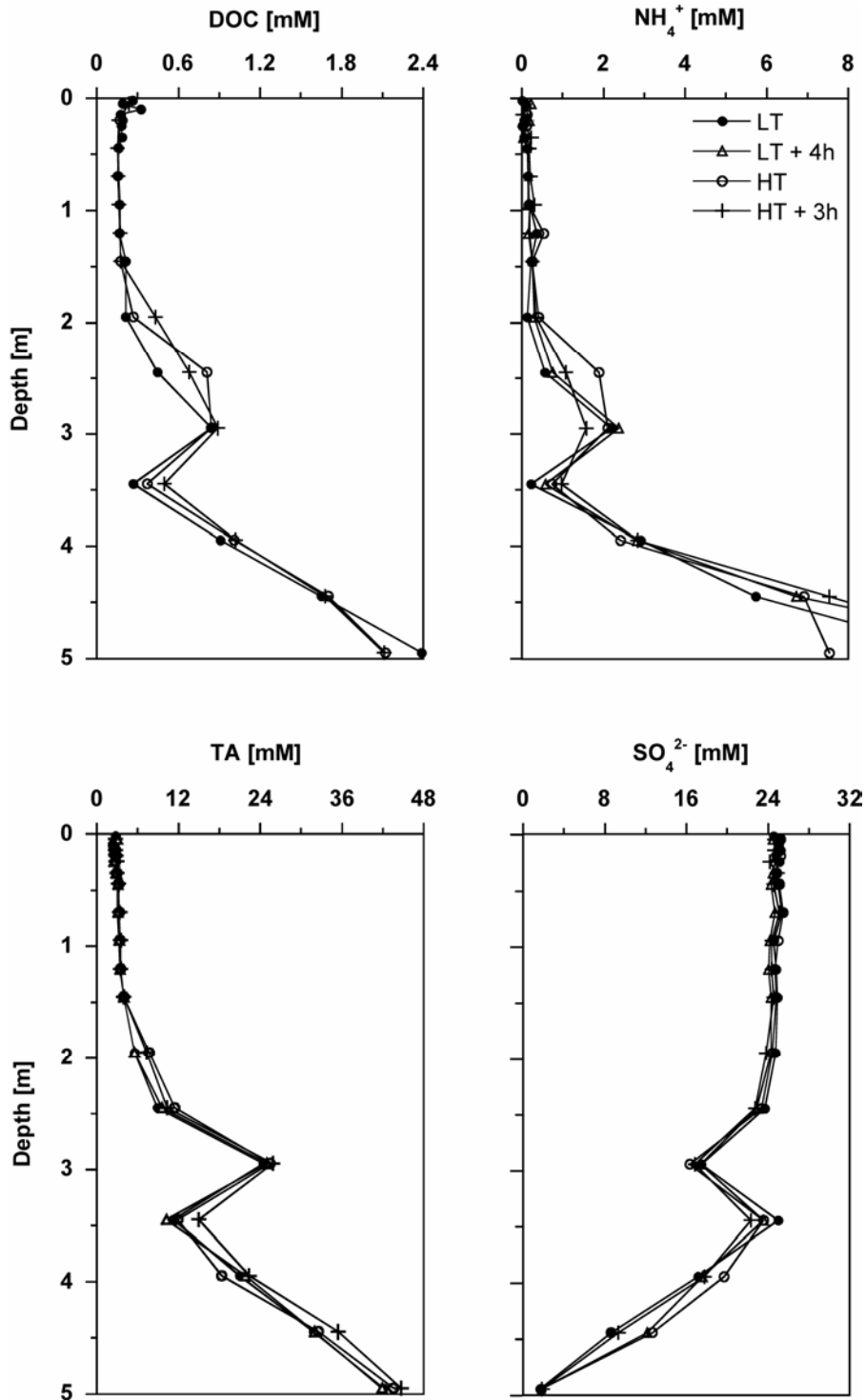


Fig. 4.7.: DOC, NH₄⁺, TA, and SO₄²⁻ pore water concentrations in samples taken at four different states in a tidal cycle, low tide (LT), rising water level (LT + 4h), high tide (HT), and falling water level (HT + 3h) in June 2006. All samples originate from exactly the same sampling location.

4.4. Discussion

4.4.1. Comparison of sand and mixed flat

In the mixed flat concentration changes with depth are more pronounced than in the sand flat area (Fig. 4.3.). Compared to sediments in the centre of the sand flat, higher clay and TOC contents are found in the mixed flat area, especially at depths exceeding 1 m. This difference in lithology can have an impact on microbial activities or pore water exchange processes, both influencing pore water composition. In clay layers lower bacterial activities are found compared to coarser-grained sediments, even when cell numbers are in the same range (Phelps et al., 1989; Chapelle and Lovley, 1990). In the NN tidal flat Köpke et al. (in prep.) detected lower microbial activities in the deep clay layers compared to the upper layers. Consequently, increased microbial activities are unlikely to explain the lower sulphate and higher nutrient concentrations in the deep clay-rich sediment layers in the mixed flat compared to the sand flat.

The difference in pore water chemistry is more likely due to reduced pore water exchange processes in clay-rich layers where small pore diameters hamper pore water diffusion and advection. Clayey sediments have higher porosities and, therefore, more interstitial pore space than sandy sediments, but at the same time reduced hydraulic conductivity and advective transport capacity as a result of increased tortuosity. Reduced pore water exchange processes lead to longer residence times of pore waters in specific sediment layers. We, therefore, suggest that the steeper pore water gradients in the mixed tidal flat are due to longer residence times of pore water within the clay-rich layers. Without a replenishment of the sulphate pool by less altered pore water, the sulphate concentrations decrease more strongly than in more permeable systems. Furthermore, species produced during organic matter mineralization such as nutrients and DOC are enriched in sediments where pore water fluxes are low. In the same study area Köpke et al. (in prep.) also identified lithology, besides the quality of the organic matter, as main factor influencing microbial activity. They concluded that the small diameter of pores in

clayey sediments limits the diffusion of substrates and affects the chemotactic behaviour of microorganisms towards substrate sources.

4.4.2. Comparison of different locations within a sand flat

In the sand flat area sediment geochemistry differs between tidal flat margin and centre. At flat margins current velocities of the overflowing water are supposed to change more frequently than in the centre of the tidal flat, for example depending on the state in the tidal cycle or due to displacements of the tidal creek. Sediment relocations and changes in sediment composition are assumed to be more pronounced at tidal flat margins. Thus, sediment geochemistry reflects several changes between sand- and clay-rich layers at site JS1, whereas sandy sediments dominate in the centre of the tidal flat (Fig. 4.2.).

Biogeochemical processes occurring at site JS1 are described in more detail in Beck et al. (submitted a). At this site a more pronounced depletion in sulphate as well as enrichment in DOC and nutrients are found in depths exceeding 3.5 m when compared to sites JS2 and JS3. The clay-rich sediment layer located between 4 and 5 m depth at site JS1 seems to lead to smaller pore water exchange rates, similar to the situation described for the mixed flat area. Considering the sediment geochemistry at site JS1, the clay-rich sediment layer is however found at less than 4 m depth (Fig. 4.2.). This discrepancy can be caused by the distance of some metres between the locations where pore water was extracted and where the sediment core was taken. Reduced pore water exchange below 3.5 m depth would lead to enrichments in DOC and nutrients in these clay layers compared to the more permeable layers above. Furthermore, the enrichment of DOC and nutrients in depths exceeding 3.5 m depth at site JS1 may as well be explained by a displacement of the tidal flat margin. Within the past 14 years the tidal flat margin moved about 100 m towards the east (B.W. Flemming, pers. comm.) suggesting that site JS1 may formerly have been located at the tidal flat margin in contrast to its recent position 75 m away from the low tide water line. In the study area the tidal flat margin, especially

close to the low water line, is microbially very active and characterized by high concentrations of pore water nutrients (Billerbeck et al., 2006b). Sediments in depths exceeding 3.5 m at site JS1, which show enrichments in nutrients and DOC, probably form part of the former tidal flat margin. The different pore water depth profiles found within the sand flat are thus due to the special sedimentological, hydrological, and biogeochemical situation at site JS1. In general, sandy sediments like those prevailing at sites JS2 and JS3 have low TOC contents leading to limited substrate availability for microorganisms and only small enrichments of metabolic products.

4.4.3. Seasonal variations – temperature and advection effects

Seasonal variations in pore water chemistry are shown for two locations on the JS tidal flat, which differ in their distance to the main tidal creek of the backbarrier area of Spiekeroog Island. At site JS1 higher sulphate depletion is determined during the summer months 2005 compared to the following months (Fig. 4.4.). The activity of sulphate reducing bacteria increases with increasing temperatures in the sediment leading to higher sulphate reduction rates in warm summer months (Vosjan, 1974; Crill and Martens, 1987; Kristensen et al., 2000; Koretsky et al., 2003). At the study site temperatures variations of 2 to 20°C are observed from winter to summer in 1 m sediment depth, of 2 to 17°C in 2 m depth, and of 8 to 12°C in 5 m depth. Temperature variations are thus significant in the upper metres of the sediment and comparably small in sediment depths of 5 m.

At site JS2, which is situated in the centre of the tidal flat, small seasonal sulphate variations are observed (Fig. 4.5.). These less pronounced seasonal variations can be due to small changes in bacterial activities. Temperature changes from the sediment surface to 5 m depth are however supposed to be in a similar range than at site JS1. Therefore, temperature changes and resulting varying activities of sulphate reducers seem to represent only one of the factors leading to the observed seasonal variations at site JS1. Besides temperature, availability and quality of the organic matter used as

substrate also influence microbial activity (Pallud and Van Capellen, 2006). At site JS1 the DOC concentration varies seasonally, with the highest DOC concentrations found in summer 2005 (Fig. 4.4.). However, the bulk parameter DOC does not provide any information about the quality of the organic material, which would be necessary to better estimate the influence on microbial activity. In the study area organic matter was shown to be mainly refractory in greater depth, while easily degradable marine organic matter was only determined in the upper sediment layers (Rusch et al., 1998; Volkman et al., 2000; Köpke et al., in prep). Refractory organic matter is not a very suitable substrate for sulphate reducing bacteria as they prefer short chain carbon molecules, e.g. acetate or lactate (Sørensen et al., 1981; Köpke et al., 2005; Finke et al., 2007).

Several microorganisms that hydrolyse, ferment, and terminally oxidize organic compounds mediate organic matter remineralization in anoxic sediments (Alperin et al., 1994). Hence, the decomposition of organic matter is controlled by a community of microorganisms, where the end product of one step serves as substrate for another. After hydrolysis of complex organic compounds, fermentative microorganisms are able to degrade mono- and polymers into small organic molecules, which are preferred by sulphate reducers (Sørensen et al., 1981). The sampling sites JS1 and JS2 show different TOC contents in the sediment with much higher contents determined at site JS1 (Fig. 4.2.). We therefore hypothesize that more substrate is available for fermentative microorganisms at site JS1 than at site JS2. Dellwig et al. (2001) for example demonstrated that sulphate reducing bacteria have to rely on the preceding decomposition of peat by fungi and/or bacteria as they are unable to use this complex organic matter as substrate. Hydrolysis rates and activities of fermentative microorganisms are enhanced at higher temperatures resulting in higher concentrations of metabolisable organic carbon in summer months (Mayer, 1989; Sansone and Martens, 1982; Alperin et al., 1994; Arnosti et al., 1998; Jahnke et al., 2005). We assume that the increased supply of metabolisable organic carbon stimulated sulphate reducers leading to a higher depletion in sulphate in summer 2005 (Sansone and Martens, 1982). The higher

rates of hydrolysis and fermentation in summer are also reflected in higher DOC concentrations determined in the same period of time (Alperin et al., 1994). The coupling of several factors thus induce the distinct depletion in sulphate at site JS1 and JS2: TOC contents, activity of fermentative microorganisms, availability of metabolisable organic carbon, activity of sulphate reducers. The effect of enhanced sulphate depletion is not seen again until June 2006, probably due to lower temperatures in the sediment compared to the year before. In June 2006 the temperature in 1 m depth is about 15°C, a value comparable to September 2005.

Increased microbial activities and higher remineralization rates of organic matter during the summer months 2005 are also reflected in increased concentrations of the degradation products NH_4^+ , PO_4^{3-} , and TA. As the seasonal pattern of NH_4^+ , PO_4^{3-} , and TA are similar to the seasonal variations of sulphate, sulphate reduction seems to be the dominant remineralization process in the sediment. Seasonal variations of H_4SiO_4 are less pronounced than those of NH_4^+ , PO_4^{3-} , and TA. The latter species are released during the degradation of most forms of organic matter, whereas H_4SiO_4 is mainly released during the degradation of diatom shells. As changes in bacterial activities are assumed to be small at site JS2, seasonal variations of nutrients and TA are hardly determined. Small seasonal variations observed at site JS3 are suspected to result of similar biogeochemical processes as described for site JS2.

After September 2005 sulphate concentrations increase in sediment depths down to 4 m at site JS1 (Fig. 4.4.). This increase in sulphate concentration can be either caused by re-oxidation of sulphide produced during sulphate reduction or by pore water advection replenishing the sulphate pool. Oxidation of sulphide in marine sediments has been described (Fossing and Jørgensen, 1990; Thamdrup et al., 1994), however most of the sulphides precipitate as FeS and FeS_2 if reactive iron is present (Howarth and Jørgensen, 1984; Moeslund et al., 1994). At our study site, the grey and black colour of the sediment gives evidence of FeS and FeS_2 precipitation. Thus, oxidation of H_2S seems to be of minor importance to replenish the sulphate pool. In contrast, a replenishment of the

sulphate pool by pore water advection is likely to occur as deep advective pore water flow is assumed to be generated at tidal flat margins driven by the hydraulic gradient between the sea water level in the tidal creek and the pore water level in the sediment (Wilson and Gardener, 2006). In several studies pore water seeps were found at tidal flat margins (Whiting et al., 1989; Howes and Goehring, 1994; Billerbeck et al., 2006b) suggesting flow in the sediment. The pore water reservoir at tidal flat margins is assumed to be replenished by pore water originating from central parts of the tidal flat where SO_4^{2-} concentrations of about 24 mM are determined down to 4.5 m depth.

Varying bacterial activities and advection seem to control seasonal pattern. Site JS1 is characterized by more pronounced pore water flow than site JS2 and JS3 due to its position closer to the tidal flat margin. We hypothesize that the pore water system at site JS1 is influenced by advection down to sediment depths of about 4 m, whereas advection is of minor importance or much slower at site JS2. The big difference between minimum and maximum concentrations found at location JS1 (Fig. 4.6.), further supports the hypothesis that biogeochemical processes are influenced by advection. At location JS2 slow pore water flow results in a smaller range between minimum and maximum concentrations. Additionally, the smaller range of concentrations determined at site JS2 compared to JS1 is due to lower TOC contents resulting in less pronounced variations in bacterial activities. To which degree seasonal concentration changes occur thus seem to depend on biogeochemical, sedimentological and hydrological properties at the sampling location. The influence of hydrological conditions is further emphasised by seasonal sampling on the mud flat. Two to three sampling campaigns carried out at sites NN1 and NN2 revealed smaller seasonal changes than at site JS1 (data not shown). Water exchange processes were shown to be more limited at the mud flat sites compared to site JS1 thus probably resulting in less fluctuating supply of substrates and bacterial activity.

4.4.4. Advection at tidal flat margins

Seasonal data of site JS1 evidence that this location, close to the tidal flat margin, is influenced by deep pore water advection. Tidal variations determined at the same location further support this assumption (Fig. 4.7.). We suggest that large concentration changes during one tidal cycle, which were particularly determined between 2 and 3 m depths, are due to pore water flow in these depths. The geochemistry of the sediment core shows that sandy sediments predominate down to 2.6 m depths. High Al_2O_3 contents between 1.8 and 2.6 m, indicating clay-rich layers, are due to very thin clay layers or lenses embedded in a sandy matrix (Fig. 4.2.). Taking additionally into account that the lithology of the sediment core does not necessarily match the lithology of the pore water sampling location, a dominantly sandy sediment seems to allow water fluxes at depths down to about 3 m. At high tide pore water shows higher DOC and nutrient concentrations in 2.5 m depth compared to low tide. The reason for this finding is not fully understood as the hydraulic gradient between the sea water level in the tidal creek and the pore water level in the sediment is not only assumed to generate pore water flow towards the tidal creek. Additionally tidal pressure gradients may lead to forward and backward flow of pore water over small distances. In general, we suggest that close to tidal flat margins where pore water is seeping out of the sediment, pore water is replenished by pore water from the central parts of the tidal flat.

Regarding our study area, Billerbeck et al. (2006b) proposed two circulation processes: 1) rapid 'skin circulation' through the upper centimetres of the sediment characterized by short flow paths, low pore water residence time, and immediate feedback to the ecosystem and 2) slow 'body circulation' through deeper layers of the sediment described by long flow paths, long pore water residence times, and enhanced nutrients concentrations, which may represent a nutrient source for the ecosystem. The hypothesis of Billerbeck et al. (2006b) that processes in permeable tidal flats are controlled by these two circulation patterns is supported by the results gained in our study. By means of seasonal and tidal studies we present evidence that deep pore water flow occurs in

permeable sediments located close to tidal flat margins. In centres of tidal flats pore water flow, however, seems to be less pronounced. Geochemical and biological factors influencing pore water concentrations as well as suspected pore water flow pathways are summarized in Figure 4.8.

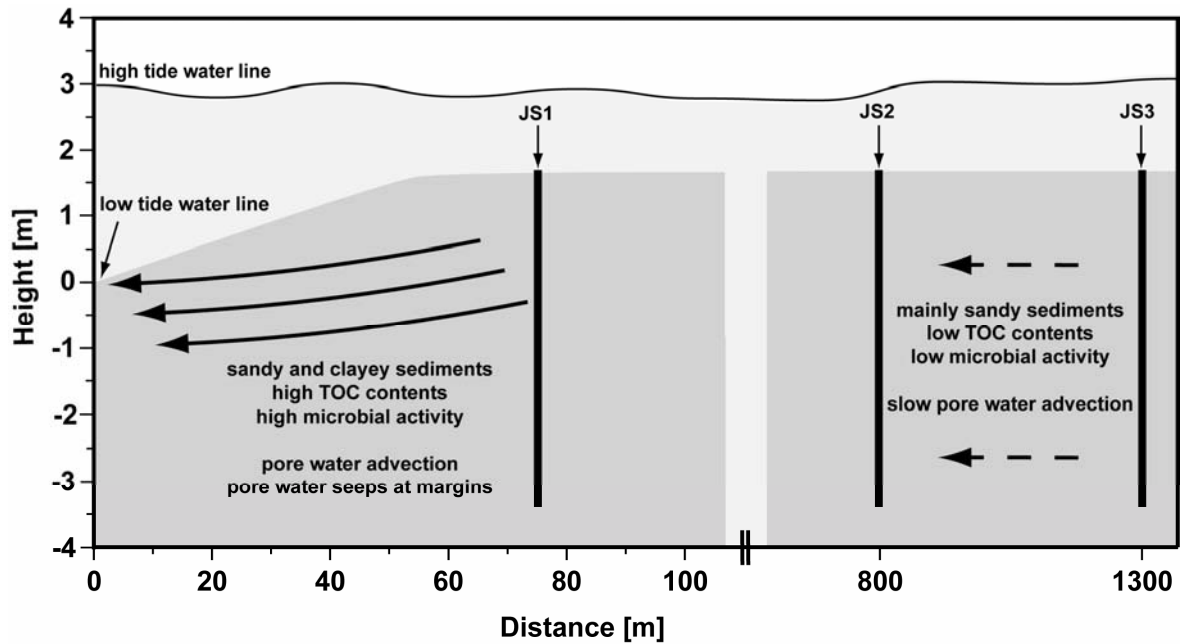


Fig. 4.8.: Summary of geochemical, biological, and hydrological factors influencing the pore water concentrations in the sand flat Janssand. JS1, JS2, and JS3 mark the locations of the pore water samplers, and arrows indicate suspected pore water flow.

4.5. Conclusions

In the tidal flat area of Spiekeroog Island spatial variations in pore water depth profiles are observed. Mixed flats show higher depletions in sulphate and stronger enrichments in DOC, nutrients, and total alkalinity compared to sand flats. The difference in pore water chemistry is likely due to reduced pore water exchange processes in mixed flat sediments which are richer in clay than sand flat sediments. Differences in sediment structure and hydrological conditions explain distinct pore water depth profiles at the JS tidal flat margin compared to central parts of the sand flat.

In permeable systems rich in TOC, seasonal variations were shown to occur down to several metres depths. If the availability of substrate is not limited, the activity of fermentative microorganisms is assumed to increase with increasing temperature even in sediment depths of some metres. Higher activities of fermentative microorganisms lead to a higher production of labile organic compounds thus stimulating the activity of sulphate reducers resulting in a higher depletion of sulphate in summer. As the sulphate pool at tidal flat margins is replenished after the summer months, the pore water system is suggested to be influenced by deep pore water flow. Changes of pore water depth profiles during one tidal cycle present further evidence that deep advection affects biogeochemical processes at tidal flat margins.

Acknowledgements

The authors would like to thank M. Groh for his valuable assistance during all sampling campaigns and C. Lehnert and E. Gründken for their assistance during laboratory work. Furthermore, we wish to thank the TERRAMARE Research Centre for providing transportation to the sampling site by boat and especially H. Nicolai for his help regarding technical questions. We thank J.M. Gieskes for his critical reading of a previous version of this manuscript. We gratefully acknowledge the financial support by the German Science Foundation (DFG, BR 775/14-4) within the framework of the Research Group 'BioGeoChemistry of Tidal Flats' (FOR 432/2).

5. Cycling of trace metals (Mn, Fe, Mo, U, V, Cr) in deep pore waters of intertidal flat sediments

Melanie Beck, Olaf Dellwig, Bernhard Schnetger, Hans-Jürgen Brumsack

This chapter has been submitted to *Geochimica et Cosmochimica Acta*.

Abstract

Trace metals (Mn, Fe, Mo, U, Cr, V) were studied in pore waters of an intertidal flat located in the German Wadden Sea. By spatial and seasonal sampling, the cycling of trace metals in coastal environments, which undergo seasonal changes in organic carbon supply, redox conditions, and deposition of particles should be clarified. *In situ* samplers were used to extract pore waters down to 5 m depth. Trace metals show similar general trends with depth close to the margin and in central parts of the tidal flat. Despite of dynamic biogeochemical, sedimentological, and hydrological conditions prevailing in intertidal flats, the general trends with depth of trace metals are remarkably similar to those observed in deep sea environments where constant sedimentation rates dominate. Seasonal sampling revealed that V and Cr vary seasonally parallel to changes in DOC concentration. This effect is most notably close to the tidal flat margin where sulphate, DOC, and nutrients vary with season down to some metres depth. Seasonal variations of Mn, Fe, Mo, and U are by contrast limited to the upper decimetres of the sediment depending on factors like organic matter supply, redox stratification, and geochemical composition of the particulate matter deposited on sediment surfaces. Pore water sampling within one tidal cycle evidences the occurrence of pore water advection in sediments close to the tidal flat margin. Pore waters originating from some metres depth are presumably escaping at tidal flat margins during low tide. Owing to the enrichment of

specific elements like Mn and V in pore water compared to sea water, seeping pore waters may have an impact on the ecosystem and the chemistry of the open water column.

5.1. Introduction

Organic matter supply and oxygen concentration of the overlying water determines the extent of reducing conditions in surface sediments. Oxygen is the primary oxidant for the degradation of organic matter. Aerobic respiration is followed by nitrate reduction, reduction of Mn and Fe oxides/hydroxides, sulphate reduction and finally methanogenesis (Froelich et al., 1979). In the absence of oxygen pore water concentrations of Mn^{2+} and/ or Fe^{2+} can be indicative of Mn and Fe oxyhydroxides reduction. However, the absence of pore water Mn and Fe does not imply that Mn and/or Fe reduction is not occurring. Precipitation of Fe^{2+} and Mn^{2+} in the form of reduced authigenic minerals, for example as Fe sulphides (Howarth and Jørgensen, 1984; Moeslund et al., 1994) or manganese carbonates (Pedersen and Price, 1982), may lead to low Fe and Mn concentrations in pore water. Furthermore, the succession of degradation processes in tidal flat sediments often slightly differs from the one described by Froelich et al. (1979) owing to distinctly different sedimentological and biogeochemical properties in individual sediment layers.

There has been extensive work on trace metal cycling in deep marine sediments (e.g., Pedersen and Price, 1982; Brumsack and Gieskes, 1983; Andersen et al., 1989a,b; Shaw et al., 1990; Barnes and Cochran, 1991; Huerta-Diaz and Morse, 1992; Wanty and Goldhaber, 1992; Crusius et al., 1996; Adelson et al., 2001; Hyacinthe et al., 2001; Nameroff et al., 2002; Sundby et al., 2004; Morford et al., 2005). However, only few studies focused on trace element cycling in estuarine and tidal flat sediments (Barnes and Cochran, 1993; Kristensen et al., 2003; Audry et al., 2006; Charette and Sholkovitz, 2006; Audry et al., 2007).

In the tidal flat area of Spiekeroog Island, NW Germany, dissolved Mn was shown to vary on tidal and seasonal time scales in the open water column (Dellwig et al., 2007a). Possible sources, which may influence the elemental composition in the study area, are the North Sea, pore water seeping from sediments during low tide, and fresh water flowing irregularly into the tidal flat area via a flood gate. A rough balance estimation revealed that pore water may represent the main source of Mn in spring and summer, whereas fresh water seems to be a potential source in winter (Dellwig et al., 2007a).

Anoxic pore waters are enriched in Mn compared to sea water (Shaw et al., 1990) thus representing a source to the open water column. In permeable sediments where surface topography features like ripples interact with bottom currents, anoxic channels are forming where anoxic pore waters may reach the sediment surface (Huettel et al., 1998). This outflow of anoxic pore water balances the oxygenated water intruding into the sediment at protruding structures. In tidal flat areas anoxic pore waters seem to be additionally released at tidal flat margins where the sediment surface slopes towards a tidal creek. Deep pore water flow is supposedly driven by the hydraulic gradient between the sea water level in the tidal creek and the pore water level in the sediment (Howes and Goehring, 1994; Billerbeck et al., 2006b; Wilson and Gardner, 2006).

In this investigation pore water is studied in surface sediments and down to 5 m depth in the backbarrier area of Spiekeroog Island (NW Germany) to better understand trace element cycling in tidal flat sediments and to extend previous studies (Barnes and Cochran, 1993; Kristensen et al., 2003; Audry et al., 2006) to deep sediment layers. To date, relatively little is known about trace metal cycling in deep tidal flat sediments. Sulphate, sulphide, dissolved organic carbon (DOC), and nutrients were already discussed in detail in previous studies (Beck et al., submitted a,b) to characterize biogeochemical processes. The intent of this study is to investigate on a spatial and seasonal scale the cycling of trace metals in coastal environments, which undergo seasonal changes in organic carbon supply, redox conditions, and sedimentation of particles. Pore water composition may further evidence the enrichment or depletion of

certain elements compared to the open water column. This allows to estimate if seeping pore waters may represent a source to the open water column. Sampling at different times within one tidal cycle may additionally demonstrate the importance of advection on pore water seeping at tidal flat margins.

5.2. Geochemical Background

5.2.1. Manganese and iron geochemistry

The oxidized forms of manganese and iron are Mn(IV) and Fe(III), which are found in nature as solid oxides and hydroxides. In sediments Mn(IV) and Fe(III) oxyhydroxides are easily dissolved under reducing conditions. The product of Mn oxyhydroxide reduction has generally been described to be Mn(II), although Mn(III) may form as well (Sundby et al., 1981; Burdige, 1993 and references therein; Trouwborst, 2006). In anoxic sediments where carbonate concentrations are high, Mn may precipitate as carbonate (e.g., Thomson et al., 1986; Middelburg et al., 1987). Reduction of Fe oxyhydroxides leads to the formation of Fe(II), which forms insoluble phases such as pyrite FeS₂ and iron monosulphides FeS (e.g., Berner, 1984; Howarth and Jørgensen, 1984; Moeslund et al., 1994). Mn and Fe oxyhydroxides can be reduced by microbial (Lovley, 1995; Todorova et al., 2005) or by abiotic pathways where for example sulphide, nitrite or Fe²⁺ (for Mn oxyhydroxides) are used as electron donors (Burdige and Nealson, 1986; Myers and Nealson, 1988; Hulth et al., 1999). Both Mn and Fe oxyhydroxides are known to scavenge a variety of trace elements (e.g., Mo, U, V) either by surface adsorption or by direct incorporation into the crystal structure (Burdige, 1993, and references therein). Thus, reduction/dissolution and oxidation/precipitation of Mn and Fe oxyhydroxides cause cycling of associated trace metals between solid sediment phases and corresponding pore waters.

5.2.2. Molybdenum and uranium geochemistry

Molybdenum – In oxic seawater molybdenum (Mo) is present in the stable oxidation form Mo(VI) as MoO_4^{2-} . The characteristics of Mo in ocean water are its conservative behaviour and its high dissolved concentration of about 110 nM at salinity 35 (Morris, 1975; Collier 1985). Several studies have shown that deviations from the conservative behaviour occur under certain biological, sedimentological, and geochemical conditions (Yamazaki and Gohda, 1990; Tuit and Ravizza, 2003; Dellwig et al., 2007b). Increased Mo concentrations are found in MnO_2 -rich oxic sediments because of Mo adsorption onto Mn oxyhydroxides (Bertine and Turekian, 1973; Crusius et al., 1996; Adelson et al., 2001; Sundby et al., 2004; Morford et al., 2005; Audry et al., 2006). In reducing sediments, a key step in Mo scavenging from seawater is the conversion of particle inert MoO_4^{2-} to particle reactive thiomolybdates ($\text{MoO}_x\text{S}_{4-x}^{2-}$, $x = 0$ to 3) (Helz et al., 1996; Erickson and Helz, 2000; Zheng et al., 2000; Vorlicek and Helz, 2002; Vorlicek et al., 2004). Thiomolybdates are readily scavenged from solution by sulphidized Fe phases and humic materials. Erickson and Helz (2000) propose that MoO_4^{2-} reacts to MoS_4^{2-} at sulphide concentrations of about 11 μM . Zheng et al. (2000) postulate that there are two thresholds for Mo precipitation, one where pore water sulphide concentrations reach a concentration of $\sim 0.1 \mu\text{M}$ and a second at sulphide concentrations of $\sim 100 \mu\text{M}$. They hypothesize that under low sulphide concentrations Mo precipitation occurs in the presence of Fe, whereas at high sulphide concentrations Fe is not required for Mo precipitation. Furthermore, Mo was shown to be associated with dissolved organic substances in sea and pore water (Brumsack and Gieskes, 1983; Yamazaki and Gohda, 1990).

Uranium – Uranium is present in sea water at a concentration of $\sim 13 \text{ nM}$ as stable, soluble U(VI) carbonate complex $\text{UO}_2(\text{CO}_3)_3^{4-}$, which shows a conservative behaviour (Ku et al., 1977). The main removal process of U is uptake from the water column to the sediment, reduction to U(IV) and subsequent adsorption or precipitation (Anderson et al., 1989a; Barnes and Cochran, 1991; Klinkhammer and Palmer, 1991). In several studies a coupling between Fe and U cycling was observed in sediments either suggesting

scavenging of U by Fe oxyhydroxides or microbially mediated conversion of both species (Cochran et al., 1986; Barnes and Cochran, 1990; Lovley et al., 1991; Lovley et al., 1993; Barnes and Cochran, 1993; Church et al., 1996; Duff et al., 2002; Sani et al., 2004; Audry et al., 2006; Morford et al., 2007). Anderson et al. (1982) showed that U is fixed to particles in surface sea water and hypothesized that organic matter is the carrier phase, which was proposed by Anderson et al. (1989b), Shaw et al. (1994), and McManus et al. (2005) as well.

5.2.3. Vanadium and chromium geochemistry

Vanadium – In oxygenated seawater V is present in the stable oxidation form V(V) as the anions H_2VO_4^- and HVO_4^{2-} (Wehrli and Stumm, 1989). V is evidently associated with Mn cycling (Wehrli and Stumm, 1989; Shaw et al., 1990; Morford et al., 2005) and with oxygenated Fe phases (Shaw et al., 1990; Morford and Emerson, 1999). Under more reducing conditions V(IV) and V(III) are the stable oxidation states, which are very particle reactive (Shaw et al., 1990; Audry et al., 2006). Wanty and Goldhaber (1992) showed that high concentrations of sulphide can result in a reduction of V(IV) to V(III), which precipitates as relatively insoluble V(III) oxyhydroxide. Furthermore, V forms stable complexes with dissolved organic material (Szalay and Szilágyi, 1967; Brumsack and Gieskes, 1983; Wanty and Goldhaber, 1992).

Chromium – Chromium exists in oxic sea water predominantly as the chromate (VI) anion CrO_4^{2-} and to a lesser extent as the cationic aquahydroxy (III) species $\text{Cr}(\text{OH})_2^+(\text{H}_2\text{O})_4$ (Cranston and Murray, 1978; Cranston, 1983; Mugo and Orians, 1993). Under reducing conditions Cr is present as the Cr(III) ion $\text{Cr}(\text{H}_2\text{O})_4(\text{OH})_2^+$ (Cranston and Murray, 1978). In anoxic sediments Cr(VI) is reduced to Cr(III) (Hursthouse et al., 2003) and removed from solution, probably by the adsorption of $\text{Cr}(\text{H}_2\text{O})_4(\text{OH})_2^+$ on particle surfaces. Furthermore, Cr was shown to be associated with dissolved organic matter (Brumsack and Gieskes, 1983).

5.3. Study area

The Wadden Sea forms one of the largest tidal flat areas extending along the coastline for almost 500 km between Den Helder (Netherlands) and Skallingen (Denmark) (Fig. 5.1.). The tidal flat areas extend between the coastline and a chain of barrier islands, which form a boundary between the North Sea and the Wadden Sea. The chain of barrier islands is separated by tidal inlets enabling water exchange between the tidal flat areas and the North Sea. The backbarrier area of each island is further characterized by a tidal channel system consisting of large main channels and smaller secondary channels (Flemming and Davis, 1994).

The study was carried out in the backbarrier area of Spiekeroog Island, which represents one of the East Frisian Islands in NW Germany (Fig. 5.1.). Sampling was conducted on the intertidal flat Janssand (JS), located in the western part of the backbarrier area (Fig. 5.1.). The study area is characterized by semi-diurnal tides and a tidal range of 2.6 m (Flemming and Davis, 1994). During high tide the JS tidal flat is covered by 1 - 2 m of water. It becomes exposed to the atmosphere for approximately 6 hours during low tide, depending on tidal range and wind direction. The tidal flat surface is almost horizontal, except for the eastern margin where the sediment surface slopes towards the main tidal creek. At low tide the difference in altitude between the sea water level and the horizontal part of the tidal flat amounts to approximately 1.5 m. Sampling was carried out at three locations on JS tidal flat (JS1: 53° 44.183' N, 007° 41.904' E; JS2: 53° 43.962' N, 007° 41.283' E; JS3: 53° 43.844' N, 007° 40.873' E). The locations are numbered according to their distance from the tidal flat margin, with number 1 being situated closest to the tidal creek. At low tide the distance between the sampling location JS1 and the water line is approximately 70 m. The distance between site JS1 and site JS2 amounts to 800 m, while site JS3 is located 500 m southeast of site JS2.

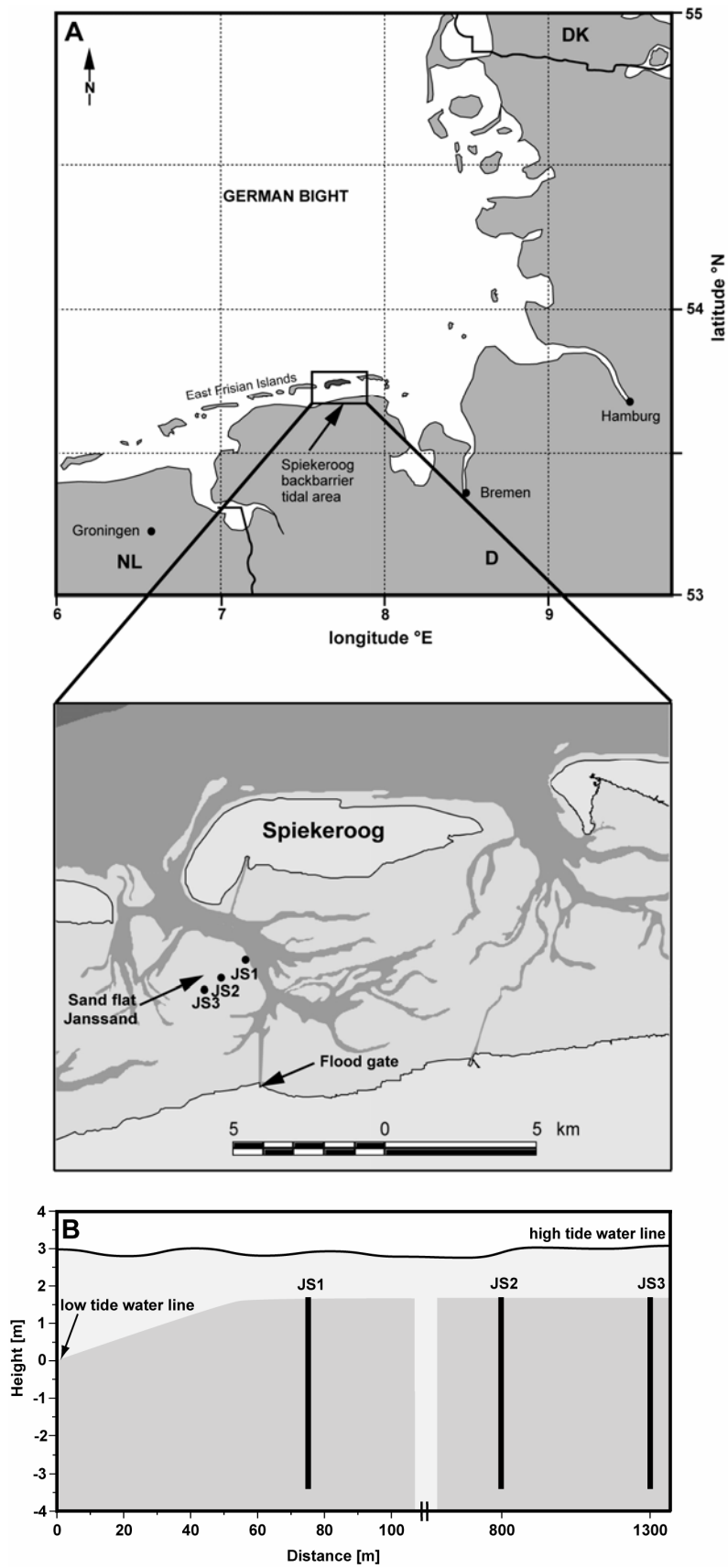


Fig. 5.1.: (A) Study sites on an intertidal sand flat (JS) in the backbarrier area of Spielerog Island, Wadden Sea, Germany. (B) Tidal flat topography.

5.4. Methods and analytical procedures

5.4.1. Pore water sampling

Pore water was extracted using *in situ* samplers described in more detail in Beck et al. (2007). The samplers remained permanently installed in the sediment to allow repetitive sampling at identical locations and depth intervals. Shortly, the sampler consists of a pipe with holes drilled into the pipe walls serving as sampling orifices. The sampling ports are linked to sampling devices located at the sediment surface by PTFE (teflon) tubings. At the top of the sampler PE (polyethylene) syringes are connected to the sampling system to extract pore water from the sediment. Pore water sampling is conducted in 20 different depths, with the upper metre sampled in higher resolution (0.05 m, 0.07 m, 0.10 m, 0.15 m, 0.20 m, 0.25 m, 0.30 m, 0.40 m, 0.50 m, 0.75 m) than deeper sediment layers (1.0 m, 1.25 m, 1.5 m, 2.0 m, 2.5 m, 3.0 m, 3.5 m, 4.0 m, 4.5 m, and 5.0 m). Depending on sampling depth and diameter of the PTFE tubes, different volumes of pore water are discarded before taking samples for analyzes. With regard to the analysis of trace metals, the sampler was constructed avoiding metal components and thus the possibility of metal contamination.

One sampling campaign carried out on April 24th and 25th 2006 on the JS tidal flat was chosen to exemplify pore water depth profiles. To study seasonal pore water variations, samples were taken on the tidal flat throughout one year. The time interval between consecutive samplings ranged from three to nine weeks. On the JS tidal flat 12 samplings campaigns were conducted at site JS1 from May 2005 to June 2006. At this site pore water was always sampled at falling water level. At locations JS2 and JS3 sampling campaigns started in July 2005, and 10 campaigns were carried out until June 2006. Furthermore, pore water was extracted four times during one tidal cycle at site JS1 on June 28th 2006. Sampling started at low tide and lasted until three hours after high tide.

All samples for trace metal analysis were immediately filtered through 0.45 µm SFCA (surfactant-free cellulose acetate) syringe filters after extraction. Subboiled HNO₃ was added to obtain a concentration of 1% (v/v) in all samples. Samples were stored in PE

bottles, which were acid washed and rinsed with ultrapure water prior to use. All samples were stored at 4-6°C until analysis. Samples for DOC and H₂S analysis were obtained according to procedures described in Beck et al. (submitted a).

5.4.2. Analytical procedures

Trace metals were analyzed using a high resolution inductively coupled plasma mass spectrometry ICP-MS (Thermo Finnigan MAT Element). The applied analytical procedure is similar to the method published by Rodushkin and Ruth (1997). Pore water samples were diluted 25-fold with 0.3 M HNO₃. To account for variations in the performance of the ICP-MS during analysis, a solution containing internal standards was added to the diluted pore water samples. As internal standards Y (for Cr, Fe, Mo, V), In (for U) and Cs (for Mn) were chosen. Calibration solutions were prepared using the same acid and the same internal standards than used for the samples. Low-resolution mode was applied to measure Y (89), Mo (98), In (115), Ba (137), and U (238), whereas V (51), Cr (52), Mn (55), Fe (56), Y (89), and Cs (133) were analyzed in medium-resolution mode.

Precision and accuracy of the analytical procedure were controlled by the reference materials Cass-4 (Nearshore seawater for trace metals) and Slew-3 (Estuarine water for trace metals, both National Research Council, Canada). A solution containing Mn and Fe was added to the reference material to control accuracy and precision of Mn and Fe analyzes as concentrations are much higher in the Wadden Sea pore water than in the original reference material. Certified and measured concentrations of the reference materials Cass-4 and Slew-3 besides accuracy and precision of the measurements are summarized in Tables 5.1. and 5.2.

5. Trace metal dynamics in intertidal flat pore waters

Table 5.1.: Replicate analyzes of Cass-4 seawater reference material (n = 105). Measured and certified values are reported as average concentration \pm standard deviation. Accuracy and precision of the measured Cass-4 samples are displayed.

Element [nM]	Cass-4 certified	Cass-4 measured	Accuracy [%]	Precision [%]
Fe	3594 ^a	3617 \pm 238	0.7	6.6
Mn	3691 ^a	3768 \pm 149	2.1	3.9
Mo	91.5 \pm 9.0	100.8 \pm 5.8	10.2	5.8
U	12.6 ^b	12.0 \pm 0.5	-5.0	4.4
V	23.2 \pm 3.1	24.2 \pm 1.8	4.4	7.2

(a) solution containing 3640 nM Mn and 3581 nM Fe was added to Cass-4

(b) U concentration in Cass-4 is only for information and not certified

Table 5.2.: Replicate analyzes of Slew-3 estuarine reference material (n = 55). Measured and certified values are reported as average concentration \pm standard deviation. Accuracy and precision of the measured Slew-3 samples are displayed.

Element [nM]	Slew-3 certified	Slew-3 measured	Accuracy [%]	Precision [%]
Fe	3592 ^a	3695 \pm 299	2.9	8.1
Mn	3670 ^a	3707 \pm 195	1.0	5.3
Mo	53.2 ^b	56.3 \pm 3.7	6.0	6.4
U	7.6 ^b	7.0 \pm 0.4	-7.2	5.7
V	50.5 \pm 1.8	58.6 \pm 3.5	15.8	6.1

(a) solution containing 3640 nM Mn and 3581 nM Fe was added to Cass-4

(b) Mo and U concentration in Slew-3 is only for information and not certified

Replicate measurements of Cass-4 and Slew-3 indicate that the precision for 25-fold sea water solutions is at least <8%. Accuracy of the measurements varies depending on the element. Measured Fe and Mn concentrations are close to the expected values, whereas measured Mo and V concentrations are slightly higher and U concentrations are somewhat lower than the certified values. The certified Cr concentration is below the detection limit of the method. DOC is analyzed according to procedures described in Beck et al. (submitted a).

5.5. Results and Discussion

In an intertidal flat the trace metals Mn, Fe, Mo, U, V, and Cr were studied in pore waters down to 5 m sediment depth. Biogeochemical parameters such as sulphate, sulphide, nutrients (ammonium, phosphate, silicate), and dissolved organic carbon (DOC) determined in pore waters of the same sites are described in detail in Beck et al. (submitted a,b). Briefly, site JS1 is situated close to the tidal flat margin and was shown to be biologically very active (Fig. 5.1.; Billerbeck et al., 2006b). Sites JS2 and JS3, which are located in central parts of the tidal flat, seem to represent a less biologically active environment as reflected in lower DOC, nutrient, and total alkalinity concentrations compared to site JS1 (Beck et al., submitted b). At site JS1 sulphate reduction was identified as dominant organic matter remineralization pathway resulting in high sulphide concentrations up to 5.5 mM. In contrast, sulphide concentrations are in the low μM range at almost all depths at sites JS2 and JS3. At the study sites the sediment is anoxic below some centimetres depth as reflected in an oxygen penetration depth of about 4 cm close to site JS1 (Billerbeck et al., 2006b).

5.5.1. Intertidal flat close to the tidal flat margin

Figure 5.2. shows trace metal (Mn, Fe, Mo, U, V, Cr) and DOC pore water depth profiles obtained at site JS1. Pore water Mn concentrations are slightly higher in the upper centimetres of the sediment than in the section below. In the study area suspended particulate matter (SPM) is enriched in Mn compared to average shale especially in summer (Dellwig et al., 2007a). During algae breakdown the release of organic compounds like transparent exopolymer particles (TEP) leads to the formation of larger aggregates (Passow, 2002; Chen et al., 2005; Lunau et al., 2006; Passow and De la Rocha, 2006). Such aggregates have higher settling velocities than their constituent particles and deposit on sediment surfaces (Chang et al., 2006c). Subsequently, they are incorporated into the sediment by pore water advection (Huettel et al., 1996; Huettel and

Rusch, 2000; Rusch and Huettel, 2000). When reducing conditions in the sediments are encountered, particulate Mn oxyhydroxides are dissolved leading to increasing Mn pore water concentrations (Fig. 5.2.). Comparable observations are reported by Sundby et al. (1981) and Morford et al. (2007) concerning marine sediments.

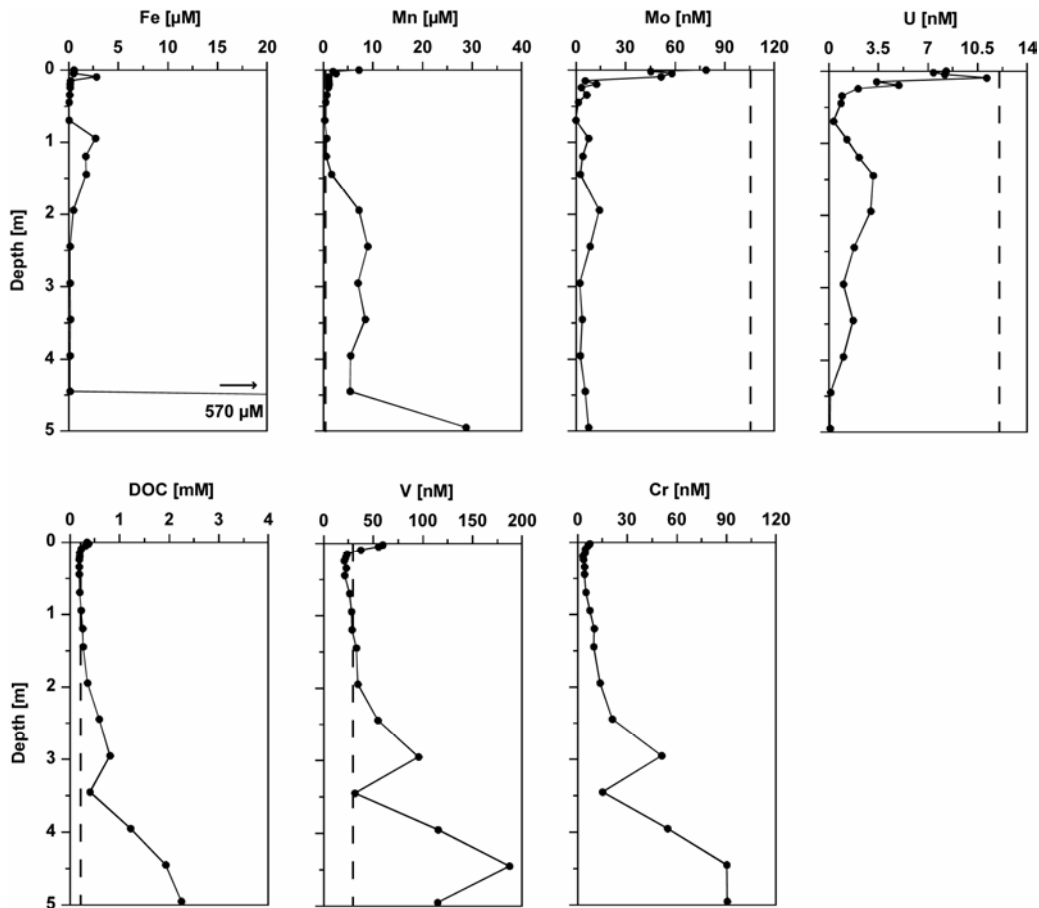


Fig. 5.2.: Trace metal (Fe, Mn, Mo, U, V, Cr) and DOC pore water profiles at site JS1, located close to the tidal flat margin of an intertidal sand flat. Samples were taken in April 2006. Fe concentration at 5 m depth is indicated by a number as it is exceeding the scale. Dashed lines mark concentrations in the open water column of the study area.

In the upper first metre of the sediment Mn concentrations are within the range of 0.01 to 1.6 μM as documented for the open water column of the study area (Dellwig et al., 2007a). This may either be due to some vertical infiltration of sea water induced by tidal sea level changes or by the formation of anoxic channels underneath of protruding

surface structures where anoxic Mn-enriched pore waters are seeping out at the sediment surface (Huettel et al., 1998). Both processes may counteract the enrichment of Mn in the upper sediment layers.

At sediment depths exceeding 1.5 m Mn increases to a concentration level of about 7 μM . In contrast to the sediments above, these layers thus show diagenetically stronger altered pore waters. This either reflects differences in the sedimented material such as Mn oxyhydroxide content, different sedimentation ages, or changing pore water exchange processes. Silt-clay lenses and very thin clay layers, which are intermingled in the sandy sediment at 1.8 to 2.5 m depths, supposedly limit water exchange with layers above resulting in a steep increase of Mn concentrations in depths exceeding 1.5 m depth.

At 5 m depth the pore water profile exhibits an unexpected high Mn concentration of 29 μM . This finding is confirmed by all sampling campaigns carried out within one year. Mn reduction rates in sediments depend on the supply of metal oxyhydroxides and on the reducing capacity of the sediment. The reducing capacity is unlikely to change at 5 m depth. We thus hypothesize that the pore water sampling orifice is located in a sediment layer formerly enriched in Mn oxyhydroxides which bears the potential to release high amounts of Mn^{2+} under reducing conditions.

Reduction of deposited particulate Fe oxyhydroxides leads to a slight increase in pore water Fe concentration close to the sediment surface (Fig. 5.2.). In general, reduction of Fe oxyhydroxides has presumably occurred at all sediment depths except for the oxic sediment surface. Below 2 m depth very low pore water Fe concentrations are determined due to the precipitation of FeS and FeS₂ phases at sulphide concentrations in excess of 0.6 mM (Beck et al., submitted a,b). Regarding the light blackish colour of the sediment above 2 m, FeS also precipitates at these depths, supposedly in smaller quantity because of lower sulphide concentrations (Böttcher et al., 2000). At 5 m depth a very high Fe concentration of almost 600 μM is encountered, which is confirmed in all sampling campaigns conducted throughout one year. As Fe and Mn are remarkably enriched in pore waters of 5 m depth, both elements have supposedly been released from

sedimentary oxyhydroxides formerly deposited at this location at high concentration levels. Fe silicates are unlikely to have reacted with sulphide thus supplying Fe to pore waters. For instance, in Peru Margin sediments this poorly reactive Fe fraction was shown to be only sulphidized on a million year time scale (Raiswell and Canfield, 1996). Furthermore, sulphate has almost completely been consumed by sulphate reducers at 5 m depth (Beck et al., submitted a,b) suggesting that little sulphide is produced at this depth. A low sulphide level limits the precipitation of Fe sulphides further explaining high pore water Fe concentrations at this depth.

Mo shows its highest concentration close to the sediment surface where Wadden Sea water infiltrates into the sediment which generally exhibits a Mo concentration slightly below the offshore value of the German Bight (103 nM). In oxic sediment layers Mo remains dissolved in pore waters and concentrations close to the sea water value are observed. For instance, Morford et al. (2007) determined Mo concentrations of about 110 nM in surface sediments of Boston Harbor, USA. However, Mo concentrations are about one third lower than 105 nM in the upper centimetres of the sediment at site JS1 suggesting that just below the sediment surface slightly reducing conditions prevail. At 0.15 m sediment depth Mo decreases sharply indicating Mo precipitation. The master variable regulating Mo precipitation is the concentration of sulphide in pore water (Helz et al., 1996; Erickson and Helz, 2000; Zheng et al., 2000; Vorlicek et al., 2004). Sulphide concentrations are higher than the threshold for the co-precipitation of Mo-Fe-S in the upper part of the sediment and at depths exceeding 1.5 m they even reach values for the onset of Mo precipitation without Fe (Zheng et al., 2000).

Depth profiles of U and Mo are rather similar (Fig. 5.2.). Close the sediment surface U concentrations are about one third lower than the average Wadden Sea value of 12 nM. U shows a sharp decrease in concentration at 0.35 m depth where U(VI) is suspected to be reduced to U(IV), which is removed from solution by adsorption or precipitation (Anderson et al., 1989a; Barnes and Cochran, 1991; Klinkhammer and Palmer, 1991; Morford et al., 2007). Slight increases in U at about 1 m depth are presumably not related to the release

of U during Fe and Mn oxyhydroxide reduction (Church et al., 1996; Elbaz-Poulichet et al., 2005; Morford et al., 2005, 2007). Instead, concentrations at this depth interval seem to be influenced by deep pore water advection (compare 5.3.). Such U increases are not always observed during our monthly sampling campaigns. Due to advection different diagenetically altered pore waters seem to be extracted at these depths.

In pore water V and Cr seem to be adsorbed by DOC because of higher concentrations in sediment depths with higher DOC levels (Fig. 5.2.; Brumsack and Gieskes, 1983; Wanty and Goldhaber, 1992). The only exception is the sample retrieved at 5 m depth where V and Cr decrease or remain constant in spite of increasing DOC. Concerning the data set obtained during twelve sampling campaigns a regression analysis of DOC against V results in a correlation coefficient of 0.90 excluding results at 5 m depth. Regression analyzes thus support the hypothesis that V is adsorbed to DOC in deep pore waters. Recycling of V with Mn oxyhydroxides likely occurs close to the sediment surface where scavenged V seems to be released during Mn oxyhydroxide reduction (Shaw et al., 1990; Morford and Emerson, 1999). This is indicated by V concentrations higher than the Wadden Sea value of about 30 nM, which is observed in surface sediments exclusively influenced by sea water infiltration. The cycling of V with Mn oxyhydroxides is not observed in deep pore waters. Furthermore, V and Cr show a decrease in concentration in the upper centimetres of the sediment suspecting a transformation of these elements into their reduced states, which are less soluble and are easily adsorbed by particles or organic matter (Shaw et al., 1990; Hursthouse et al., 2003).

5.5.2. Central parts of the intertidal flat

The general features describing pore water geochemistry close to the tidal flat margin are also valid in central parts of the tidal flat (Fig. 5.3.). The exception is Fe, which exhibits quite different depth profiles. At site JS1 Fe concentrations are low due to precipitation of Fe sulphides. In the centre of the tidal flat sulphide concentrations are, however, much

lower compared to site JS1 (Beck et al., submitted b). At site JS2 high pore water Fe concentrations, especially at 2.5 to 4 m depth, thus seem to be due to limited Fe sulphide precipitation. Besides sulphide concentration, reactive sedimentary Fe is a further key factor in controlling pore water Fe concentrations. For example, sulphide concentrations are comparable at sites JS2 and JS3 (Beck et al., submitted b), but Fe^{2+} remains low at greater depths at site JS3 in contrast to site JS2. We thus assume that less reactive sedimentary Fe is present at site JS3.

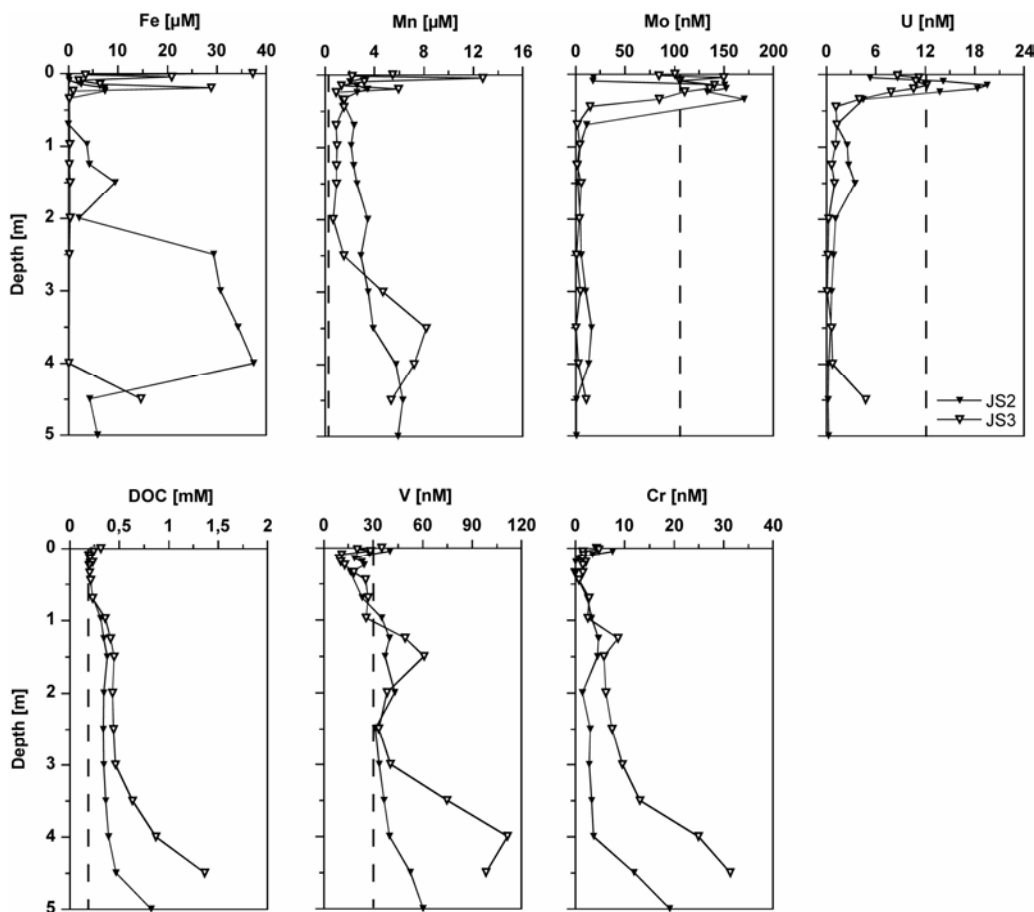


Fig. 5.3.: Trace metal (Fe, Mn, Mo, U, V, Cr) and DOC pore water profiles at sites JS2 and JS3, located in the central parts of an intertidal sand flat. Samples were taken in April 2006. Dashed lines mark concentrations in the open water column of the study area.

In central parts of the tidal flat Mn and Fe are also determined in higher concentrations at the sediment surface than in some decimetres depth illustrating the

deposition of Mn- and Fe-rich particles at the surface and their subsequent reduction after incorporation into the sediment (Fig. 5.3.). Pore water Mn increases to a lower extent with depth in the centre of the tidal flat compared to the margin. The lower Mn concentrations seem to be due to a lower content of Mn oxyhydroxides in the sandy sediments of the central flat where clay layers like at site JS1 are rare (Beck et al., submitted b).

The general shape of Mo and U depth profiles is similar at all sites, however the sharp decrease in concentration is found at different depths depending on location (Fig. 5.3.). In April 2006 the gradient between oxic and anoxic conditions seems to be steepest at site JS1 indicating the reduction of Mo(VI) and U(VI) at shallower depths compared to sites JS2 and JS3. More organic material is presumably introduced into the sediment at site JS1 due to surface advection induced by ripples, resulting in a faster consumption of oxygen. The organic material may be derived from an algae bloom, which occurred in the study area at the beginning of April (M. Grunwald, pers. comm.). In contrast to site JS1 where Mo and U concentrations are below the sea water value at the sediment surface, Mo and U are enriched in pore waters close to the surface at sites JS2 and JS3. We assume that the material deposited at the sediment surface at sites JS2 and JS3 is enriched in Mo (Dellwig et al., 2007b), whereas U is scavenged by organic material produced at these sites (Anderson et al., 1989b). Thus, Mn and U are released when the material is degraded in the upper sediment layers (Dellwig et al., 2007b; compare 5.2.3., 5.2.4.).

At sites JS2 and JS3 V and Cr depth profiles are comparables to those at site JS1 with sea water concentrations close to the sediment surface, decreasing concentrations below and coupling of V and Cr with DOC in deeper pore waters (Fig. 5.3.). However, the correlation between DOC and V or Cr is less pronounced than at site JS1.

5.5.3. Comparison with pore waters of marine sediments

Despite of more dynamic biogeochemical, sedimentological, and hydrological conditions prevailing at tidal flat margins (Billerbeck et al., 2006b; Beck et al., submitted

a,b), trace metals show similar general trends with depth at the margin and in central parts of the tidal flat (Figs. 5.2., 5.3.). These general trends with depth observed in deep pore waters of an intertidal flat are comparable to those determined in the upper decimetres of anoxic marine sediments. Concerning Mo and U, a consistent decrease from the sediment surface to non-zero asymptotic values were observed in several pore water studies of marine sediments (Anderson et al., 1989b; Barnes and Cochran, 1991; Klinkhammer and Palmer, 1991; Elbaz-Poulichet et al., 2005; McManus et al., 2005; Morford et al., 2007). In marine sediments depth profiles comparable to those in tidal flat sediment are recognized, suggesting that similar processes lead to Mn and U removal from pore waters in both environments. In contrast to most marine sediments, concentration-depth profiles in tidal flat sediments are not solely dominated by diffusion but often influenced by advection. Furthermore, sedimentation rates are not constant in tidal flat environments where erosion dominates in winter and periodic deposition occurs in summer (Chang et al., 2006b,c). Both aspects may lead to the shifting of comparable biogeochemical processes into different depth intervals. By fitting a diffusion-reaction model to measured profiles, Morford et al. (2007) showed that the depth order in which trace metals are removed is $U < Mo$. This depth order is not confirmed by our study suggesting that the depths of metal removal are influenced by advective sea water infiltration into the tidal flat sediment and the presence/absence of e.g. DOC and sulphide.

In sulphide bearing sediments Fe is rapidly removed from pore waters by precipitation of Fe sulphides (Howarth and Jørgensen, 1984; Böttcher et al., 2000). Consequently, pore water Fe is expected to decrease in those depths where sulphide increases (Morford et al., 2007). This inverse correlation between Fe and sulphide is not seen in our study area. It is suggested that alternations of material with different clay, organic carbon, and Fe oxyhydroxide contents cause the discrepancy to the suspected inverse correlation. However, the general finding that high pore water Fe concentrations are only detected in layers where little sulphide is present is still valid in our study area. An increase in Mn pore water concentrations with depth due to the dissolution of Mn oxyhydroxides was

shown for marine sediments (Shaw et al., 1990; Hyacinthe et al., 2001). Besides an initial rise, Pedersen and Price (1982) describe that an apparent equilibrium between dissolution of Mn oxyhydroxides and precipitation of Mn carbonates is attained below. In the studied tidal flat Mn carbonates do not precipitate as either Mn or alkalinity concentrations are too low to initiate this reaction.

V porewater concentration was shown to decrease close to sediment surfaces (Shaw et al., 1990; Swarzenski and Baskaran, 2007). In some studies V was described to increase again in some centimetres depth, which was either attributed to V release when Mn oxyhydroxides are reduced (Wehrli and Stumm, 1989; Shaw et al., 1990; Morford et al., 2005) or to complexation of V by soluble organic material (Brumsack and Gieskes, 1983). In intertidal flat pore waters we see decreasing V concentrations close to the surface and increasing ones in deeper sediment layers, which were closely coupled to increases in DOC. In both, intertidal flat and marine sediments Cr exhibits a similar behaviour in pore waters like V (Brumsack and Gieskes, 1983; Shaw et al., 1990).

5.5.4. Seasonal variations of trace metals

Vanadium and chromium

Seasonal variations in pore water chemistry are shown for three locations on the JS tidal flat. V and Cr prevail a seasonal pattern very similar to DOC (Fig. 5.4.). In deep sediment depths increasing V and Cr concentrations are always coupled to increasing DOC concentrations and vice versa supporting the hypothesis that V and Cr are associated with dissolved organic carbon molecules in deep pore waters. The coupling is particularly evident at site JS1. The enhanced availability of substrate at the tidal flat margin presumably leads to increasing microbial activity with rising temperature thus fostering the production of labile organic compounds (Beck et al., submitted b). Because of the simultaneous concentration changes of DOC, V, and Cr, we hypothesize that in reducing sediment layers V and Cr are first adsorbed to organic material and are

transferred to the dissolved organic carbon fraction when organic matter is degraded by hydrolysis and fermentation.

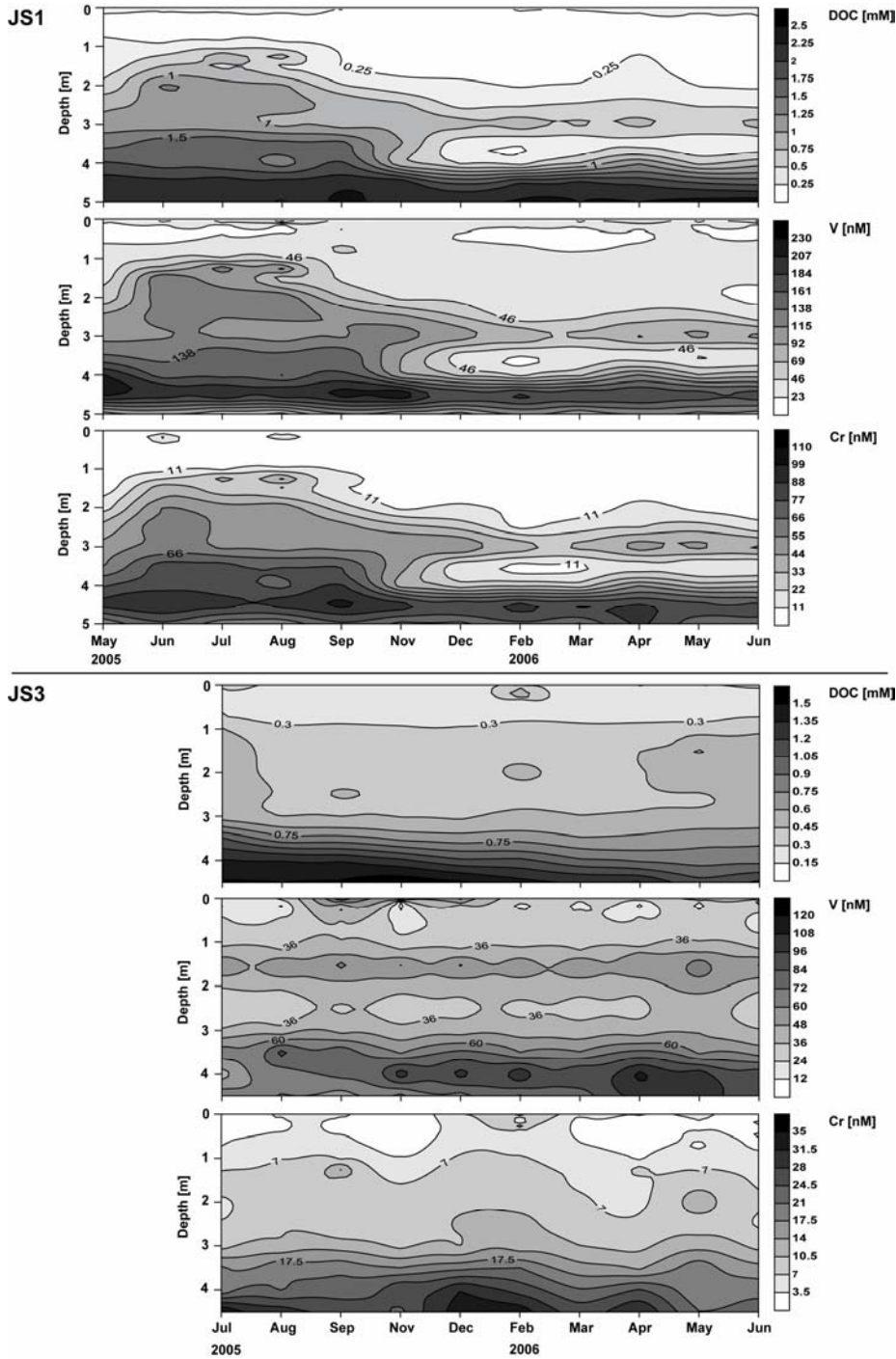


Fig. 5.4.: Seasonal variation of DOC, V, and Cr at site JS1 close to the tidal creek and at site JS3 in the central parts of the tidal flat. Samples were extracted at the same location from May 2005 to June 2006. Data are interpolated according to Kriging using the program Surfer. Note the different concentration scales of site JS1 and JS3.

The decrease in DOC observed after September 2005 presumably results from advective pore water flow, which led to the exchange of water masses down to some metres depth (Beck et al., submitted b; compare 5.3.). The diminishment of the DOC pool leads to decreasing pore water concentrations of adsorbed V and Cr. In central parts of the tidal flat no seasonal variation of DOC is observed in deep pore waters due to limited organic matter availability (Beck et al., submitted b). The absence of DOC concentration changes with season may explain the seasonally relative constant V and Cr concentrations.

Manganese and iron

Mn shows little seasonal variation at all sites (Fig. 5.5.). At site JS1 seasonal changes in Mn concentration are observed at 2 to 3 m depths with higher concentrations in summer and autumn 2005. These changes are rather small, however they may be resulting from higher microbial activity in summer months as described for sulphate and DOC (Beck et al., submitted b). Reduction of Mn oxyhydroxides most likely is microbially mediated (Myers and Nealson, 1988; Lovley, 1995) and thus higher microbial activity may lead to increased Mn oxyhydroxide reduction. At site JS2 an increase in Mn pore water concentration is observed in surface sediments in September 2005 implying that Mn-enriched particles are decomposed in the sediment, which formerly settled from the open water column (Schoemann et al., 1998; Dellwig et al., 2007b; compare 5.2.3.). Seasonal Mn pore water data give no evidence for scavenging of Mo by Mn oxyhydroxides in deposited particles. In JS2 surface sediments the enrichment in pore water Mn succeeds the maximum in Mo enrichment in summer 2005 (Figs. 5.5., 5.6., compare 5.2.3.). Seasonal variations of Fe are also small (Fig. 5.5.). In deep pore waters Fe show low concentrations throughout the whole year at site JS1, except at 5 m depth, and concentrations remain high in the depth interval from 2.5 to 4 m at site JS2.

5. Trace metal dynamics in intertidal flat pore waters

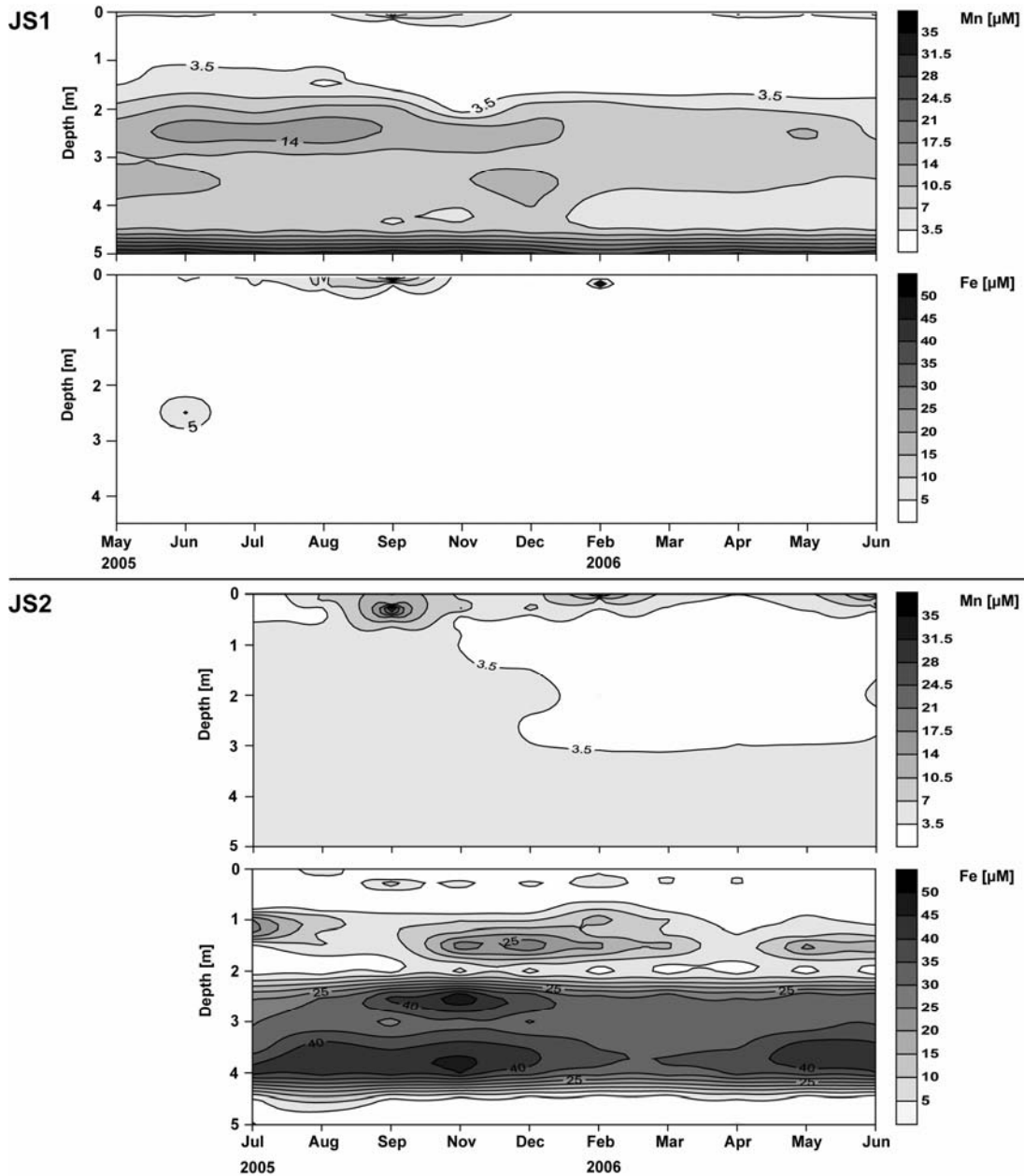


Fig. 5.5.: Seasonal variation of Mn and Fe at sites JS1 and JS2. Samples were extracted at the same location from May 2005 to June 2006. Data are interpolated according to Kriging using the program Surfer. Note that high Fe concentrations determined at 5 m depth at site JS1 are neglected in this figure.

Molybdenum

Molybdenum only exhibits seasonal variations in the upper 50 cm, whereas below concentrations remain at very low levels during the whole year (Fig. 5.6.). In summer and autumn Mo is enriched in pore waters, while the extent of enrichment depends on the

sampling location. Comparing central parts of the JS tidal flat with the margin, the sediment surface structure is different. Water current velocities during falling and rising tide are supposedly smaller in the centre than at margins where the sediment surface slopes towards a tidal creek. Consequently, the sediment surface is covered by ripples at site JS1, whereas fluffy particulate material is deposited on the sediment surface in central parts especially in summer (Chang et al., 2006a). In the open water column large voluminous flocs form during summer when organic compounds released during bacterial decomposition of algae promote aggregation of suspended mineral particles (Chen et al., 2005; Chang et al., 2006c; Lunau et al., 2006; Dellwig et al., 2007b). The sites in the central flats are further characterized by large colonies of *Cerastoderma edule*, most notably at site JS2.

Dellwig et al. (2007b) postulated that during the breakdown of algae blooms MoO_4^{2-} is reduced in oxygen-depleted micro-zones of large flocs suspended in the open water column and/or scavenged by fresh organic material. This leads to an enrichment of Mo in suspended particulate matter. In central parts of the tidal flat where large flocs are preferentially deposited, Mo concentrations above the expected sea water level are determined in summer and autumn several weeks after the aggregation event. This reflects the supply of Mo to pore waters by Mo-enriched particles (Fig. 5.6.). The hypothesis that reduction of Mo occurs in oxygen-depleted micro-zones of large flocs suspended in the open water column implies that Mo has to be re-oxidized at the sediment surface. Without any oxidation step at the sediment surface, an increase in Mo pore water concentration would not be observed. Scavenging of Mo by fresh organic material in the open water column suggests that Mo is released during organic matter degradation in surface sediments without changes in the Mo redox state. No conclusions can, however, be drawn whether the first or second process is the dominant pathway leading to pore water Mo enrichments.

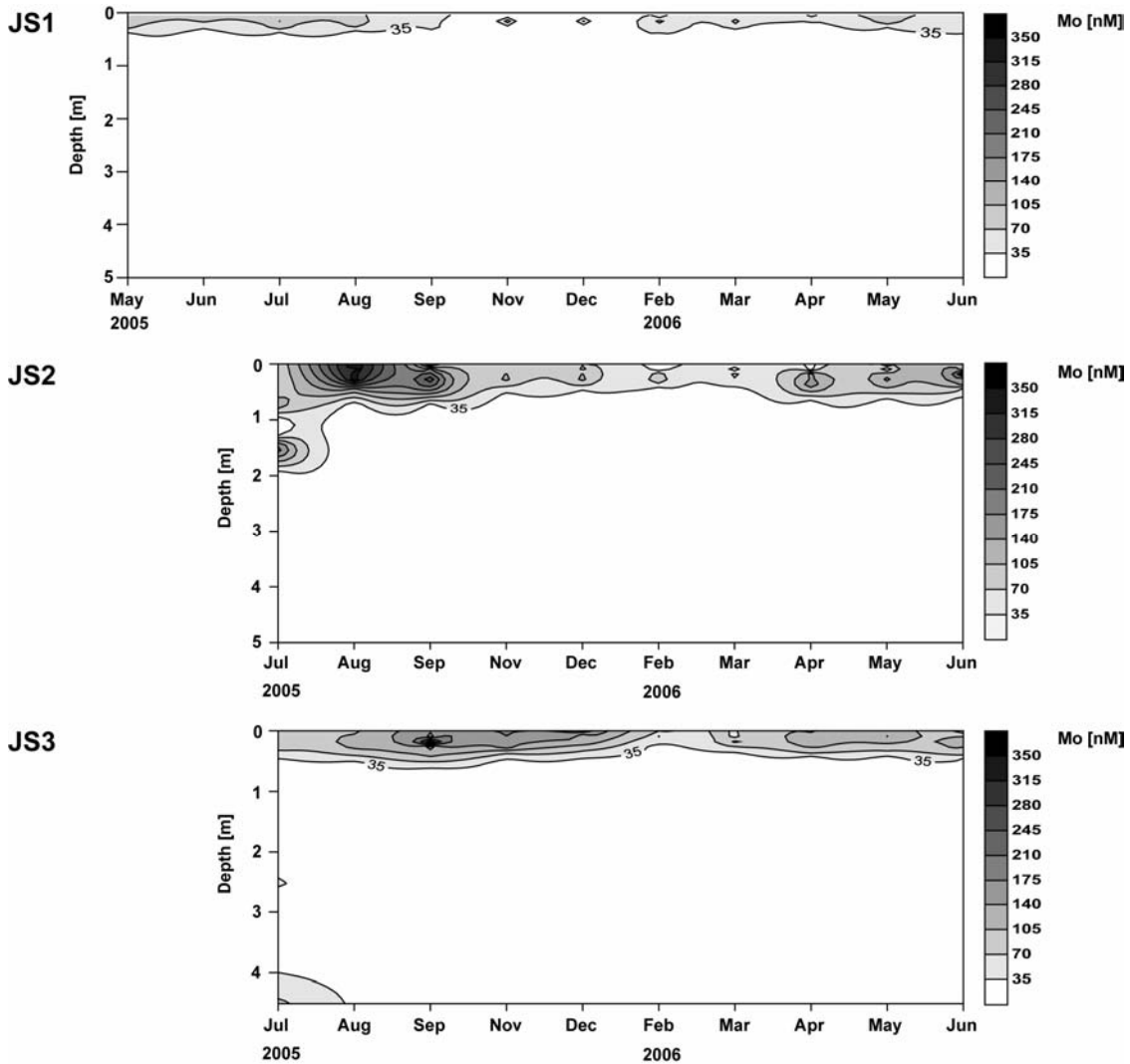


Fig. 5.6.: Seasonal variation of Mo at sites JS1, JS2, and JS3. Samples were extracted at the same location from May 2005 to June 2006. Data are interpolated according to Kriging using the program Surfer.

At site JS2 Mo is enriched in pore waters down to 0.5 m depth. *Cerastoderma edule* and *Arenicola marina* seem to support the transport of particles in sediment depths of some decimetres by burrowing activities. Mussels further may attack aggregate constituents during digestive processes thus presumably accelerating the degradation of deposited particles. Consequently, colonies of *Cerastoderma edule* seem to influence time and depth of Mo enrichments in pore waters. At site JS2 Mo enrichments are seen earlier and at greater depths compared to site JS3, which may be due to higher *Cerastoderma edule* activities.

At site JS1 pore water Mo concentrations vary slightly around 105 nM in summer showing no enrichments. Negative Mo concentration anomalies are, however, observed in autumn and winter 2005/2006. Here, except for 0.15 m depth, Mo concentrations below 30 nM are determined in the upper decimetres (Fig. 5.6.). In this case it is rather unlikely that Mo is scavenged by Mn oxyhydroxides as proposed by Crusius et al. (1996), Sundby et al. (2004), and Morford et al. (2005) because of elevated pore water Mn concentrations in the same time period. The results indicate that the sediment is anoxic just below the surface leading to the precipitation of Mo. In November 2005 the number of free-living and aggregate-associated bacteria in the open water column is surprisingly as high as in July (Dellwig et al., 2007b). Furthermore, DOC concentrations even higher than those in July are determined in November. An algae bloom in autumn thus presumably has caused reducing conditions in the sediment.

Uranium

Seasonal variations in U are particularly observed in the upper 0.5 m of the sediment, whereas only small changes are seen below (Fig. 5.7.). Similar to Mo, the extent and time of U enrichment or depletion in pore water depends on the sampling location. At site JS1 U exhibits concentrations below the Wadden Sea level of 12 nM in surface sediments in November and December 2005. It is suspected that reducing conditions prevailing in surface sediments during this time of the year led to the precipitation of U (Klinkhammer and Palmer, 1991).

In contrast to site JS1, U shows concentrations above 12 nM at site JS2 from September 2005 until April 2006 at depths of about 0.2 m (Fig. 5.7.). This finding is also observed at site JS3, however limited to a shorter time period. During the breakdown of an algae bloom in summer 2005 when Mo concentrations decreased about one third in the open water column of the study area, no decrease in U concentrations is observed. Particulate U concentrations further vary little from spring to winter. Suspended particulate matter deposited on sediment surfaces thus has relatively constant U contents throughout

one year. Therefore, it is suggested that SPM does not contribute to deviations of U pore water concentrations from the Wadden Sea level of 12 nM.

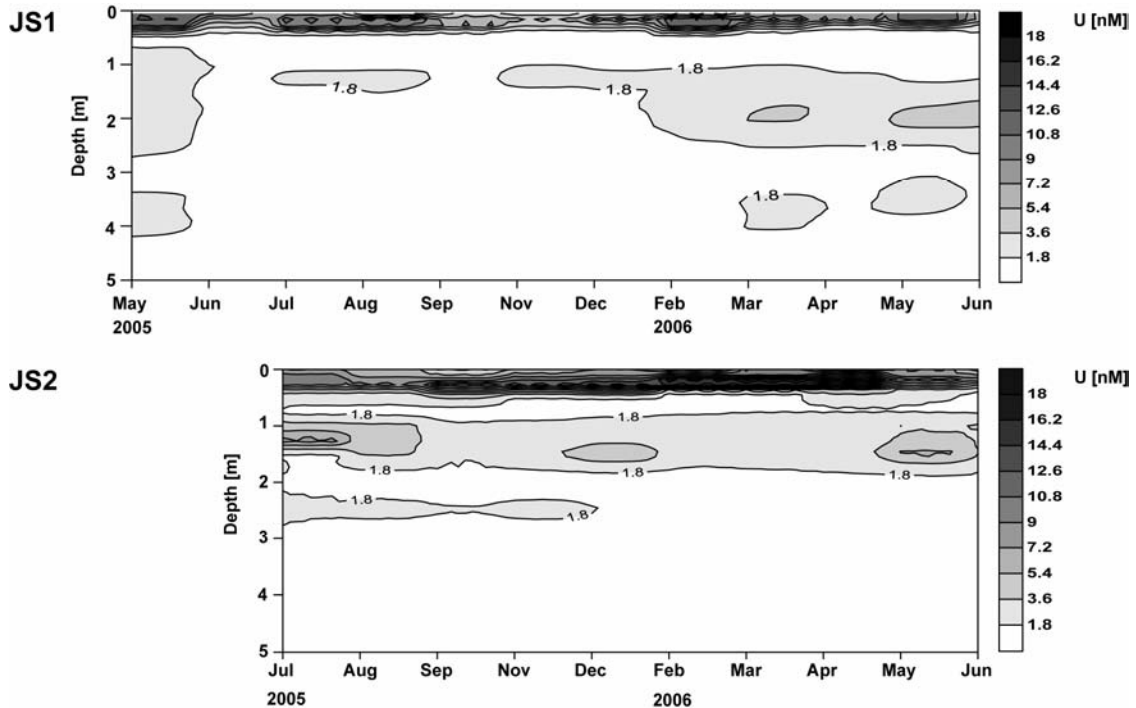


Fig. 5.7.: Seasonal variation of U at sites JS1 and JS2. Samples were extracted at the same location from May 2005 to June 2006. Data are interpolated according to Kriging using the program Surfer.

Coupling of U to organic matter was proposed by Anderson et al. (1982, 1989b). We hypothesize that U is bound to biodeposits of *Cerastoderma edule*, which colonizes especially site JS2. During the productive season the organic carbon content of *Mytilus edulis* biodeposits is higher than that of naturally sedimenting particles (Kautsky and Evans, 1987). We therefore postulate that U is scavenged by biodeposits of *Cerastoderma edule* resulting in an enrichment of U in these biodeposits. Sediments in central parts further are more densely colonized by benthic diatoms compared to margin sediments. Benthic diatoms produce extracellular polymeric substances (EPS), which bind sediment particles thus enhancing sediment cohesiveness and stability (Blanchard et al., 2000; Stal, 2003). Therefore, U is presumably also adsorbed to EPS which are known as

chelating agents and may bind trace metals. Normalization of U concentrations to salinities of the German Bight reveal that U may be depleted in the open water column in summer (Fig. 5.9.). This presumably supports the hypothesis that U is adsorbed on to organic constituents in surface sediments in summer.

The growing season of *Cerastoderma edule* takes place from April to September, coinciding with the phytoplankton cycle in the area (Ramón, 2003). In winter mussels are less active thus limiting biodeposit production. More frequent high-energy events in winter further cause resuspension of biodeposits (Chang et al., 2006a). From September to April U is thus presumably to a lesser extent scavenged by biodeposits. Instead, U is released during the degradation of biodeposits, which were transported to subsurface layers by *Cerastoderma edule*. Therefore, degradation of U-enriched biodeposits probably leads to pore water U enrichments, which from September to April are observed at a narrow depth interval from 0.15 to 0.25 m at site JS2.

In deep pore waters trace metals show smaller seasonal variations than sulphate, DOC, and nutrients where large variations were observed at site JS1 (Beck et al., submitted b). Nevertheless, trace metals like Mo and U exhibit remarkable seasonal variations in pore waters of the upper sediment layers. These variations are due to seasonal changes in the material deposited or produced at the sediment surface and in the redox conditions prevailing in surface sediments.

5.5.5. Tidal variations of deep pore water profiles

In June 2006 pore water samples were retrieved at four different time intervals during one tidal cycle at site JS1: at low tide, at mid-tide with rising water level, at high tide, and at mid-tide with falling water level. Depth profiles for Fe, Mn, U, Mo, V, and Cr are shown in Figure 5.8. Trace metal concentrations remain quite stable in the upper decimetres of the sediment regardless if the sediment surface is exposed to the atmosphere or covered by 1.2 m of water. The redox stratification of the sediment thus seems to change little within one tidal cycle. From low tide to high tide Mn concentrations increase about two fold

from 1.5 to 2.5 m depth, whereas smaller changes are observed at 3.5 m depth. It is assumed that depths layers where concentration changes occur within one tidal cycle are strongly influenced by pore water advection. Several studies hypothesize that advection influences the pore water system at tidal flat margins where at low tide a hydraulic gradient between the sea water level in the tidal creek and the pore water level in the sediment induces flow (Howes and Goehring, 1994; Billerbeck et al., 2006b; Wilson and Gardner, 2006; Beck et al., submitted b). In contrast, no tidal changes in Mn concentration are determined at 3 m and below 4 m depth. The sediment geochemistry shows that sandy sediments predominate down to 2.6 m depths (Beck et al., submitted a,b). A sandy layer at about 3.5 m depth further seems to enable pore water flow, whereas layers with higher clay contents inhibit advective processes at 3 m and below 4 m depth (Beck et al., submitted a,b).

Fe shows an increase in concentration from low tide to high tide comparable to that observed for Mn, however the increase is limited to depths between 1 and 2 m (Fig. 5.8.). Strongly increasing H₂S concentrations below 2 m depth may be responsible for the fact that concentrations remain at a very low level without showing any tidal cyclicity at depths exceeding 2 m. U concentrations change in a similar depth range compared to Mn. However, in contrast to Mn, concentrations decrease from low tide to high tide. Deep Mo pore water concentrations remain very low during the whole tidal cycle and do not show any concentration changes. Concentrations of V and Cr vary at about 2.5 m depth in parallel to DOC concentration changes found at these depths (Beck et al., submitted b).

Tidal variations of Mn, Fe, and U imply that at low tide pore water is sampled, which is less diagenetically altered compared to pore water extracted at high tide. At low tide pore water is less enriched in Mn and Fe and less depleted in U compared to high tide. This phenomenon is also observed regarding DOC, ammonia, and silicate where lower concentrations are determined at low tide compared to high tide (Beck et al., submitted b). The reason for this finding is not yet fully understood as the hydraulic gradient between the sea water level in the tidal creek and the pore water level in the sediment is not only

assumed to generate pore water flow towards the tidal creek. Additionally tidal pressure gradients may lead to forward and backward flow of pore water over small distances.

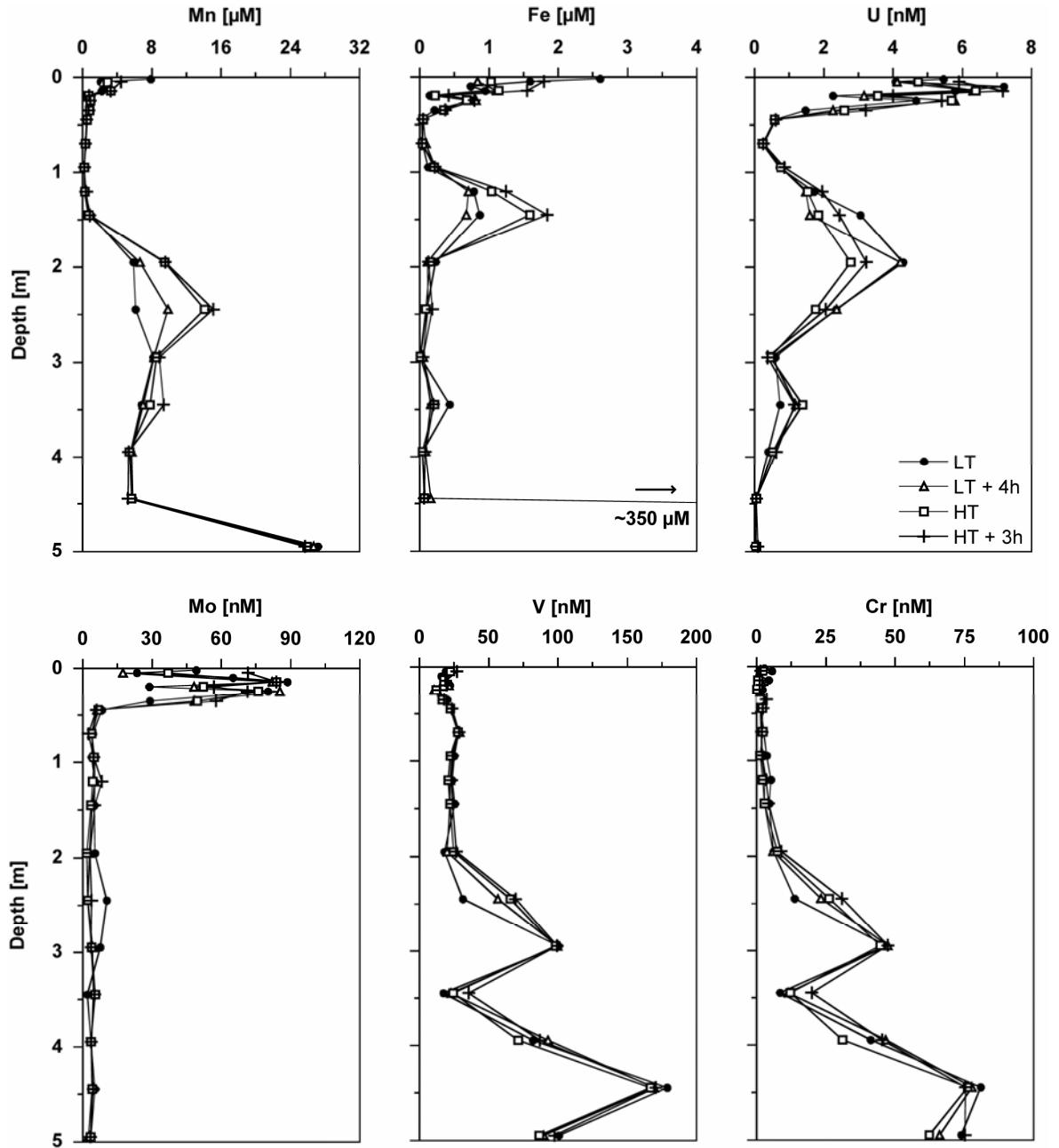


Fig. 5.8.: Mn, Fe, U, Mo, V, and Cr pore water concentrations in samples taken at four different states during one tidal cycle; low tide (LT), rising water level (LT + 4h), high tide (HT), and falling water level (HT + 3h) in June 2006. All samples originate from the identical sampling location.

As already hypothesized by Billerbeck et al. (2006b) and Beck et al. (submitted b), the pore water system of the study area is influenced by advection at tidal flat margins. In

central parts of the JS tidal flat, repetitive sampling within one tidal cycle was not carried out. Deep pore waters however showed little seasonal variation in central parts, which is assumed to be due to slow advection processes, besides low organic matter contents and thus low bacterial activity. This is in accordance with the assumption that pore water advection is especially generated at tidal flat margins because a hydraulic gradient is needed to induce it. By seasonal and tidal studies we thus present evidence that deep pore water flow occurs in permeable sediments located close to tidal flat margins. Deep pore waters escaping at tidal flat margins during low tide presumably form a major source of trace metals, which are enriched in pore water compared to sea water. Concentrations of Fe, Mo, and U are close to or below sea water level in deep pore waters, however elements like Mn, V, and Cr with high concentrations in seeping pore waters will have an impact on the composition of the open water column.

In Fig. 5.9. surface concentrations of Mn, V, and U obtained in the tidal inlet in February and August 2002 are presented as an example. Mn, V, and U exhibit different concentration levels in the open water column depending on season, state of the phytoplankton bloom, and salinity (Fig. 5.9.; Dellwig et al., 2007a,b). Salinities in the Wadden Sea are mostly lower than offshore as reflected in lower U concentrations compared to the German Bight (Fig. 5.9.). In the open water column of the study area Mn and V concentrations show a tidal cyclicity with maximum values during low tide (Fig. 5.9.). Fresh water is an important Mn source averaging 4 μM during sampling campaigns in 2002 and 2003 (Dellwig et al., 2007a). However, fresh water inflow is irregular and does not happen at every low tide. Mixing processes in the open water column further limit the influence of fresh water on Mn concentrations in the backbarrier area. Increasing Mn and V concentrations at low tide are also not caused by imports of North Sea water because water outflow from the backbarrier area into the North Sea dominates at low tide periods.

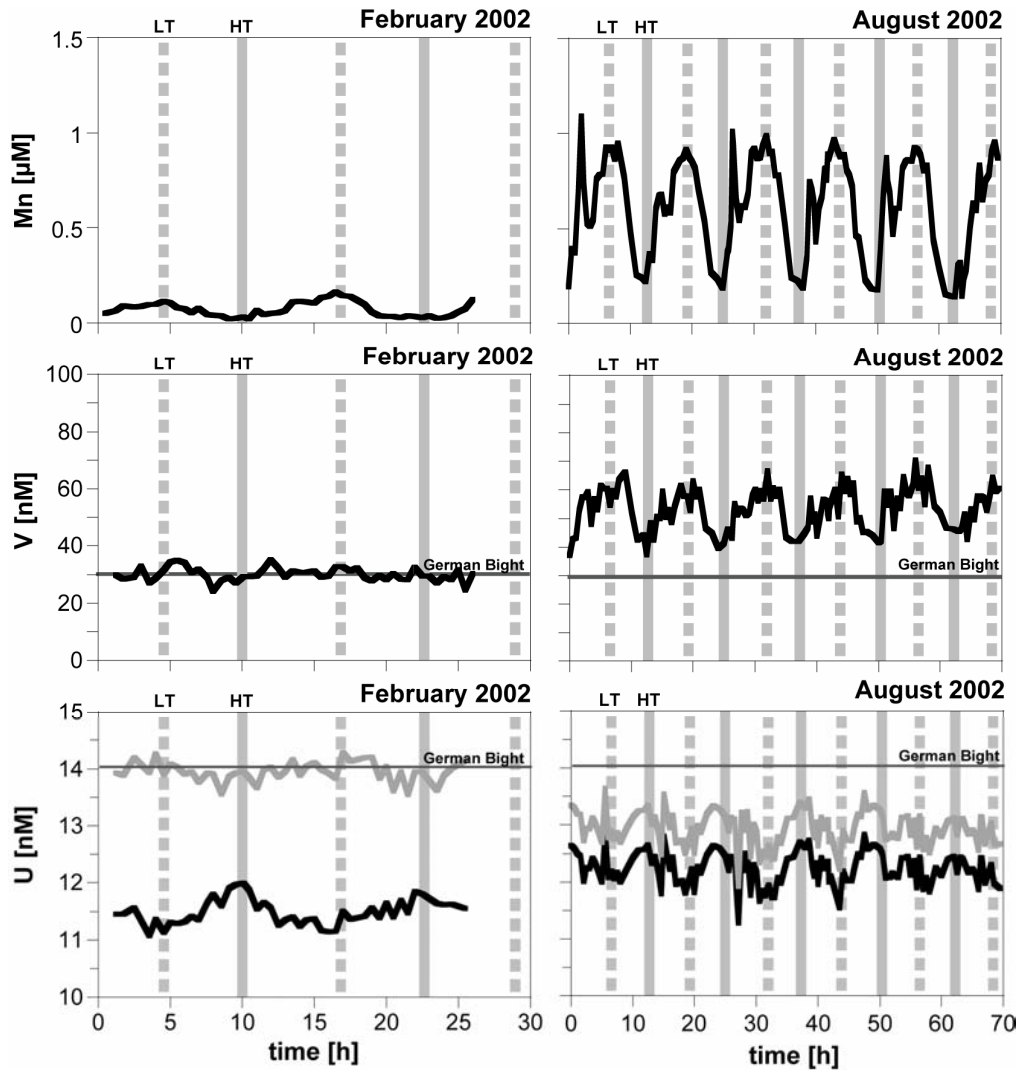


Fig. 5.9.: Mn, V, and U concentrations in the open water column of the backbarrier area of Spiekeroog Island in August 2002. Samples were obtained close to the tidal inlet of the backbarrier area. The vertical grey and dashed lines denote high tide (HT) and low tide (LT). U concentrations are displayed at *in situ* salinities (black line) and normalized to offshore salinities (grey line).

The release of Mn- and V-enriched pore waters at low tide may thus largely account for maximum Mn and V concentrations in the open water column at this time within the tidal cycle. Wadden Sea U concentrations show a tidal pattern with maximum concentrations during high tide (Fig. 5.9.). Deep pore waters seeping at creek banks are depleted in U compared to sea water thus implying that seeping pore water lead to a slight decrease in U concentration in the open water column at low tide (Fig. 5.9.).

5.6. Conclusions

Sampling of deep pore waters in an intertidal flat revealed trace metal features comparable to those observed in surface sediments of deep marine environments. Despite of more dynamic biogeochemical, sedimentological, and hydrological conditions prevailing in intertidal flats, trace metals show similar general trends with depth like in continental margin environments where sedimentation rates are essentially constant.

Seasonal sampling revealed that the trace metals Mn, Fe, Mo, and U vary little in deep intertidal flat pore waters within a time span of one year. Thus, in contrast to sulphate, nutrients, and DOC where seasonal variations were observed down to 4 m depth in sediments close to a tidal flat margin (Beck et al., submitted b), changes in temperature and bacterial activity seem to have little effect on Mn, Fe, Mo, and U dynamics in deep layers. However, the trace metals V and Cr vary seasonally parallel to changes in dissolved organic carbon. Close to the sediment surface, seasonal patterns of trace metals further exhibit large concentration changes in Mo and U from summer to winter. In summer Mo-enriched particulate matter of the open water column is deposited on sediment surfaces. When this particulate matter is decomposed in the sediment, Mo is released into surface pore waters. In contrast, U is presumably scavenged by biodeposits of *Cerastoderma edule* in summer leading to pore water U enrichments when biodeposits are remineralized. In time periods where redox stratification is less pronounced due to lower primary production, scavenging of Mo and U by Mn and Fe oxyhydroxides is further suspected to occur in surface sediments.

Pore water sampling at different times within one tidal cycle evidences that the pore water system close tidal flat margins is affected by advection down to some metres depth. Therefore, pore waters originating from such depths presumably escape at tidal flat margins at low tide. Owing to the enrichment of specific elements like Mn and V in pore water compared to sea water, seeping pore waters may represent a source for the ecosystem in the open water column.

Acknowledgements

The authors would like to thank Malte Groh for his invaluable assistance during sampling campaigns. We wish to thank the TERRAMARE Research Centre, especially Helmo Nicolai, for providing transportation to the sampling site by boat. Financial support for this work was provided by the German Science Foundation (DFG, BR 775/14-4) within the framework of the Research Group 'BioGeoChemistry of Tidal Flats' (FOR 432/2).

6. Non-conservative behaviour of molybdenum in coastal waters: Coupling geochemical, biological, and sedimentological processes

Olaf Dellwig, Melanie Beck, Andreas Lemke, Mirko Lunau, Kerstin Kolditz, Bernhard Schnetger, Hans-Jürgen Brumsack

This chapter is published in *Geochimica et Cosmochimica Acta* **71**, 2745-2761.

Abstract

Non-conservative behaviour of dissolved Mo was observed during specific time periods in the water column of the Wadden Sea of NW Germany. In July 2005 dissolved Mo declined within 36 hours from a level only slightly below seawater (82 nM) to a minimum value of 30 nM, whereas in August 2002 dissolved Mo revealed a tidal cyclicity with maximum values up to 158 nM at low tide. In contrast, cruises in August 2003 and 2004 displayed an almost conservative behaviour of Mo. The decrease in dissolved Mo during July 2005 and elevated values in August 2002 were accompanied by Mo enrichments on aggregates in the water column of the Wadden Sea. Along with Mo, dissolved Mn showed unusual concentration patterns in July 2005, with values distinctly below the common summer level (factor 5). A direct relation between the loss of Mo and scavenging by freshly formed MnO_x phases could not be inferred from our data because both metals revealed inverse patterns. Parallel to decreasing dissolved Mo concentrations dissolved Mn showed an increasing trend while particulate Mn decreased. Such finding is compatible with the formation of oxygen-depleted zones in aggregates, which provide suitable conditions for the rapid fixation of Mo and parallel release of Mn by chemically

and/or microbially mediated processes. Our assumption is supported by biological (e.g. number of aggregate-associated bacteria) and sedimentological (e.g. aggregate abundance and size) parameters. The production of organic components (e.g. TEP) during breakdown of an algae bloom in July 2005 led to the formation of larger Mo-enriched aggregates, thus depleting the water column in dissolved Mo. After deposition on and incorporation into sandy tidal flats these aggregates are rapidly decomposed by microbial activity. Pore water profiles document that during microbial decomposition of these aggregates substantial amounts of Mo are released and may replenish and even enrich Mo in the open water column. We postulate a conceptual model for the observed non-conservative behaviour of Mo in coastal waters, which is based on the tight coupling of geochemical, biological, and sedimentological processes.

6.1. Introduction

Molybdenum is an essential trace metal for planktonic organisms, e.g. cyanobacteria, as it plays an important role in nitrogen metabolism. Mo forms a cofactor for various nitrogen-fixation and nitrate reductase systems (e.g. Fogg and Wolfe, 1954; Arnold, 1955; Fogg, 1962; Robson et al., 1986). Despite its biological requirement, Mo is the most abundant trace metal in ocean water (about 107 nM) and generally displays a conservative behavior unaffected by biological activity (Morris, 1975; Collier, 1985). However, Berrang and Grill (1974) found variable Mo concentrations in coastal waters of Saanich Inlet ranging from 73 to 107 nM. The authors suggested a non-biotic coupling to Mn oxidation and subsequent scavenging by freshly formed MnO_x phases. Adelson et al. (2001) also ascribed importance to Mn cycling on Mo behaviour. They proposed a model for the removal of MoO_4^{2-} from surface waters and its pre-concentration at the sediment/water interface by settling $\text{Mn}(\text{Mo})\text{O}_x$ phases. A special feature of this model is that MoO_4^{2-} is not necessarily reduced during transfer to the sediment. Moreover, MoO_4^{2-} is released at the sediment/water interface from where it may diffuse back into the water

column and/or into the sediment. Within the sediment MoO_4^{2-} can be fixed by thiol or covalent bondings to transition metals followed by reduction and final burial as sulphide, which leads to typical Mo enrichments frequently observed in TOC-rich marine sediments (e.g. Brumsack, 2006).

In contrast, Head and Burton (1970) observed decreasing Mo concentration in the estuary of Southampton Water during spring, which they attributed to its utilisation by plankton and/or complexing by organic particles. Yamazaki and Gohda (1990) also observed Mo depletion in coastal waters (Seto Inland Sea, North Pacific, minimum 69 nM), which was explained by scavenging of Mo as an organically associated species; a relationship, which was suggested earlier by Szalay and Szilagyi (1967) and Brumsack and Gieskes (1983). More recently, Tuit and Ravizza (2003) reported both, positive and negative Mo concentration anomalies in a region of nitrogen-fixation in the Eastern Equatorial Pacific (+ 5nM, -3 nM), which presumably are related to biological processes. A coupling of Mo anomalies to Mn was not observed by these authors. Recent publications by Engel et al. (2004) and Lunau et al. (2006) emphasise the importance of organic macromolecules produced during algae blooms on particle dynamics in the water column. These compounds are supposed to maintain aggregate formation in the water column, which possibly also influences the cycles of trace metals via scavenging by organic matter or reduction in the suboxic interior of larger particles. Evidence for the existence of oxygen-depleted zones is provided by studies of Alldredge and Cohen (1987) who demonstrated substantial oxygen depletion in marine snow. In addition, Ploug et al. (1997) measured microscale distributions of oxygen in laboratory-made aggregates and concluded that anoxic conditions can prevail for a few hours. Stable anoxic conditions, however, would require a high and continuous carbon supply.

In this contribution we present data, which show distinct non-conservative behaviour of Mo (positive and negative anomalies) in coastal waters of the Southern North Sea during certain time-periods in summer. These data were obtained during several ship cruises in the backbarrier tidal flat of Spiekeroog Island and the adjoining near-coastal

German Bight between 2002 and 2005. Along with Mo, we present Mn data, which also reflect a much more complex seasonal variability as assumed so far (e.g. Dellwig et al., 2007). Earlier investigations suggested a simple seasonal behaviour of Mn, with concentrations of dissolved Mn increasing from winter to summer by a factor of about 10 due to elevated release from the tidal flat sediments. In contrast, data from 2005 point towards a distinctly higher variability of Mn during summer which seems to be controlled by internal recycling processes in the Wadden Sea system. Thus, the major goal of this paper is to provide possible explanations for the observed unusual behaviour of both metals. Previous work in the study area has shown that Mn-oxidation forms a prominent process in the Wadden Sea (Dellwig et al., 2007), which can influence the patterns of other trace metals like Mo via scavenging. However, we strongly focus on the influence of microbial and sedimentological processes on the geochemistry of Mo and Mn, and postulate a tight coupling between these processes.

6.2. Geographical setting

The Wadden Sea of the Southern North Sea with its tidal flats and barrier Islands has formed about 7,500 BP as a result of the Holocene sea-level rise (Streif, 1990). Today, the morphology of the coastline, which stretches about 500 km from Den Helder in the Netherlands to Esbjerg in Denmark, is largely determined by human activities (e.g. dike building). The East-Frisian Wadden Sea, which represents about 15% of the entire Wadden Sea, forms our major study area. It is characterized by mesotidal conditions (tidal range 2.2-2.8 m).

Fig. 6.1. a shows the sampling locations during the cruises in the German Bight and the adjacent backbarrier tidal flats. This contribution is based on data from the following cruises: RV Heincke 220 (October 2004), RV Heincke 234 (July 2005), RV Senckenberg (January 2004, 2005; February 2002, 2003; April 2003, 2005; May 2002; July 2005;

August 2002, 2003; November 2002-2005). Further sampling was done on a time-series station in the tidal inlet of Spiekeroog Island in August, September, and October 2005.

Sampling was performed in intervals of 10 to 30 min during transects (RV Heincke 220: 54°29.94'N/7°19.92'E to 53°47.92'N/7°32.79'E and 234: 53°48.04'N/7°30.62'E to 54°06.09'N/7°45.47'E) and every 30 min during time-series in 2002-2004 (RV Senckenberg). In 2005 sampling intervals were raised to 60 min. While samples between 2002 and 2004 originate exclusively from surface waters, sampling on RV Senckenberg in 2005 was done almost simultaneously at three depth intervals.

Figure 6.1. b shows our main study area in the backbarrier tidal flats of the Islands of Spiekeroog and Langeoog. The locations OB1 in the tidal inlet of Spiekeroog Island (Otzumer Balje; 53°44.87'N/7°40.29'E) and CBA (central backbarrier area; 53°43.43'N/7°43.32'E) mark the sampling campaigns with RV Senckenberg. OB2 (53°48.21'N/7°26.95'E) is positioned at the 10m-depth line where sampling was performed during one cruise with RV Heincke in July 2005. Additionally, a sampling campaign was carried out in the tidal inlet of Langeoog Island at position AE in July 2005 (Accumer Ee; 53°43.53'N/7°26.95'E). In the transition zone between tidal flats and salt marshes of the Island of Langeoog (53°44.77'N/7°31.46'E) samples from sediment traps were taken monthly between March and November 2005.

The light grey areas in Fig. 6.1. b indicate tidal flats emerging at low tide. The Janssand is one of the flats in the backbarrier area of Spiekeroog Island. In this area sandy sediments predominate, however at depths exceeding 3 m these are intermingled with silt-clay layers. Pore water samples were taken at two locations on this flat (asterisks in Fig. 6.1. b). Location 1 is situated very close to the main tidal channel of the backbarrier area of Spiekeroog Island (53° 44,183' N, 007° 41,904' E), whereas location 2 is positioned further towards the centre of the sand flat (53°43.96' N/7°41.28' E). Pore waters were retrieved *in situ* from the sediment using permanently installed samplers. The construction and the use of these samplers are described in more detail by Beck et al. (2007).

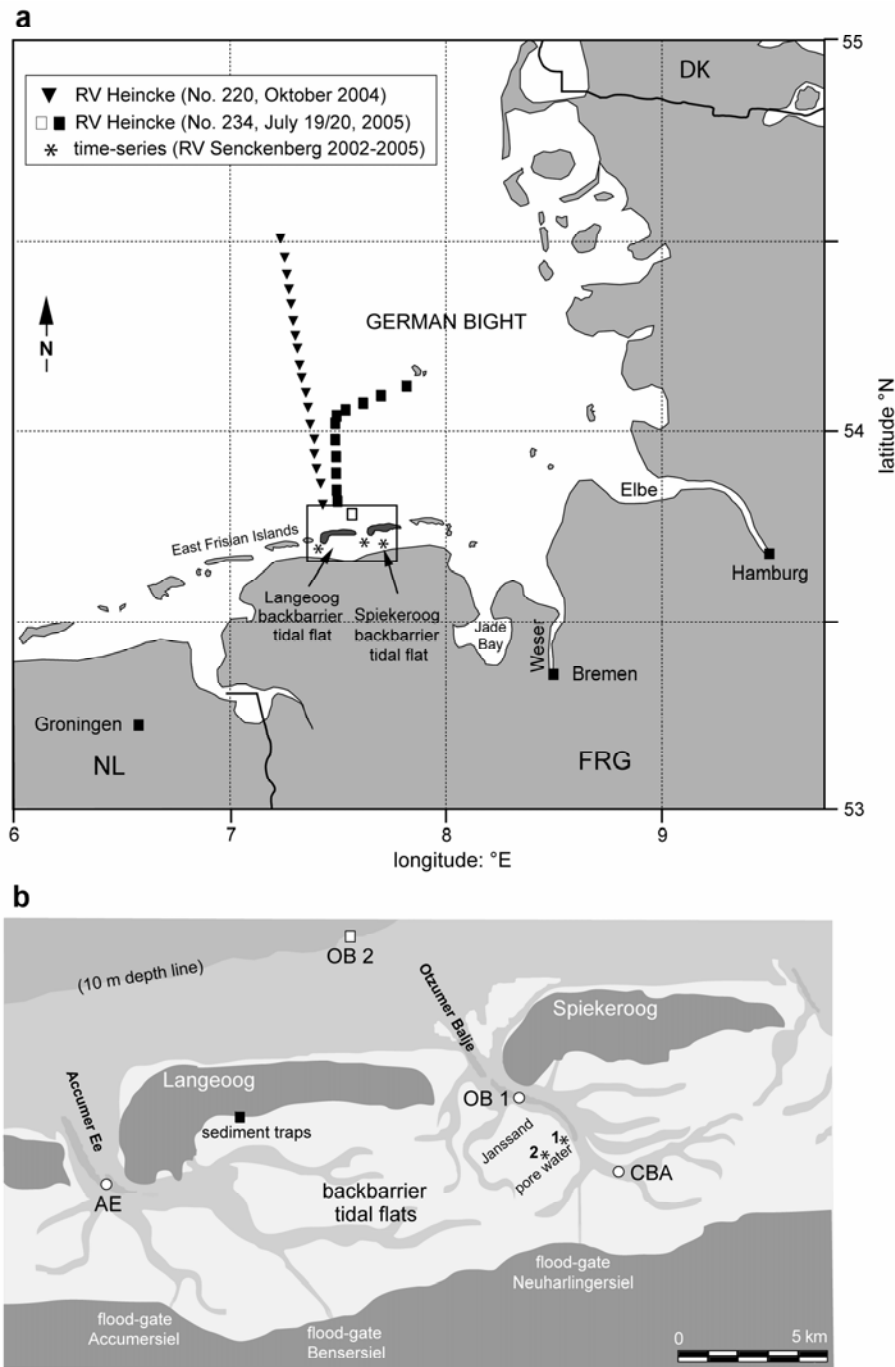


Fig. 6.1.: (a) map of the study area showing the sampling sites during several cruises in the Wadden Sea of NW Germany. The square denotes the main study area in the backbarrier tidal flats of the Islands of Spiekeroog and Langeoog. (b) detailed map of the backbarrier areas of the Islands of Spiekeroog and Langeoog showing the time-series locations in the tidal inlets (Otzumer Balje, OB 1; Accumer Ee, AE), at the 10 m depth line (OB2), and in the central backbarrier area (CBA). The asterisks mark the locations of the pore water sampling sites on the Janssand tidal flat. The black square indicates the location of sediment traps at the transition zone of tidal flats and salt marshes of Langeoog Island. The light grey areas indicate tidal flats emerging at low tide.

6.3. Material and Methods

6.3.1. Geochemistry

Mo, Mn, Al – Depending on SPM contents, 0.25 to 1.5 l of seawater were filtered through pre-weighed Millipore Isopore membrane filters (0.4 µm polycarbonate PC) for multi-element analyzes. Filters were rinsed with 60 ml purified water, dried at 60°C for 48 h and re-weighed for the determination of total SPM. Samples for analysis of dissolved metals in seawater and pore water were taken with pre-cleaned PE-syringes and 0.45 µm SFCA syringe filters. These samples were acidified to 1 vol. % HNO₃ in pre-cleaned PE-bottles.

For multi-element analysis the PC filters were treated overnight with 1 ml HNO₃ and 2 ml HClO₄ in closed PTFE autoclaves (PDS-6; Heinrichs et al., 1986) at room temperature to oxidise organic matter. Then the filters were decomposed at 160°C. SPM residues were digested in the same PTFE vessels at 180°C after adding a mixture of 1 ml HClO₄ and 3 ml HF. After digestion acids were evaporated at 180°C, residues were re-dissolved and fumed off three times with 2 ml semi-concentrated HCl and diluted with 2 vol. % HNO₃ to a final dilution of 2,500 or 5,000. All acids were pre-cleaned by sub-boiling distillation, except for HF (suprapure quality). Material from sediment traps was sieved and the <63 µm fraction was digested with HClO₄ and HF.

Particulate Al and Mn were analyzed by ICP-OES (Perkin Elmer Optima 3000XL), whereas particulate Mo as well as dissolved Mn and Mo were measured by ICP-MS (Thermo Finnigan MAT ELEMENT). Dissolved trace metals were determined directly from 25-fold diluted samples. The analytical procedure applied is similar to the method published by Rodushkin and Ruth (1997). Data presented here are based on measurements of Mo98 in low resolution and Mn55 in medium resolution with Y89 and Cs133 as internal standards, respectively. As we measured Mo98 instead of Mo95, the interference of BrO was negligible. However, Mo showed significant memory effects within the sample introducing system (e.g. tubings, nebuliser), which required sufficient wash and take up times (60-90 s). Contamination effects were excluded by measurement of

filter and onboard procedural blanks. As filters for the analysis of particulate Mn and Mo were thoroughly rinsed with purified water any corrections for residual salt were unnecessary. This is also supported by measurement of particulate Na, which only reflected the normal detrital background level.

Precision (1σ) and accuracy of all measurements were checked by parallel analysis of international and in-house reference materials. GSD-4 and our in-house shale standard TW-TUC were used as a reference for particulate samples (Al: precision 2.2%, accuracy -0.6%; Mn: 1.5%, -0.9%; Mo: 9.0%, -2.1%), whereas reference seawater standards CASS-3 and CASS-4 (Canada) were used for dissolved samples (Mn: 6.1%, 6.7%; Mo: 2.6%, 1.8%). For the analysis of Mn in pore water, a spike solution was added to these reference standards as the concentration for Mn was much higher in the Wadden Sea pore waters than in the original reference materials. The final Mn concentration in the reference standards was 3640 nM.

Particulate organic carbon (POC) and total particulate nitrogen (TPN) – Subsamples of 100 mL were filtered onto precombusted and preweighed GF/F filters (Whatman, 25 mm diameter), rinsed with 2-5 ml of distilled water to remove salt and kept frozen at -20°C until further analysis. Prior to analysis the filters were exposed to the fume of concentrated hydrochloric acid for 12 h to remove carbonates. Thereafter, filters were transferred into tin capsules (IVA, Meerbusch, Germany) and analyzed for POC and TPN by a FlashEA 1112 CHN-analyzer (Thermo Finnigan). Analysis was done at a combustion temperature of 1000°C and a column temperature of 35°C . Concentrations were calculated by an external calibration curve with Methionin (0.1-2.5 mg).

Chlorophyll-a and Phaeopigments – Subsamples of 500 ml were filtered onto GF/F filters (Whatman, 47 mm diameter), immediately wrapped into aluminum foil and kept frozen at -20°C until further analysis in the shaded lab within one week. Filters were mechanically hacked and extracted in hot ethanol (75°C) for 1 h in the dark. Concentrations of chlorophyll-a and phaeopigments were determined spectrophotometrically and calculated following the procedure described by von Tümpling

and Friedrich (1999). Chlorophyll_{total} was calculated as the sum of chlorophyll-a and phaeopigments.

Dissolved organic carbon – The measurements of dissolved organic carbon (DOC) were performed on GF/F-filtrates by combustion and IR-detection with a multi N/C 3000 analyzer (Analytik Jena). The filtrate was stored in brown glass bottles and acidified with semi-concentrated HCl (500 µl per 100 ml). The analysis was checked by measurements of K-hydrogenphthalate solutions containing 2 and 3 mg l⁻¹ C (precision 4.6%; accuracy - 0.4%).

6.3.2. Sedimentology

Documentation of aggregate abundance and size – Photos were taken with an *in situ* camera device. Samples were illuminated by a red light diode laser ($\lambda=658$ nm, 50 mW), and the abundance and size distribution of the aggregates were documented by digital photography using a Sony Cybershot DSC-F828. The resolution of the DSC-F828 is 15 µm per pixel. Further data processing and image analysis was done in the lab using the software package analySIS V 3.0 (Soft Imaging System, Münster, Germany). We determined abundance, size distribution, equivalent circular diameter (ECD), and surface area of the aggregates. For further details of data analysis see Lunau et al. (2004).

Suspended particulate matter (SPM) – Subsamples of 500-1000 ml were filtered onto precombusted (2 h, 450°C) and preweighed GF/F filters (Whatman, 47 mm diameter). Filters were rinsed with 10-20 ml of distilled water to remove salt and kept frozen at -20°C until further analysis in the lab within one week. After drying for 12 h at 60°C, filters were adapted to room temperature for 30 min and weighed again. SPM was calculated as the difference between filter weight before and after sample filtration and normalised per litre.

6.3.3. Microbiology

Bacterial cell counts – Subsamples were transferred into 5 ml cryotubes (Nunc) onboard ship, preserved with 2% (final concentration) glutardialdehyde (resp. 1%/0.05% PFA/GDA mixture in April 2005) and stored at -20°C until further processing. Abundances of total and free-living bacteria (FL) were enumerated by epifluorescence microscopy after staining with SybrGreen I, applying a new detachment procedure. In brief: for the determination of the free living bacteria cells were washed with 3-5 ml of a TAE-methanol mix (1:1, pH 7.4) before the filters were transferred to a microscope slide and stained by SybrGreen I mixed into the mounting solution (1:40) containing moviol 4-88 (polyvinylalcohol 4-88). For the determination of total bacteria samples were treated with 10-30% methanol (35°C) and ultrasonicated before centrifugation. The number of aggregate-associated bacteria (AGG) was calculated as the difference of total bacteria and FL bacteria. This procedure is particularly suitable for samples with high loads of SPM and results in a very efficient detachment of AGG bacteria, yielding reliable numbers of the latter with a standard error of <15%. For further details of the method see Lunau et al. (2005).

Stained cells were counted with a Zeiss Axiolab 2 microscope at 1,000x magnification by using a 100x Plan-Apochromat oil-immersion objective (lamp: HBO 50, filter set: Zeiss, Ex 450-490, FT 510, LP 515). The filtered sample volume yielded 60-150 stained cells in the counting grid. For each sample ten grids and a minimum of 600 cells per filter were enumerated.

6.3.4. CTD

CTD data were determined with a CTD probing system (Model OTS 1500, ME Meerestechnik-Elektronik, Germany) equipped with sensors for measuring pressure, conductivity and temperature. Salinity and density were calculated according to UNESCO standards (UNESCO 1981).

6.4. Results

6.4.1. Biological properties

The data presented in Table 6.1. provide an overview about several biological parameters in surface samples from the Wadden Sea cruises in 2005. These data were obtained from surface samples. Concentrations of chlorophyll-*a* increase roughly by a factor of two from January to April and July and decrease again towards November. This finding is consistent with the occurrence of spring and summer algae blooms, whereas the generally less pronounced autumn bloom is not covered by our cruises. The ratio of phaeopigments to total chlorophyll designates the quality of the algae material and provides information about the state of the bloom. This ratio shows highest values during January and November when resuspension of formerly deposited algal detritus is highest. In contrast April and July ratios are distinctly lower as both cruises cover algae blooms and indicate fresh algal material. However, the ratio of July is slightly higher when compared with the value from April, which may be indicative for a final stage of the bloom.

Tab. 6.1.: Average surface values and ranges (in parentheses) of several biological, meteorological, and sedimentological parameters for the Wadden Sea of Spiekeroog Island (tidal inlet OB1 and central backbarrier area CBA).

	Wadden Sea January 2005	Wadden Sea April 2005	Wadden Sea July 2005	Wadden Sea November 2005
Chlorophyll- <i>a</i> [$\mu\text{g l}^{-1}$]	2.3 (1.2-3.3)	4.8 (3.2-6.4)	5.0 (3.1-6.7)	2.2 (0.6-3.2)
Phaeopigments [$\mu\text{g l}^{-1}$]	162 (103-239)	118 (55-145)	184 (28-284)	150 (50-231)
Phaeopigments / Chlorophyll _{total}	71	25	36	71
DOC [mM]	0.20 (0.17-0.24)	0.19 (0.15-0.24)	0.25 (0.2-0.32)	0.28 (0.22-0.44)
POC [%]	3.4 (2.5-5.0)	7.1 (2.9-16.3)	7.6 (1.1-28.7)	2.4 (0.5-4.5)
free-living bacteria (FL) [cells $\times 10^6 \text{ ml}^{-1}$]	1.0 (0.6-1.4)	0.9 (0.4-1.6)	2.2 (1.3-3.0)	1.9 (1.4-3.2)
aggregate-associated bacteria (AGG) [cells $\times 10^6 \text{ ml}^{-1}$]	0.7 (0.2-1.0)	0.9 (0.3-2.3)	1.6 (0.4-4.2)	1.9 (0.6-3.7)
av. wind speed [m s^{-1}]	11.2	3.7	12.5	4.6
av. wind direction [$^{\circ}$]	230	171	265	216
SPM [mg l^{-1}]	72 (29-128)	8 (2-18)	22 (6-66)	52 (21-95)
aggregate number (AGA) [ml^{-1}]	500 (60-2400)*	-	280 (110-420)	-
aggregate size (ECD) [μm]	88 (64-110)*	-	118 (91-139)	-

*Data from 2003 (Lunau et al., 2006)

A further difference during the algae blooms in April and July 2005 is seen in DOC data, which are higher in July due to release of organic compounds during the breakdown of the bloom (Table 6.1.). The occurrence of algae blooms also leads to elevated organic matter contents of particles as seen in POC values during April and July. Additionally, Table 6.1. presents the number of free-living bacteria (FL) and aggregate-associated bacteria (AGG) in surface water of the Wadden Sea for the cruises in 2005. Interestingly, the number of FL and AGG bacteria is comparable in January and April, which may be due to pronounced resuspension in January. In contrast, the number of FL and AGG bacteria is distinctly higher in July when compared with the previous cruises, which implies elevated microbial activity in the water column during summer. Unusually high numbers are seen in November, which is most likely caused by remnants of prior blooms and resuspension.

6.4.2. Sedimentological properties

Average surface values of SPM concentrations for the cruises in 2005 are given in Table 6.1. Generally, maximum SPM concentrations coincide with maximum current velocities, particularly in surface samples. In addition, wind speed and direction are important factors controlling the SPM load of the water column. Similar values for both parameters are seen during the cruises in January and July 2005. Highest concentrations of SPM are observed in January while in April data are considerably lower and amount to only 10 to 20% of the winter values. From July towards November SPM values increase again. Distinctive features in July 2005 are differences for the three sampling depths, which are less pronounced in January 2005 (Fig. 6.2.). Especially the SPM concentrations of the bottom samples are remarkably high when compared with the surface values. In addition, the difference between both locations in the tidal inlet (OB1) and the central part of the tidal basin (CBA) is more pronounced in July 2005.

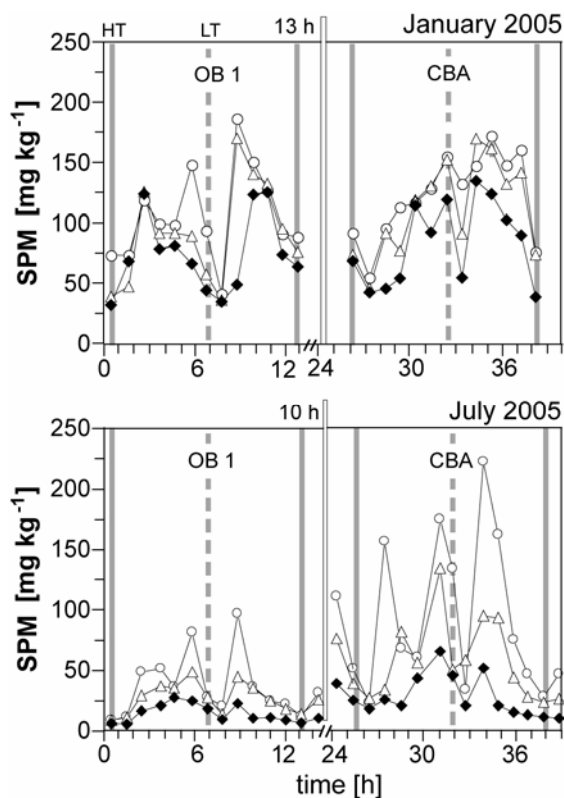


Fig. 6.2.: Tidal patterns of suspended particulate matter (SPM) for the Wadden Sea cruises in January and July 2005 (Spiekeroog Island). The vertical grey and dashed lines denote high tide (HT) and low tide (LT). The vertical rectangle marks a time gap between the sampling campaigns. Please note that wind speed and direction are comparable during both cruises (Table 6.1.).

Furthermore aggregate properties differ between winter and summer times (Table 6.1.). Even if we cannot provide data for the winter of 2005, a statistical comparison of February 2003 (Lunau et al, 2006) with July 2005 (this study) showed significant differences in aggregate numbers (Mann-Whitney-Test, $P = 0.026$) and size (t-Test, $P = 0.002$). Mean aggregate abundance over a tidal cycle was almost twice as high in February compared to July (500 ml^{-1} vs. 280 ml^{-1}), while aggregate size revealed distinctly higher values during the growing season (ECD: $118 \mu\text{m}$ in July vs. $88 \mu\text{m}$ in February).

6.4.3. Mo and Mn in the water column of the Wadden Sea

Molybdenum

Table 6.2. presents concentrations of dissolved Mo (Mo_{diss}) in the backbarrier tidal flat of Spiekeroog Island (tidal inlet Otzumer Balje OB1; central backbarrier area CBA) for the cruises in January, April, July, and November 2005. Values of Mo_{diss} normalised to a salinity of 33.7 (offshore value from October 2004) are shown as well. During the cruises in January, April, and November salinity normalised Mo_{diss} shows the expected conservative behaviour. Values are essentially identical to the offshore concentration, which was determined on samples from a cruise in October 2004 ($54^{\circ}30'$, $7^{\circ}20'$ to $54^{\circ}20'$, $7^{\circ}23'$) during a period of low biological activity. Previous Wadden Sea cruises in winter, spring, and autumn 2002 to 2004 confirm this conservative behaviour (not shown) with normalised values similar or slightly above the offshore value.

Tab. 6.2.: Average surface values and ranges (in parentheses) of water temperature, salinity as well as dissolved and particulate geochemical parameters for the Wadden Sea (tidal inlet OB1 and central backbarrier area CBA) and the German Bight. $\text{Mo}_{\text{diss},33.7\text{psu}}$ indicates values normalized to offshore salinity.

	Wadden Sea January 2005	Wadden Sea April 2005	Wadden Sea July 2005	Wadden Sea November 2005	German Bight offshore October 2004
temperature [$^{\circ}\text{C}$]	7.1 (6.5-7.4)	10.1 (8.8-12.2)	19.3 (18.6-20.1)	8.9 (7.4-9.8)	15.7 (15.6-15.8)
salinity [psu]	31.1 (29.7-32.0)	32.4 (32.1-32.6)	31.9 (31.5-32.1)	29.9 (29.3-30.3)	33.7 (33.6-33.8)
Mo_{diss} [nM]	95 (90-101)	99 (95-101)	57 (30-82)	91 (87-94)	103 (100-105)
$\text{Mo}_{\text{diss},33.7\text{psu}}$ [nM]	103 (98-107)	102 (97-105)	60 (32-86-30)	103 (98-108)	
Mo_{part} [mg kg^{-1}]	1.3 (1.1-1.5)	2.0 (1.2-3.6)	15.3 (3.8-39.6)	3.3 (1.9-4.2)	2.0 (0.7-3.2)
Mn_{diss} [nM]	48 (20-113)	331 (121-679)	135 (51-256)	65 (36-125)	12 (9-20)
Mn_{part} [mg kg^{-1}]	714 (653-754)	461 (178-703)	1205 (803-1636)	875 (678-1045)	1020 (996-1039)
Al_{part} [%]	5.7 (5.4-6.1)	4.1 (1.8-5.8)	5.3 (4.5-5.9)	5.8 (5.0-6.4)	4.1 (3.8-4.6)

Non-conservative behaviour of Mo_{diss} was observed in July 2005 with values distinctly below the seawater level. Based on almost identical salinities during that time interval (Table 6.2.), a noticeable influence of fresh water via the flood-gate in Neuharlingersiel can be excluded (compare Fig. 6.1. b). The tidal pattern of Mo_{diss} in July 2005 is visualised

in Figure 6.3. a. As salinity variations were comparatively small and close to the offshore value during these cruises, we present only absolute concentrations in Figure 6.3.

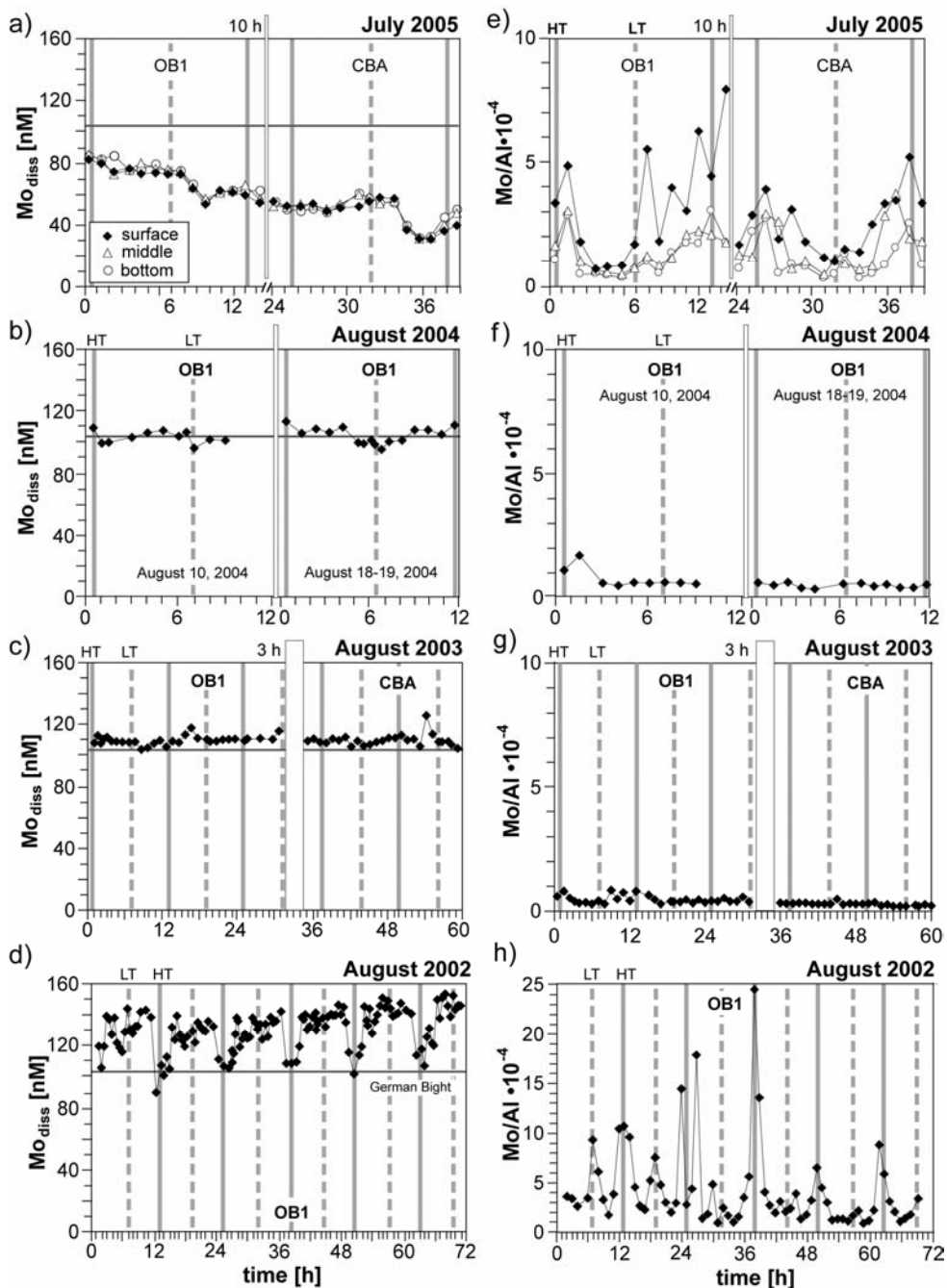


Fig. 6.3.: Tidal patterns of dissolved Mo and Mo/Al ratios for the Wadden Sea cruises (Spiekeroog Island) from summer 2002 to 2005. The vertical grey and dashed lines denote high tide (HT) and low tide (LT). The vertical rectangle marks a time gap between both sampling campaigns. The gray line denotes the Mo level for the offshore German Bight (data from October 2004).

At the beginning of the cruise in July 2005 Mo_{diss} displays a value of 82 nM and within the following 36 hours its concentration decreases dramatically to a minimum value of 30 nM, which is less than one third of the seawater value. This rapid loss in Mo_{diss} is seen in the entire water column as indicated by the similar patterns of the three depth intervals investigated (surface, middle app. 7 m above seafloor, and bottom app. 1.5 m above seafloor) and seems to be independent of the tidal exchange, i.e., input of Mo-rich seawater during high tide. Furthermore, this phenomenon spans the whole tidal basin because data from both, the tidal inlet (OB1) and the central part of the backbarrier tidal flat (CBA) show the same trend of decreasing Mo_{diss} concentrations. The rate of Mo_{diss} loss is about 2 nM h^{-1} at location OB1 and 1.5 nM h^{-1} at CBA, with a more pronounced linearity of Mo loss in the tidal inlet (OB1: $r = 0.89$; CBA: $r = 0.69$).

The decreases in Mo_{diss} were also observed in July 2005 during parallel sampling at position OB2 off Spiekeroog Island at the 10 m depth line and in the western backbarrier tidal flat of Langeoog Island (AE) where sampling started about 14 hours prior to the campaign at Spiekeroog Island (compare Fig. 6.1. b). The concentration of Mo_{diss} at position OB2 and AE (not shown) decrease from 93 nM to 74 nM and from 70 to 47 nM, respectively. Additionally, a transect from Langeoog Island towards Helgoland Island was carried out about 2 hours before sampling at location CBA in the backbarrier tidal flat of Spiekeroog (Figs. 6.1. a [black squares] and 6.4. a). Measurements of Mo_{diss} reveal that the non-conservative behaviour of Mo in the Wadden Sea is seen further offshore, too. Thus, the “normal” seawater concentration of Mo is only observed at a distance of more than 25 km offshore the barrier islands, reflecting that this phenomenon of drastically decreasing Mo_{diss} concentrations covers the entire Wadden Sea system and parts of the Southern German Bight.

Subsequent sampling campaigns in the tidal inlet of Spiekeroog at position OB1 show that the concentrations of Mo_{diss} are still below 66 nM in mid-August (Fig. 6.4. b). In mid-September a level close to the seawater value is attained, which suggests that Mo_{diss} depletion lasts at minimum for one month. During mid-October Mo_{diss} increases further

and exceeds the seawater level with an average value of 112 nM and 124 nM when normalised to offshore salinity, respectively. In contrast, the sampling campaign in November 2005 again reveals a seawater-like level of 91 nM, which is identical with the German Bight value when normalised to salinity (Fig. 6.3. d, Table 6.2.).

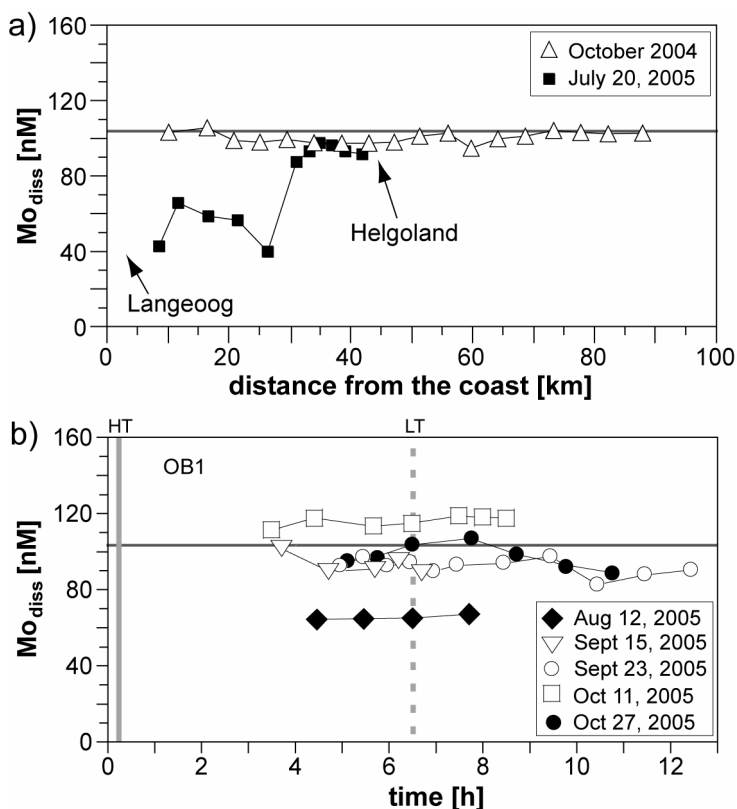


Fig. 6.4.: Dissolved Mo of (a) transects from Langeoog Island into the German Bight, and (b) several sampling campaigns at position OB 1 in the tidal inlet of Spiekeroog Island. The grey line denotes the Mo level for the offshore German Bight (data from October 2004).

Comparison with previous summer cruises from August 2002 to 2004 provides evidence about this variable behaviour of Mo in the Wadden Sea water column (Figs. 6.3. b-d). While the data from July 2005 reveal a negative anomaly of Mo_{diss} , the cruise in August 2002 is characterized by a distinct positive anomaly with maximum concentrations (158 nM) at low tide. In contrast to this, data from August 2003 and 2004 reveal an almost conservative pattern with concentrations close to the seawater value.

Regarding the values of particulate Mo (Mo_{part}) during the cruises in 2005 (Table 6.2.) it becomes evident that along with decreasing concentrations of Mo_{diss} substantial enrichments of Mo are seen on aggregates in summer when compared with the other seasons. In comparison to the geogenic background (Mo/Al : 0.15; Wedepohl, 2004) aggregates are enriched on average by a factor of 20. Despite of the general enrichment, Mo/Al -ratios in July 2005 (Fig. 6.3. e) display a variable pattern with a certain trend to higher values during high tide and more pronounced enrichments in surface samples. The comparison to other summer cruises from 2002 to 2004 (Figs. 6.3. f-h) reveals that Mo enrichments on aggregates are only seen during phases of Mo_{diss} anomalies, i.e. during July 2005 and August 2002.

Certain Mo enrichments are also observed in samples of sediment traps (<63 μm) from Langeoog Island between March and November 2005 (Fig. 6.5.). The pattern of Mo/Al -ratios reveals elevated values during July 2005, which coincides with the observed increase in Mo/Al -ratios on SPM from the water column of the Spiekeroog backbarrier tidal flat during that time (Fig. 6.3. e).

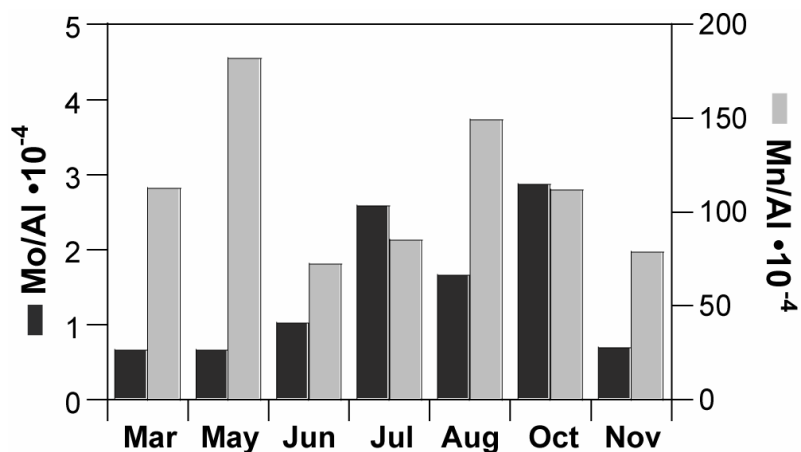


Fig. 6.5.: Mo/Al and Mn/Al ratios of material (<63 μm) from sediment traps of the backbarrier salt marsh of Langeoog Island from March to November 2005.

Manganese

The Wadden Sea cruise in July 2005 is not only special regarding Mo_{diss} but also with respect to Mn_{diss} . Earlier investigations on the behaviour of Mn in the Wadden Sea environment revealed a clear seasonal dependence with concentrations increasing by a factor of about 10 from winter towards summer (Dellwig et al., 2007) and vice versa. This behaviour was explained by elevated Mn concentrations in the pore fluids of the tidal flat sediments in summer due to more pronounced reducing conditions and therefore a higher release of Mn during ebb tide. Average concentrations of 700 nM were reported for Mn_{diss} in August 2002 and 2003 while values in winter (February 2002, 2003: 70 nM), spring (May 2002, April 2003: 300 nM), and autumn (November 2002, 2003: 80 nM) were distinctly lower. During the cruises in January and April 2005 Mn_{diss} follows this increasing trend (Figs. 6.6. a-d, Table 6.2.). Based on the results of cruises in 2002 and 2003, Mn_{diss} should have been twice as high as the spring values in summer. However, a converse behaviour without any tidal dependence is observed in July 2005, with Mn_{diss} values distinctly lower than in spring.

Ensuing sampling in the tidal inlet of Spiekeroog Island revealed that an increase in Mn_{diss} occurred somewhat later than it was observed for Mo_{diss} (Figs. 6.4. b and 6.7.). In the case of Mn_{diss} increasing values are not observed until the end of September. The average value of 300 nM on September 23 is similar to previous cruises in the Wadden Sea during September (av. 280 nM, Hinrichs, 2001). Concentrations of Mn_{diss} continue to increase until early October and reach a maximum value of 530 nM. Two weeks later, Mn_{diss} dropped to values between 140 to 278 nM, which reflects the general decrease towards the November level seen in Fig. 6.6. d.

In contrast, particulate Mn (Figs. 6.6. e-h) shows the typical enrichments in summer when compared with the other seasons, as observed during earlier cruises as well (Dellwig et al., 2007). However, the pattern from July 2005 reveals a certain trend of decreasing Mn/Al-ratios parallel to increasing concentrations of Mn_{diss} .

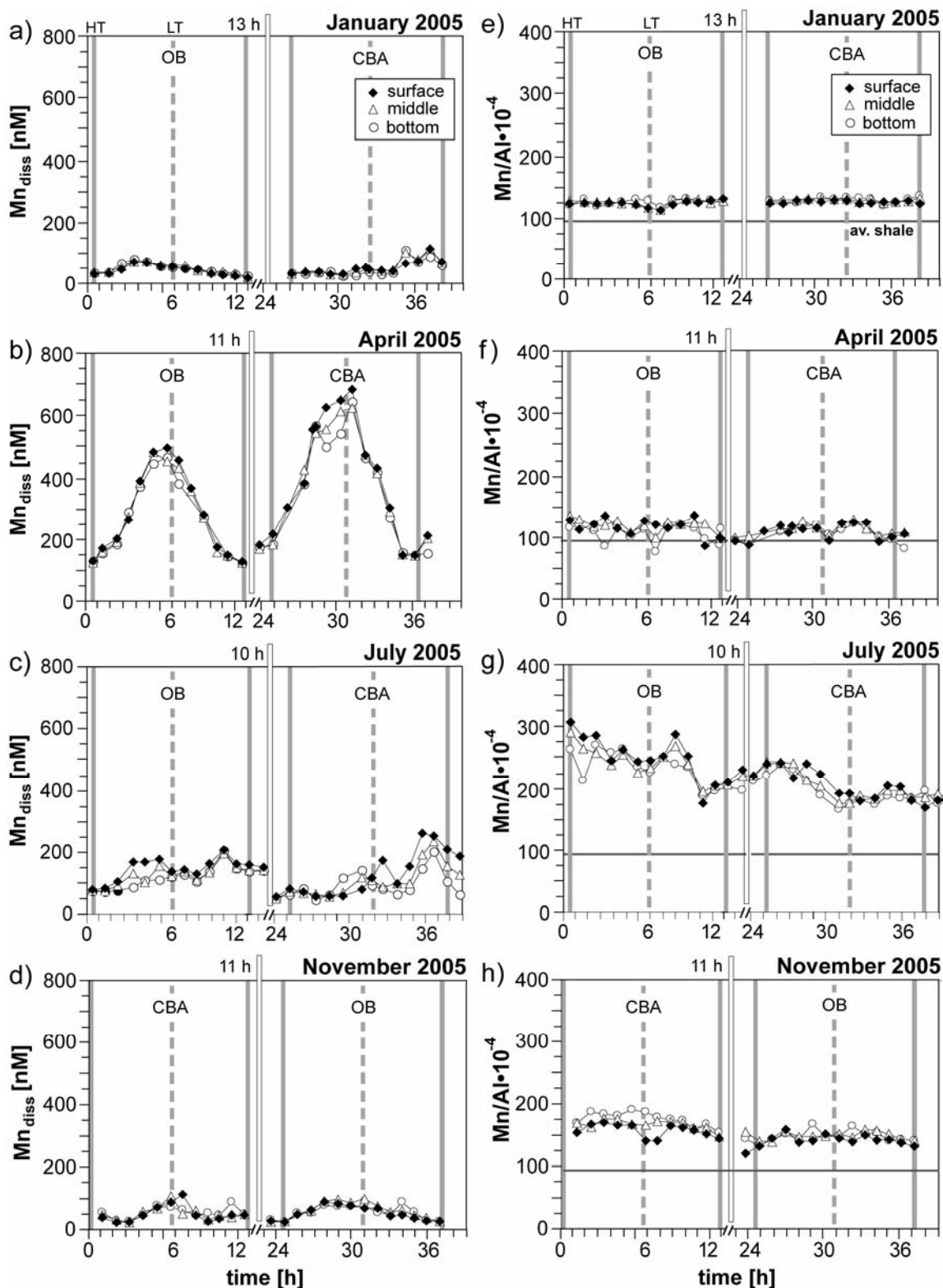


Fig. 6.6.: Tidal patterns of dissolved Mn and Mn/Al ratios for the Wadden Sea cruises in 2005 (Spiekeroog Island). The vertical grey and dashed lines denote high tide (HT) and low tide (LT). The vertical rectangle marks a time gap between the sampling campaigns. The grey line denotes the average shale level (Wedepohl, 2004).

6.4.4. Mo and Mn in the pore water of the Wadden Sea

Figure 6.8. shows pore water profiles of Mo_{diss} and Mn_{diss} for the sampling sites close to the low water line (location 1) and for the centre of the sand flat (location 2). At both sites (see Fig 6.1. b), concentrations of Mo_{diss} reveal elevated levels in the uppermost portion of the sediment and a strong decline at a sediment depth of about 0.5 m. Especially at location 2 an increase in Mo_{diss} concentrations in the upper part of the sediment is observed from July to August. Maximum values reach 370 nM, which suggests pore waters as a significant Mo source during that time when compared with the concentration in the water column in August (av. 66 nM). Elevated values lasted until September, whereas in November the profile is similar to the one in July. In contrast, at location 1, which is close to the main tidal channel, Mo_{diss} shows a high variability but does not significantly exceed the seawater level.

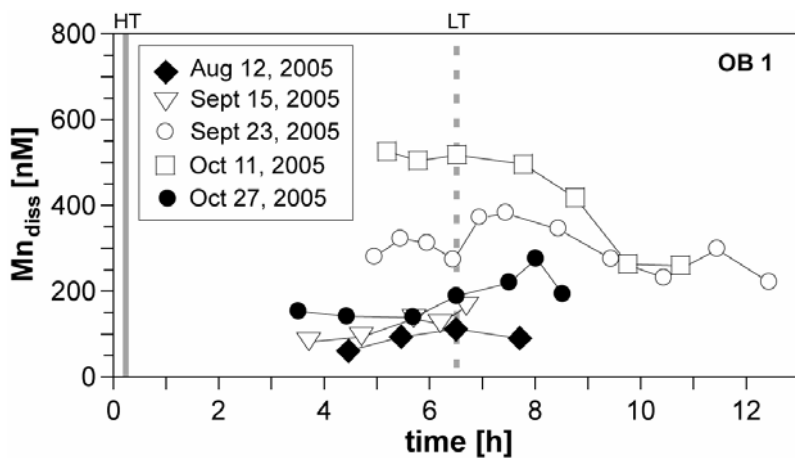


Fig. 6.7.: Dissolved Mn from several sampling campaigns at position OB 1 in the tidal inlet of Spiekeroog Island during summer and autumn 2005. The vertical grey and dashed line denotes high tide (HT) and low tide (LT).

Pore water Mn_{diss} concentrations increase about 10-fold from 1,400 nM to a maximum concentration of 15,000 nM from July to August in the upper centimetres of the sediment at location 2. Extremely high values are also observed in September, especially at 0.3 m depth. Similar to Mo_{diss} , location 1 reveals less pronounced enrichments in Mn_{diss} . An

exception forms the uppermost sample in September, when Mn_{diss} exceeds 15,000 nM. When comparing these results with the development of Mn_{diss} concentrations in the water column (Fig. 6.7.) it seems evident that the pore waters represent a significant source for Mn_{diss} as well.

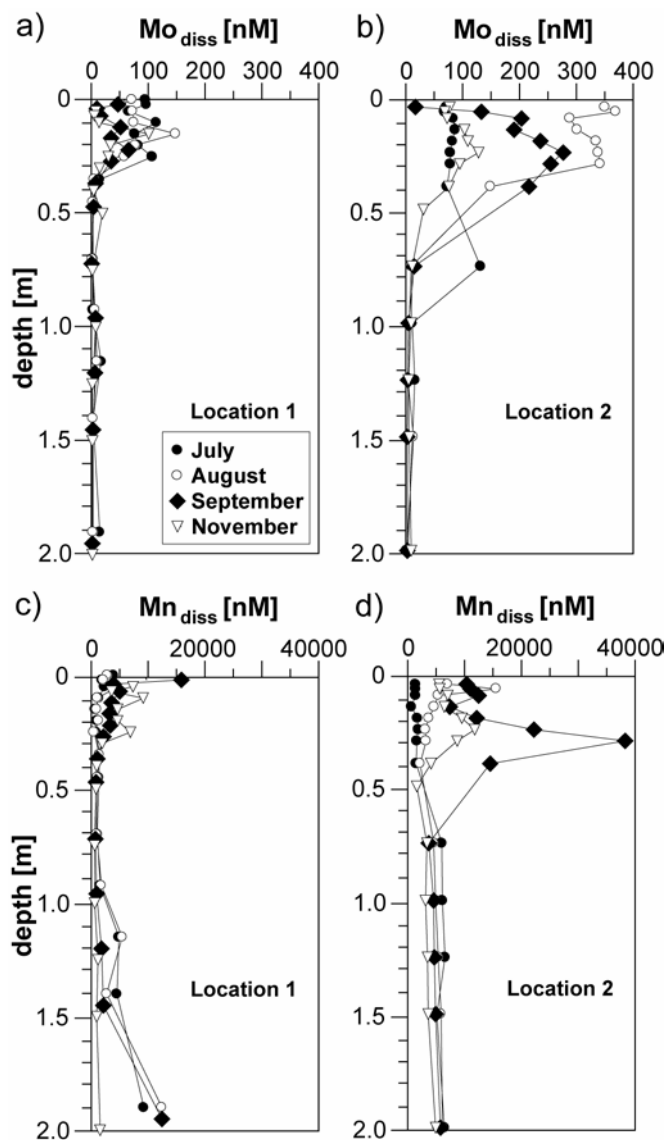


Fig. 6.8.: Comparison of Mo and Mn pore water profiles between July and November 2005 from two locations at the Janssand tidal flat of the backbarrier area of Spiekeroog Island (compare Fig. 6.1. b).

6.5. Discussion

6.5.1. Biological and sedimentological conditions

The results presented so far document non-conservative behaviour of Mo_{diss} in the Wadden Sea during specific time intervals in summer as reflected by both, negative but also positive concentration anomalies (Figs. 6.3. a, d). In contrast, cruises in August 2003 and 2004 (Figs. 6.3. b, c) displayed a more or less conservative pattern, which may reflect a transitional behaviour between extreme situations. Decreasing concentrations were also observed in the western backbarrier area of Langeoog Island (not shown) and in the adjoining near-coastal waters of the German Bight (Fig. 6.4. a), which gives evidence that a larger area is affected by this phenomenon.

Processes causing removal and at a later stage release of Mo_{diss} are necessary to explain such differing concentration signatures. For understanding the individual mechanisms causing such phenomena, it is essential to know about the distinctive characteristics of the individual summer cruises. For that reason, the first part of the discussion deals with the biological and sedimentological aspects, while in the following chapters we will discuss the processes of removal and release of Mo.

The chlorophyll-*a* concentrations (Table 6.1.) point towards the occurrence of algae blooms during both cruises in April and July 2005. However, taking the ratios of phaeopigments to total chlorophyll into account, which are indicative for the quality of algae material, it becomes obvious that in July 2005 the algae bloom was in a later stage, most likely in a phase of breakdown. Consequently, the onset of lyses of algae may have led to a release of elevated amounts of labile organic compounds. It is well known that such fresh and labile DOC is very rapidly degraded by bacteria (Coveney and Wetzel, 1989; Muenster, 1993). It also has the potential to form transparent exopolymer particles (TEP) from dissolved precursors. Thus we postulate, that the degradation of such algal material by free-living bacteria, which are twice as abundant in July as in April (Table 6.1.), initiates the formation of larger aggregates in the Wadden Sea water column as recently observed by several authors (e.g. Engel et al., 2004; Chen et al., 2005; Lunau

et al., 2006; Passow and De la Rocha, 2006). A further indication of degradation and release of organic compounds is given by elevated DOC values in July when compared with the bloom in April (Table 6.1.). Former cruises in August 2002 and 2003 showed lower DOC values as well (av. 0.21 mM; Dellwig et al., 2007) and shed light on the special situation during the cruise in July 2005.

Aggregation is documented by the comparison of ECD values between winter and summer (Table 6.1.). Along with POC, our data suggest the occurrence of larger organic-rich aggregates in summer, whereas the winter situation is dominated by smaller inorganic particles. These larger aggregates offer favourable conditions for the formation of suboxic micro-zones, an assumption that is supported by investigations of Alldredge and Cohen (1987) and Ploug et al. (1997). The authors detected significant oxygen depletion in marine snow and laboratory-made aggregates by the use of microelectrodes. Additionally, Nielsen et al. (2005) found a distinctly higher potential for anammox inside larger aggregates when compared with smaller ones. For the formation of suboxic zones within the aggregates elevated microbial activity is necessary, a prerequisite, that is indicated by distinctly higher numbers of aggregate-associated bacteria in July 2005 (Table 6.1.).

Aggregation during breakdown of algae blooms is of crucial importance for sedimentological and geochemical budgets of the Wadden Sea environment as the larger aggregates behave hydraulically different (Chang et al., 2006a,c). This change is seen in the varying SPM loads during the cruises in 2005 (Fig. 6.2.), which are mainly attributed to three variables: (i) the tidal state, (ii) weather conditions, and (iii) hydrological properties of aggregates. The tidal influence can be regarded in a first approximation as constant as the cruises took place during similar tidal states (spring tide at the end of the campaign). The second parameter, i.e., wind speed and wind direction, is of major importance for the hydrodynamic conditions in the Wadden Sea. For that reason it is essential that weather conditions are almost identical when comparing SPM concentrations of different cruises, which is only the case for January and July 2005 (Table 6.1.). Nonetheless, surface SPM concentrations and the number of aggregates are considerably higher in January when

compared with July, which has to be attributed to the different hydraulic properties of SPM in winter and summer (Table 6.1.). To solve this discrepancy in SPM load between both cruises, huge amounts of larger aggregates have to be deposited on the tidal flats during summer. This assumption is in accordance with sedimentological investigations carried out in the backbarrier area of Spiekeroog Island by Chang et al. (2006a, c). The authors report that in summer, the surface sediment comprises a mud drape, whereas during winter the same tidal flats are dominated by sand. They also suggest that the finer particles deposited in summer are incorporated into larger flocs and aggregates and are therefore hydraulically similar to co-deposited sand.

Overall, from a biological and sedimentological view the distinctive feature in July is the breakdown of an algae bloom, which accelerated bacterial activity and growth. As a result organic matter is released by lyses and bacterial decomposition of algal material initiates the formation of larger aggregates. Huge amounts of these organic-rich aggregates are deposited on the tidal flats, thereby serving as a potential shuttle for the transfer of material and compounds from the open water column to the sediment layer. In contrast, earlier cruises in August 2002-2004 did not record this development at its initial stage. Thus, the question remains whether this special situation in July 2005 can be made responsible for the observed behaviour of Mo?

6.5.2. Removal of Mo from the water column

For the removal of Mo_{diss} from the water column several processes are conceivable, which comprise uptake by phytoplankton, fixation in reducing tidal flat sediments, scavenging by Mn-oxides, complexation by organic matter as well as processes in the suboxic interior of larger aggregates.

Although Mo forms an essential micro-nutrient for the nitrogen-metabolism of phytoplankton and bacteria (Howarth and Cole, 1985; Paerl et al., 1987), which can be enriched in marine cyanobacteria during nitrogen fixation (Tuit and Ravizza, 2003), culture experiments have shown that Mo uptake rates are too low ($0.4 \text{ pM } \mu\text{g chl}^{-1} \text{ h}^{-1}$; Marino et

al., 2003) for explaining the Mo_{diss} depletion rate of 2 nM h^{-1} observed in July 2005. A further possibility may be the fixation of Mo_{diss} as sulphide in reducing tidal flat sediments. Again, this possibility seems to be less plausible as such process cannot explain the observed rapid loss of more than 60% of Mo_{diss} from the water column within 36 hours. Moreover, Mo burial in sediments prevails during the entire summer when microbial activity is high and reducing conditions in the sediments are most pronounced. Even though the settling of aggregates transfers high amounts of organic matter to the sediment, which accelerates microbial activity, our pore water profiles do not proof elevated Mo fixation in July 2005 (Figs. 6.8. a, b).

One important mechanism may be the scavenging of Mo_{diss} by freshly formed MnO_x phases during bacterial oxidation of Mn_{diss} . Adelson et al. (2001) postulated a model for scavenging of Mo by MnO_x phases in order to explain Mo enrichments in sediments of Chesapeake Bay. Mn^{2+} refluxing from sediments is converted to particulate $\text{Mn}(\text{Mo})\text{O}_x$ during oxidation in the upper water column. Sedimentation of these particles leads to preconcentration of Mo at the sediment-water interface. Mo is liberated during reduction of Mn-oxide phases at or close to the sediment surface from where it may diffuse downward until it is fixed by organic thiols or HS^- . Extremely low Mn_{diss} concentrations and associated enrichments in Mn_{part} in Wadden Sea samples from July 2005 (Figs. 6.6. c, g) point towards intense oxidation of Mn^{2+} . Therefore, formation of $\text{Mn}(\text{Mo})\text{O}_x$ phases might explain the depletion in Mo_{diss} (Fig. 6.3. c) or vice versa the enrichment of Mo_{part} on SPM (Fig. 6.3. e) observed in July 2005. Unfortunately, we do not know whether Mn-oxidising bacteria exhibit enhanced activity during an algae breakdown, which would be important information as Mn-oxidation forms a common process in the study area during summer (Dellwig et al., 2007). Comparing the Mn/Al-ratios of the summer aggregates (August 2002: 260; August 2003: 316; August 2004: 302; July 2005: 227) no unusual enrichments are observed for the cruises in July 2005 and August 2002. SPM from the latter cruises is even slightly depleted in Mn, which contradicts a relation between Mo_{diss} depletion and Mn oxidation. In addition, unusually low values of Mn_{diss} in July 2005 (Fig. 6.6. c) are most

likely not due to elevated bacterial Mn oxidation but rather caused by exhaustion of the sedimentary reservoir. A finding that is supported by low Mn_{diss} concentrations in pore waters especially at location 2 in July 2005 (Fig. 6.8. d).

Moreover, the patterns of Mn_{diss} and Mn_{part} display an opposite trend in July 2005. While Mn_{diss} tends to increase, the contents of Mn_{part} decline, which points towards release of Mn from SPM and argues against elevated Mn oxidation and associated Mo scavenging. The conversion of the contents of Mn_{part} into volume specific units reveals an average concentration of 272 nM, which is twice as high as the average concentration of Mn_{diss} (135 nM). Therefore, the gain in Mn_{diss} during the investigated time-period in July 2005 could be explained by release from SPM (Fig. 6.6. c). However, release from the particulate phase would require suboxic zones in aggregates, which can be caused by an elevated number and activity of aggregate-associated bacteria, respectively (Table 6.1.). A similar process was already postulated by Klinkhammer and McManus (2001). They explained mid-depth Mn maxima in the Columbia River estuary by reduction of Mn in the suboxic interior of aggregates. In addition, the authors point out the connection between Mn release and bacterial activity. Therefore, on the basis of our data, a relation between Mn-oxidation and Mo depletion can only hardly be deduced. Nevertheless, the possible adsorption of Mo on still existing MnO_x coatings on aggregates cannot be completely disregarded.

Despite the aforementioned reduction of MnO_x phases, oxygen-depleted micro-zones in aggregates may be the loci for Mo_{diss} reduction and removal from the water column as well. In view of the xy-plots shown in Figure 6.9. a relationship between bacterial abundance on aggregates and Mo_{diss} and Mn_{diss} concentrations becomes obvious. Thus, we postulate that increasing abundance and activity of bacteria on organic-rich aggregates produces oxygen-depleted micro-zones, which enable fixation of Mo and release of Mn from the aggregates. Unfortunately, our data do not provide information about the particular mechanism of Mo fixation. In addition to chemical processes, reduction by bacteria is also conceivable as shown by Ghani et al. (1993). The same is

true for Mn, either bacteria may start to reduce Mn_{part} directly, or Mn may be reduced chemically in suboxic zones.

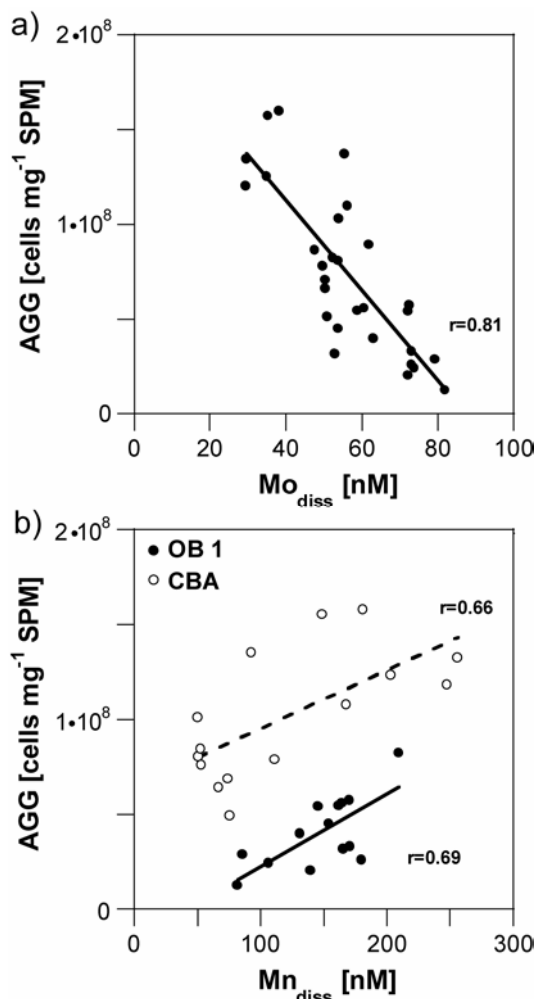


Fig. 6.9.: Correlation diagrams of dissolved Mn and Mo versus aggregate-associated bacteria (normalized to SPM) for surface water samples from the backbarrier area of Spiekeroog Island in July 2005.

Besides this direct fixation of Mo in micro-zones, fresh algal organic matter and certain humic substances are also capable to capture MoO_4^{2-} from solution (Szilagyi, 1967; Bertine, 1972; Volkov and Formina, 1974; Nissenbaum and Swaine, 1976; Disnar, 1981; Brumsack and Gieskes, 1983; Alberic et al., 2000), particularly when the organic matter is sulphurised (Tribovillard et al., 2004). An increase in organic matter content of SPM is evident from POC data, which show elevated values in spring and especially

during summer (max. 28.7%; Table 6.1.). Additionally, Bertine (1972) reported a pH dependency of Mo scavenging and/or reduction by organic acids with increasing rates during decreasing pH. This should be the case in the suboxic interior of aggregates as shown by Alldredge and Cohen (1987) and Ploug et al. (1997).

Both processes, reduction in oxygen-depleted zones and scavenging by organic matter are strongly coupled to biological activity. The release/bacterial degradation of fresh algal organic matter especially during breakdown of blooms causes aggregation, and is therefore limited to a certain time interval. Only such processes are able to explain the abrupt decrease in Mo_{diss} , whereas the processes mentioned before are not limited to a certain time interval or event. For instance, fixation of Mo in sediments as well as scavenging of Mo by MnO_x should occur during the entire summer.

6.5.3. Fate of Mo on aggregates

As seen in Figures 6.3. a and e, the rapid loss of Mo_{diss} in July 2005 corresponds with substantial enrichments of Mo_{part} on aggregates. However, it is of crucial importance whether the Mo enrichment on SPM is balanced by the loss in Mo_{diss} . This requires the direct comparison of dissolved and particulate metal concentrations per volume unit. For that reason, we calculated excess element concentrations, which reflect the amount of Mo added to SPM in addition to the geogenic background. This excess fraction is calculated according to the following equations (average shale data from Wedepohl, 2004):

$$Mo_{background} = (Mo/Al)_{av. \text{ shale}} \times Al_{sample}$$

$$Mo_{excess} = Mo_{sample} - Mo_{background}$$

The conversion of Mo_{excess} into volume specific Mo concentrations (Mo_{xs}) is done by multiplication with SPM concentrations. The resulting concentrations of Mo_{xs} indicate that the particulate phase, even though highly enriched in Mo, cannot explain the observed loss in Mo_{diss} in the water column. The average value of Mo_{xs} (2.5 nM) only explains 6% of the loss in Mo_{diss} . In our view, this discrepancy can only be explained by the rapid

sedimentation of Mo-rich particles following particle aggregation during breakdown of an algae bloom (see Chapter 5.1.).

According to M. Beck (pers. comm.) deposited aggregates formed a widespread fluffy layer on the tidal flat sediments next to the pore water sampling site 2. Unfortunately, this fluffy material is not available for geochemical analyzes. However, the geochemical composition of these aggregates is most likely reflected in sediment trap samples collected in the backbarrier salt marsh of Langeoog Island (Fig. 6.5). This material shows enrichments in Mo from summer to early autumn. Furthermore, the pattern of Mn is in accordance with an alternating dominance of Mn-oxidation and Mn-reduction. Mn-oxidation prevails in spring and late summer, whereas in June and July, when aggregation along with the development of suboxic micro-zones in aggregates becomes more important, decreasing values are due to intense Mn-reduction.

In our view it is rather likely that the deposition of such aggregates may explain the discrepancy in the balance between Mo_{diss} loss and the apparent lack of particulate Mo_{xs} to compensate for this loss. Thus, we propose that large amounts of Mo_{diss} are removed from the water column owing to deposition of Mo-rich and still Mn-rich aggregates during breakdown of an algae bloom in early summer. Additionally, with the transfer of Mo and Mn into the upper sediment layer by settling aggregates organic matter is added to the sediment, which favours microbial activity and therefore the decomposition of buried aggregates.

6.5.4. Fate of Mo in the sediments: Implications from the pore water

Aggregates formed in the open water column were deposited on the sand flat Janssand in July 2005 especially at location 2 (Fig. 6.1. b), leading to the accumulation of a fine layer of Mo- and still Mn-rich particulate matter at the sediment surface. Although still under debate, adherence of deposited aggregates on the tidal flats may be favoured by release of extracellular polymeric substances (EPS) from benthic diatoms and cyanobacteria. As EPS compounds exhibit a certain stickiness, they are presumably

increasing the erosion threshold (Stal, 2003). This material is supposed to be subsequently incorporated into subsurface layers of the sediment. The transport of particulate matter into permeable sandy sediment by boundary flows, which interact with sea bed topography, for example sediment wave ripples, has often been described and modelled (Huettel and Rusch, 2000; Rusch and Huettel, 2000; Precht and Huettel, 2003; de Beer et al., 2005). While these aggregates are incorporated into the sediment, Mn and Mo are released once the aggregates experience reducing conditions in slightly deeper sections of the sediment (Duinker et al., 1974; Burdige, 1993). Stabilisation of Mo in the pore water is probably assured by complexation with dissolved organic matter (Brumsack and Gieskes, 1983). The microbially induced release of both metals, which is caused by decomposition of organic aggregates, reasonably well explains the observed increases in Mo_{diss} and Mn_{diss} in the pore water at location 2 from July to September 2005 (Figs. 6.8. b, d).

Due to tidal dynamics, exchange processes occur between the surface sediment pore waters and the open water column (Huettel et al., 1998). This process contributes Mo_{diss} and Mn_{diss} to the water column as seen in increasing concentrations in August and September 2005 (Figs. 6.4. b and 6.7.). The same phenomenon of Mo_{diss} release from pore water may explain the positive anomaly in Mo_{diss} at low tide observed in August 2002 (Fig. 6.5. a). The hypothesis of Mo release from pore water is supported by observations of Dalai et al. (2005) who explained excess concentrations of Mo at salinity >5 in the Chao Phraya Estuary by release from pore waters and changing redox conditions. Furthermore, experiments with *in situ* benthic flux chambers carried out by Morford et al. (2007) revealed substantial release of Mo from Boston Harbor sediments.

In case of Mn, settling of Mn-rich aggregates forms an important process for the Mn budget of the Wadden Sea environment. The comparison of Mn_{diss} between July 2005 and April 2005 (Table 6.2.) reveals an unusually low level during the summer cruise. In addition to intense Mn-oxidation in the water column, this observation seems to be caused to a certain degree by exhaustion of the tidal flat sediments in reactive Mn. This

assumption is in accordance with the findings of Dellwig et al. (2007) who showed that during spring and especially summer, the Mn budget of the Wadden Sea water column is almost completely controlled by release from pore waters. Therefore, deposition of aggregates and concomitant Mn reduction form a recharge mechanism explaining the increasing Mn_{diss} values observed in September and early October 2005 (Fig. 6.7.).

6.6. Summary and concluding remarks

Non-conservative behaviour of dissolved Mo was observed in the Wadden Sea of NW Germany, i.e., negative but also positive anomalies. In the backbarrier tidal flat of Spiekeroog Island concentrations of dissolved Mo declined from a seawater-like level to a minimum value of 30 nM within 36 hours during July 2005. This phenomenon was also observed in the adjoining backbarrier tidal flat of Langeoog Island and in near-coastal water masses about 25 km offshore. Further measurements provide evidence that this depletion, which is accompanied by significant Mo enrichments on SPM, lasted for at minimum four weeks. In contrast, elevated Mo_{diss} values (maximum 158 nM) were observed in August 2002. During this period Mo_{diss} displayed a tidal cyclicity with maximum concentrations during low tide, which points towards the tidal flat sediments as the dominant source.

This non-conservative behaviour of Mo can only be explained by the tight coupling of biological, sedimentological, and geochemical processes, as summarized in the sketch shown in Figure 6.10. The controlling forces are algae blooms and the associated growth of bacteria. While the algae spring bloom does not influence the total number of bacteria, this does not seem to be the case for the algae bloom in summer, when bacterial activity and number increased significantly. Bacterial decomposition of algae releases organic compounds, which promote aggregation of suspended mineral particles. MoO_4^{2-} seems to be reduced in oxygen-depleted zones of larger aggregates and/or is “scavenged” by

freshly formed organic matter resulting in prominent Mo_{part} enrichment. A relation between the depletion of Mo and the formation of MnO_x phases is not indicated by our data.

Mn_{diss} concentrations are unusually low during this specific time period, which is either caused by exhaustion of the tidal flat sedimentary pool in reactive Mn or Mn-oxidation in the water column, which also diminishes the concentration in Mn_{diss} and leads to Mn enrichments on aggregates.

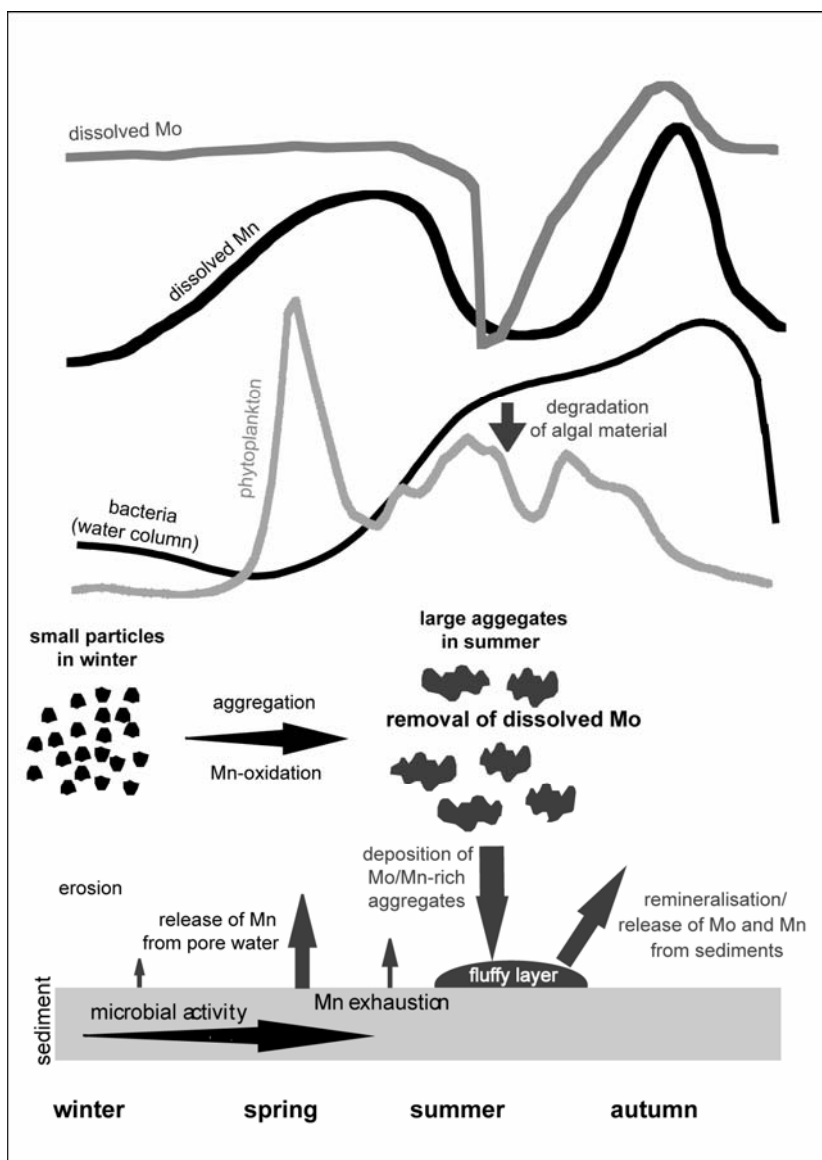


Figure 6.10.: Illustration of the postulated model for non-conservative behaviour of Mo in coastal waters, which is based on the tight coupling between geochemical, biological, and sedimentological processes. Phytoplankton pattern bases on model results by Kohlmeier (2004).

Huge amounts of larger aggregates and associated Mo and Mn are deposited on the tidal flats, leading to a depletion of these elements in the water column. Microbial decomposition of shallowly buried aggregates leads to release of Mo and Mn from the sediments and replenishes the trace metal pool in the water column, as seen in increasing trace metal concentrations in the pore water pool in late summer as well as subsequently in the water column.

In addition to the transfer of trace metals into the sediments via deposition of aggregates, this process also leads to a sudden deposition of huge amounts of organic matter, which enhances microbial activity in the sediments.

The postulated coupling of biological, sedimentological, and geochemical processes may also be of significant relevance for Mo and possibly other trace metal enrichments in TOC-rich marine deposits. Thus, the transfer of Mo to the sediments via settling aggregates will concentrate Mo at the sediment/water interface from where it may diffuse into the deeper anoxic zone where it may finally be fixed as a sulphide.

Acknowledgements

The authors wish to thank the crews of the research vessels RV Senckenberg and RV Heincke for active support during the cruises. Maik Grunwald, Alexander “Josi” Josefowicz, Sibylle Kölsch, and Laura Wehrmann are thanked for their great assistance during several sampling campaigns. We thank Holger Freund and Jan Barkowski (ICBM, Marine Station) for making material from the sediment traps available. Further thanks are due to Andrea Lübben and Frank Terjung (Marine Physics, University of Oldenburg) for providing several salinity and water temperature data of the cruises with RV Senckenberg and RV Heincke. Two anonymous reviewers and Tim Shaw are thanked for their helpful and constructive comments. This study was funded by the Deutsche Forschungsgemeinschaft (DFG) through grants BR 775/14-1/2 and forms part of the Research Group “BioGeoChemistry of Tidal Flats”.

7. Conclusions and perspectives

Biogeochemical processes and trace metal dynamics were studied in pore waters of intertidal flat sediments located in the backbarrier area of Spiekeroog Island. The studies focused on the sandy tidal flat called Janssand (JS), whereas some results are also shown from the Neuharlingersieler Nacken (NN) tidal flat, which is characterized by higher clay contents. The Janssand tidal flat was chosen as the main study area because it shows typical characteristics of backbarrier areas of the West- and East-Frisian Islands.

Sulphate, dissolved organic carbon, nutrients, and some metabolic products were determined in pore waters to identify spatial, seasonal, and tidal variations of biogeochemical processes. Spatial samplings revealed that pore water depth profiles show some different characteristics in the JS and NN tidal flats. Sulphate displays a more pronounced depletion and metabolic products are stronger enriched in the NN tidal flat compared to the JS tidal flat. Clay-rich layers seem to hinder pore water exchange processes in the NN tidal flat resulting in longer residence times of pore waters and thus enrichments of metabolic products. Differences in sediment structure and hydrological conditions were further identified as key factors leading to spatial variations in pore water depth profiles of tidal flat margins compared to central parts of tidal flats.

Deep pore water studies in the JS tidal flat further illustrate that seasonal variations of sulphate, dissolved organic carbon, and nutrients are not limited to the sediment surface, but are also observed in some metres depth of permeable sandy sediments. Close to the JS tidal flat margin, lower sulphate concentrations are determined at 1 to 4 m depth in summer 2005 compared to the remaining months of the year. Temporal pattern of DOC, total alkalinity, and the nutrients ammonium and phosphate are very similar to those of sulphate, however show the opposite seasonal pattern. Increasing activity of sulphate reducing bacteria with increasing temperature only partly explains the observed finding. No seasonal variations in sulphate are found in central parts of the tidal flat. The site close

to the tidal flat margin prevails higher TOC contents than central parts thus leading to the suggestion that better substrate availability induced a higher activity of fermentative microorganisms in summer 2005. By the production of labile organic matter they seem to stimulate the activity of sulphate reducers even in depths of some metres.

Trace metals show similar general trends with depth in pore waters of sites close to the margin and in central parts of the tidal flat. Despite of dynamic biogeochemical, sedimentological, and hydrological conditions prevailing in intertidal flats, the general trends with depth of trace metals are similar to those observed in continental margin environments where constant sedimentation rates dominate. V and Cr show seasonal variations down to some metres depth parallel to changes in dissolved organic carbon. Seasonal variations of Mn, Fe, Mo, and U are by contrast limited to the upper decimetres of the sediment depending on factors like organic matter supply, redox stratification, and geochemical composition of the particulate matter deposited on the sediment surface. In July 2005 a non-conservative behaviour of Mo was observed in the open water column of the study area, which resulted in a decrease in Mo by about two thirds. Bacterial decomposition of algae releases organic compounds promoting the aggregation of suspended mineral particles. It is suspected that Mo is reduced in oxygen-depleted zones of larger aggregates and/or scavenged by freshly formed organic matter resulting in a decrease of dissolved Mo concentrations in the water column. Deposition of Mo-enriched particulate matter on tidal flat sediment surfaces and consequently incorporation of these particles into the sediment leads to pore water Mo concentrations significantly above the sea water level.

Several results of this study present evidence that deep pore water advection affects biogeochemical processes in sediments of tidal flat margins. Changes in pore water depth profiles are observed in some metres depth during one tidal cycle. The replenishment of the sulphate pool after the summer months in 2005 further evidence that tidal flat margins are influenced by deep pore water flow. We thus hypothesize that the Janssand tidal flat is influenced by deep pore water advection at its margins, which triggers seeps of anoxic

pore waters. Seeping anoxic pore waters presumably originate from some metres depth as sampling at different times within a tidal cycle revealed largest changes in depth profiles in about 1.5 to 3 m depth. Concerning species enriched in pore water compared to sea water like nutrients or Mn, seeping pore water may represent an important source for the ecosystem in the open water column.

The Janssand tidal flat was thus identified as an important “bio-reactor” where organic matter is recycled, and nutrients, DOC, and several other terminal metabolic products are produced and consecutively released at creek banks. For the exchange of solutes and particles, transport processes at the sediment-water interface and in the sediment body were shown to be essential. Transport processes include molecular diffusion and pore water advection, where advection is suggested to be the dominant transport process in permeable sandy sediments like the Janssand tidal flat.

Little is however known about flow pathways in the Janssand tidal flat. We suspect that close to tidal flat margin where pore water is seeping out of the sediment, pore water is replenished by pore water from central parts of the tidal flat. Additionally tidal pressure gradients may lead to forward and backward flow of pore water over small distances. However, we can only speculate about flow pathways and flow velocities in deep pore waters and about sediment layers especially affected by advection processes. Further studies concerning the sedimentological and stratigraphical structure of the tidal flat may help to identify permeable sediment layers allowing deep pore water flow over longer distances. These studies should not be limited to marginal regions of the tidal flat, but extended far into central parts to elucidate possible long flow pathways. Furthermore, tracer experiments would verify pore water flow velocities. Inserting a dye into sediment layers where this study gave indications for water flow would provide data about possible maximum flow velocities in deep layers.

Temperature changes in the sediment also provide information about thermal conductivity and permeability of the sediment. Within the framework of this thesis continuous temperature measurements (Pt 100; Ahlborn, Germany) were conducted in

1 m intervals down to 5 m depth close to the margin on the Janssand tidal flat. Seasonal temperature variations are significant in the upper metres of the sediment and comparably small in sediment depths of 5 m. Interpretation of these data is however complicated due to technical questions and data will be presented at a later stage. A second temperature measuring system (CeraDiver; Schlumberger, Eigenbrodt, Germany) has recently been installed at different locations at the Janssand tidal flat margin. Both systems will be used to better understand hydrological processes in the tidal flat sediments.

The knowledge gained about sedimentological structure, flow pathways, and pore water flow velocities would help to establish a model setup finally enabling to calculate pore water discharge at tidal flat margins. Pore water discharge in turn is essential to better estimate the influence of seeping pore waters on the ecosystem in the open water column. Furthermore, these results would be important for the establishment of material budgets concerning all compartments influencing biogeochemical processes in the backbarrier area, such as the water column and including suspended particles, the sediment-water interface, deep sediments, North Sea, and fresh water. These material budgets are an essential tool to predict whether species are imported from the North Sea or exported from the backbarrier area.

8. References

- Adelson J.M., Helz G.R., and Miller C.V. (2001) Reconstructing the rise of recent coastal anoxia; molybdenum in Chesapeake Bay sediments. *Geochim. Cosmochim. Acta* **65**(2), 237-252.
- Alberic P., Viollier E., Jezequel D., Grosbois C., and Michard, G. (2000) Interactions between trace elements and dissolved organic matter in the stagnant anoxic deep layer of a meromictic lake. *Limnol. Oceanogr.* **45**(5), 1088-1096.
- Allredge A.L. and Cohen Y. (1987) Can microscale chemical patches persist in the sea? Microelectrode study of marine snow, fecal pellets. *Science*, **235**, 689-691.
- Alperin M.J., Albert D.B., and Martens C.S. (1994) Seasonal variations in production and consumption rates of dissolved organic carbon in an organic rich coastal sediment. *Geochim. Cosmochim. Acta* **58**(22), 4909-4930.
- Andersen F.O. and Helder W. (1987) Comparison of oxygen microgradients, oxygen flux rates and electron transport system activity in coastal marine sediments. *Mar. Ecol. Prog. Ser.* **37**(2-3), 259-264.
- Andersen M.S., Jakobsen V.N.R., and Postma D. (2005) Geochemical processes and solute transport at the seawater/freshwater interface of a sandy aquifer. *Geochim. Cosmochim. Acta* **69**(16), 3979-3994.
- Anderson R.F. (1982) Concentration, vertical flux, and remineralization of particulate uranium in seawater. *Geochim. Cosmochim. Acta* **46**(7), 1293-1299.
- Anderson R.F., Fleisher M.Q., and Leheray A.P. (1989a) Concentration, oxidation state, and particulate flux of uranium in the Black Sea. *Geochim. Cosmochim. Acta* **53**(9), 2215-2224.
- Anderson R.F., Leheray A.P., Fleisher M.Q., and Murray J.W. (1989b) Uranium deposition in Saanich Inlet sediments, Vancouver Island. *Geochim. Cosmochim. Acta* **53**(9), 2205-2213.

- Arnosti C., Jørgensen B.B., Sagemann J., and Thamdrup B. (1998) Temperature dependence of microbial degradation of organic matter in marine sediments: polysaccharide hydrolysis, oxygen consumption, and sulfate reduction. *Mar. Ecol. Prog. Ser.* **165**, 59-70.
- Atkinson M.J. and Smith S.V. (1983) C:N:P ratios of benthic marine plants. *Limnol. Oceanogr.* **28**(3), 568-574.
- Audry S., Blanc G., Schäfer J., Chaillou G., and Robert S. (2006) Early diagenesis of trace metals (Cd, Cu, Co, Ni, U, Mo, and V) in the freshwater reaches of a macrotidal estuary. *Geochim. Cosmochim. Acta* **70**(9), 2264-2282.
- Audry S., Blanc G., Schäfer J., and Robert S. (2007) Effect of estuarine sediment resuspension on early diagenesis, sulfide oxidation and dissolved molybdenum and uranium distribution in the Gironde estuary, France. *Chem. Geol.* **238**(3-4), 149-167.
- Baldock J.A., Masiello C.A., Gelin Y., and Hedges J.I. (2004) Cycling and composition of organic matter in terrestrial and marine ecosystems. *Mar. Chem.* **92**(1-4), 39-64.
- Barnes C.E. and Cochran J.K. (1990) Uranium removal in oceanic sediments and the oceanic U balance. *Earth Planet. Sci. Lett.* **97**(1-2), 94-101.
- Barnes C.E. and Cochran J.K. (1991) Geochemistry of uranium in Black Sea sediments. *Deep-Sea Res.* **38**, S1237-S1254.
- Barnes C.E. and Cochran J.K. (1993) Uranium geochemistry in estuarine sediments - Controls on removal and release processes. *Geochim. Cosmochim. Acta* **57**(3), 555-569.
- Beck M., Dellwig O., Kolditz K., Freund H., Liebezeit G., Schnetger B., and Brumsack H.-J. (2007) In situ pore water sampling in deep intertidal flat sediments. *Limnol. Oceanogr.: Meth.* **5**, 136-144.
- Beck M., Dellwig O., Holstein J.M., Grunwald M., Liebezeit G., Schnetger B., and Brumsack H.-J. Sulphate, dissolved organic carbon, nutrients and terminal metabolic products in deep pore waters of an intertidal flat. (submitted a).

- Beck M., Dellwig O., Liebezeit G., Schnetger B., and Brumsack H.-J. Spatial, seasonal and tidal variations of sulphate, dissolved organic carbon, and nutrients in deep pore waters of intertidal flat sediments. (submitted b).
- Bender M., Martin W., Hess J., Sayles F., Ball L., and Lambert C. (1987) A whole-core squeezer for interfacial pore-water sampling. *Limnol. Oceanogr.* **32**(6), 1214-1225.
- Berg P. and McGlathery K.J. (2001) A high-resolution pore water sampler for sandy sediments. *Limnol. Oceanogr.* **46**(1), 203-210.
- Berner R.A. (1984) Sedimentary pyrite formation - an update. *Geochim. Cosmochim. Acta* **48**(4), 605-615.
- Berrang P.G. and Grill E.V. (1974) The effect of manganese oxide scavenging on molybdenum in Saanich Inlet, British Columbia. *Mar. Chem.* **2**, 125-148.
- Bertine K.K. (1972) The deposition of molybdenum in anoxic waters. *Mar. Chem.* **1**, 43-53.
- Bertine K.K. and Turekian K.K. (1973) Molybdenum in marine deposits. *Geochim. Cosmochim. Acta* **37**(6), 1415-1434.
- Bertolin A., Rudello D., and Ugo P. (1995) A new device for in-situ pore-water sampling. *Mar. Chem.* **49**(2-3), 233-239.
- Billerbeck M., Werner U., Bosselmann K., Walpersdorf E., and Huettel M. (2006a) Nutrient release from an exposed intertidal sand flat. *Mar. Ecol. Prog. Ser.* **316**, 35-51.
- Billerbeck M., Werner U., Polerecky L., Walpersdorf E., de Beer D., and Huettel M. (2006b) Surficial and deep pore water circulation governs spatial and temporal scales of nutrient recycling in intertidal sand flat sediment. *Mar. Ecol. Prog. Ser.* **326**, 61-76.
- Bischoff J.L., Greer R.E., and Luistro A.O. (1970) Composition of interstitial waters of marine sediments: temperature of squeezing effect. *Science* **167**(3922): 1245-1246.
- Blanchard G.F., Paterson D.M., Stal L.J., Richard P., Galois R., Huet V., Kelly J., Honeywill C., de Brouwer J., Dyer K., Christie M., Seguignes M. (2000) The effect of geomorphological structures on potential biostabilisation by microphytobenthos on intertidal mudflats. *Cont. Shelf Res.* **20**, 1243-1256.

- Böttcher M.E., Rusch A., Höpner T., and Brumsack H.-J. (1997) Stable sulfur isotope effects related to local intense sulfate reduction in a tidal sandflat (southern North Sea): Results from loading experiments. *Isot. Environ. Health Stud.* **33**(1-2), 109-129.
- Böttcher M.E., Oelschlager B., Höpner T., Brumsack H.-J., and Rullkötter J. (1998) Sulfate reduction related to the early diagenetic degradation of organic matter and "black spot" formation in tidal sandflats of the German Wadden Sea (southern North Sea): stable isotope (^{13}C , ^{34}S , ^{18}O) and other geochemical results. *Org. Geochem.* **29**(5-7), 1517-1530.
- Böttcher M.E., Hespeneide B., Llobet-Brossa E., Beardsley C., Larsen O., Schramm A., Wieland A., Böttcher G., Berninger U.G., and Amann R. (2000) The biogeochemistry, stable isotope geochemistry, and microbial community structure of a temperate intertidal mudflat: an integrated study. *Cont. Shelf Res.* **20**(12-13), 1749-1769.
- Boudreau B.P. (1992) A kinetic model for microbic organic-matter decomposition in marine sediments. *FEMS Microbiol. Ecol.* **102**:1-14.
- Boudreau B.P. (1997) Diagenetic models and their implications. Springer, Berlin.
- Brotas V., Amorim-Ferreira A., Vale C., and Catarino F. (1990) Oxygen profiles in intertidal sediments of Ria Formosa (S. Portugal). *Hydrobiologia* **207**, 123-129.
- Brumsack H.-J. and Gieskes J.M. (1983) Interstitial water trace metal chemistry of laminated sediments from the Gulf of California, Mexico. *Mar. Chem.* **14**(1), 89-106.
- Brumsack H.-J. (2006) The trace metal content of recent organic carbon-rich sediments: Implications for Cretaceous black shale formation. *Paleogeogr. Paleoclimatol. Paleoecol.* **232**(2-4), 344-361.
- Bufflap S.E. and Allen H.E. (1995) Sediment pore-water collection methods for trace-metal analysis - a review. *Water Res.* **29**(1), 165-177.
- Burdige D.J. and Nealson K.H. (1986) Chemical and microbiological studies of sulfide-mediated manganese reduction. *Geomicrobiol. J.* **4**(4), 361-387.
- Burdige D.J. (1993) The biogeochemistry of manganese and iron reduction in marine sediments. *Earth Sci. Rev.* **35**(3), 249-284.

- Burnett W.C., Bokuniewicz H., Huettel M., Moore W.S., and Taniguchi M. (2003) Groundwater and pore water inputs to the coastal zone. *Biogeochemistry* **66**(1-2), 3-33.
- Caetano M., Falcão M., Vale C., and Bebianno M.J. (1997) Tidal flushing of ammonium, iron and manganese from inter-tidal sediment pore waters. *Mar. Chem.* **58**(1-2), 203-211.
- Chang T.S., Bartholomä A., and Flemming B.W. (2006a) Seasonal dynamics of fine-grained sediments in a back-barrier tidal basin of the German Wadden Sea (southern North Sea). *J. Coast. Res.* **22**(2), 328-338.
- Chang T.S., Flemming B.W., Tilch E., Bartholomä A., and Wöstmann R. (2006b) Late Holocene stratigraphic evolution of a back-barrier tidal basin in the East Frisian Wadden Sea, southern North Sea: transgressive deposition and its preservation potential. *Facies* **52**(3), 329-340.
- Chang T.S., Joerdel O., Flemming B.W., and Bartholomä A. (2006c) The role of particle aggregation/disaggregation in muddy sediment dynamics and seasonal sediment turnover in a back-barrier tidal basin, East Frisian Wadden Sea, southern North Sea. *Mar. Geol.* **235**(1-4), 49-61.
- Chapelle F.H. and Lovley D.R. (1990) Rates of microbial metabolism in deep coastal plain aquifers. *Appl. Environ. Microbiol.* **56**(6), 1865-1874.
- Charette M.A. and Allen M.C. (2006) Precision groundwater sampling in coastal aquifers using a direct-push, shielded-screen well-point system. *Ground Water Monit. R.* **26**(2): 87-93.
- Charette M.A. and Sholkovitz E.R. (2006) Trace element cycling in a subterranean estuary: Part 2. Geochemistry of the pore water. *Geochim. Cosmochim. Acta* **70**(4), 811-826.
- Chen M.S., Wartel S., and Temmerman S. (2005) Seasonal variation of flocculation characteristics on tidal flats, the Scheldt estuary. *Hydrobiologia* **540**, 181-195.

- Christiansen C., Volund G., Lund-Hansen L.C., and Bartholdy J. (2006) Wind influence on tidal flat sediment dynamics: Field investigations in the Ho Bugt, Danish Wadden Sea. *Mar. Geol.* **235**(1-4), 75-86.
- Church T.M., Sarin M.M., Fleisher M.Q., and Ferdelman T.G. (1996) Salt marshes: An important coastal sink for dissolved uranium. *Geochim. Cosmochim. Acta* **60**(20), 3879-3887.
- Cochran J.K., Carey A.E., Sholkovitz E.R., and Surprenant L.D. (1986) The geochemistry of uranium and thorium in coastal marine sediments and sediment pore waters. *Geochim. Cosmochim. Acta* **50**(5), 663-680.
- Collier R.W. (1985) Molybdenum in the Northeast Pacific Ocean. *Limnol. Oceanogr.* **30**(6), 1351-1354.
- Coveney M.F. and Wetzel R.G. (1989) Bacterial metabolism of algal extracellular carbon. *Hydrobiologia* **173**: 141-149.
- Cranston R.E. and Murray J.W. (1978) Determination of chromium species in natural waters. *Anal. Chim. Acta* **99**(2), 275-282.
- Cranston R.E. (1983) Chromium in Cascadia Basin, Northeast Pacific Ocean. *Mar. Chem.* **13**, 109-125.
- Crill P.M. and Martens C.S. (1987) Biogeochemical cycling in an organic-rich coastal marine basin. 6. Temporal and spatial variations in sulfate reduction rates. *Geochim. Cosmochim. Acta* **51**(5), 1175-1186.
- Crusius J., Calvert S., Pedersen T., and Sage D. (1996) Rhenium and molybdenum enrichments in sediments as indicators of oxic, suboxic and sulfidic conditions of deposition. *Earth Planet. Sci. Lett.* **145**(1-4), 65-78.
- Dalai T.K., Nishimura K., and Nozaki Y. (2005) Geochemistry of molybdenum in the Chao Phraya River estuary, Thailand: Role of suboxic diagenesis and porewater transport. *Chem. Geol.* **218**(3-4): 189-202.

- D'Andrea A.F., Aller R.C., and Lopez G.R. (2002) Organic matter flux and reactivity on a South Carolina sandflat: The impacts of porewater advection and macrobiological structures. *Limnol. Oceanogr.* **47**(4), 1056-1070.
- de Beer D., Wenzhofer F., Ferdelman T.G., Boehme S.E., Huettel M., van Beusekom J.E.E., Böttcher M.E., Musat N., and Dubilier N. (2005) Transport and mineralization rates in North Sea sandy intertidal sediments, Sylt-Rømø Basin, Wadden Sea. *Limnol. Oceanogr.* **50**(1), 113-127.
- Delafontaine M.T., Flemming B.W., and Thimm M. (2004) Large-scale trends in some mass physical properties of Danish Wadden Sea sediments, and implications for organism-sediment interactions. *Danish J. Geogr.* **104**, 27-36.
- Dellwig O., Gramberg D., Vetter D., Watermann F., Barckhausen J., Brumsack H.-J., Gerdes G., Liebezeit G., Rullkötter J., Scholz-Böttcher B.M., and Streif H. (1998) Geochemical and microfacies characterization of a Holocene depositional sequence in northwest Germany. *Org. Geochem.* **29**(5-7), 1687-1699.
- Dellwig O., Hinrichs J., Hild A., and Brumsack H.-J. (2000) Changing sedimentation in tidal flat sediments of the southern North Sea from the Holocene to the present: a geochemical approach. *J. Sea Res.* **44**(3-4), 195-208.
- Dellwig O., Watermann F., Brumsack H.-J., Gerdes G., and Krumbein W.E. (2001) Sulphur and iron geochemistry of Holocene coastal peats (NW Germany): a tool for palaeoenvironmental reconstruction. *Paleogeogr. Paleoclimatol. Paleoecol.* **167**(3-4), 359-379.
- Dellwig O., Bosselmann K., Kölsch S., Hentscher M., Hinrichs J., Böttcher M.E., Reuter R., and Brumsack H.-J. (2007) Sources and fate of manganese in a tidal basin of the German Wadden Sea. *J. Sea Res.* **57**(1), 1-18.
- Dellwig O., Beck M., Lemke A., Lunau M., Kolditz K., Schnetger B., and Brumsack H.-J. (2007) Non-conservative behaviour of molybdenum in coastal waters: Coupling geochemical, biological, and sedimentological processes. *Geochim. Cosmochim. Acta* **71**: 2745-2761.

- Disnar J.-R. (1981) Experimental study on metal fixation by a recent sedimentary organic-matter of algal origin - 2. Invitro fixation of UO_3^- , Cu^{2+} , Ni^{2+} , Zn^{2+} , Pb^{2+} , Co^{2+} , Mn^{2+} , and of VO_3^- , MoO_4^{2-} et GeO_3^{3-} . *Geochim. Cosmochim. Acta* **45**(3), 363-379.
- Duff M.C., Coughlin J.U., and Hunter D.B. (2002) Uranium co-precipitation with iron oxide minerals. *Geochim. Cosmochim. Acta* **66**(20), 3533-3547.
- Duinker J.C., van Eck G.T.M., and Nolting R.F. (1974) On the behaviour of copper, zinc, iron and manganese, and evidence for mobilization processes in the Dutch Wadden Sea. *Neth. J. Sea Res.* **8**(2-3), 214-239.
- Elbaz-Poulichet F., Seidel J.L., Jezequel D., Metzger E., Prevot F., Simonucci C., Sarazin G., Viollier E., Etcheber H., Jouanneau J.M., Weber O., and Radakovitch O. (2005) Sedimentary record of redox-sensitive elements (U, Mn, Mo) in a transitory anoxic basin (the Thau lagoon, France). *Mar. Chem.* **95**(3-4), 271-281.
- Engel A., Thoms S., Riebesell U., Rochelle-Newall E., and Zondervan I. (2004) Polysaccharide aggregation as a potential sink of marine dissolved organic carbon. *Nature* **428**(6986), 929-932.
- Erickson B.E. and Helz G.R. (2000) Molybdenum(VI) speciation in sulfidic waters: Stability and lability of thiomolybdates. *Geochim. Cosmochim. Acta* **64**(7), 1149-1158.
- Finke N., Vandieken V., and Jørgensen B.B. (2007) Acetate, lactate, propionate, and isobutyrate as electron donors for iron and sulfate reduction in Arctic marine sediments, Svalbard. *FEMS Microbiol. Ecol.* **59**(1), 10-22.
- Flemming B.W. and Davis J., R.A. (1994) Holocene evolution, morphodynamics and sedimentology of the Spiekeroog barrier island system (southern North Sea). *Senckenbergiana maritima* **24**(1/6), 117-155.
- Flemming B.W. and Nyandwi N. (1994) Land reclamation as a cause of fine-grained sediment depletion in backbarrier tidal flats (southern North Sea). *Netherlands Journal of Aquatic Ecology* **28**(3-4), 299-307.

- Flemming B.W. and Ziegler K. (1995) High resolution grain size distribution patterns and textural trends in the backbarrier environment of Spiekeroog Island (southern North Sea). *Senckenbergiana maritima* **26**(1/2), 1-24.
- Flemming B.W. and Delafontaine M.T. (2000) Mass physical properties of intertidal muddy sediments: some applications, misapplications, and non-applications. *Cont. Shelf Res.* **20**, 1179-1197.
- Fogg G.E. and Wolfe M. (1954) Nitrogen metabolization of blue-green algae. *Symp. Soc. Gen. Microbiol.* **4**: 99-125.
- Fogg G.E. (1962) Extracellular products. In *Physiology and biogeochemistry of algae* (eds. Baldwin R.A.). Academic Press Inc., New York, pp. 475-489.
- Fossing H. and Jørgensen B.B. (1990) Oxidation and reduction of radiolabeled inorganic sulfur-compounds in an estuarine sediment, Kysing Fjord, Denmark. *Geochim. Cosmochim. Acta* **54**(10), 2731-2742.
- Froelich P.N., Klinkhammer G.P., Bender M.L., Luedtke N.A., Heath G.R., Cullen D., Dauphin P., Hammond D., Hartman B., and Maynard V. (1979) Early oxidation of organic matter in pelagic sediments of the Eastern Equatorial Atlantic - Suboxic diagenesis. *Geochim. Cosmochim. Acta* **43**(7), 1075-1090.
- Ghani B., Masataka T., Hisham N.Z., Kishimoto N., Ismail A.K.M., Tano T., and Sugio T. (1993) Isolation and characterization of a Mo⁶⁺-reducing bacterium. *App. Environ. Microbiol.* **59**(4), 1176-1180.
- Grasshoff K., Kremling K., and Ehrhardt M. (1999) Methods of seawater analysis. Wiley-VCH, New York, N.Y.
- Gribsholt B. and Kristensen E. (2003) Benthic metabolism and sulfur cycling along an inundation gradient in a tidal *Spartina anglica* salt marsh. *Limnol. Oceanogr.* **48**(6), 2151-2162.
- Grunwald M., Dellwig O., Liebezeit G., Schnetger B., Reuter R., and Brumsack H.-J. (2007) Continuous measurements of methane and nutrients on a Wadden Sea time-series station (NW Germany). *Mar. Chem.* doi:10.1016/j.marchem.2007.04.003.

- Head P.C. and Burton J.D. (1970) Molybdenum in some ocean and estuarine waters. *J. Mar. Biol. Assoc. U.K.* **50**, 439-448.
- Heinrichs H., Brumsack H.-J., Löffler N., and König N. (1986) Verbessertes Druckaufschlußsystem für biologische und anorganische Materialien. *Z. Pflanzenernährung Bodenkunde* **149**, 350-353.
- Helz G.R., Miller C.V., Charnock J.M., Mosselmans J.F.W., Patrick R.A.D., Garner C.D., and Vaughan D.J. (1996) Mechanism of molybdenum removal from the sea and its concentration in black shales: EXAFS evidence. *Geochim. Cosmochim. Acta* **60**(19), 3631-3642.
- Hesslein R.H. (1976) In situ sampler for close interval pore water studies. *Limnol. Oceanogr.* **21**(6), 912-914.
- Hinrichs J. (2001) Geochemical tracers in the deep-sea and the North Sea. Ph.D. Thesis, University of Oldenburg, Germany.
- Howarth R.W. and Jørgensen B.B. (1984) Formation of ^{35}S -labeled elemental sulfur and pyrite in coastal marine sediments (Limfjorden and Kysing Fjord, Denmark) during short-term $^{35}\text{SO}_4^{2-}$ reduction measurements. *Geochim. Cosmochim. Acta* **48**(9), 1807-1818.
- Howarth R.W. and Cole J.J. (1985) Molybdenum availability, nitrogen limitation, and phytoplankton growth in natural waters. *Science* **229**(4714), 653-655.
- Howes B.L., Dacey J.W.H., and Wakeham S.G. (1985) Effects of sampling technique on measurements of porewater constituents in salt-marsh sediments. *Limnol. Oceanogr.* **30**(1), 221-227.
- Howes B.L. and Goehring D.D. (1994) Porewater drainage and dissolved organic carbon and nutrient losses through the intertidal creekbanks of a New-England salt-marsh. *Mar. Ecol. Prog. Ser.* **114**(3), 289-301.
- Huerta-Diaz M.A. and Morse J.W. (1992) Pyritization of trace metals in anoxic marine sediments. *Geochim. Cosmochim. Acta* **56**(7), 2681-2702.

- Huettel M. and Gust G. (1992) Impact of bioroughness on interfacial solute exchange in permeable sediments. *Mar. Ecol. Prog. Ser.* **89**(2-3), 253-267.
- Huettel M., Ziebis W., and Forster S. (1996) Flow-induced uptake of particulate matter in permeable sediments. *Limnol. Oceanogr.* **41**(2), 309-322.
- Huettel M., Ziebis W., Forster S., and Luther G.W. (1998) Advective transport affecting metal and nutrient distributions and interfacial fluxes in permeable sediments. *Geochim. Cosmochim. Acta* **62**(4), 613-631.
- Huettel M. and Rusch A. (2000) Transport and degradation of phytoplankton in permeable sediment. *Limnol. Oceanogr.* **45**(3), 534-549.
- Huettel M., Røy H., Precht E., and Ehrenhauss S. (2003) Hydrodynamical impact on biogeochemical processes in aquatic sediments. *Hydrobiologia* **494**(1-3), 231-236.
- Hulth S., Aller R.C., and Gilbert F. (1999) Coupled anoxic nitrification manganese reduction in marine sediments. *Geochim. Cosmochim. Acta* **63**(1), 49-66.
- Hursthouse A.S., Iqbal P.P., and Denman R. (1993) Sampling interstitial waters from intertidal sediments - an inexpensive device to overcome an expensive problem. *Analyst* **118**(11), 1461-1462.
- Hursthouse A.S., Matthews J.M., Figures J.E., Iqbal-Zahid P., Davies I.M., and Vaughan D.H. (2003) Chromium in intertidal sediments of the Clyde, UK: Potential for remobilisation and bioaccumulation. *Environ. Geochem. Health* **25**(2), 171-203.
- Hyacinthe C., Anschutz P., Carbonel P., Jouanneau J.-M., and Jorissen F.J. (2001) Early diagenetic processes in the muddy sediments of the Bay of Biscay. *Mar. Geol.* **177**, 111-128.
- Jahnke R.A. (1988) A simple, reliable, and inexpensive pore-water sampler. *Limnol. Oceanogr.* **33**(3), 483-487.
- Jahnke R.A., Alexander C.R., and Kostka J.E. (2003) Advective pore water input of nutrients to the Satilla River Estuary, Georgia, USA. *Estuar. Coast. Shelf Sci.* **56**(3-4), 641-653.

- Jahnke R., Richards M., Nelson J., Robertson C., Rao A., and Jahnke D. (2005) Organic matter remineralization and porewater exchange rates in permeable South Atlantic Bight continental shelf sediments. *Cont. Shelf Res.* **25**(12-13), 1433-1452.
- Jannasch H.W., Wheat C.G., Plant J.N., Kastner M., and Stakes D.S. (2004) Continuous chemical monitoring with osmotically pumped water samplers: OsmoSampler design and applications. *Limnol. Oceanogr. Meth.* **2**, 102-113.
- Jørgensen B.B. (1982) Mineralization of organic matter in the sea bed - the role of sulfate reduction. *Nature* **296**(5858), 643-645.
- Jørgensen B.B. (2006) Bacteria and marine biogeochemistry. In *Marine Geochemistry* (eds. Schulz H.D., Zabel M.). Springer Verlag, Berlin, pp. 169-201.
- Kautsky N. and Evans S. (1987) Role of biodeposition by *Mytilus edulis* in the circulation of matter and nutrients in a Baltic coastal ecosystem. *Mar. Ecol. Prog. Ser.* **38**, 201-212.
- Klinkhammer G.P. and Palmer M.R. (1991) Uranium in the oceans - Where it goes and why. *Geochim. Cosmochim. Acta* **55**(7), 1799-1806.
- Klinkhammer G.P. and McManus J. (2001). Dissolved manganese in the Columbia River estuary: Production in the water column. *Geochim. Cosmochim. Acta* **65**, 2835-2841.
- Kohlmeier C. (2004) Modellierung des Spiekerooger Rückseitenwatts mit einem gekoppelten Euler-Lagrange-Modell auf der Basis von ERSEM. Ph.D. Thesis, University of Oldenburg, Germany.
- Köpke B., Wilms R., Engelen B., Cypionka H., and Sass H. (2005) Microbial diversity in coastal subsurface sediments: a cultivation approach using various electron acceptors and substrate gradients. *Appl. Environ. Microbiol.* **71**(12), 7819-7830.
- Köpke B., Böttcher M.E., Köster J., Freese E., Wilms R., Engelen B., Cypionka H., Rullkötter J., and Sass H. Presence and activity of microbial populations in the subsurface of a tidal flat. (in prep.).

- Koretsky C.M., Moore C.M., Lowe K.L., Meile C., Dichristina T.J., and Van Cappellen P. (2003) Seasonal oscillation of microbial iron and sulfate reduction in saltmarsh sediments (Sapelo Island, GA, USA). *Biogeochemistry* **64**(2), 179-203.
- Kristensen E., Jensen M.H., and Jensen K.M. (1997) Temporal variations in microbenthic metabolism and inorganic nitrogen fluxes in sandy and muddy sediments of a tidally dominated bay in the northern Wadden Sea. *Helgol. Meeresunters.* **51**(3), 295-320.
- Kristensen E., Bodenbender J., Jensen M.H., Rennenberg H., and Jensen K.M. (2000) Sulfur cycling of intertidal Wadden Sea sediments (Königshafen, Island of Sylt, Germany): sulfate reduction and sulfur gas emission. *J. Sea Res.* **43**(2), 93-104.
- Kristensen E., Kristiansen K.D., and Jensen M.H. (2003) Temporal behaviour of manganese and iron in a sandy coastal sediment exposed to water column anoxia. *Estuaries* **26**(3), 690-699.
- Ku T.L., Knauss K.G., and Mathieu G.G. (1977) Uranium in open ocean - Concentration and isotopic composition. *Deep-Sea Res.* **24**(11), 1005-1017.
- Kuwae T., Kibe E., and Nakamura Y. (2003) Effect of emersion and immersion on the porewater nutrient dynamics of an intertidal sandflat in Tokyo Bay. *Estuar. Coast. Shelf Sci.* **57**(5-6), 929-940.
- Laima M., Brossard D., Sauriau P.G., Girard M., Richard P., Gouleau D., and Joassard L. (2002) The influence of long emersion on biota, ammonium fluxes and nitrification in intertidal sediments of Marennes-Oléron Bay, France. *Mar. Environ. Res.* **53**(4), 381-402.
- Lerat Y., Lasserre P., and Lecorre P. (1990) Seasonal changes in pore water concentrations of nutrients and their diffusive fluxes at the sediment water interface. *J. Exp. Mar. Biol. Ecol.* **135**(2), 135-160.
- Liebezeit G., Behrends B., and Kraul T. (1996) Variability of nutrients and particulate matter in backbarrier tidal flats of the East Frisian Wadden Sea. *Senckenbergiana maritima* **26**(3/6), 195-202.

- Lovley D.R., Phillips E.J.P., Gorby Y.A., and Landa E.R. (1991) Microbial reduction of uranium. *Nature* **350**(6317), 413-416.
- Lovley D.R., Roden E.E., Phillips E.J.P., and Woodward J.C. (1993) Enzymatic iron and uranium reduction by sulfate-reducing bacteria. *Mar. Geol.* **113**(1-2), 41-53.
- Lovley D.R. (1995) Microbial reduction of iron, manganese, and other metals. In *Advances in Agronomy*, Vol. 54, pp. 175-231.
- Lunau M., Sommer A., Lemke A., Grossart H.-P., and Simon M. (2004) A new sampling device for microaggregates in turbid aquatic systems. *Limnol. Oceanogr.: Meth.* **2**, 387-397.
- Lunau M., Lemke A., Walther K., Martens-Habbenha W., and Simon M. (2005) An improved method for counting bacteria from sediments and turbid environments by epifluorescence microscopy. *Environ. Microbiol.* **7**, 961-968.
- Lunau M., Lemke A., Dellwig O., and Simon M. (2006) Physical and biogeochemical controls of microaggregate dynamics in a tidally affected coastal ecosystem. *Limnol. Oceanogr.* **51**(2), 847-859.
- Magni P. and Montani S. (2006) Seasonal patterns of pore-water nutrients, benthic chlorophyll a and sedimentary AVS in a macrobenthos-rich tidal flat. *Hydrobiologia* **571**, 297-311.
- Makemson J.C. (1972) Interstitial water sampler for sandy beaches. *Limnol. Oceanogr.* **17**(4), 626-8.
- Marencic H., Essink K., Kellermann A., and Eskildsen K. (2005) Introduction. In *Wadden Sea quality status report 2004* (eds. Essink K., Dettmann C., Farke H., Laursen K., Lüerßen G., Marencic H., Wiersinga W.). Wadden Sea ecosystem No. 19. Trilateral monitoring and assessment group. Common Wadden Sea Secretariat (CWSS), Wilhelmshaven, Germany, pp. 11-25.
- Mayer L.M. (1989) Extracellular proteolytic enzyme activity in sediments of an intertidal mudflat. *Limnol. Oceanogr.* **34**(6), 973-981.

- McManus J., Berelson W.M., Klinkhammer G.P., Hammond D.E., and Holm C. (2005) Authigenic uranium: relationship to oxygen penetration depth and organic carbon rain. *Geochim. Cosmochim. Acta* **69**(1), 95-108.
- Mendel R.R. (2005) Molybdenum: biological activity and metabolism. *Dalton T.* 3404-3409.
- Middelburg J.J., Delange G.J., and Vanderweijden C.H. (1987) Manganese solubility control in marine pore waters. *Geochim. Cosmochim. Acta* **51**(3), 759-763.
- Moeslund L., Thamdrup B., and Jørgensen B.B. (1994) Sulfur and iron cycling in a coastal sediment - Radiotracer studies and seasonal dynamics. *Biogeochemistry* **27**(2), 129-152.
- Montgomery J.R., Price M.T., Holt J., and Zimmermann C. (1981) A close-interval sampler for collection of sediment pore waters for nutrient analyses. *Estuaries* **4**(1), 75-77.
- Morford J.L. and Emerson S. (1999) The geochemistry of redox sensitive trace metals in sediments. *Geochim. Cosmochim. Acta* **63**(11-12), 1735-1750.
- Morford J.L., Emerson S.R., Breckel E.J., and Kim S.H. (2005) Diagenesis of oxyanions (V, U, Re, and Mo) in pore waters and sediments from a continental margin. *Geochim. Cosmochim. Acta* **69**(21), 5021-5032.
- Morford J.L., Martin W.R., Kalnejais L.H., Francois R., Bothner M., and Karle I.M. (2007) Insights on geochemical cycling of U, Re and Mo from seasonal sampling in Boston Harbor, Massachusetts, USA. *Geochim. Cosmochim. Acta* **71**, 895-917.
- Morgan J.J. (2005) Kinetics of reaction between O₂ and Mn(II) species in aqueous solutions. *Geochim. Cosmochim. Acta* **69**(1), 35-48.
- Morris A.W. (1975) Dissolved molybdenum and vanadium in Northeast Atlantic Ocean. *Deep-Sea Res.* **22**(1), 49-54.
- Muenster U. (1993) Concentrations and fluxes of organic carbon substrates in the aquatic environment. *Antonie Van Leeuwenhoek* **63**, 243-274.

- Mugo R.K. and Orians K.J. (1993) Seagoing method for the determination of chromium(III) and total chromium in sea water by electron-capture detection gas-chromatography. *Anal. Chim. Acta* **271**(1), 1-9.
- Murray L.G., Mudge S.M., Newton A., and Icely J.D. (2006) The effect of benthic sediments on dissolved nutrient concentrations and fluxes. *Biogeochemistry* **81**(2), 159-178.
- Myers C.R. and Nealson K.H. (1988) Microbial reduction of manganese oxides - Interactions with iron and sulfur. *Geochim. Cosmochim. Acta* **52**(11), 2727-2732.
- Nameroff T.J., Balistrieri L.S., and Murray J.W. (2002) Suboxic trace metal geochemistry in the eastern tropical North Pacific. *Geochim. Cosmochim. Acta* **66**(7), 1139-1158.
- Nayar S., Miller D., Bryars S., and Cheshire A.C. (2006) A simple, inexpensive and large volume pore water sampler for sandy and muddy substrates. *Estuar. Coast. Shelf Sci.* **66**(1-2), 298-302.
- Nielsen M., Bollmann A., Sliekers O., Jetten M., Schmid M., Strous M., Schmidt I., Larsen L.H. Nielsen L.P., and Revsbech N.P. (2005) Kinetics, diffusional limitation and microscale distribution of chemistry and organisms in a CANON reactor. *FEMS Microbiol. Ecol.* **51**(2), 247-256.
- Nissenbaum A. and Swaine D.J. (1976) Organic matter-metal interaction in recent sediments, the role of humic substances. *Geochim. Cosmochim. Acta* **40**, 809-816.
- Pallud C. and Van Cappellen P. (2006) Kinetics of microbial sulfate reduction in estuarine sediments. *Geochim. Cosmochim. Acta* **70**(5), 1148-1162.
- Paerl H.W., Crocker K.M., and Prufert L.E. (1987) Limitation of N₂ fixation in coastal marine waters - Relative importance of molybdenum, iron, phosphorus, and organic matter availability. *Limnol. Oceanogr.* **32**(3), 525-536.
- Passow U. (2002) Transparent exopolymer particles (TEP) in aquatic environments. *Progress Oceanogr.* **55**(3-4), 287-333.
- Passow U. and De la Rocha C.L. (2006) Accumulation of mineral ballast on organic aggregates. *Global Biogeochem. Cycles* **20**(1).

- Pedersen T.F. and Price N.B. (1982) The geochemistry of manganese carbonate in Panama Basin sediments. *Geochim. Cosmochim. Acta* **46**(1), 59-68.
- Phelps T.J., Raione E.G., White D.C., and Fliermans C.B. (1989) Microbial activities in deep subsurface environments. *Geomicrobiol. J.* **7**: 79-91.
- Pingitore N.E. and Eastman M.E. (1985) Barium partitioning during the transformation of corals from aragonite to calcite. *Chem. Geol.* **48**:183-187.
- Ploug H., Kühl M., Buchholz-Cleven B., and Jørgensen B.B. (1997) Anoxic aggregates – an ephemeral phenomenon in the pelagic environment? *Aquat. Microb. Ecol.* **13**, 285-294.
- Precht E. and Huettel M. (2003) Advective pore-water exchange driven by surface gravity waves and its ecological implications. *Limnol. Oceanogr.* **48**(4), 1674-1684.
- Precht E., Franke U., Polerecky L., and Huettel M. (2004) Oxygen dynamics in permeable sediments with wave-driven pore water exchange. *Limnol. Oceanogr.* **49**, 693-705.
- Precht E. and Huettel M. (2004) Rapid wave-driven advective pore water exchange in a permeable coastal sediment. *J. Sea Res.* **51**(2), 93-107.
- Ramón M. (2003) Population dynamics and secondary production of the cockle *Cerastoderma edule* (L.) in a backbarrier tidal flat of the Wadden Sea. *Scientia marina* **67**(4), 429-443.
- Raiswell R. and Canfield D.E. (1996) Rates of reaction between silicate iron and dissolved sulfide in Peru Margin sediments. *Geochim. Cosmochim. Acta* **60**(15), 2777-2787.
- Redfield A.C. (1958) The biological control of chemical factors in the environment. *Am. Scientist* **46**(3), 205-221.
- Reeburgh W.S. (1967) An improved interstitial water sampler. *Limnol. Oceanogr.* **12**(1), 163-165.
- Reise K. (2005) Coast of change: habitat loss and transformations in the Wadden Sea. *Helgol. Mar. Res.* **59**(1), 9-21.
- Riedl R.J., Machan R., and Huang N. (1972) Subtidal pump - Mechanism of interstitial water exchange by wave action. *Mar. Biol.* **13**(3), 210-221.

- Robbins J.A. and Gustinis J. (1976) Squeezer for efficient extraction of pore water from small volumes of anoxic sediment. *Limnol. Oceanogr.* **21**(6), 905-909.
- Robson R.L., Eady R.R., Richardson T.H., Miller R.W., Hawkins M., and Postgate J.R. (1986) The alternative nitrogenase of azotobacter-chroococcum is a vanadium enzyme. *Nature* **322**(6077), 388-390.
- Rocha C. (1998) Rhythmic ammonium regeneration and flushing in intertidal sediments of the Sado estuary. *Limnol. Oceanogr.* **43**(5), 823-831.
- Rodushkin I. and Ruth T. (1997) Determination of trace metals in estuarine and sea-water reference materials by high resolution inductively coupled plasma mass spectrometry. *J. Anal. At. Spectrom.* **12**(10), 1181-1185.
- Rusch A., Töpken H., Böttcher M.E., and Höpner T. (1998) Recovery from black spots: results of a loading experiment in the Wadden Sea. *J. Sea Res.* **40**(3-4), 205-219.
- Rusch A. and Huettel M. (2000) Advective particle transport into permeable sediments - evidence from experiments in an intertidal sandflat. *Limnol. Oceanogr.* **45**(3), 525-533.
- Rusch A., Forster S., and Huettel M. (2001) Bacteria, diatoms and detritus in an intertidal sandflat subject to advective transport across the water-sediment interface. *Biogeochemistry* **55**(1), 1-27.
- Rusch A., Huettel M., Wild C., and Reimers C.E. (2006) Benthic oxygen consumption and organic matter turnover in organic-poor, permeable shelf sands. *Aquat. Geochem.* **12**(1), 1-19.
- Saager P.M., Sweerts J.P., and Ellermeijer H.J. (1990) A simple pore-water sampler for coarse, sandy sediments of low porosity. *Limnol. Oceanogr.* **35**(3), 747-751.
- Sakamaki T., Nishimura O., and Sudo R. (2006) Tidal time-scale variation in nutrient flux across the sediment-water interface of an estuarine tidal flat. *Estuar. Coast. Shelf Sci.* **67**(4), 653-663.
- Sani R.K., Peyton B.M., Amonette J.E., and Geesey G.G. (2004) Reduction of uranium(VI) under sulfate-reducing conditions in the presence of Fe(III)-(hydr)oxides. *Geochim. Cosmochim. Acta* **68**(12), 2639-2648.

- Sansone F.J. and Martens C.S. (1982) Volatile fatty acid cycling in organic-rich marine sediments. *Geochim. Cosmochim. Acta* **46**(9), 1575-1589.
- Sarazin G., Michard G., and Prevot F. (1999) A rapid and accurate spectroscopic method for alkalinity measurements in sea water samples. *Water Res.* **33**(1), 290-294.
- Sasseville D.R., Takacs A.P., Norton S.A., and Davis R.B. (1974) Large-volume interstitial water sediment squeezer for lake sediments. *Limnol. Oceanogr.* **19**(6), 1001-1004.
- Sayles F.L., Wilson T.R.S., Hume D.N., and Mangelsdorf P.C. (1973) In-situ sampler for marine sedimentary pore waters - Evidence for potassium depletion and calcium enrichment. *Science* **181**(4095), 154-156.
- Schnetger B., Hinrichs J., Dellwig O., Shaw T., and Brumsack H.-J. (2001) The significance of radionuclides and trace elements in a back barrier tidal area: results from the German Wadden Sea. In *Distribution and Speciation of Radionuclides in the Environment* (eds. Inaba J., Hisamatsu S., Ohtsuka Y.). Proceedings of the International Workshop on Distribution and Speciation of Radionuclides in the Environment, Rokkasho, Aomori, Japan, October 2000, pp 99-106.
- Schoemann V., de Baar H.J.W., de Jong J.T.M., and Lancelot C. (1998) Effects of phytoplankton blooms on the cycling of manganese and iron in coastal waters. *Limnol. Oceanogr.* **43**(7), 1427-1441.
- Seeberg-Elverfeldt J., Schlüter M., Feseker T., and Kölling M. (2005) Rhizon sampling of porewaters near the sediment-water interface of aquatic systems. *Limnol. Oceanogr. Meth.* **3**, 361-371.
- Serpa D., Falcão M., Duarte P., Cancela da Fonseca L., and Vale C. (2007) Evaluation of ammonium and phosphate release from intertidal and subtidal sediments of a shallow coastal lagoon (Ria Formosa – Portugal): a modelling approach. *Biogeochemistry* **82**:291-304.
- Shaw T.J., Gieskes J.M., and Jahnke R.A. (1990) Early diagenesis in differing depositional environments - the response of transition metals in pore water. *Geochim. Cosmochim. Acta* **54**(5), 1233-1246.

- Sholkovitz E. (1973) Interstitial water chemistry of Santa Barbara Basin sediments. *Geochim. Cosmochim. Acta* **37**(9), 2043-2073.
- Sørensen J., Christensen D., and Jørgensen B.B. (1981) Volatile fatty-acids and hydrogen as substrates for sulfate-reducing bacteria in anaerobic marine sediment. *Appl. Environ. Microbiol.* **42**(1), 5-11.
- Stal L.J. (2003) Microphytobenthos, their extracellular polymeric substances, and the morphogenesis of intertidal sediments. *Geomicrobiol. J.* **20**, 463-478.
- Sundby B., Martinez P., and Gobeil C. (2004) Comparative geochemistry of cadmium, rhenium, uranium, and molybdenum in continental margin sediments. *Geochim. Cosmochim. Acta* **68**(11), 2485-2493.
- Sundby B. and Silverberg N. (1981) Pathways of manganese in an open estuarine system. *Geochim. Cosmochim. Acta* **45**(3), 293-307.
- Stal L.J. (2003) Microphytobenthos, their extracellular polymeric substances, and the morphogenesis of intertidal sediments. *Geomicrobiol. J.* **20**(5), 463-478.
- Streif H. (1990) Das ostfriesische Küstengebiet. Gebrüder Borntraeger, Berlin.
- Swarzenski P.W. and Baskaran M. (2007) Uranium distribution in the coastal waters and pore waters of Tampa Bay, Florida. *Mar. Chem.* **104**(1-2), 43-57.
- Szalay A. and Szilagyi M. (1967) Association of vanadium with humic acids. *Geochim. Cosmochim. Acta* **31**(1), 1-6.
- Szilagyi M. (1967) Sorption of molybdenum by humus preparations. *Geochem. Int.* **4**, 1165-1167.
- Thamdrup B., Fossing H., and Jørgensen B.B. (1994) Manganese, iron, and sulfur cycling in a coastal marine sediment, Aarhus Bay, Denmark. *Geochim. Cosmochim. Acta* **58**(23), 5115-5129.
- Thomson J., Higgs N.C., Jarvis I., Hydes D.J., Colley S., and Wilson T.R.S. (1986) The behavior of manganese in Atlantic carbonate sediments. *Geochim. Cosmochim. Acta* **50**(8), 1807-1818.

- Tishchenko P.Y., Pavlova G.Y., Suess E., Nedashkovskii A.P., Domeier B., and Greinert I. (2001) The alkali reserve of interstitial water at the sites of methane emission in the Sea of Okhotsk. *Geochem. Int.* **39**(6), 597-603.
- Tribovillard N., Riboulleau A., Lyons T., and Baudin F.O. (2004) Enhanced trapping of molybdenum by sulfurized marine organic matter of marine origin in Mesozoic limestones and shales. *Chem. Geol.* **213**(4), 385-401.
- Trouwborst R.E., Clement B.G., Tebo B.M., Glazer B.T., and Luther III G.W. (2006) Soluble Mn(III) in suboxic zones. *Science* **313**, 1955-1957.
- Todorova S.G., Siegel D.I., and Costello A.M. (2005) Microbial Fe(III) reduction in a minerotrophic wetland - geochemical controls and involvement in organic matter decomposition. *Appl. Geochem.* **20**(6), 1120-1130.
- Tuit C.B. and Ravizza G. (2003) The marine distribution of molybdenum. *Geochim. Cosmochim. Acta* **67**(18), Suppl. 1, A495.
- UNESCO (1981) The practical salinity scale 1978 and the international equation of state of seawater 1980. Tenth report on the joint panel on oceanographic tables and standards. UNESCO Technical Paper in Marine Science 36, UNESCO, Paris.
- Volkman J.K., Rohjans D., Rullkötter J., Scholz-Böttcher B.M., and Liebezeit G. (2000) Sources and diagenesis of organic matter in tidal flat sediments from the German Wadden Sea. *Cont. Shelf Res.* **20**(10-11), 1139-1158.
- Volkov I.I. and Formina L.S. (1974) Influence of organic material and processes of sulphide formation on distribution of some trace elements in deep-water sediment of Black Sea. *AAPG Memoir* **20**, 457-476.
- von Tuempling W. and Friedrich G. (1999) *Biologische Gewässeruntersuchung*. Jena; Stuttgart; Lübeck; Ulm, G. Fischer.
- Vorlicek T.P. and Helz G.R. (2002) Catalysis by mineral surfaces: Implications for Mo geochemistry in anoxic environments. *Geochim. Cosmochim. Acta* **66**(21), 3679-3692.

- Vorlicek T.P., Kahn M.D., Kasuya Y., and Helz G.R. (2004) Capture of molybdenum in pyrite-forming sediments: Role of ligand-induced reduction by polysulfides. *Geochim. Cosmochim. Acta* **68**(3), 547-556.
- Vosjan J.H. (1974) Sulphate in water and sediment of the Dutch Wadden Sea. *Neth. J. Sea Res.* **8**:208-213.
- Wanty R.B. and Goldhaber M.B. (1992) Thermodynamics and kinetics of reactions involving vanadium in natural systems - Accumulation of vanadium in sedimentary rocks. *Geochim. Cosmochim. Acta* **56**(4), 1471-1483.
- Watson P.G. and Frickers T.E. (1990) A multilevel, in situ pore-water sampler for use in intertidal sediments and laboratory microcosms. *Limnol. Oceanogr.* **35**(6), 1381-1389.
- Wedepohl K.H. (1971) Environmental influence on the chemical composition of shales and clays. In *Physics and Chemistry of the Earth* (eds. Ahrens L.H., Press F., Runcorn S.K., Urey H.C.), Vol. 8, Pergamon, Oxford, pp 305-333.
- Wedepohl K.H. (2004) The composition of earth's upper crust, natural cycles of elements, natural resources. In *Elements and their Compounds in the Environment* (eds. Merian E., Anke M., Ihnat M., Stoepler M.), 2nd Edition. Wiley-VCH, pp. 3-17.
- Wehrli B. and Stumm W. (1989) Vanadyl in natural waters - Adsorption and hydrolysis promote oxygenation. *Geochim. Cosmochim. Acta* **53**(1), 69-77.
- Weston N.B., Porubsky W.P., Samarkin V.A., Erickson M., Macavoy S.E., and Joye S.B. (2006) Porewater stoichiometry of terminal metabolic products, sulfate, and dissolved organic carbon and nitrogen in estuarine intertidal creek-bank sediments. *Biogeochemistry* **77**(3), 375-408.
- Whiting G.J. and Childers D.L. (1989) Subtidal advective water flux as a potentially important nutrient input to Southeastern USA saltmarsh estuaries. *Estuar. Coast. Shelf Sci.* **28**(4), 417-431.
- Wilms R., Köpke B., Sass H., Chang T.S., Cypionka H., and Engelen B. (2006) Deep biosphere-related bacteria within the subsurface of tidal flat sediments. *Environ. Microbiol.* **8**(4), 709-719.

- Wilms R., Sass H., Köpke B., Cypionka H., and Engelen B. (2007a) Methane and sulfate profiles within the subsurface of a tidal flat are reflected by the distribution of sulfate-reducing bacteria and methanogenic archaea. *FEMS Microbiol. Ecol.* **59**(3), 611-621.
- Wilms R., Sass H., Köpke B., Köster J., Cypionka H., and Engelen B. (2006b) Specific bacterial, archaeal, and eukaryotic communities in tidal-flat sediments along a vertical profile of several meters. *Appl. Environ. Microbiol.* **72**(4), 2756-2764.
- Wilson A.M. and Gardner L.R. (2006c) Tidally driven groundwater flow and solute exchange in a marsh: Numerical simulations. *Water Resour. Res.* **42**(1), Art. No. W01405.
- Wirtz K.W. (2003) Control of biogeochemical cycling by mobility and metabolic strategies of microbes in the sediments: an integrated model study. *FEMS Microbiol. Ecol.* **46**(3), 295-306.
- Yamazaki H. and Gohda S. (1990) Distribution of dissolved molybdenum in the Seto Inland Sea, the Japan Sea, the Bering Sea and the Northwest Pacific Ocean. *Geochem. J.* **24**(4), 273-281.
- Yin K.D. and Harrison P.J. (2000) Influences of flood and ebb tides on nutrient fluxes and chlorophyll on an intertidal flat. *Mar. Ecol. Prog. Ser.* **196**, 75-85.
- Zheng Y., Anderson R.F., van Geen A., and Kuwabara J. (2000) Authigenic molybdenum formation in marine sediments: A link to pore water sulfide in the Santa Barbara Basin. *Geochim. Cosmochim. Acta* **64**(24), 4165-4178.
- Ziebis W., Huettel M., and Forster S. (1996) Impact of biogenic sediment topography on oxygen fluxes in permeable seabeds. *Mar. Ecol. Prog. Ser.* **140**(1-3), 227-237.

Acknowledgements / Danksagung

Die vorliegende Arbeit ist durch die Anleitung, Mitarbeit und Unterstützung vieler Menschen möglich geworden, die ich in den vergangenen Jahren kennen gelernt habe.

An erster Stelle gilt mein Dank Prof. Dr. H.-J. Brumsack, der es mir ermöglicht hat in der Arbeitsgruppe Mikrobiogeochemie über ein sehr interessantes Thema meine Promotion zu machen. Darüber hinaus bin ich für die fortwährende Unterstützung und die vielen interessanten Diskussionen sehr dankbar, die mir den Einstieg in die Meeresforschung erleichtert und wesentlich zum Gelingen der Arbeit beigetragen haben.

Prof. Dr. J. Rullkötter danke ich für sein Engagement für die Forschergruppe „BioGeoChemie des Watts“ und für seine Bereitschaft das Zweitgutachten zu übernehmen.

In den vergangenen Jahren haben Olaf Dellwig und Bernhard Schnetger meine Arbeit eng begleitet und ich habe sehr von ihrem geochemischen und analytischen Wissen profitiert. Olaf Dellwig bin ich für die Unterstützung bei analytischen Fragen und die vielen fachlichen Diskussionen sehr dankbar. Bernhard Schnetger danke ich dafür, dass er mir die analytische Denkweise näher gebracht hat und mir beim Lösen von Problemen mit Geräten und bei fachlichen Fragen immer wieder geholfen hat.

Almut Hetzel, Kerstin Kolditz, Maik Grunwald und Frank Schoster danke ich für die schöne Zeit in der Arbeitsgruppe und die vielseitige Unterstützung. Danke Alexander Josefowicz ‚Josi‘ für das unkomplizierte Erfüllen unserer Literaturwünsche. Eleonore Gründken, Carola Lehnert, Martina Wagner und Nicole Becker ein großes Dankeschön für ihr großes Engagement und ihre Hilfsbereitschaft im Labor. Bei meinen Kollegen im Büro möchte ich mich für die tolle Arbeitsatmosphäre bedanken. Malte Groh hat mich bei den Arbeiten im Watt wunderbar unterstützt.

Allen Mitstreitern in der Forschergruppe danke ich herzlich für die tolle Zusammenarbeit. Das Bearbeiten von interdisziplinären Fragen hat dazu beigetragen, dass die eigene Arbeit noch spannender wurde.

Den Mitarbeitern der Werkstatt des Forschungszentrums Terramare, besonders Helmo Nicolai, möchte ich für den Bau meiner Probenahmesysteme und für ihren unermüdlichen Einsatz bei Arbeiten im Watt danken.

Meinen Eltern möchte ich herzlich für den großen Rückhalt und die Unterstützung während der vorliegenden Arbeit danken.

Diese Arbeit wurde von der Deutschen Forschungsgemeinschaft (DFG) im Rahmen der Forschergruppe FOR 432/2 „BioGeoChemie des Watts“ gefördert.

Curriculum vitae

Name: Melanie Beck

Geburtsdatum: 12.10.1978

Geburtsort: Wertingen

1985 – 1989 Grundschule in Wertingen

1989 – 1998 Gymnasium in Wertingen (Abschluss: Allgemeine Hochschulreife)

1998 – 2004 Studium Diplom Geoökologie an der Universität Bayreuth

Vordiplom: 17. Oktober 2000

Diplomarbeit am Lehrstuhl für Hydrologie zum Thema „Zusammenhang von Steroidkonzentrationen im Abwasser und in abwasserbürtigen Aerosolpartikeln“

Diplom: 20. Januar 2004

seit Juni 2004 wissenschaftliche Mitarbeiterin in der Arbeitsgruppe Mikrobiogeochemie am Institut für Chemie und Biologie des Meeres (ICBM) der Carl von Ossietzky Universität Oldenburg

Experimentelle Arbeiten zur vorliegenden Promotion im Rahmen der DFG-Forschergruppe „BioGeoChemie des Watts“ unter der Leitung von Herrn Prof. Dr. H.-J. Brumsack

Erklärung

Hiermit versichere ich, dass ich die vorliegende Arbeit selbstständig angefertigt und keine anderen als die angegebenen Quellen und Hilfsmittel verwendet habe. Zusätzlich erkläre ich, dass diese Dissertation weder in ihrer Gesamtheit noch in Teilen einer anderen wissenschaftlichen Hochschule zur Begutachtung in einem Promotionsverfahren vorliegt oder vorgelegen hat.

Oldenburg, im Juni 2007

Melanie Beck